ABSTRACT

Title of Document: NOVEL PRECISION POLYOLEFINS FROM LIVING COORDINATIVE CHAIN-TRANSFER POLYMERIZATION

Rennisha R. Wickham
Doctor of Philosophy, 2012

Directed By: Professor Lawrence. R. Sita
Department of Chemistry and Biochemistry

Polyolefins (POs), especially polyethene (PE) and polypropene (PP), are by far the largest volume synthetic polymers in the plastic industry, with annual global production exceeding 1.4×10^8 metric tons and projected to increase to 200 million tons by the year 2020 according to the 2007 National Petrochemical and Refiners Association Report. This is primarily due to their benign nature, excellent cost performance value, as well as ease of recycling, processing and fabrication. With societal dependence on polyolefins steadily increasing, efforts have been placed on the development of living coordinative chain-transfer polymerization (LCCTP) towards the large scale production of functionalized copolymers and block copolymers from commodity volume monomers, ethene (E) and propene (P) with α-olefins, cyclic and sterically encumbered olefin comonomers that could potentially be used as compatibilizers in polymer mixtures, thermoplastic elastomeric substitutes of EPDM rubber, and macro-initiators in anionic and free radical polymerizations methods. Copolymerizations of E and P with monomers that can be obtained in industrially significant volumes from renewable biomass-derived

feedstocks or waste product streams are investigated. The diterpene β-citronellene, represents an ideal target as a potential co-monomer since after incorporation through Ziegler-Natta enchainment of the terminal vinyl group, the remaining tri-substituted double bond is available for further chemical modification or cross-linking. Norbornene is also a desirable comonomer for ethene copolymerization as the resulting polyolefin materials are optically transparent and can be used as replacements for polycarbonates. Another non-conjugated diene, 1,5-hexadiene, has been utilized in conjunction with 1-hexene or 1-octene to produce rod-coil block copolymers that could potentially give way to polyolefins having new end-use properties through microphase separation into various nanostructures. Moreover, post-functionalization of PE and PP materials with I, N_3, OH, and PPh_3 etc., is investigated as a route towards the production of value-added polymers. Finally, this work utilizes aims to develop new spectroscopic and analytical tools for the structural analysis of hydrocarbons materials, as these properties directly influence the chemical and physical properties. Therefore, the practicality of MALDI-TOF MS as a routine characterization method for the evaluation of new polyolefins was probed. Overall this thesis will discuss the tailored synthesis, functionalization and characterization of ethene and propene based polymers.

NOVEL PRECISION POLYOLEFINS FROM LIVING COORDINATIVE CHAIN-TRANSFER POLYMERIZATION

by

Rennisha R. Wickham

Dissertation submitted to the Faculty of the Graduate School of the
University of Maryland, College Park, in partial fulfillment
of the requirements for the degree of
Doctor of Philosophy
2012

Advisory Committee:
Professor Lawrence R. Sita, Chair
Professor Kyu Choi, Dean's Representative
Professor Jeffrey T. Davis
Professor Andrei Vedernikov
Professor Philip DeShong

Dedication

To my loving and supportive family and friends, and in memory of my brother Derek Wickham, grandmother Merle Roberts, and grandfather Andreas Miller.

Acknowledgments

I would like to express my sincere gratitude to my PhD advisor, Professor Lawrence Sita, for motivating me to do my best and put forth maximum effort under all circumstances.

I would also like extend my gratitude to my candidacy and thesis committee members, Dr. Davis, Dr. Vedernikov, Dr. Eichhorn, Dr. DeShong and Dr. Choi, for their excellent advice and guidance. I am also very grateful to Dr. Yiu-Fai Lam, Dr. Yinde Wang, and Frederick Nytko for their help with NMR experiments as well as Dr. Yu Li for his assistance with MALDI-TOF MS experiments. TEM assistance from Dr. Wen-An Chiou and Dr. LiChung Lai of the University of Maryland Nanocenter is also greatly appreciated.

Next, I would like to thank all past and present Sita group members with whom I have had the pleasure of working, Dr. Philip Fontaine, Dr. Wei Zhang, Emily Trunkley, Dr. Jia Wei, Wonseok Hwang, Brendan Yonke, Gail Blakely, Andrew Keane, Wesley Farrell, Kaitlyn Crawford, and Dr. Jonathan Reeds for their meaningful discussions and for making my time at the University of Maryland memorable and exciting. I would also like to thank Dr. Domonique Downing, Melantha Jackson, Dr. Williamson Oloo, and Petrina Boucher, for their unwavering friendship, support, and encouragement throughout my graduate school career. You all will always have a special place in my heart and a place in my life. Additionally, I would like to thank the University of Maryland NOBCChE organization for being a support system where I could establish friendships and identify leadership opportunities early in my scientific career.

I sincerely would like to thank my mother Shermaine Miller, sisters Rennica Wickham and Orniqua Edney, and my brothers Orson Edney and Derek Wickham for their love and encouragement throughout my lifetime. Had it not been for them I would never have endeavored to become a doctorate of philosophy nor would I have accomplished this feat given all the obstacles that I encountered on my journey to this goal. Their confidence in me is unwavering and limitless and their love unconditional, and with them I will forever be inspired to become a better me! Derek, thanks for being my guardian angel and my source of confidence, because of you I now know that no goal is insurmountable. Mom, thank you for instilling in me the importance of a quality education and more significantly for ensuring that I understood that with hardwork and dedication I could achieve all things. Rennica, had it not been for you forcing me unto that airplane six years ago and babysitting me in Maryland my first year in graduate school I would never have made it. For this, I will be forever grateful. Also, thank you to Orniqua and Orson for being a source of encouragment; I hope that I have proven to you both that all goals are achievable. Also, thank you all for taking care of Gucci while I wrote my thesis.

Love, support and motivation from other family members and friends, especially Edward Wickham, Russel Bodley, Lewanda and Peter James, Joel Wynter, Mercedes Bell, Latoya Javois, Mrs. Grullon, Charles Gee, and small group members at The Bridge are also deeply appreciated. I would also like to extend a special thank you to my perfect person, Glenn Rogers. Additionally, I would like to thank my mentors Attorney Joel H. Holt and Jerri Farrante for teaching me to be fearless and to always chase my dreams. Lastly, I would like to thank my high school English and Chemistry teachers at the St.

Croix Central High School Ms. Cummings and Mr. Woods and members of HOVENSA's Shining Stars tutorial program for sparking my interest in chemistry and encouraging me to pursue that interest early on.

It has become unequivocally clear to me that all things are possible with God and his angels, so I thank him whole-heartedly for placing all of these extraordinary people in my life!

Table of Contents

List of Tables

List of Figures

List of Abbreviations

POs	polyolefins
PE	polyethene
PP	polypropene
LCP	living coordination polymerization
CCTP	coordinative chain-transfer polymerization
LCCTP	living coordinative chain-transfer polymerization
E	ethene
P	propene
M_n	number average molecular weight
M_w	weight average molecular weight
PDI	polydispersity index
DP	degree of polymerization
CRP	controlled radical polymerization
SFRP	stable free radical polymerization
ATRP	atom transfer radical polymerization
RAFT	reversible addition-fragmentation transfer
ROMP	ring opening metathesis polymerization
ZN	Ziegler-Natta
GPC	gel permeation chromatography or size exclusion chromatography
DSC	differential scanning calorimetry
TGA	thermogravemetric analysis

NMR	nuclear magnetic resonance
PH	poly(1-hexene)
PO	poly(1-octene)
PMCP	poly(methylene-1,3-cyclopentane)
Ps-TM-AFM	phase sensitive tapping mode atomic force microscopy
MALDI-TOF MS	matrix-assisted laser desorption/ionization time-of-flight mass spectroscopy
°C	(-)-β-Citronellene
NB	norbornene
VCH	vinylcyclohexane
T_g	glass transition temperature
T_m	melting temperature
T_c	crystallization temperature
LP	laser power
DP	degree of polymerization
$[M]_o$	initial monomer concentration
$[I]_o$	initial initiator concentration
SIS	polystyrene-*b*-polyisoprene-*b*-polystyrene
SBS	polystyrene-*b*-polybutadiene- *b*-polystyrene
PS	polystyrene
PB	polybutadiene

Chapter 1 : Introduction

1.1 Background

Polyolefins (POs), especially polyethene (PE) and polypropene (PP), are by far the largest volume synthetic polymers in the plastic industry, with annual global production exceeding 1.4×10^8 metric tons and projected to increase to 200 million tons by the year 2020 according to the 2007 National Petrochemical and Refiners Association Report.[1-3] Despite society's steadfast dependence on these synthetic materials and over 50 years of academic and industrial research in the area of olefin polymerization, we have yet to completely elucidate the structural, compositional, and architectural intricacies surrounding polyolefin.[4] This information is crucial to the development of novel polyolefin-based materials, as the end-use applications of polymers are dictated by their physical and mechanical properties. These properties are defined by the polymer morphology, which is largely influenced by the composition and architecture of the polymeric material.[5] As such, the precise synthesis of well-defined polymers having specific molecular weight, molecular weight distribution, stereochemistry, tacticity, end-group functionality, comonomer incorporations, and block sequence from a variety of monomers is vital.

Several types of polymerization methods have been explored towards the synthesis of these hydrocarbon-based polymers. However, each method has both advantages and disadvantages, which will be discussed herein to determine the best method for the production of polyolefins having specific properties. These polymerization methods include anionic, cationic, radical, ring opening metathesis, and coordination polymerization.

Living polymerization, first described by Szwarc[6,7], is a method that allows the tailored synthesis of polyolefins through consecutive enchainment of monomer units void of termination. Both the irreversible chain transfer to metal alkyls and β-elimination reactions on the metal polymeryl species are circumvented in a truly living system.[8] Though the term "living" has been used rather laxly since its discovery in 1956, there does exist a set of well-defined criteria that summarize the capabilities a living polymerization catalyst system.[9] These guidelines are as follows[8]:

1. polymerization proceeds to complete monomer conversion, and further monomer addition results in continued chain growth;
2. number average molecular weight (M_n) of the polymer increases linearly as a function of conversion;
3. the number of active centers remain constant throughout the polymerization process;
4. molecular weight can be precisely controlled through manipulation of reaction stoichiometry, related to the degree of polymerization, DP = $[M]_o$ / $[I]_o$, where $[M]_o$ is the initial monomer concentration and $[I]_o$ is the initial initiator concentration;
5. polymers produced display narrow molecular weight distributions, as described by the ratio of the weight average molecular weight to the number average molecular weight, PDI = M_w/M_n = 1.01;
6. block copolymers can be prepared by sequential monomer addition;
7. end-functionalized polymers can be prepared.

Though many systems can meet at least one of the aforementioned guidelines, no one criterion defines a living catalyst system. In contrast, very few polymerization systems whether ionic, radical, or metal-mediated, meet all these rules. Thus, it is usually necessary to meet many of the above listed criteria before declaring a system to be living. In this chapter the various classes of living polymerizations will be discussed. Ergo, living anionic, cationic, radical, ring opening metathesis, and coordination polymerization will be examined briefly.

1.1.2 Anionic Polymerization

In 1910, Ziegler and Schlenk demonstrated that dienes could be polymerized, using sodium metal as an initiator.[10] Almost three decades later, Scott et al. showed that arylmetals could be used for the anionic polymerization of styrene.[10] However, it was not until the late 50's that the mechanism of anionic polymerization was unambiguously demonstrated by Szwarc.[11]

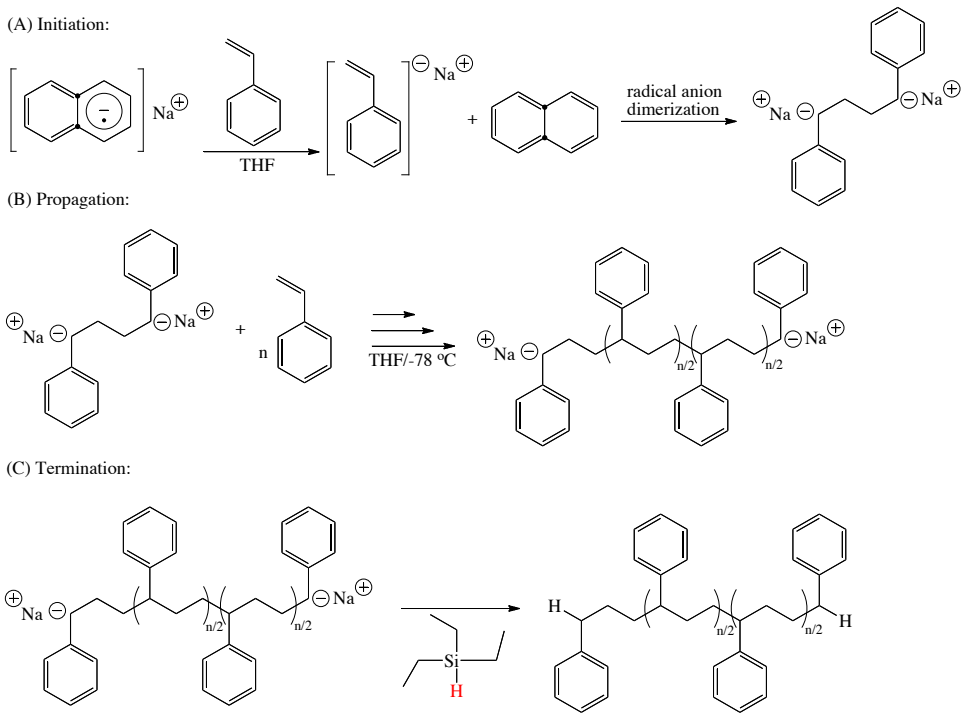

Figure 1.1. Proposed mechanism for synthesis of polystyrene using sodium naphthalenide as an initiator in THF.

In 1956, Szwarc was able to synthesize a polystyrene-*β*-polyisoprene block copolymer via "living" anionic polymerization using sodium naphthalenide as an initaitor.[11] Upon the addition of styrene to the radical napthalenide initiator, styryl radical anions were generated through electron transfer from the sodium naphthalenide radical anion to the styrene monomer (Figure 1.1A). The onset of initiation resulted in a change of the reaction color from green to red. Further addition of styrene monomer lead to a gradual increase in the viscosity of the THF polymeryl solution until all the styrene was consumed to produce polystyrene, Figure 1.1B. The persistence of the red color after complete monomer consumption indicated the presence of intact styryl anionic centers necessary for further chain propagation. This "living" system was subsequently treated with another aliquot of styrene, then an aliquot of isoprene monomer added. This

triggered a further increase in the viscosity of the polymeryl solution, indicating successful extension of the polystyrene chain to include isoprene units. The active chain ends were only terminated after the deliberate addition of triethylsilane to produce the targeted styrene/isoprene block copolymer. Interestingly, polystyrene and polyisoprene homopolymers were absent in the reaction mixture, Figure 1.1C.

Since Szwarc's discovery of "living" anionic polymerization, a variety of monomers have been investigated to determine the scope of this polymerization technique. The living anionic polymerization of styrene is often referred to as the best example of living polymerization[12], meeting all the criteria[9], although a couple drawbacks to this mode of polymerization do exist.[10] Firstly, monomers that are polymerizable are generally limited to those that are void of functional groups. Monomers containing electron-withdrawing groups react with propagating radical anions, in addition to the intiator, resulting in the undesirable termination of propagating species. However, it has been shown that the introduction of protecting groups can allow the polymerization of these more difficult monomers.[10,12-17] This significantly broadens the types of monomers that can be polymerized via anionic means to include hydrocarbon dienes and styrenes, polar vinyl monomers (such as vinyl pyridines), acrylates, vinyl ketones, acrylonitriles, cyclic monomers containing oxirane, lactones, carbonates, and siloxanes, and monomers bearing protected electrophilic functional groups. Secondly, proper selection of the anionic initiator (radical anions, carbanions, and oxyanions) and solvent for each monomer is integral. Solvent selection influences the type and concentration of ions (aggregated ion pairs, contact ion pairs, solvent separated ion pairs, and/or free ion pairs) present in the reaction solution, which impacts the rate of initiation.

The initiation rate is particularly important because if it is not at least comparable to that of the propagating species initiation will not be homogeneous which will likely result in a polyolefin having a broad molecular weight distribution. When initiation is indeed efficient, the reaction kinetics is influenced mainly by the rate of propagation, and can therefore produce polymers having narrow polydispersity indices in the absence of side reactions that cause uncontrolled chain termination, Figure 1.2.[10]

Szwarc's synthesis of block copolymers based on styrene and isoprene via anionic polymerization had tremendous impact on the synthetic rubber industry. In fact, Milkovich, Szwarc's PhD student, facilitated the commercialization of the first anionic polyisoprene material at the Shell Company. Shortly after, a number of commercial styrene block copolymers from anionic polymerization were synthesized and found wide use applicability in the footwear, adhesive and automotive industries. Polystyrene-*b*-polyisoprene-*b*-polystyrene (SIS) and polystyrene-*b*-polybutadiene-*b*-polystyrene (SBS) thermoplastic elastomers for example, were prepared via anionic polymerization using butyllithium as the initiator in nonpolar solvents.[18] Sequential monomer addition provided polymers with rubber-like properties at room temperature due to the ability of the polymer chains to microphase separate into ordered domains, eliminating the need for crosslinking.[10,18] These unsaturated materials and their hydrogenated analogs have since been manufactured under the name *Kraton*®. Anionic polymerization can be utilized to produce other polymeric architectures, such as star type. As a matter of fact, polystyrene-*b*-polybutadiene (PS-PB) block copolymers having star-block and star-tapered architectures are produced by coupling four living PS-PB chains having variable PB

content, resulting in high-impact thermoplastic *Styrolux*® and highly flexible *Styroflex*®, respectively.[19,20]

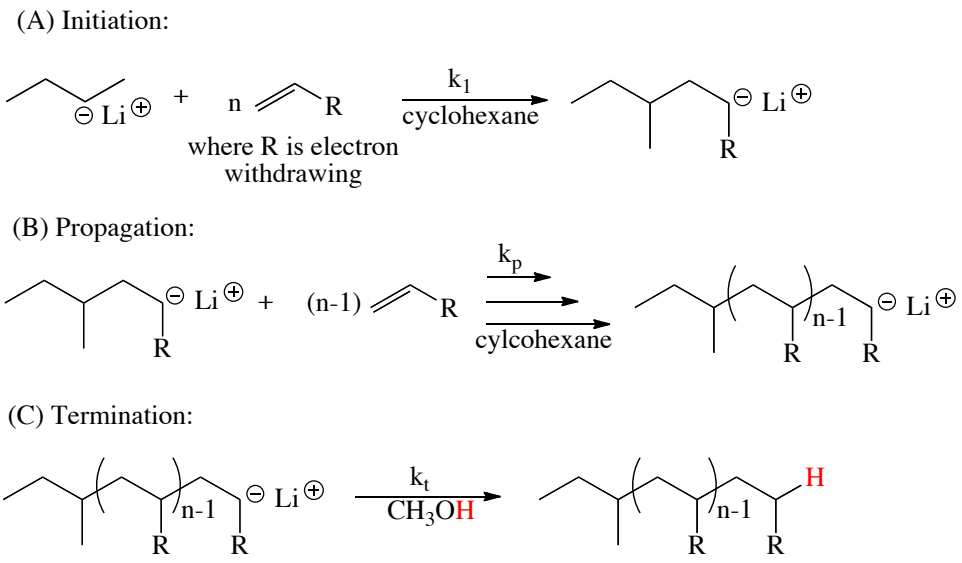

Figure 1.2. General mechanism of anionic polymerization.

Though a number of materials are produced via anionic polymerization on a commercial scale and this methodology is mechanistically well understood and developed, there still remain limitations on anionic polymerization. Some of these limitations are a result of the reaction conditions that are necessary for polymerization.[10] For instance, initiation of anionic polymerizations use sodium or pyrophoric organometals, which require special handling, storage, disposal procedures, and low reaction temperatures that can be costly to implement. Moreover, reactions must be carried out under inert atmosphere (nitrogen or argon) and all reagents (even quenching agent) must be rigorously purified to remove moisture in order to avoid chain termination or electron transfer with oxygen and carboanions.[21] Also, a special high vacuum apparatus equipped with glass cylinders are required for the synthesis of high molecular

weight polymers that require very low initiator concentrations.[22] As mentioned previously, monomers are limited to those that are void of electrophiles unless they can be protected and initiators used must be carefully selected to insure the homogeneity of the resulting polymer. Lastly, ethylene and propene cannot be polymerized via this method. Overall, advantages of anionic polymerization include the controlled synthesis of various polymeric materials (i.e. polystyrene) and access to various architectures (star, comb dendrimer, and multiblock) through chain-end functionalization of polymeric anions.

1.1.3 Cationic Polymerization

Unlike anionic polymerization, "living" cationic polymerization was not even deemed possible until the late 1970s, when long-lived cationic species were observed during the polymerization of styrene derivatives.[23,24] Prior to this discovery, the instability of the propagating cationic species was known to result in uncontrollable side reactions irrespective of the monomer used. However a few years following this discovery, Higashimura et al.[25,26] and Kenndy et al.[27,28] facilitated the growth of this field with their report of the first examples of "living" cationic polymerization of vinyl ethers and isobutene respectively. Since then, the method has expanded to include many functional monomers, such as α-methyl vinylether, α-methyl styrene, functional vinylethers, styrene derivatives, and N-vinylcarbazole.[29-32] In cationic polymerization, monomers are added to the active cationic species and undergo electrophilic addition in the presence of a nucleophilic additive or proton trap that helps to stabilize the propagating cationic species, Scheme 1.1. As such, viable monomers must be nucleophilic, possessing electron-donating groups that can stabilize the resulting

positively charged species. The acid initiator used to activate the polymerization greatly impacts the reaction kinetics and monomer reactivity and therefore must be chosen carefully and specifically for each monomer of interest. The strength of the Lewis acid being used to activate polymerization should be inversely proportional to the reactivity of the monomer. Moreover, the co-initiator (nucleophilic additive or proton trap/scavenger or salt used to stabilize the carbocation, scavenge protogenic impurities, or impede dissociation the ion pairs into free ions respectively) must also be selected wisely, as their presence should not impact the polymerization rates, molecular weights, or polydispersity indices of the resulting polymer.

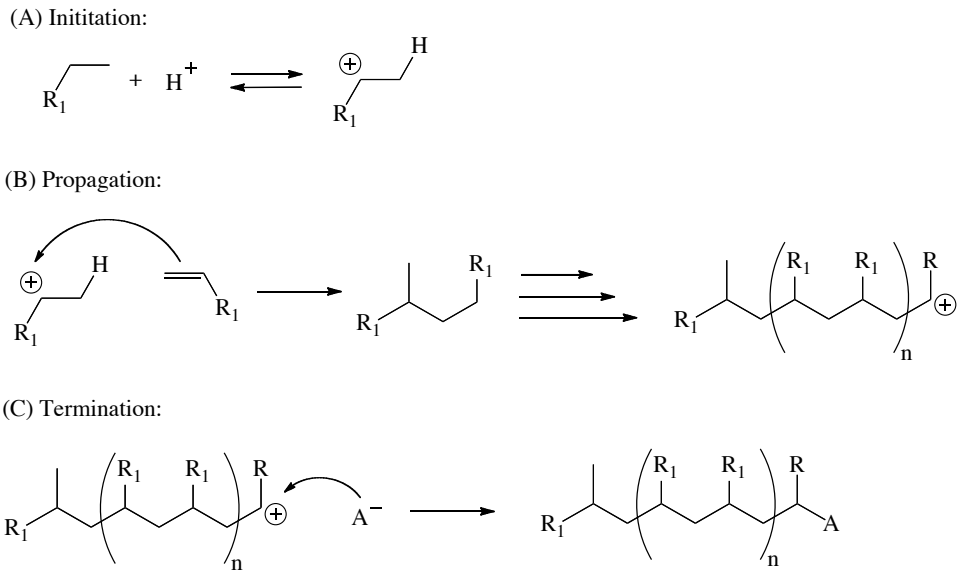

Scheme 1.1. Mechanism for cationic polymerization.

The impact of cationic polymerization of vinyl monomers is far reaching as evidenced by the 2.5 million tons of polymer produced via this method annually.[33] In fact, telechelic polymers based on poly(styrene-*b*-isobutylene-*b*-styrene) block copolymers produced by Kaneka Corporation in Japan (Sibstar) have excellent elastomeric properties. Additionally, these triblock copolymers of styrene and

isobutylene have found use as drug carriers for a coronary stent system and is manufactured under the name *Translute* by Boston Scientific Corporation.[10]

Compared to controlled anionic polymerization, controlled cationic polymerization requires less strenuous experimental conditions. Although rigorous purification of reagents is recommended for best control over polymer properties, this method is more tolerant to moisture so high vacuum requirements can be circumvented in some cases. Furthermore, functional monomers (with electron-donating groups) used for this polymerization are more accessible but there are no universal initiators as in the case of anionic polymerization.[10,32] Lastly, cationic polymerization also gives way to architectures such as multiblock copolymers, telechelic (α,ω-bifunctional and multifunctional polymers that can contain different functional groups at each terminal position.[32]

1.1.4 Radical Polymerization

Radical polymerization is the most commercially utilized method of polymerization, as approximately 50% of the world's synthetic polymers are produced via this method.[10] This is likely because radical polymerization, unlike ionic polymerizations methods, can be carried out on a wide array on monomers (given that radicals are tolerant to functionalities like acidic, hydroxyl, and amino groups). The reactions require only mild conditions (ca. 25 ^{o}C - 100 ^{o}C and ambient pressure), and minimal solvent purification is necessary because reactions are not affected by water and protic impurities and can be carried out in bulk solution, aqueous suspensions, emulsions and dispersions.[34] Moreover, although conventional radical polymerization does not produce "living" polymers due to unavoidable termination events, control over polymer

structure and properties can be acquired through controlled radical polymerization (CRP) processes by manipulating reaction parameters that influence initiation, propagation, and termination kinetics.

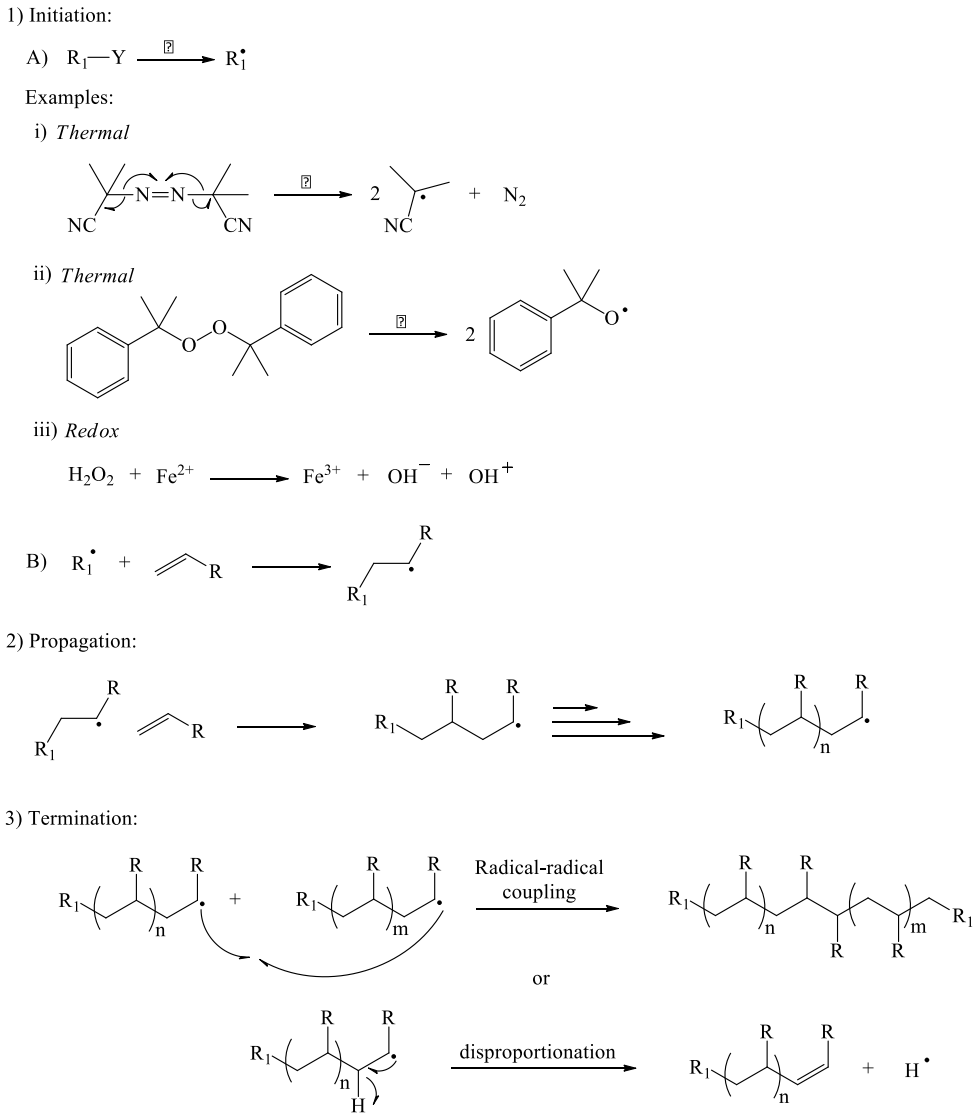

Scheme 1.2. General mechanism for radical polymerization.

The mechanism of radical polymerization involves four separate reaction steps (initiation, propagation, termination and chain transfer), as shown in Scheme 1.2. The

initiation step involves both the generation of active radical species (In*) and the reaction of those free radicals with a monomer of choice, Scheme 1.2A. The former is the rate-determining step. Subsequent addition of monomer units to the actively propagating polymer chain continues until termination takes place via the coupling of two growing radical chains or by disproportionation. While the rate of propagation is not dependent on the chain length of the polymer once the degree of polymerization is ten or greater, the rate of termination is strongly chain length and conversion dependent. Typically, termination by coupling occurs with most monosubstituted radicals and those having minimal steric effects, while termination by disproportionation occurs for substituted radical such as methyl methacrylate. Another reaction that can take place during radical polymerization is that of transfer (to monomer, polymer or transfer agent). Though less likely than termination, transfer can inhibit propagation if re-initiation is not prompt, and can produce branched or crosslinked polymers. The key to traditional radical polymerization is to balance the rates of initiation and termination such that a low and steady concentration of radicals is achieved. However, under these conditions the rate of propagation exceeds the rate of initiation, which results in the continuous production of homopolymer chains, preventing the synthesis of well-defined copolymers with novel compositions, architectures, and functionalities. Additionally, if the reaction proceeds too quickly (at higher temperatures or concentrations of initiator) the molecular weight decreases due to the presence of more radicals in solution.

When the reactivities of monomers are very similar, the synthesis of statistically random copolymers can be easily achieved by radical polymerization. Electrophilic and nucleophilic radicals react easily with electron rich monomers and alkenes with electron

withdrawing substituents, respectively. The homopolymerization of high molecular weight polymers from less reactive monomers (those that don't provide stability through resonance and/or polar and steric effects) such as ethylene and α-olefins is however challenging. Ethylene polymerization in particular requires extremely high temperatures (> 200 ^{o}C) and pressures (>20,000 psi) in order to overcome the slow propagation rate. Though these conditions suppress termination events therefore allowing high molecular weights to be achieved, transfer reactions are more significant resulting in branched polyethylene (LDPE), which has different properties (flexible, solvent resistant, good flow properties, and good impact resistance) than its linear counterpart. Even with a vibrant market for LDPE (6 million tons of LDPE was produced in Europe alone in 2007) polystyrene and polyvinyl chloride remain the largest volume polymers produced by radical polymerization.

Although traditional radical polymerization offers a number of advantages, one significant disadvantage is the lack of "livingness" or control over polymer architectures that results from a fundamental requirement that the rate of initiation and termination be balanced such that there exists a steady state of radicals throughout the polymerization. As discussed in Section 1.1, one criteria of living polymerization is that termination is non-existent, which would require fast initiation and slow termination at the very least. However this condition is difficult to achieve during radical polymerization. As a work around to this problem, several controlled radical polymerization techniques are utilized towards the design of polymers having various architectures, composition, and end-group functionalities. Two main approaches can be taken to harness control during radical polymerization. In the first and most popular approach, the steady state of radicals is

achieved via the trapping of newly generated radicals in a deactivation/ activation process.[35-37] Deactivation can be carried out using a stable radical (nitroxide)[38,39] or organometallic species (cobalt porphyrine)[40,41], while activation occurs thermally, in the presence of light, or with the use of a catalyst that regenerates the growing radical centers.[42,43] Stable free radical polymerization (SFRP) and atom transfer radical polymerization (ATRP) are examples of controlled radical polymerization that use this approach. The second controlled approach utilizes an excess of transfer agent (relative to the radical initiator), which acts as a dormant species that undergoes degenerative transfer with actively growing radical species.[44] Using this technique the propagation process is extended (from about 1 s to approximately 1000 min) thereby allowing good control over molecular weight, polydispersity, and architecture. Reversible addition-fragmentation transfer (RAFT)[45-47] is an example of this methodology.

1.1.5 Ring Opening Metathesis Polymerization

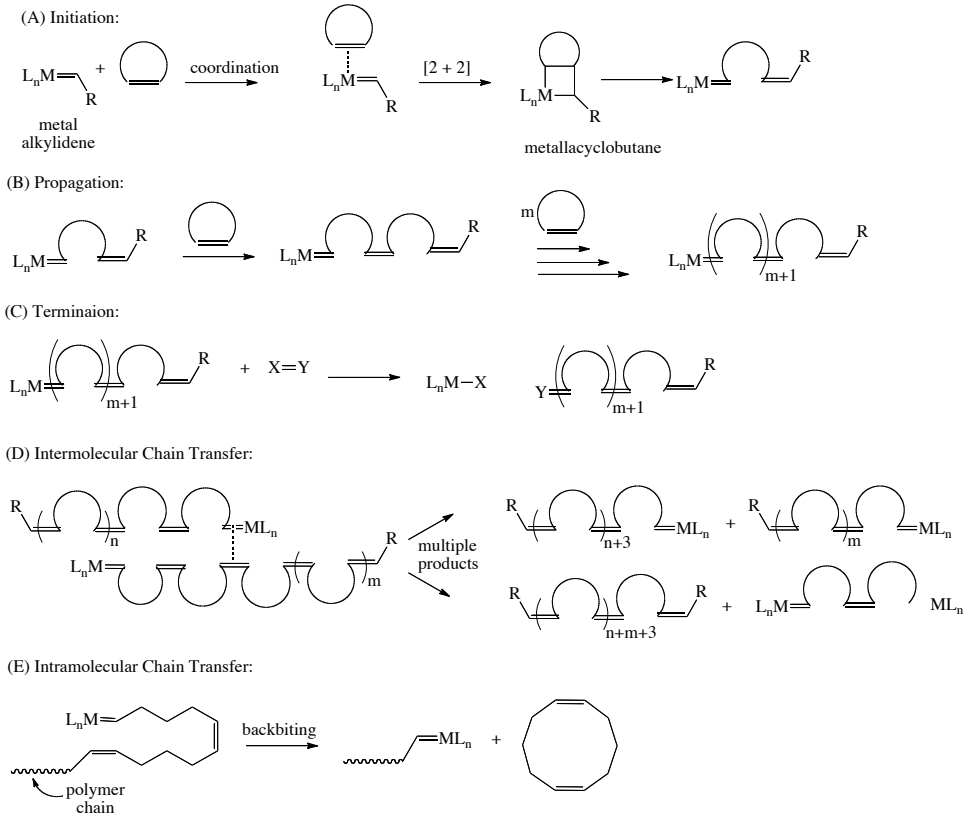

Scheme 1.3. General mechanism for transition metal catalyzed ring opening metathesis polymerization (A-C). Examples of chain transfer side reactions that can occur during ROMP (D-E).

Ring opening metathesis polymerization (ROMP), first discovered in the mid-1950s[48-50], has become a primer method for the synthesis of well-defined polymer materials from a mixture of cyclic olefins.[51-53] This polymerization mechanism involves the carbon-carbon double bond exchange, thus allowing the preservation of double bonds along the polymer backbone. ROMP reactions are initiated using transition-metal alkylidene complexes, which coordinate to cyclic olefins and then undergo [2+2] cycloaddition to generate a strained four-membered metallacyclobutane intermediate that generates the propagating polymer chain, as shown in Scheme 1.3B.[54] The polymer

chain can also propagate from the newly generated metal alkylidene complex, which can be generated from cycloreversion reactions of the strained metalocyclobutane intermediate. The nature of the transition metal and ligands used in the catalyst as well as the reaction conditions serves as the determining factor.[55] Subsequent addition of monomer to the propagating species results in increased polymer chain growth until the reaction is terminated either through spontaneous or deliberate quenching, Scheme 1.3C. Access to new functional groups can therefore be achieved with the selection of an appropriate quenching reagent.[56] ROMP can sometimes fall prey to unwanted side reactions, such as intermolecular and intramolecular chain transfer reactions that can lead to heterogeneity with the polymer sample when reaction conditions, such as monomer concentration and temperature, are not adequately controlled. Intermolecular chain transfer in particular, produces multiple polymer products having various degrees of monomer incorporation per polymer chain. The inconsistency is a result of the reaction of the active alkylidene terminus of a propagating polymer chain reacting with the unsaturated polymer backbone of another polymer chain in the same reaction flask, Scheme 1.3D.[57-59] Intramolecular chain transfer on the other hand, produces cyclic polymers after the active terminus of the alkylidene species reacts with itself, Scheme 1.3E. While these reactions are not preferred in living polymerizations, they do allow access to unique cyclic polymers. It is important to note that ROMP reactions are enthalpically favored due to the release of ring strain associated with the cyclic monomer. Therefore proper monomer selection is imperative in order to maintain balance over entropic penalties. Consequently, cyclic monomers with a reasonable degree of ring strain (>5 cal mol^{-1}), such as norbornene, cyclooctene, cyclobutene and derivatives

thereof are mostly utilized. Moreover, a number of requirements should be met for an effective ROMP: a) the transition metal complex used must rapidly and quantitatively react with the monomer to form a transition metal-polymer chain; b) during propagation, chain transfer or spontaneous termination should not readily occur; c) quenching of the polymerization reaction with a terminating agent must be facile to avoid broad molecular weight distributions; d) the polymerization catalyst should have good solubility in organic solvents and should be stable towards moisture and common organic functional groups. Although there exist no "universal" initiator, transition metal complexes (based on metals such as titanium, tantalum, tungsten, molybdenum, and ruthenium) have allowed the synthesis of unique materials that have found use in automotive, rubber and biomedical fields. For example, ROMP of norbornene and cyclooctene monomers yield elastomeric materials that are marketed under the trade names Norsorex® and Vestenamer®, respectively and utilized in applications that require viscoelastic damping. Monomers having multiple strained olefins can produce crosslinked polymers that are more robust, as in the case of the dicyclopentadiene monomer.[60] Polydicyclopentadiene materials are used extensively in the automotive industry in parts like bumpers and moldings and are available commercially as Metton®, Telene® and Pentam®. The living nature of ROMP has also been exploited for the preparation of functionalized synthetic polymers that can act as drug delivery systems for treatment of illnesses such as lymphatic leukemia and malignant melanomas, as in the case of Nguyen and coworkers.[61]

1.1.6 Coordination Polymerization

The works of Szwarc *et al*[11] had a tremendous role in the advancement of macromolecular chemistry, however enormous progress in the field of transition metal coordination polymerization would not have been as significant without the contributions of Karl Zeigler and Giulio Natta, Chemistry Nobel Prize winners of 1963. In 1953, Ziegler uncovered that triethylaluminum could be used to generate olefin dimers in the presence of nickel.[62-64] This discovery prompted the examination of other transition metals towards the preparation of higher order α-olefins, which ultimately led to the discovery of heterogeneous catalysts for preparation of linear polyethene.[62] Increased catalytic activity was observed when Group IV and V metal halides and aluminum alkyls were utilized.[62] Shortly thereafter, Natta was able produce highly crystalline, high melting isotactic polypropene (where isotactic refers to the uniformed placement of substituents on the same side of the carbon backbone) using methods similar to that of Ziegler.[63] The successful preparation of high molecular weight, stereoselective polypropene was immediately recognized for its practical significance. Given the more robust nature of the isotactic form (white solid), which is in direct contrast with its atactic (where atactic refers to the random placement of substituents along the carbon backbone of the polymer) counterpart, which is a highly viscous liquid. The combined discoveries of Ziegler and Natta resulted in a burst of intense industrial and academic research that focused on the exploration of organometallic materials in the presence of metal alkyls in polymerization systems.[8] Over the years, Ziegler-Natta catalysts have evolved from heterogeneous systems composed of a transitional metal species (generally titanium or

vanadium) and a main group metal alkyl compound, to homogeneous transition metal complexes with greatly improved catalytic activities. In fact, a number of homogenous transition metal catalysts are now available, that are unparalleled in all of polymer chemistry. Some of these catalysts even allow precise control over stereochemistry, structure, composition, molecular weight, and molecular weight distributions.[8] Given these significant improvements, living coordination polymerization catalyzed by homogeneous transition metal complexes is now regarded as the premier method for the controlled synthesis of polyolefins. Living coordination polymerization is initiated using a transition metal catalyst, which is activated by a cocatalyst to generate the active initiator species (cationic transition metal complex and a bulky non-coordinating anion), Scheme 1.4A. Monomers can then coordinate to the open coordination site of the initiator species and then insert into the metal-carbon bond via [2+2] cycloaddition to form the propagating polymer chain, Scheme 1.4B. Subsequent monomer coordination and insertion results in growth of the polymer chain until the reaction is terminated either spontaneously (via chain transfer reactions) or intentionally using a terminating agent such as methanol (see Scheme 1.4C).

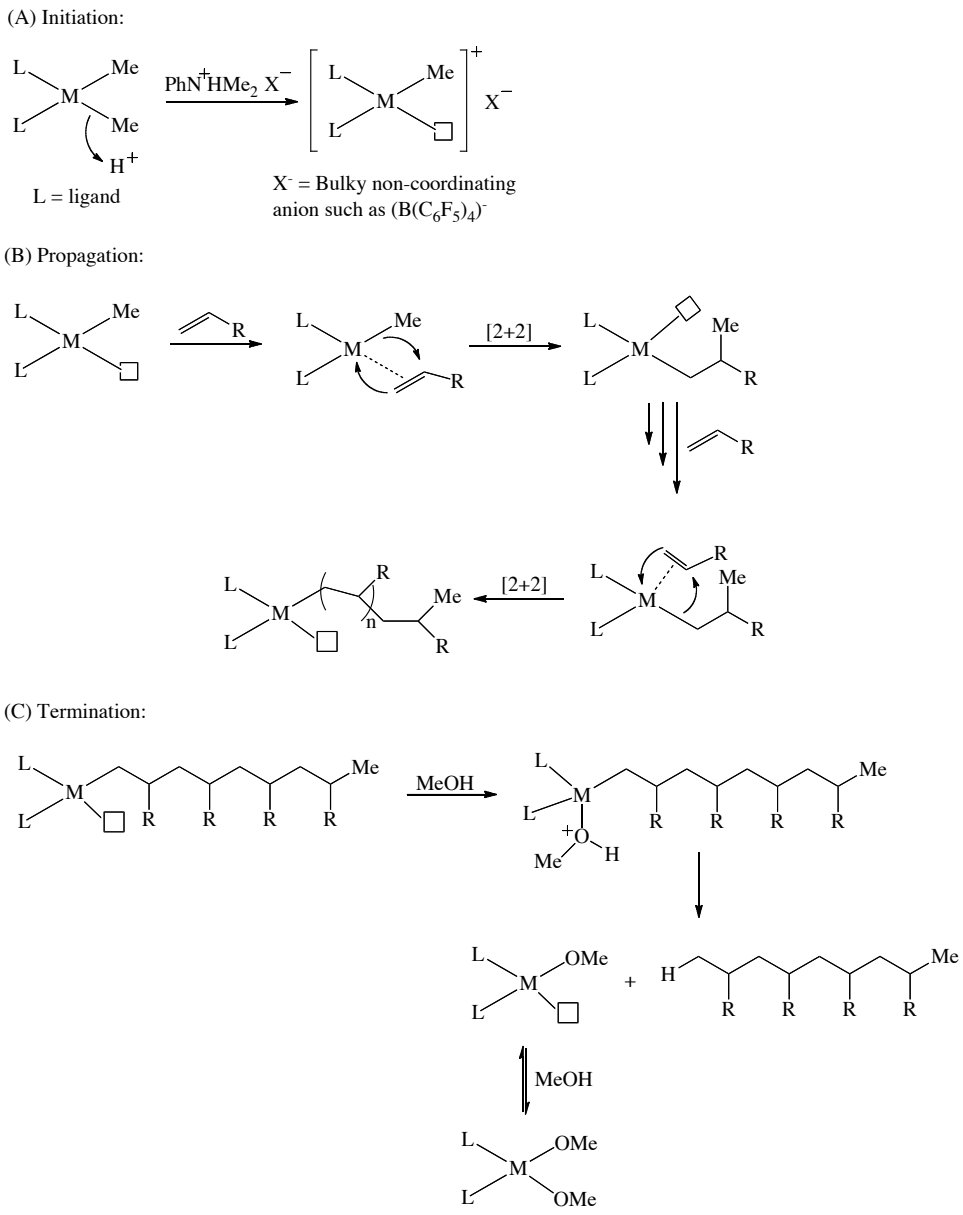

Scheme 1.4. General mechanism for coordination polymerization.

1.1.7 Sita Catalyst System

More than 50 years following the discovery and commercialization of Ziegler-Natta (ZN) catalysts, there still remains a need for new ZN catalysts. This is likely due to the absence of a "universal" catalyst that allows the controlled synthesis of polyolefins with specifically targeted molecular weight, composition, micro- and macromolecular

architecture and stereospecificity. Although many transition-metal-based complexes have found extensive use as catalysts for olefin polymerization, only few are considered living for polyolefin synthesis.[8] Over the past decade, Sita and coworkers have developed several homogeneous (soluble) "single-center" transition-metal-based coordination catalysts that are living in nature, see Figure 1.3 for examples. Upon activation with boron-based cocatalysts (Figure 1.3), these catalysts have shown living behavior for polymerization of propene and higher α-olefins. This was first demonstrated for 1-hexene polymerization at -10 ^{o}C in chlorobenzene solvent, which yielded isotactic poly(1-hexene) ([*mmmm*] > 0.95) with narrow polydispersity indices (M_w/M_n = 1.03-1.13). In fact, the C_1-symmeteric monocyclopentadienyl acetamidinate zirconium dimethyl catalyst (**Precatalyst I** shown in Figure 1.3A) in particular was the first ZN catalyst reported that was both living and highly isospecific for α-olefin polymerization when activated by **Cocatalyst I** (see Figure 1.3B).[65] In attempts to further increase the activity for this class of catalysts, Sita and coworkers strived to minimize the steric interactions at the metal center by replacing the pentamethylcyclopentadienyl (Cp*) moiety with its less bulky counterpart, the cyclopentadienyl (Cp) moiety, which is less sterically demanding because of the absence of the methyl groups on the cyclopentene ring. This resulted in the preparation of a N,N-dicyclohexyl zirconium derivative, **Precatalyst II** of Figure 1.3A. As expected, this derivative was living in nature and displayed higher activity towards α-olefins and more difficult monomers (such as vinylcyclohexane) given the more accessible active site. However, a decrease in enantiofacial selectivity was observed given the C_s-symmetry of the precatalyst.

(A) Sita's Precatalysts:

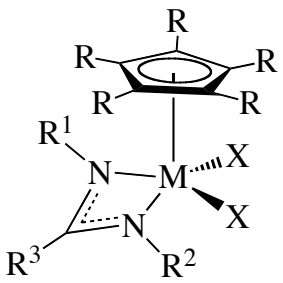

	M	X	R	R^1	R^2	R^3
Precatalyst I	Zr	Me	Me	tBu	Et	Me
Precatalyst II	Zr	Me	H	Cy	Cy	Me
Precatalyst III	Hf	Me	Me	Et	Et	Me

(B) Sita's Cocatalysts:

Cocatalyst I $[PhHNMe_2][B(C_6F_5)_4]$

Cocatalyst II $[PhHNMe_2][B(C_6F_5)_3]$

Figure 1.3. Sita's catalyst system.

Sita *et al*. studied the mechanistic intricacies and scope of monomers that could be produced from their class of group 4 transition-metal complexes.[65-68] By 2007, substantial emphasis had been focused on overcoming the problem of limited polyolefin production from living Ziegler-Natta polymerization. Even with an established method towards the controlled synthesis of polyolefins having exact molecular weights, narrow molecular weight distributions, end-group functionalities, and architecture, the promise of large scale production of polyolefins was in jeopardy. This production limitation is intrinsic to living polymerization in that the criterion requires that the number of catalytically active centers remain constant throughout polymerization thus allowing only one polymer chain to grow per catalytic center. As such, the amount of polyolefin produced would be directly proportional to the amount of catalyst utilized in the polymerization process. Given the cost incurred in the preparation of group 4 transition-metal catalysts, large-scale production would be uneconomical. In light of these facts, Sita and coworkers

aimed to couple coordinative chain-transfer polymerization (CCTP) with living Ziegler-Natta polymerization for the preparation of ethene and higher α-olefins. CCTP utilizes an excess of inexpensive main-group-metal alkyl species, such as ZnR_2 and AlR_3, which act as 'surrogate' chain growth centers that undergo rapid reversible chain-transfer with the active transition metal propagating species. Initial attempts to couple these two methods were investigated using **Precatalyst I**, however low activity was observed in the polymerization of propene under CCTP conditions.[69] These observations were in agreement with computational studies reported by Busico *et al*.[70] which identified the sterically crowded nature of the propagating metal center of **Precatalyst I** as the likely cause of decreased activity. In light of this information, efforts were focused on reducing the steric interactions within the metal ligand sphere. This investigation resulted in the synthesis of a N,N-diethyl hafnium derivative, **Precatalyst III**. Activation of **Precatalyst III** with equimolar amounts of **Cocatalyst I** at -10 °C in chlorobenzene yielded a highly active initiator species that successfully polymerized propene to ultrahigh molecular weights (Mw > 2000 kDa) in a controlled fashion under non-CCTP conditions.[69] ^{13}C stereochemical NMR analysis, differential scanning calorimetry, and X-ray diffraction studies of the resulting polypropene materials generated from **Precatalyst III**, revealed no sign of crystallinity evidencing its atactic stereochemistry. This observation is consistent with the use of a C_s-symmetric catalyst. With a viable homogeneous single-site catalyst in hand (**Precatalyst III**) living CCTP of propene was attempted in toluene at low temperatures (-20 °C to 0 °C) and constant propene pressure (5 psi) using 5 to 200 equiv. diethylzinc. These experiments provided low molecular weight oligomers in practical quantities. For example, in two hours 9.1 mg of transition

metal **Precatalyst III** activated by **Cocatalyst I** can be used to produce 1.6 g of atactic propene (M_n = 3.63 kDa) under CCTP conditions when 20 equiv. of $ZnEt_2$ is used or 4.93 g of atactic propene (M_n = 1.45 kDa) when 200 equiv. of $ZnEt_2$ is used, both of which have narrow polydispersities. These experiments not only marked the first successful coupling of CCTP with living Ziegler-Natta polymerization of α-olefins, but also marked the onset of the pursuit of block copolymers, chain-end functionalized polyolefins, and polymers based on monomers that are typically "difficult" to polymerize, in substantial quantities.

Since the first successful coupling of CCTP with living Ziegler-Natta polymerization (referred to as living coordinative chain-transfer polymerization (LCCTP) throughout this thesis) was demonstrated for the polymerization of polypropene, Sita and coworkers have aimed to determine the scope of this method for the large-scale synthesis of ethene, propene, α-olefins and α,ω-nonconjugated diene-based homopolymers and copolymers based on the cationic hafnium species (**Precatalyst III**).[71]

In route to this goal, a mechanism for LCCTP was proposed, see Scheme 1.5 for illustration. The key to this reaction is that the rate of chain transfer (k_{ct}) of the polymeryl group between the active transition-metal propagating centers and the inactive surrogate main-group-metal species is much faster than the rate of the transition-metal-mediated propagation (k_p). This assures the appearance of uniform chain growth rates for all active (A) and surrogate (S) species, which enables production of polyolefins having narrow molecular weight distributions. Under LCCTP conditions, the number average degree of polymerization (X_n) is defined by $X_n = ([\text{monomer}]_0 - [\text{monomer}]_t) / [A + n \times S]_0$, where x is the initial number of molar equivalents of main-group-metal alkyl

species relative to the transition-metal initiator and n is the number of alkyl groups of the surrogate species that engage in rapid and reversible chain transfer (e.g. n = 2 for $ZnEt_2$). When LCCTP is employed, the overall yield depends on the initial amount of $ZnEt_2$ used, which bypasses the one chain per metal center criterion of traditional Ziegler-Natta polymerization that limits scalability of novel polyolefins.[69,71] Additionally, the polydispersity index (PDI) is defined by $D = M_w/M_n = 1 + k_p/k_{ct}$, where M_w and M_n are the weight-average and number-average molecular weight indices, respectively. In cases where the rate of chain-transfer is indeed much faster the rate of propagation, molecular weight distributions are narrow (PDI's range from 1.04-1.09 when $ZnEt_2$ and **Precatalyst III** are utilized for polymerization).

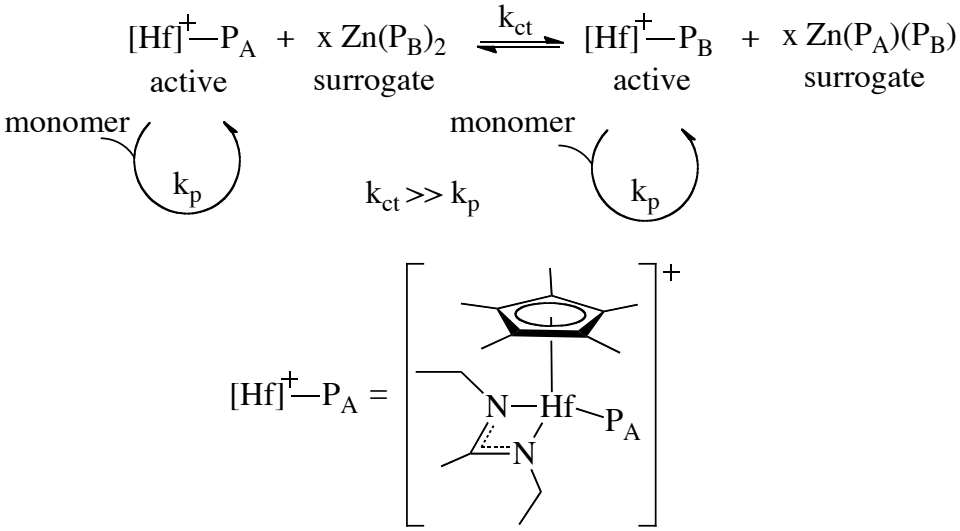

Scheme 1.5. Binary living coordinative chain transfer of α-olefins employing **Precatalsyt III** as the active chain-growth initiator and $ZnEt_2$ as a chain-transfer agent. P_n is a polymeryl group that is produced after multiple α-olefin insertions involving **Precatalyst III**. All other parameters are defined in the main text.

Even with a method to scalable production of polyolefins in hand, the commercial practicality of LCCTP has been a matter of debate, given the cost and safety procedures associated with the use of diethylzinc as a chain-transfer agent. In order to address these

concerns, the use of less expensive and pyrophoric trialkylaluminum species such as triisobutylaluminum (TIBA) was investigated for use as a chain-transfer agent in the polymerization of propene. TIBA was not only successful in the preparation of polypropene, but also afforded access to larger overall yields given that all three alkyl groups can equally engage in rapid reversible chain transfer. It is worth noting however that to achieve more narrow polydispersities, a catalytic amount of diethylzinc had to be utilized. This catalytic amount of $ZnEt_2$ (< 5 mol %) served as a primary surrogate chain-growth species and as a chain-transfer mediator (CTM) as shown in Scheme 1.6. This extension of LCCTP was coined ternary LCCTP.[72] The key to the synergistic ternary exchange between the three different metal species, is that the relative rates and rate constants for polymeryl group exchange amongst all the metals, as well as that for chain-growth propagation at hafnium, must be of the following order: (n_{ct}, k_{ct})[Zn,Hf], (n_{ct}, k_{ct})[Zn,Al] >>> (n_{ct}, k_{ct})[Al,Hf] > (n_p, k_p)[Hf]. When these conditions are met with control of molecular weight and narrow polydispersities maintained, the number average degree of polymerization can be defined by $X_n = ([\text{monomer}]_0 - [\text{monomer}]_t) / [(\text{Hf}) + 2\,x(\text{Zn}) + 3\,y(\text{Al})]_0$ and the polydispersity can be defined by $D = 1 + k_p/k_{ct[obs]}$, where $k_{ct[obs]}$ is the overall apparent rate constant for chain transfer.

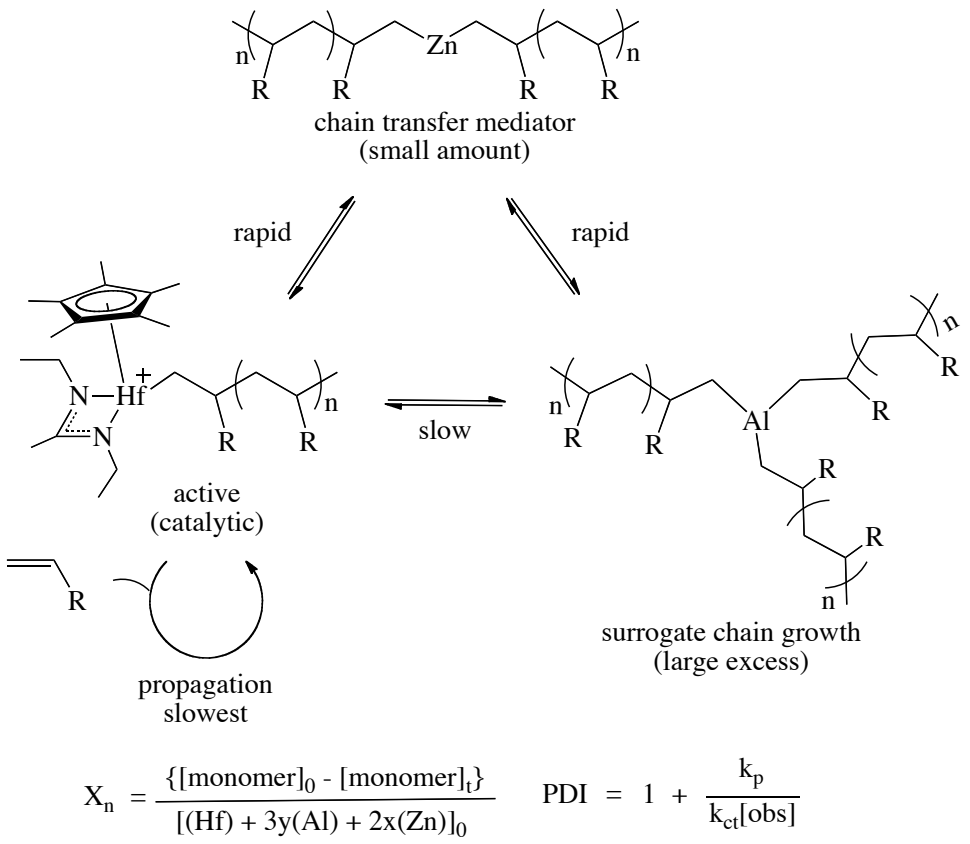

$$X_n = \frac{\{[\text{monomer}]_0 - [\text{monomer}]_t\}}{[(\text{Hf}) + 3y(\text{Al}) + 2x(\text{Zn})]_0} \qquad \text{PDI} = 1 + \frac{k_p}{k_{ct}[\text{obs}]}$$

Scheme 1.6. Ternary living coordinative chain transfer polymerization of α-olefins employing **Precatalyst III** as the active chain-growth initiator, AlR_3 (R = Et, *n*Pr, or *i*Bu) as primary surrogate chain-growth species, and $ZnEt_2$ as both a secondary surrogate and as a chain-transfer mediator (CTM). P_n is a polymeryl group that is produced after multiple a-olefin insertions involving **Precatalyst III**.

Having provided binary and ternary LCCTP as work-around solutions to the 'one-polymer chain-per-metal' limitation that prevents the production of significant amounts precise polyolefin materials, efforts were placed on developing a new methodology that would greatly increase the number of new polyolefins materials that can be synthesized from a single catalyst. This is a significant feat, because there are only a limited number of catalysts available for polyolefin synthesis and each catalyst typically gives only one type/class of polymer with specific material properties. Successful realization of this goal was achieved via an extension of LCCTP to include rapid and reversible polymeryl

chain transfer between two populations of "tight" and "loose" propagating ion pairs. This facile exchange between ion pairs is mediated by a dialkyl zinc species (such as $ZnEt_2$), which also acts as a "surrogate" allowing scalability, according to Scheme 1.6.[73] The differences in the strength of the ion pairing interaction between the cationic transition metal precatalyst (**Precatalyst II** or **Precatalyst III**) and a counteranion, such as $[B(C_6F_5)_4]^-$ and $[MeB(C_6F_5)_3]^-$, generated from activation of the precatalyst with the boron-based **Cocatalyst I** and **Cocatalyst II** respectively, influence the extent of comonomer incorporation in resultant poly(ethene-*co*-1-hexene) and poly (ethene-*co*-cyclopentene) materials.[73] When the active catalyst species is prepared using **Cocatalyst I** the bulkiness of the $[B(C_6F_5)_4]^-$ counteranion prevents tight binding to the cationic transition metal species, which results in a electropositive and more sterically accessible coordination site that can accommodate the higher olefin (comonomer) more adequately. This ion pair is therefore referred to as "loose" and provides higher comonomer reactivity. Conversely, when the active transition metal species is generated from **Cocatalyst II**, the less bulky counter anion $[MeB(C_6F_5)_3]^-$ is produced which can coordinate more closely/strongly to the cationic transition metal species. This ion pair is therefore regarded as "tight" and results in lower comonomer incorporation relative to the former. When a mixture of **Cocatalyst I** and **Cocatalyst II** is utilized to activate either **Precatalyst II** or **Precatalyst III** and intermediate interaction between the counteranion and the transition-metal center, which provides comonomer incorporation that is in between that of the "tight" and "loose" ion pairs. This methodology therefore allows the production of various grades of polyethene-based materials from one precatalyst activated with various ratios of two cocatalysts under otherwise identical conditions. In

particular, reversible chain transfer between the tight ion pair, formed using the borane cocatalyst, and the loose ion pair, formed using borate cocatlayst, provided ethylene copolymers having levels of 1-hexene incorporation ranging from 7-74%. Matrix Assisted Laser Ionization/Desportion Time-of-Flight Mass Spectroscopy of copolymers based on ethene and cyclopentene produced via the method to verify this methodology. This will be discussed in Chapter 5 of this thesis.

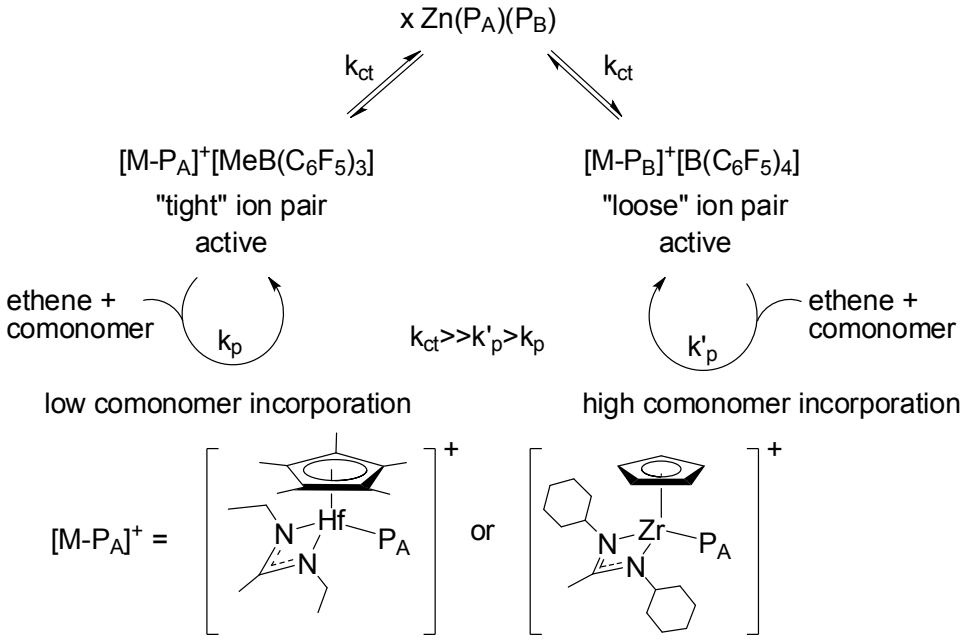

Scheme 1.7. Proposed mechanism of living coordinative chain-transfer copolymerization between tight and loose ion pairs for modulating the comonomer relative reactivities of ethene and 1-hexene or cyclopentene. P_A and P_B are polymeryl groups of chain length A and B, respectively.

With the demand for polyolefins projected to increase steadily over the next decade, this thesis aims to utilize the methodologies discussed above towards the design and precise synthesis of novel hydrocarbon-based plastics and elastomers that do not require plasticizers or other chemical additives to achieve desired physical properties. Living coordination polymerization (LCP), is a technique that produces polyolefins with

well-defined polymer architectures, tunable molecular weights and narrow polydispersities. Binary and ternary living coordination chain-transfer polymerization (LCCTP), allow for the cost-effective large-scale synthesis of polyolefins while maintaining control over molecular weight and structure. Reversible chain transfer between "tight" and "loose" ion pairs enables modulation of comonomer incorporation using a single precatalyst. Together these three concepts will be used to produce new classes of polyolefins having a potentially endless array of end-use properties.

The copolymerization of ethene and propene with longer chain α-olefins and sterically hindered monomers, such as β-citronellene and norbornene was investigated to produce a range of polyolefins having variable architectures. The monoterpene β-citronellene is a non-conjugated diene available from renewable biomass-derived feedstocks. This co-monomer is ideal because when incorporated through Ziegler-Natta enchainment of the terminal vinyl group, there still remains an internal double bond available for chemical modification or cross-linking. Norbornene is a cyclic olefin that is also of interest because copolymerization with ethene gives way to highly transparent materials that are possible polycarbonate replacements. The microphase separation of rod-coil block copolymers is also being investigated as another means of expanding the range of available polyolefin materials. Block copolymers of 1-hexene or 1-octene, which serve as the coil component with 1,5-hexadiene, are being used as model systems for this study. The phase morphologies of these polymeric materials are studied by phase sensitive tapping mode atomic force microscopy (ps-TM-AFM) and will be coupled with tensile strength data and dynamic mechanical analysis data to establish a relationship between specific morphologies and physical properties. This would then allow the

design of materials having some targeted material properties from a simple subset of monomers.

In order to improve the interaction between polyolefins and other materials, copolymers based on ethene, propene, and α-olefins are being functionalized from the zinc polymeryl species with iodine and oxygen gas to achieve iodide and hydroxyl terminated materials, respectively. Iodide-terminated polyolefin materials underwent further reactions to convert them to methylhydroxyl, carboxyl, and phosphonium terminated polymers, thus increasing their potential applicability.

In addition to developing new classes of polyolefin materials through LCP and LCCTP processes, this thesis details the development of new spectroscopic and analytical tools that can be used to quantify compositions and structures on polyolefin materials. Molecular weight and compositional information was attained for low molecular weight polyolefins using matrix-assisted laser desorption/ionization time-of-flight mass spectroscopy (MALDI-TOF MS), by exploiting the ability to produce end-terminated phosphonium polyolefins. Random copolymers of ethene with cyclopentene were synthesized via LCCTP for the first time and used to demonstrate the value of reversible chain transfer between "tight" and "loose" ion pairs for the modulation of comonomer incorporation, and MALDI-TOF MS provided in depth structural analysis of these materials. MALDI-TOF MS was also used to analyze other narrow molecular weight distribution ethene, propene, and α-olefin copolymers having various architectures that could be useful as standards given knowledge of their exact molecular weight.

To promote the use of polyolefins as a reasonable substitute to more harmful plastics for use in everyday products, LCP, LCCTP and reversible chain transfer between

ion pairs were exploited in the copolymerization of ethene and/or propene with α- olefins and sterically encumbered monomers. Microphase separation of rod-coil block copolymers is also being investigated as a means of creating a greater array of polyolefin materials having specifically targeted physical properties through simple changes in the materials' microstructure. Polyolefin copolymers were terminally functionalized to produce novel materials that can better react with other materials acting as macroinitiators for other synthetic processes. Structural analysis of phosphonium terminated polyolefin copolymers was carried out via MALDI-TOF MS revealing exact molecular weight and compositional arrangements of the comonomer within the polyethene backbone demonstrating the utility MALDI-TOF as a powerful tool for polyolefin analysis.

Transition catalyst systems used for living coordination polymerizations are useful for the controlled synthesis of polyolefins. However several limitations exist for the use of these catalysts for the preparation of functionalized polymers. For example, the majority of early transition metal catalysts described to date (including Sita's catalysts) are readily poisoned by heteroatom-containing moieties. This is unfortunate because heteroatoms provide nice handles to further functionalize polymers with other groups that could impact useful properties to the polymers for end-use applications. Sita's catalyst systems, however, promote living polymerization and hence provide a unique opportunity for polymer chain functionalization that would give way to unique or novel polyolefins with improved physical properties. Polymerizations of alkene monomers that are more sterically encumbered than ethene could lead to materials that have interesting properties but these olefins do not always polymerize as readily as ethylene.

1.2 Thesis Overview

In the remainder of the thesis, the polymerization and characterization of precision polyolefins via LCCTP with Sita's catalyst systems will be discussed. Additionally, the polymers discussed herein will focus on broadening the applicability of hydrocarbon polyolefins. In Chapter 2, new synthetic strategies will be utilized to generate value-added materials through the introduction of functional groups that can allow access to improved material properties either directly or via subsequent reactions. The use of sterically encumbered cyclic olefins and non-conjugated towards the synthesis of novel copolymers will be discussed in Chapter 3. The phase behavior of olefin-based rod-coil block copolymers will be examined in Chapter 4. Lastly, Chapter 5 will address the characterization of polyolefins by matrix-assisted laser desorption/ionization time-of-flight mass spectrometry.

Chapter 2 : End-Group Functionalization of Polyolefins

2.1 Background

Polyolefins are a very important class of materials given their excellent combination of chemical and physical properties; low cost, ease of proccessability and recyclability contribute significantly to their commercial interest. Polyolefins currently remain the most largely produced thermoplastics in the world, having applicability in consumer goods such as garbage bags, food packaging products, and structural plastics such as hoses, carpets and automobile bumpers. However despite their importance, polyolefins still suffer physical shortcomings that limit the expansion of their applicability to areas monopolized by more costly and less environmentally friendly polymeric materials (i.e. polyvinylchloride (PVC), polyethylene terephthalate (PETE), and polycarbonate (PC)). These shortcomings can be attributed to two key issues. The first disadvantage is the absence of control over key structural components such as molecular weight, molecular weight distributions, and architecture. The second issue is the lack of polarity, which limits their adhesion, paintability and compatibility with other polyolefins and polymeric materials and surfaces; the absence of chemical functionalities along the polymer chain and the inherently low surface energy of polyolefins cause this phenomenon. In order to overcome these difficulties, new strategies for the incorporation of value-added moieties within the well-defined polyolefin motif must be introduced, as the resulting functionalized materials would potentially allow access to new architectures and desirable material properties.[74-76] Examples of commercial polymers that have desirable properties are the Amplify EA functional polymers (from ethylene-ethyl acrylate (EEA) copolymers), made by The Dow Chemical Company. These products

possess excellent pigment retention and feature functional adhesion to various substrates such as metals, polyolefins, cellulose, polyester, polycarbonate, polyvinylidene chloride (PVDC), and glass. These properties are therefore ideal for applications such as flexible tubing, lamination film, and thin layer adhesives.[77]

Three approaches are commonly employed to functionalize polyolefins: (i) direct copolymerization with polar monomers[74,78-81]; (ii) post-polymerization modification[82-86] and (iii) copolymerization with reactive comonomers that can be selectively and effectively interconverted to functional groups[87-89] as shown in Scheme 2.1.[76] Ideally, direct copolymerization would be the most straightforward mode of functionalization, as it would only require a single step to produce the value-added polymers. However, issues of functional group tolerance and catalyst poisoning caused by the complexation of the transition metal species with lone pairs of the functional monomers plague this method, especially when early transition metal catalysts are employed thus making this strategy commercially inferior. Although the use of protecting groups and/or less-oxophilic catalysts that are more stable to heteroatoms have been investigated to remedy this problem there still remain limitations to these solutions. More specifically, the protection and deprotection processes are not only expensive and yield polymers that have decreased solubility, but they also produce byproducts that are of environmental concern. Late transition metals work better with substrates with coordinating moieties but these catalysts do not allow the same degree of architectural control resulting in the production of branched polymers having minimal crystallinity.[74]

The aforementioned issues with the incorporation of coordinating moieties into polymers, using transition metals have been solved in a roundabout way via post-polymerization modification. However because polyolefins are mainly made up of hydrocarbons, the functionalization of these materials using mild methods is not trivial and remains a longstanding scientific challenge. A popular strategy to functionalize polyolefins is to use monomers that contain "latent" groups that are tolerated by the transition metal catalysts and which could be readily transformed into other functionalities after polymerization. A classic example is the polymerization of dienes to afford polyolefins that contain terminal alkene units. Subsequent transformation of the alkene unit via a myriad of methods such as hydration, dihydroxylation, oxidative cleavage, etc. could then afford a heteroatom-terminated polymer, which would otherwise be difficult to access via a direct polymerization method. These heteroatom-terminated polyolefins could potentially be transformed into other value-added polyolefin products. In this chapter, the use of living coordinative chain-transfer polymerization (LCCTP) as a practical route towards the scalable synthesis of bulk quantities of well-defined end-group functionalized precision polyolefins will be discussed.

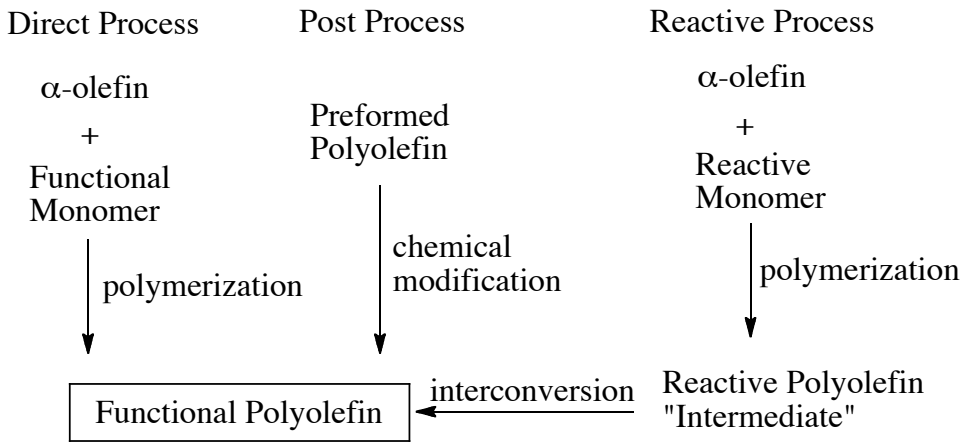

Scheme 2.1. Different strategies to make functionalized polyolefins. Reproduced from T.C Chung. [76]

In order to endow polyolefins with desirable properties, such as adhesion to various surfaces, living coordination polymerization in tandem with chain transfer (LCCTP) has been used to make functionalized polymers, *vide infra*. As described in Chapter 1, LCCTP unlike other polymerization strategies gives access to a potentially endless variety of polyolefin-based materials having well-defined polymer structures in a scalable fashion.

The approach to prepare functionalized polyolefins via living coordinative chain transfer polymerization exploited in this study utilized the carbon-metal moiety of the actively propagating polymeryl species. In this process the metal could be zirconium, hafnium, zinc or aluminum. The carbon-metal moiety, being nucleophilic, could then react with an electrophile. These metallated polymers are stable enough to allow for the storage of bulk quantities of the active polymer species in toluene at low temperature for weeks at a time, after the removal of olefin monomers in *vacuo*. This stability of the metallated polymer is a tremendous advantage because it allows for facile subsequent reactions to be carried out on the polymer without the need for special handling or

procedure, as shown in Scheme 2.2. In subsequent sections, the details of these transformations will be discussed.

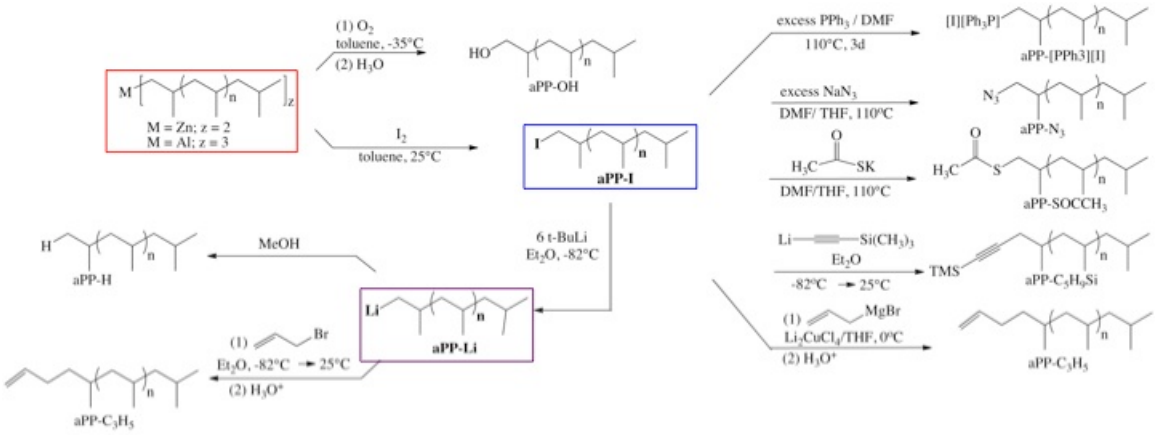

Scheme 2.2. Transformation of metallated-polymer into various functionalities.

2.2 Iodo-terminated polyolefins

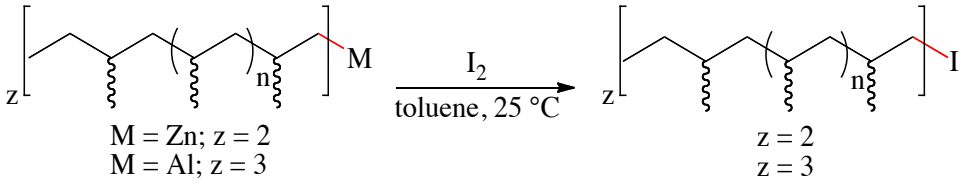

Scheme 2.3. Reaction of metal-carbon bond of the polymeryl species to yield iodo-terminated polypropene.

Electrophilic addition of iodine to the metal-carbon bond was first targeted to generate iodide-terminated polyolefins. The functionalization of polymers with halogens (especially with iodides), which are excellent leaving groups, allows for further functionalization of the polymers via the nucleophilic displacement of the halides. This can generate other value-added moieties at the polymer terminus. The nucleophilic displacement of halogens is not the only strategy that could be used to convert the halogenated polymer into other products. For example, the reaction of the iodo-

terminated polymer with radical generators would yield polymers bearing radical centers, which would then react with other radicals to give other value-added functionalities. It must be pointed out that control over radical reactions, especially when the generated radical is of a primary nature, is non-trivial and mixtures of products could be obtained. Therefore efforts were concentrated on reactions that utilized the cleaner nucleophilic displacement of the iodide functionality. Iodo-terminated precision polyolefins have been prepared in the Sita group[90] by titration of a stock solution of either Zn(polymeryl)$_2$ or Al(polymeryl)$_3$ with a solution of I_2 in toluene until a slight, persistent pink color is obtained. To isolate the product from the residual iodine and metal the following procedures have been followed: a) Firstly, the reaction mixture is rinsed with aqueous NaOH solution (1 M) three times (using a separatory funnel); b) additional acidic rinses (10% aqueous HCl, three times) is then performed and c) the product is rinsed with deionized water (also three times). After the rinses, titration of the toluene-polymer solution with basic methanol usually results in the precipitation of the final polymer product. Near quantitative conversion of the corresponding 1-iodo polyolefin materials has been obtained by several workers in the group. Figure 2.1 presents the ^{1}H NMR for 1-iodo-polyethylene and 2-methyl-ω-iodo-PE which were prepared by binary LCCTP using Zn(Et)$_2$ and Zn(^{i}Pr)$_2$as the respective main group metal alkyl surrogates. As can be seen in the proton NMR (courtesy of Jia Wei), the use of $ZnEt_2$ gave a polymer that has a CH_3 group at the chain end (evidenced by a resonance at 0.9 with a triplet multiplicity, see Figure 2.1A) whereas Zn^iPr_2 gave a polymer bearing an isopropyl group (the proton NMR showed characteristic isopropyl doublet and septet peaks, see Figure 2.1B).

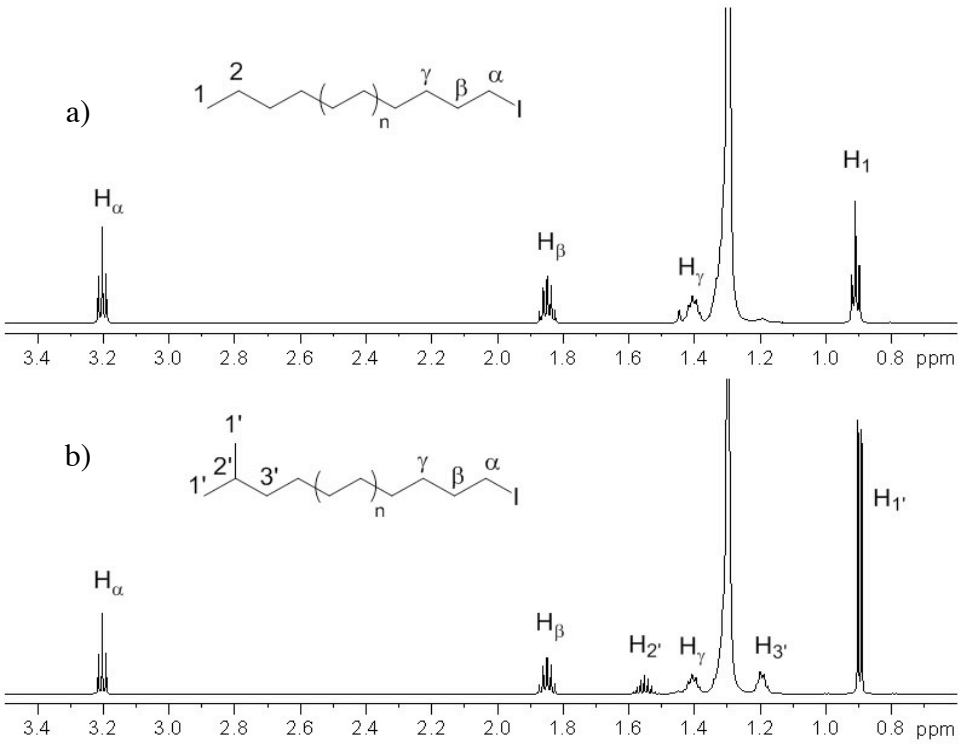

Figure 2.1. Differential chain-end modification via the use of different reagents. $Zn(Et)_2$ gives a primary terminal (A) and $Zn(^iPr)_2$ gives a tertiary end (B). ^1H NMR (600 MHz, 1,1,2,2-$C_2D_2Cl_4$, 90 °C. Polymers were synthesized by Jia Wei.

The successful introduction of an iodide group into the linear polymer chain was confirmed by the ^1H NMR spectra of 1-iodo-polyethylene (PE-*t*-I) and 2-methyl-ω-iodo-PE (*i*Pr-PE-*t*-I), which both showed a triplet at 3.20 ppm corresponding to the methylene group adjacent to the iodine atom. Based on the NMR resonance integrations, it was adjudged that the end-group functionalization process (i.e. iodination) was quantitative. The ratio of the integrations of a unique multiplet at 1.55 ppm, which corresponds to the tertiary carbon of the ^{i}Pr-PE-*t*-I, and a triplet at 3.2 ppm, which corresponds to the protons that are alpha to the iodide, was 1:2. This ratio augments the assertion that the conversion was quantitative, as it shows that both ends of the PE chain were fully capped with modification groups; one end with isopropyl and the other end with iodide. Overall,

these data revealed the well-defined structures of these precision polyolefin materials for which quantitative end-group functionalization was also confirmed. Also noteworthy was the absence of vinyl end-group resonances, which is consistent with the living character of these polymerizations.

As described in Chapter 1.1, a living polymerization is a process whereby polymerization comes to a halt after all of the monomers are used up but then polymerization can be resumed upon the addition of fresh monomers. Some polymerization methods can be quasi living for a period of time but upon catalyst decomposition or chain termination (such as beta hydride elimination) the system ceases to become living. In this regard, it is plausible to have a polymerization method that is living for monomers that have rapid polymerization kinetics (i.e. polymerization rate >>> catalyst decomposition or chain termination) but non-living for monomers that polymerize slowly. To avoid the stoichiometric use of metal catalyst during polymerization, the transfer of the polymeryl group to a surrogate metal has been used. For a successful living coordinative chain transfer polymerization, the rate of chain transfer between the active catalyst and the surrogate metal has to be faster than the polymerization process in order to achieve a narrow polydispersity. An important distinguishing feature of LCCTP using [Cp*HfMe{N(Et)C(Me)N(Et)}][$B(C_6F_5)_4$] (generated from **Precatalyst III** in combination with one equivalent of **Cocatalyst I**) as the initiator is that the catalyst does not "die" quickly. As a result, it is possible to obtain a broader range of precision polyolefins compared to previous reports of CCTP that have been restricted to the production of only PE and end-group functionalized PE materials.[91-94] For instance, *a*PP was prepared via *binary*-LCCTP of propene, using 200 equivalents

of $ZnEt_2$ (relative to catalyst 1) as the chain transfer mediator. The $Zn(aPP)_2$ solutions were subsequently treated with I_2, yielding 1-iodo-atactic PP materials having an ethyl group at the opposite chain end, as summarized in Scheme 2. 3. As in the case of PE-*t*-I, ^1H and ^{13}C NMR spectra shown in Figures 2.2 and 2.3 indicated near quantitative conversion to the expected 1-iodo *a*PP products.

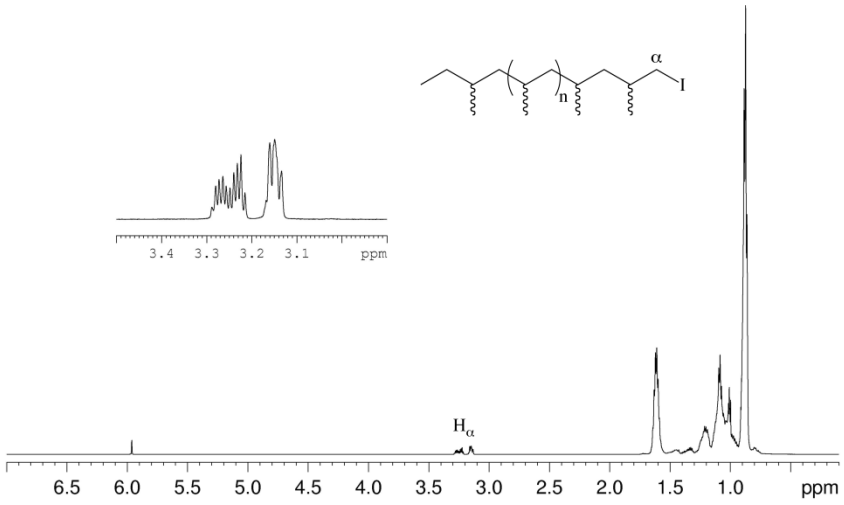

Figure 2.2. ^1H NMR (600 MHz, 1,1,2,2-$C_2D_2Cl_4$, 90 ºC) spectrum and resonance assignments of 1-iodo-*a*PP.

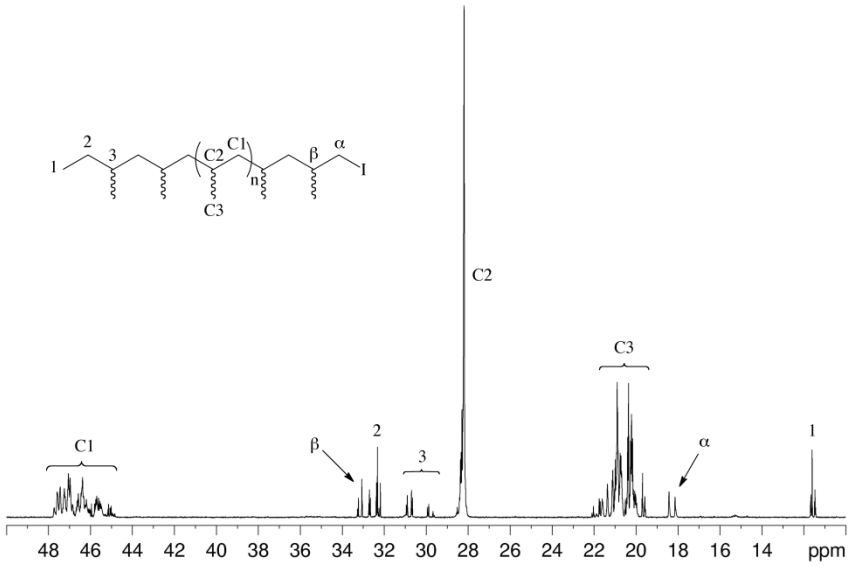

Figure 2.3. ^{13}C NMR (150 MHz, 1,1,2,2-$C_2D_2Cl_4$, 90 ºC) spectra and resonance assignments of 1-iodo-*a*PP.

The tacticity of the prepared 1-iodo-*a*PP was found to be atactic. Atactic stereochemical microstructures for these materials arise from both the C_s-symmetric nature of the propagating species, as well as, due to the rapid and reversible chain-transfer between active and surrogate species. In fact, DSC revealed the absence of any degree of crystallinity that might possibly arise from short runs of stereoregularity, as shown in Figure 2.4.

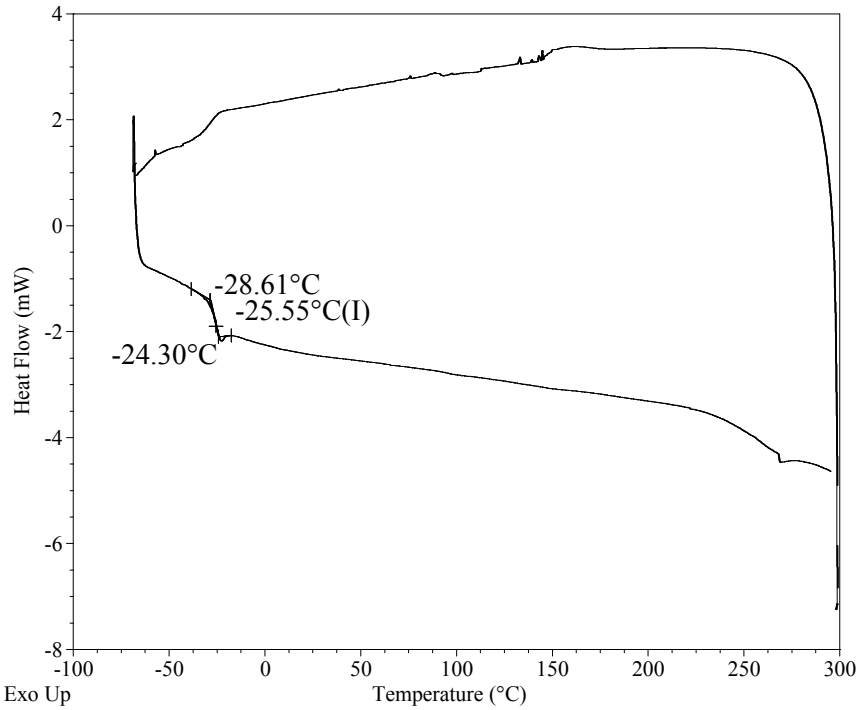

Figure 2.4. Differential scanning calorimetry of atactic iodide terminated polypropene with a glass transition temperature of -25.6 °C.

2.3 Hydroxyl-terminated polypropene

There is great interest in methodologies that allow for the preparation of hydroxyl-terminated polymers. This is because hydroxyl-terminated polymers are versatile intermediates that can be transformed into various functional groups. For example, the hydroxyl group can undergo either one or two electron aerobic alcohol oxidation to generate aldehyde or carboxyl functionalized polyolefins, respectively. The aldehyde group is versatile and can be converted to several functional groups via mild chemistries. For example, amine-functionalized moieties could be added to aldehydes to give an imine, which could then be reduced with a reducing agent, such as sodium cyanoborohydride, to give a permanent linkage, as shown in Scheme 2.4.[95]

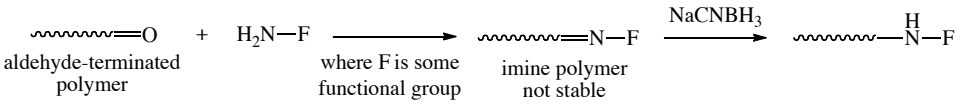

Scheme 2.4. Potential conversion of aldehyde-functionalized polymer to an amino terminated polymer. F is a functional unit that impacts specific properties to the polymer, such as carboxylate to give wetting ability, etc.

Another strategy that could be used to link other functional groups to aldehyde-terminated polymers is nucleophilic additions. For example, the addition of organometallics (e.g. RLi or RMgX) to the aldehyde unit in the polymer[96] allows for the simultaneous introduction of both a hydroxyl and other functional groups to the polymer terminus (see Scheme 2.5). This is especially useful for functionalities that are not compatible with the polymerization conditions and would require a post-functionalization means to affix to the polymer.

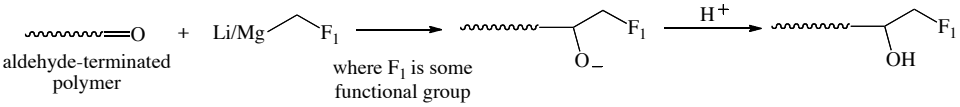

Scheme 2.5. Potential conversion of aldehyde-functionalized polymer using organometallic reagents. F_1 is a functional unit that impacts specific properties to the polymer, such as carboxylate to give wetting ability, etc.

As already mentioned, functionalization of aldehyde-terminated polymers with organometallic reagents will not only lead to the attachment of other functional groups to the polymer but also give rise to a secondary alcohol functionality within the polymer. For hydrocarbons that are hydrophobic and have limited interactions with the environment or other materials, the addition of a hydroxyl group to the polymer might endow the new polymer with an amphiphilic nature and hence increase the interactions that the polymer could make with other materials. Recent advances in transition metal chemistry have now made possible the addition of several aromatic groups bearing

sensitive groups that are incompatible with organolithium or Grignard chemistries to aldehydes via palladium, nickel, rhodium and other transition metal catalysis.[97] For example, various functionalized boronic acids could be added to the aldehyde-terminated polymers using established catalysts and protocols, as summarized in Scheme 2.6.[98]

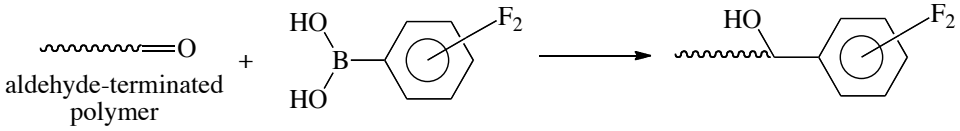

Scheme 2.6. Potential conversion of aldehyde terminated polymer using boronic acids to yield aryl functionalized polymers. F_2 is a functional unit that impacts specific properties to the polymer, such as carboxylate to give wetting ability etc.

Additions of aromatics to aldehyde-terminated polymers would lead to aryl functionalized polymers, with potentially interesting properties. Aromatic groups within polymers could pi-stack with each other and endow the functionalized polymers with new optical properties.

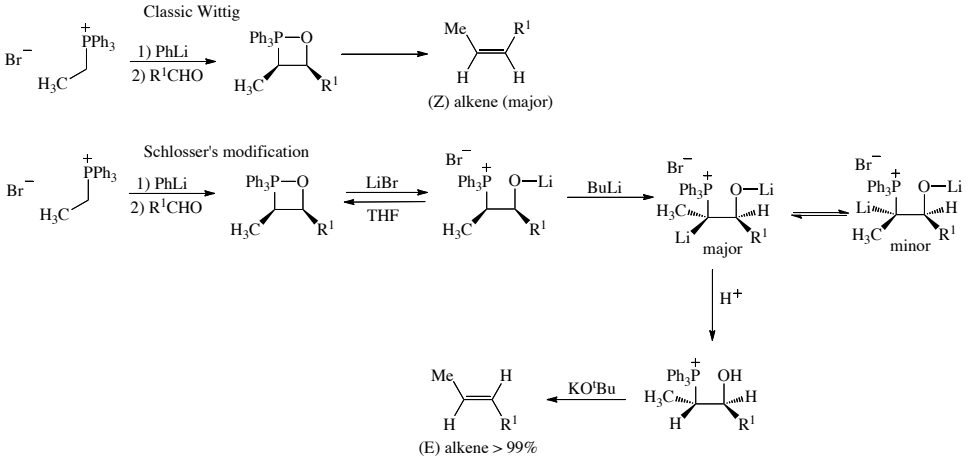

Scheme 2.7. Selective formation of E- or Z-alkenes via classic Wittig (Z-alkene) or Schlosser modification modification[99] (E-alkene) .

Various other strategies to further functionalize aldehyde-containing polymers exist. For example, the Wittig reaction, discovered by George Wittig[100], is an old reaction

for the preparation of a wide variety of alkenes from aldehydes.[101-104] It uses phosphonium ylides (which are readily prepared via the nucleophilic addition of phosphines to alkyl halides, followed by deprotonation by a non-nucleophilic base) and an aldehyde to give alkenes. The Wittig reaction is however not very selective and it is difficult to control the geometry of the alkene formed, although Z-alkenes are predominantly obtained with simple ylides,[101] The Schlosser modification allows for the formation of E-alkenes.[105] (see Scheme 2.7) Other olefination methods utilized by others to incorporate alkene units into molecules include Horner–Wadsworth–Emmons reaction[106-109], Julia–Lythgoe olefination[110,111], Peterson olefination[112-114] and olefination using the Tebbe's reagent[115] (see Scheme 2.8 for brief overviews of these reactions).

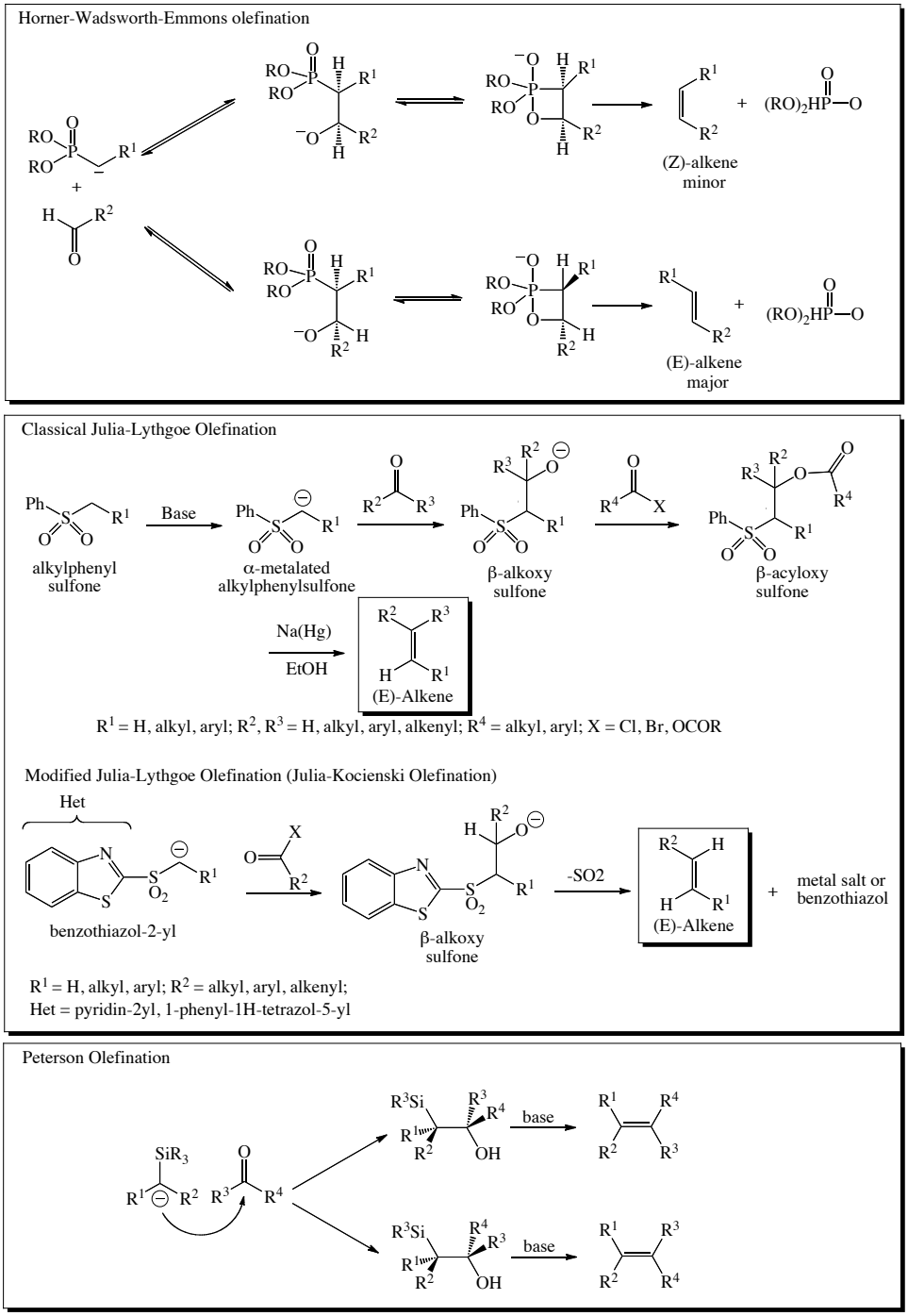

Scheme 2.8. Overview of olefination reactions.

The reagents required for the olefination methods discussed above are commercially available so it is possible to transform aldehyde-terminated polymers into

alkene-terminated polymers (see Scheme 2.9). These alkene-terminated polymers could then be further transformed into other value-added products.

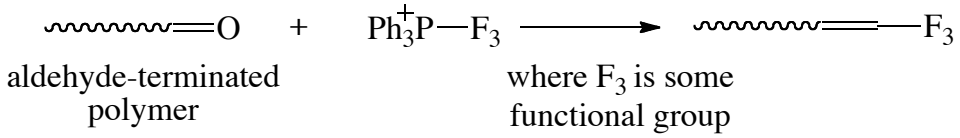

Scheme 2.9. Conversion of aldehyde-terminated polymer into alkene-terminated polymer via a Witting reaction. F_3 is a functional unit that impacts specific properties to the polymer, such as carboxylate to give wetting ability, etc.

There has been a recent surge in the use of copper catalyzed azide-alkyne cycloaddition (CuAAC) reactions to make triazoles from azides and alkynes (discussed more extensively in Section 2.7). Consequently, the conversion of aldehyde-terminated polymers into alkyne-terminated polymers (via the addition of diazophosphonates to aldehydes, Seyferth-Gilbert Homologation[116]) provides an alkyne handle to "click" together several interesting moieties to the polymer, as shown in Scheme 2.10.

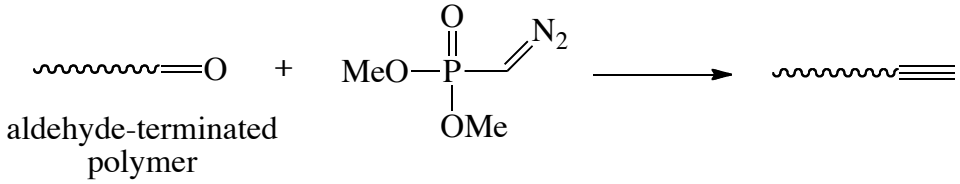

Scheme 2.10. Synthesis of alkyne-terminated polymer from the aldehyde.

Both alkene and alkyne polymers are also versatile and could be further functionalized. In the case of an alkene-terminated polymer, the polymer could yet still be used in other polymerization reactions.

Another versatile reaction of aldehydes that could be used to functionalize aldehyde-terminated polymers is to use hydrazines and alkoxy amines to form hydrazones and oximes.[117,118] The X-N=C (where X = O or N) moieties are more stable

than imines and do not require a reductive step to make the functionalization permanent, although the addition of sodium cyanoborohydride to these hydrazones and oximes could impart more stability to these functionalized polymers as shown in Scheme 2.11.

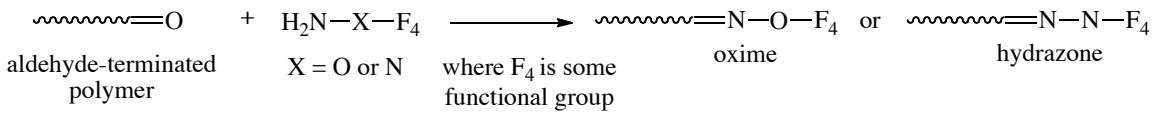

Scheme 2.11. Synthesis of oxime and hydrazone from aldehyde terminated polymer. F_4 is a functional unit that impacts specific properties to the polymer, such as carboxylate to give wetting ability, etc.

The aforementioned discussions about the potential uses of aldehyde-functionalized polymers, which are obtained from hydroxyl-terminated polymers via oxidation, places importance on methodologies that allow for the synthesis of hydroxyl-terminated polymers. Hydroxyl functionalized precision polyolefins are also of significant interest due to their ability to act as macroinitiators for anionic and controlled free radical polymerizations to produce amphiphilic block copolymers. For example, previous work by Kim *et al*. described the formation of poly(ethylene-*b*-ε-caprolactone) from hydroxyl functionalized PE by ring opening anionic polymerization of ε-caprolactone catalyzed by stannous octoate.[92] Amphiphilic block copolymers often find application in important materials given their ability to improve interfacial interactions in blends by acting as compatibilizers resulting in increased adhesion. The functional polymer segments provide good adhesion to polar surfaces, while the polyolefin block interpenetrates the more robust pure olefin domains.[119]

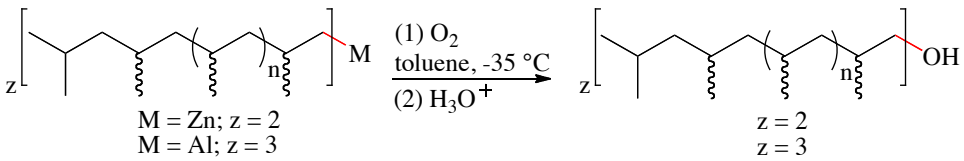

Scheme 2.12. Hydroxyl functionalization of metallated polymeryl species.

Table 2.1. Synthesis of 1-hydroxy-*a*PP.

Entry	t_p [h]	Yield [g]	Mn [kDa]	D	T_g (°C)	$T_{thermal}$ (°C)	$T_{oxidative}$ (°C)
t-LCCTP							
1	20.5	6.2	2.43	1.06	-23.4	441.8	403.0
2	38.0	13.9	4.60	1.04	-12.9	452.1	425.6
3	36.0	17.7	6.79	1.04	-11.3	454.2	423.5

Conditions: All reactions were carried out in toluene with 1 equiv. $ZnEt_2$ and 100 equiv. $Al(^iBu)_3$ at 0 °C.

Hydroxyl terminated precision polyolefins were therefore prepared through oxygen insertion into the corresponding $Al(aPP)_3$ reagents at -35 °C over 3 h using dioxygen followed by quenching with a hydrogen source (MeOH) and isolation by standard procedures (Scheme 2.12). The desired 1-hydroxy-aPP product was generated cleanly in excellent conversion. ^1H and ^{13}C NMR data indicated the formation of the hydroxyl group. New peaks centered around 3.4 and 3.5 ppm in the ^1H NMR (see Figure 2.5) of the 1-hydroxy-*a*PP spectrum are attributed to the diastereotopic hydrogens *alpha* to the hydroxyl group. In the ^{13}C NMR, weak resonances around 69 ppm are attributed to the carbon bearing the hydroxyl group (Figure 2.6). It is also worth mentioning that this synthetic transformation can be finicky with both $Al(aPP)_3$ and $Zn(aPP)_2$ reagents. For the $Al(aPP)_3$ reagent, when the dioxygen was added at temperatures higher than -25 °C, hydroperoxide and peroxide products were also obtained. For the corresponding $Zn(aPP)_2$ reagents, even adding the oxygen at temperatures below -25 °C still afforded 1-

hydroxy-*a*PP that was contaminated with hydroperoxide and peroxide side products that required additional chemical transformations to remove.

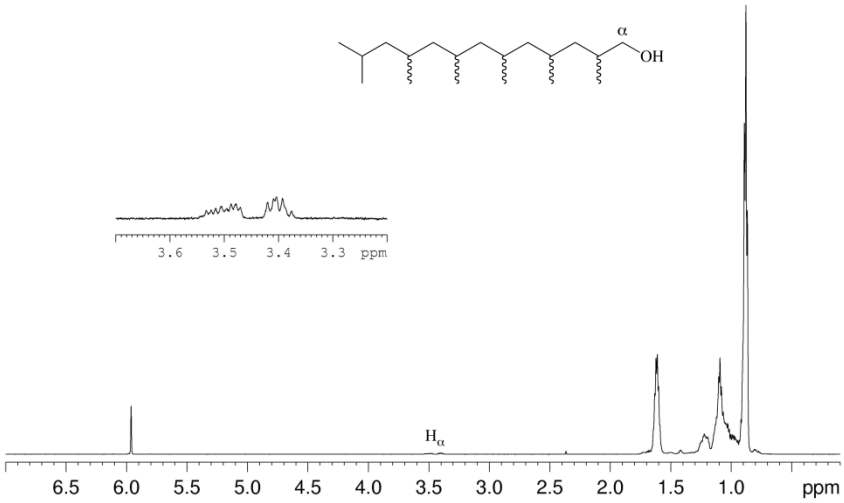

Figure 2.5. ^{1}H NMR of hydroxyl-terminated. Insert is an enlarged region showing the alpha protons next to the hydroxyl functionality.

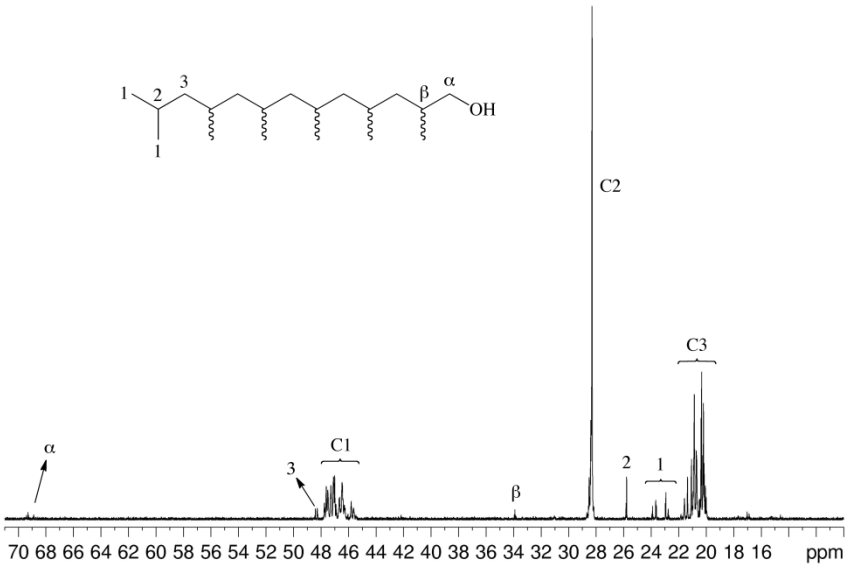

Figure 2.6. ^{13}C NMR hydroxyl-terminated *a*PP showing weak peaks around 69 ppm, indicative of carbon bearing hydroxyl group.

The amorphous nature of the resulting *a*PP-*t*-OH materials were evidenced by DSC (see Figure 2.7), which revealed glass transition temperatures ranging from -11 °C to -23°C based on second cycle data of samples heated and cooled at 10 °C/min as shown in Table 1. Degradation data for these hydroxyl functionalized materials were observed to be uniform in nature, having virtually 100% maximum mass loss between 403 °C to 454 °C; the data was consistent under both thermal and oxidative conditions with N_2 and dioxygen as the flow gas, respectively. This degradation data is of importance given that the substitution of metals with polymers is becoming increasing popular in the automotive, aerospace and computer industries due to significant weight and cost advantages.[120] The viability of these substitutions are dependent upon the degradation of the polymers.

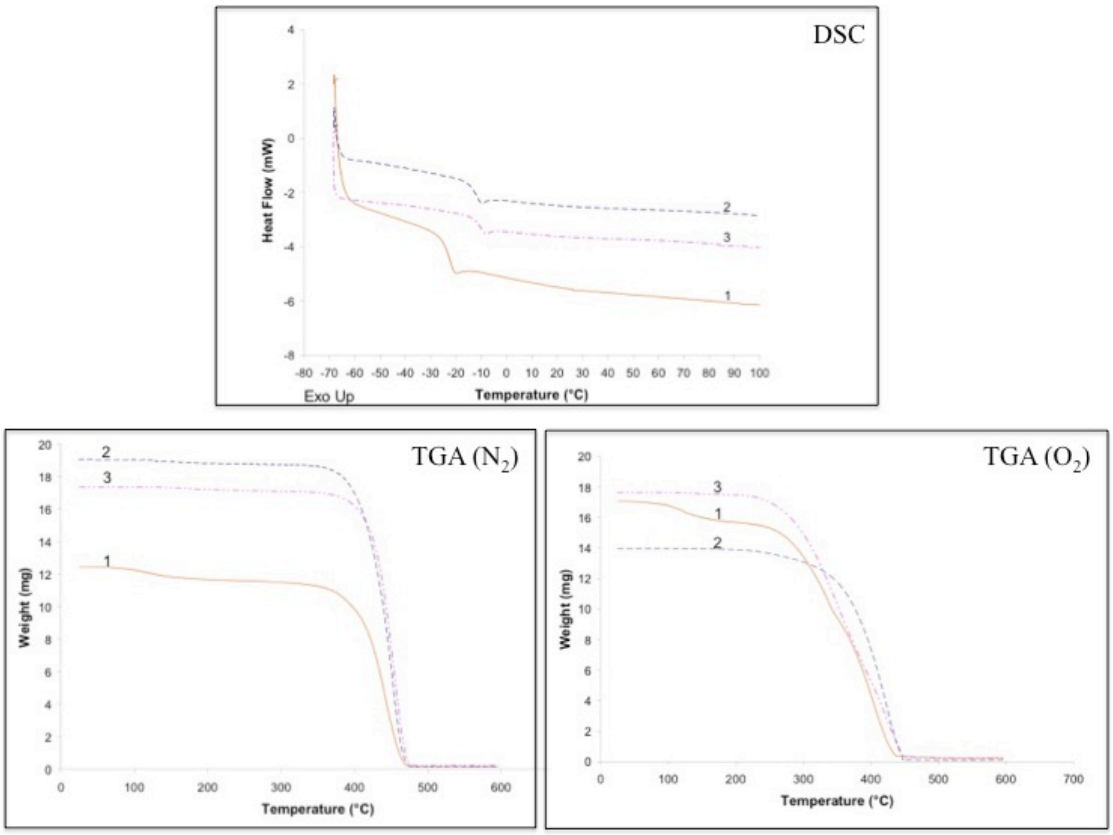

Figure 2.7. DSC and TGA heating curves of 1-hydroxyl-*a*PP polymers where the orange, blue and pink curves correspond to entries 1-3, respectively.

2.4 Phosphonium-terminated polypropene

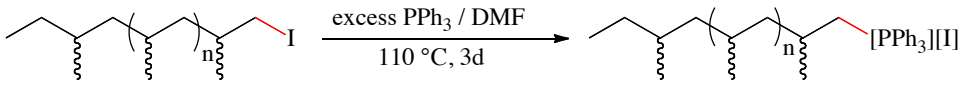

Scheme 2.13. Transformation of iodide-terminated polymer into phosphonium-terminated polymer.

Phosphonium-functionalized polymers are also of interest due to their potential to be used for making olefins through Wittig reactions, as discussed in Section 2.2, and also for mass spectrometry analysis (see Chapter 5 for details). The [PPh_3][I]-terminated polyolefins have been shown to be excellent analytes for determining absolute molecular

weights and molecular weight distributions via MALDI-TOF mass spectrometry according to the method reported by Wallace and co-workers.[14,81,82] Triphenylphosphonium-terminated polyolefins were targeted in current studies through simple nucleophilic displacement of iodide on the iodide-terminated polymer with triphenylphosphine at elevated temperatures in dimethylformamide (Scheme 2.13). The reaction was adjudged to be complete based on the disappearance of resonances centered around 3.2 ppm (Figure 2.8C), corresponding to α-protons adjacent to the iodide group. The NMR of the presumed phosphonium functionalized PP (Figure 2.8B) contained resonances between 7.2 and 8.0 ppm and importantly some of these resonances were not identical to those of the pure triphenylphosphine starting material (see Figure 2.8A). Additionally, the ^{1}H NMR of the phosphonium PP contained new peaks centered at 4.0 and 3.4 ppm, which could be due to the two diastereotopic protons *alpha* to the phosphonium group. Based on these observations, it was concluded that the polymer contained the triphenylphosphonium group.

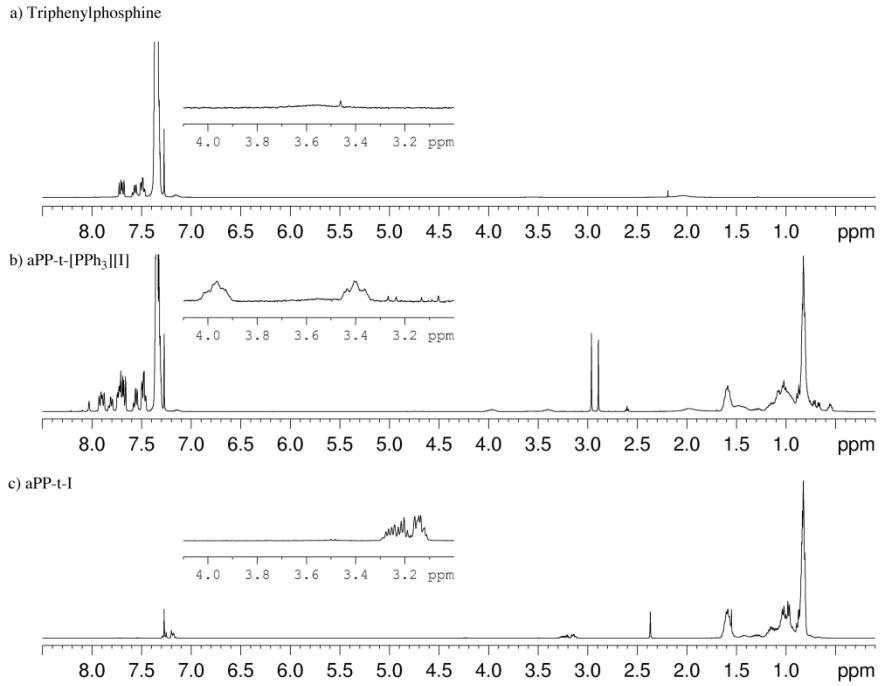

Figure 2.8. ^{1}H NMR of Ph_3P (A), phosphonium-functionalized PP (B) and iodo-terminated PP (C).

2.5 Allyl-terminated polypropene

The alkene is amongst the most versatile functional groups, as they not only find utility in post-modification transformations to other useful functionalities, but vinyl groups have also shown broad applicability inpolymerization[121,122], crosslinking[123], and radical coupling[124] reactions.[8] For instance vinyl monomers such as styrene, acrylates and dienes can be polymerized to generate useful materials, and polymers having multiple pendant vinyl groups can also act as macromonomers towards the synthesis of polymeric materials having very complex architectures[8]. Coates and coworkers[82] for example, utilized bis(phenoxyimine) titanium catalysts to incorporate 1,5-hexadiene monomer via a secondary insertion/isomerization mechanism that leads to the incorporation of 3-vinyltetramethylene (VTM) as well as methylenecyclopentane (MCP)

units as shown in Scheme 2.14. This material was later polymerized with a poly(ethene-co-propene) copolymer to generate amorphous poly(ethene-*co*-propene)-*block*-poly(MCP-*co*-VTM) diblock copolymers.[125] Coates' copolymer could be further functionalized given the prevalence of the terminal vinyl functionalities.

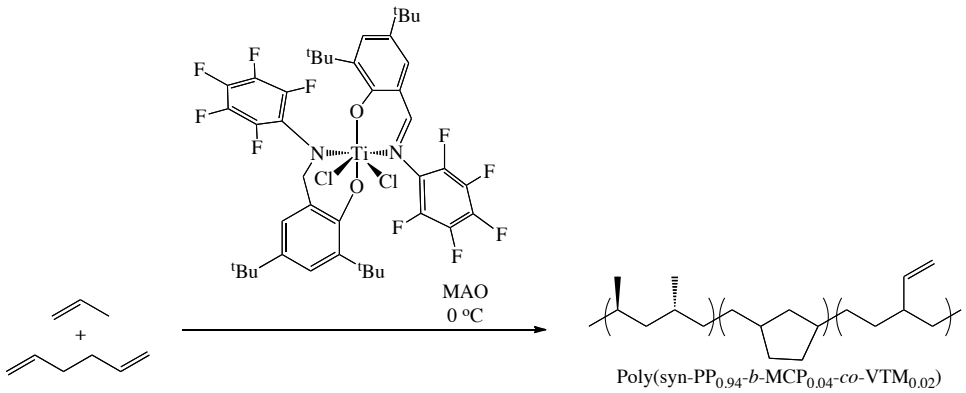

Scheme 2.14. Synthesis of diblock by Coates *et al*. via 1,5-hexadiene cycloaddition.[125]

In 2007, Coates and Sheiko later demonstrated the utility of vinyl macromonomers towards the production of intramolecularly crosslinked polymeric nanoparticles that have potential use in electronic materials.[126] Vinyl functionalized polycarbonates were prepared via terpolymerization of cylcohexene oxide (CHO), vinylcylcohexane oxide (VCHO), and CO_2 with a β-diiminate zinc(II) acetate catalyst ([(BDI)ZnOAc]$_2$). The pendant vinyl groups along the polycarbonate chain were subsequently cross-metathesized using Grubbs' catalyst as shown in Scheme 2.15.

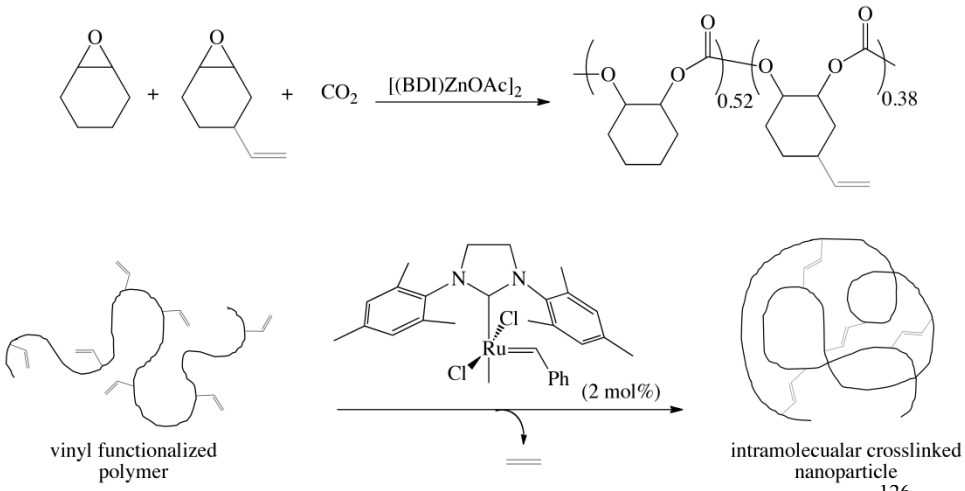

Scheme 2.15. Synthesis of alkene crosslinked polycarbonate nanoparticles.[126]

The utility of controlled radical coupling of vinyl functionalized polymers towards the engineering of unique macromolecules was reported by Debuigne and coworkers through the synthesis of symmetrical poly(vinyl acetate)-*b*-poly(N-vinylpyrrolidone)-*b*-poly(vinyl acetate) triblock copolymers (PVAc-*b*-PNVP-*b*-PVAc) in the presence of a bis(acetylacetonato)cobalt(II) complex as shown in Scheme 2.16.[127]

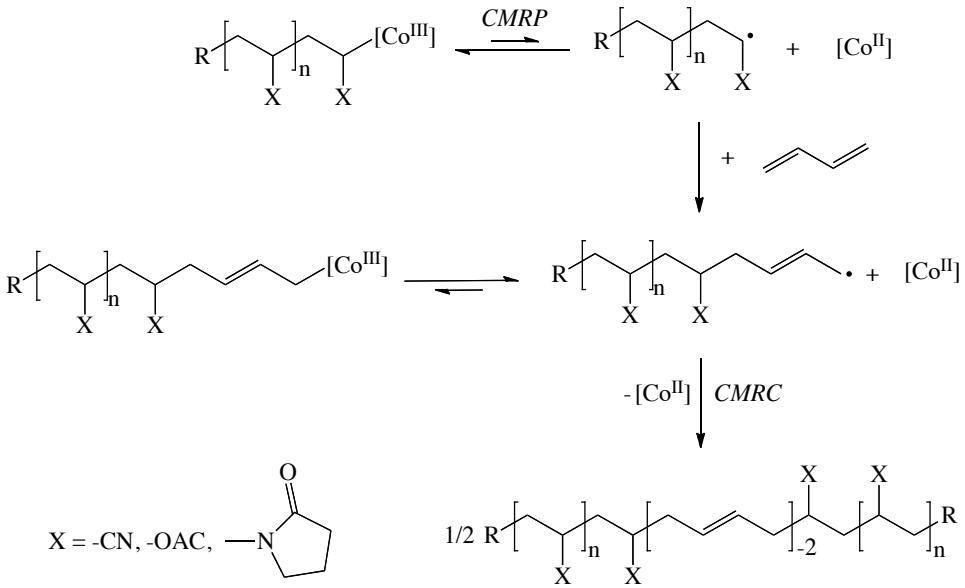

Scheme 2.16. General scheme for the synthesis of block copolymers from alkene macromonomers via cobalt-mediated radical polymerization (CMRP) and coupling (CMRC) reactions.

Due to the versatility of alkenes, as discussed above, it was of interest to convert the iodide-terminated polypropene into an alkene-terminated polymer.

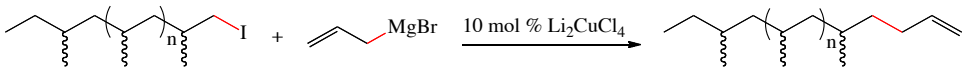

Scheme 2.17. Preparation of alkene-terminated polymer from iodide-terminated polymer.

To prepare an alkene-terminated polymer from the iodide-terminated polymer, allyl magnesium bromide was reacted with the polymer iodide in THF under copper catalysis (Scheme 2.17). A 0.1 M THF solution of Li_2CuCl_4 (obtained from Sigma-Aldrich) was added to a mixture of allylmagnesium bromide and iodide-terminated polypropene in THF at 0 ^{o}C. The solution turned from orange to clear. The mixture was allowed to warm up from 0 ^{o}C to room temperature overnight and the reaction mixture turned from clear to black, in line with literature observation.[128] The reaction was quenched with aqueous acetic acid and diethyl ether was added. After standard workup, the crude product was analyzed by ^{1}H NMR and GPC. The ^{1}H NMR spectrum (Figure 2.9) showed olefinic resonances (centered around 5.0 and 5.8 ppm), indicating possible product formation. GPC analysis (Figure 2.10) showed bimodal distribution hinting at the formation of homocoupled products. A mechanism (via magnesium-halogen exchange) [129-131] to account for the formation of the homocoupled product is shown in Scheme 2.18. The copper-catalyzed allylation of the iodo polymer was therefore not selective enough to cleanly give the desired functionalized polymer void of the homocoupled impurity.

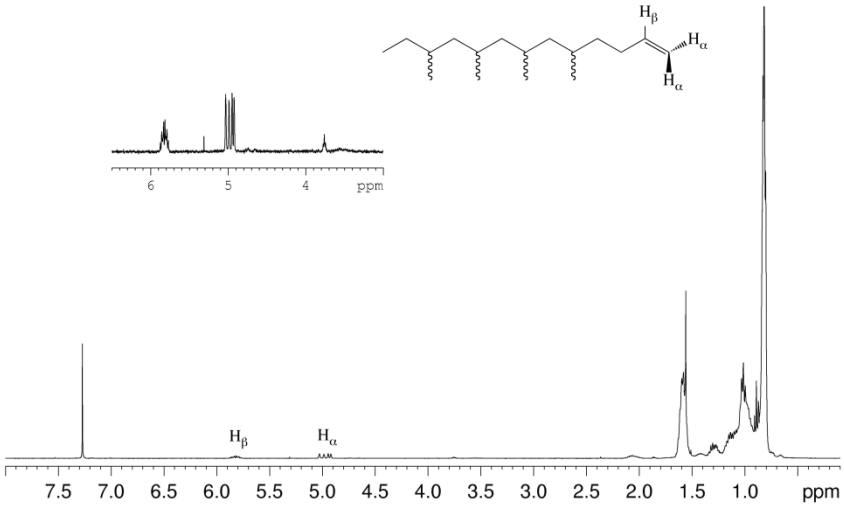

Figure 2.9. ^{1}H NMR (400 MHz, chloroform-d_1) of *a*PP-*t*-allyl. Insert is expanded region to show the olefinic resonances.

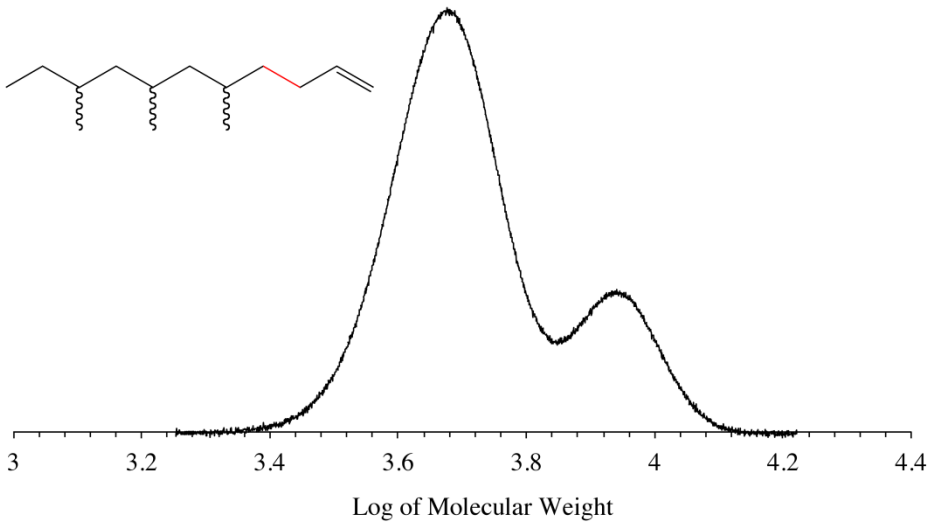

Figure 2.10. GPC showing the presence of a putative homocoupled product in addition to ally-terminated polypropene.

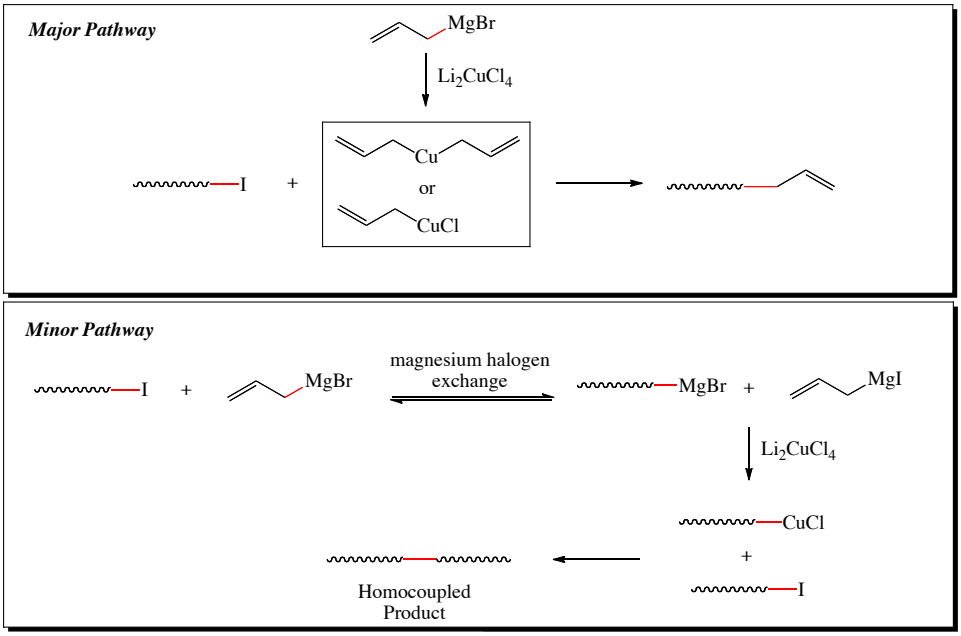

Scheme 2.18. Copper-catalyzed coupling of Grignards with alkyl iodide.

An alternative allylation method was then employed, using direct nucleophilic displacement of the bromide on allyl bromide with a lithiated polymer which was generated from the iodo polymer and *t*-BuLi (see Scheme 2.19).

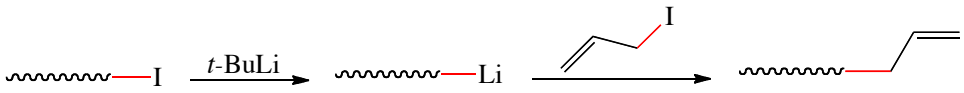

Scheme 2.19. Generation of lithiated polymeryl species followed by attempted alkylation.

Addition of *t*-BuLi to iodo polypropene in diethyl ether at -82 ^{o}C resulted in a lithium-halogen exchange. To ascertain the extent of polymer lithiation, the reaction was quenched with methanol and analyzed by both ^{1}H NMR and GPC. ^{1}H NMR showed the disappearance of the peaks corresponding to the alpha protons next to the iodo group in the starting material (see Figure 2.11). GPC analysis (Figure 2.12) showed a bimodal molecular weight distribution (Mn = 8.4 kDa and 4.0 kDa); thus indicating the presence

of a high molecular weight polymer, having a molecular weight that is almost double that of the starting iodo-terminated polypropene, in addition to the expected product as shown in Scheme 2.20. The homo-coupled polymer likely arose from the co-existence of lithiated polymer and iodo-polymer leading to self-reaction. See Scheme 2.21 for plausible mechanism.

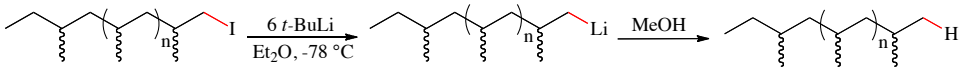

Scheme 2.20. Generation of lithiated polymer and subsequent quench with methanol.

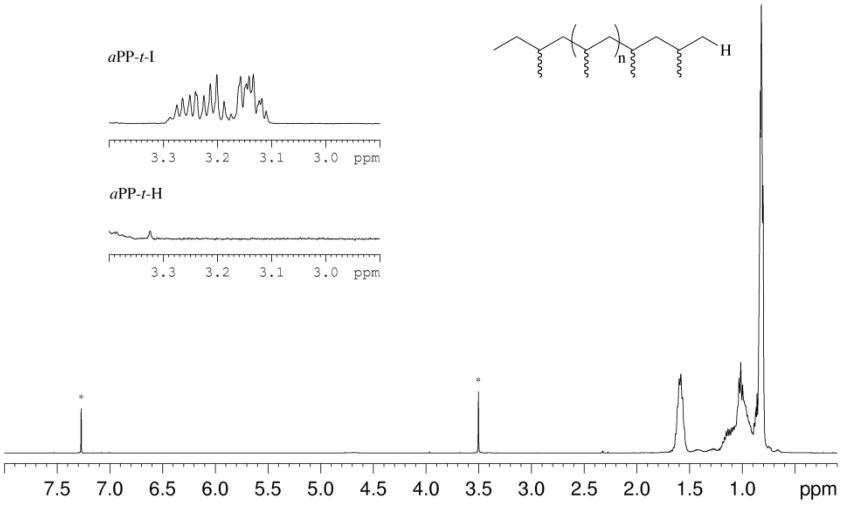

Figure 2.11. ^{1}H NMR (400 MHz, chloroform-d_1) of quenched lithiation reaction indicates that iodo group is removed from polymer in line with expectation if halogen is exchanged with lithium and then quenched with a proton.

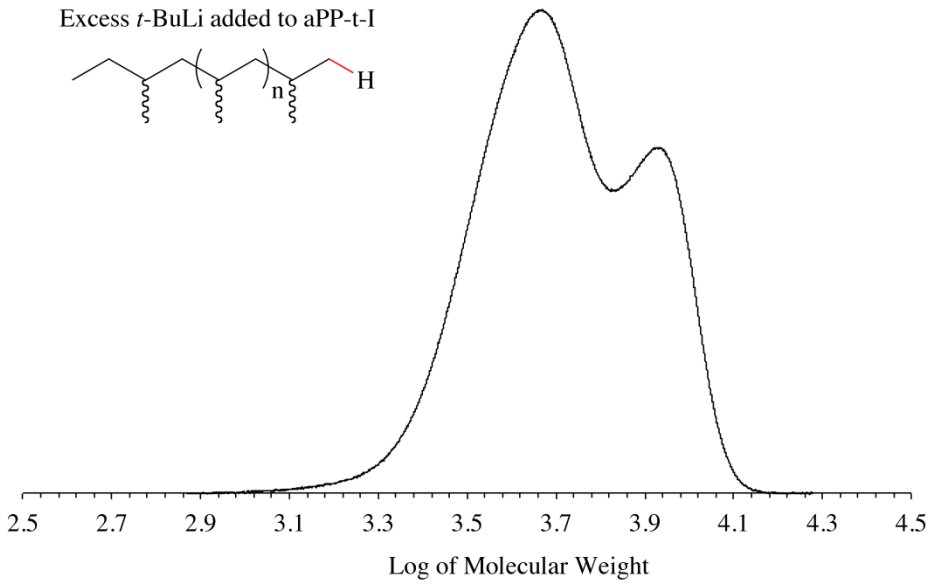

Figure 2.12. GPC analysis shows bimodal distribution of polymer and a putative homocoupled PP.

Scheme 2.21. Plausible mechanism for homocoupling during lithiation step.

To prevent the homocoupling from happening, the iodo-terminated polymer was then added dropwise to a solution of *t*-BuLi to minimize the presence of both the lithiated and iodo-terminated polymers in solution. Using the aforementioned method to generate the lithiated polymer and then quenching with methanol, gave a product with narrow molecular weight distribution.

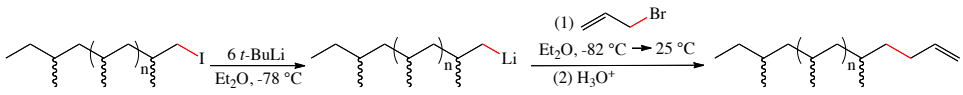

Scheme 2.22. Olefination of iodo-terminated polypropene via lithium-halogen exchange and subsequent alkylation.

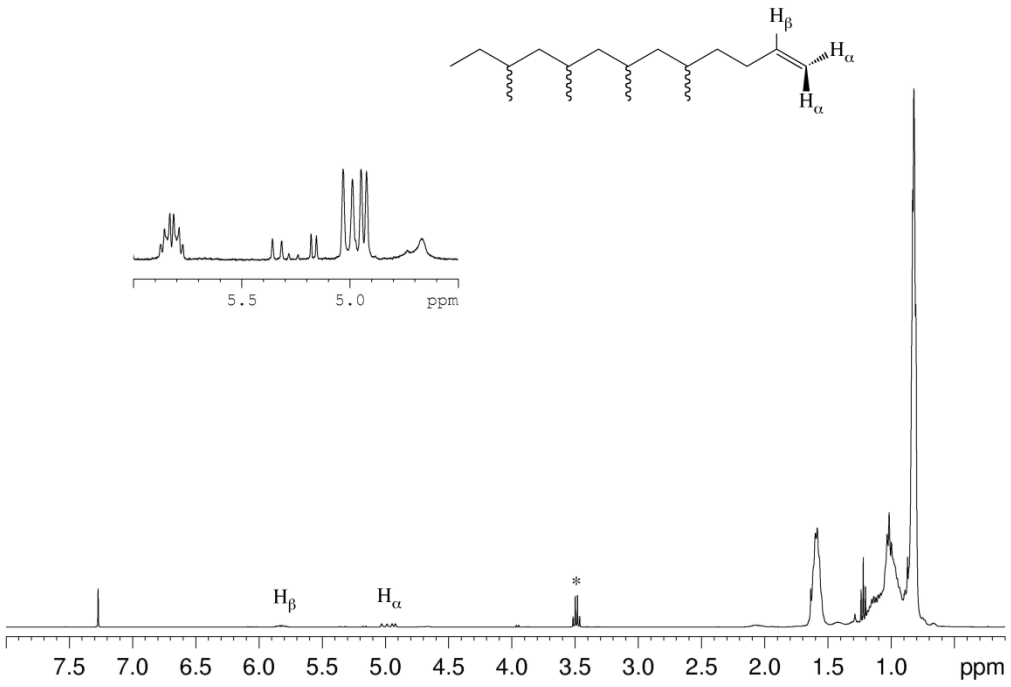

Figure 2.13. ^{1}H NMR of allyl-terminated PP, synthesized via lithiated polymer intermediate.

Having established a protocol to access the lithiated polypropene polymer, without significant formation of the homocoupled product, optimism was high that the addition of allyl bromide to this lithiated polymeryl species would finally afford a polymer with an alkene unit at the termini. Therefore allyl bromide was added to the lithiated polymer at -82 ^{o}C, followed by warming of the reaction mixture to room temperature overnight and quenching with methanol gave a crude product that was analyzed by ^{1}H NMR and GPC (Scheme 2.22). ^{1}H NMR showed disappearance of iodo-starting material and appearances of new peaks centered around 5.0 and 5.8 ppm, see Figure 2.13. ^{1}H NMR also indicated the formation of side products with chemical shifts centered around 4.5

ppm. Importantly, the presumed olefinic peaks centered around 5.0 and 5.8 ppm for the product obtained from the lithiated polymer intermediate have similar chemical shifts and multiplicities relative to the peaks observed when the product was made via copper catalysis (compare Figures 2.9 and 2.13). This time GPC analysis (see Figure 2.14) showed that the overall molecular weight distribution was monomodal, with a slight high molecular weight shoulder.

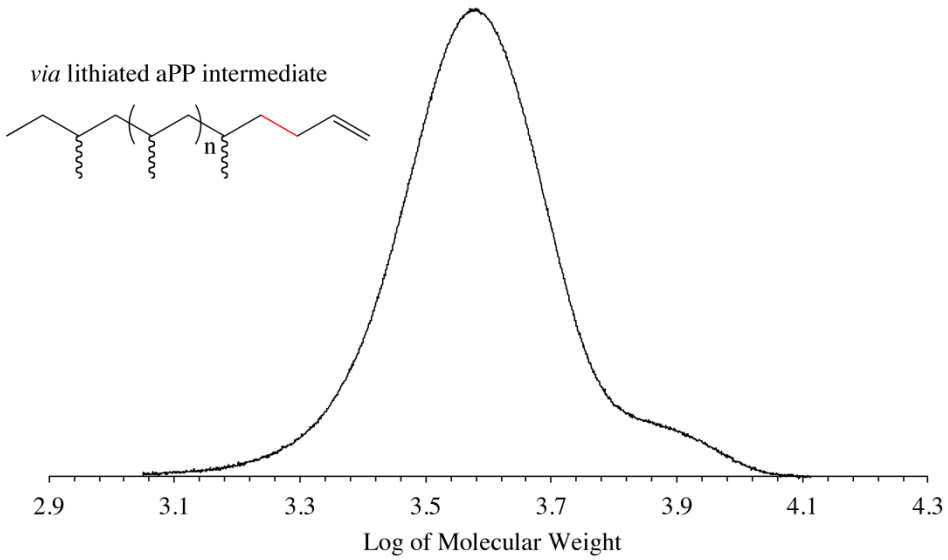

Figure 2.14. GPC of the allyl-functionalized PP.

2.6 Azide-terminated polypropene

As stated previously, the introduction of polar groups to the terminus of the polyolefin motif is one strategy utilized for the diversification of polyolefin end-use properties. One functionalized polyolefin material whose acquisition was of high priority was the azide-terminated polymer. Azide-functionalized materials are of importance because they can potentially serve as building blocks for the construction of

architecturally complex polyolefins that could translate to variability in end-use properties. A range of reactive functional groups can be easily incorporated thereafter with the use of azide/alkyne click reactions.[132] Click is a general term, popularized by Sharpless[133], to describe reactions that are facile and give almost quantitative yields under mild reaction conditions. Apart from their high efficiency click reactions are also highly tolerant of functional groups and solvents, including water and can be conducted under both homogeneous and heterogeneous conditions. Therefore click reactions provide endless opportunities to functionalize polymers to afford diverse architectures in ways that were formerly unreachable via controlled polymerization methods.

In the last decade, the alkyne-azide click, catalyzed by copper (I) (called CuAAC) [133,134] or the newly developed "copper-free" [31,32] click methodologies [135,136], have emerged as powerful tools to functionalize myriads of compounds, ranging from small molecules that are diversified into drug-like structures[137,138], ligands for catalysis[139-141], macromolecules[142] (including proteins, nucleic acids, oligosaccharides) and other synthetic polymeric materials. [132,143] In exciting new applications of click chemistry, others have even shown that this enabling methodology can be used to label macromolecules such as proteins inside live cells.[144] Indeed it is surprising that the alkyne-azide click reaction, which is really a 1,3 Huisgen dipolar cycloaddition, originally described by Michael[145] and developed by Huisgen[146-150], was underutilized for decades and it was not until the publication of Meldal's important paper on the copper-catalyzed 1,3 Huigsen dipolar cycloaddition papers[151,152] followed by a beautifully written paper by Sharpless on this topic[153] that the community became aware of the importance of this reaction.[133] One could therefore call Sharpless' paper as a "wake-up"

paper. The copper-catalyzed click reaction follows a mechanism[143] that is different from the thermal 1,3-dipolar cycloaddition of azides and alkynes, in that the former is a stepwise process (see Figure 2.15) whereas the later is a pericyclic reaction that likely goes through an aromatic transition state and controlled by frontier orbitals (see Figure 2.16). The frontier-orbital theory used to analyze the thermal, non-Cu-catalyzed azide/alkyne cycloaddition has been excellently reviewed by Lwowski.[154] The mechanism of the Cu(I)-catalyzed CuAAC is not fully understood and it has been postulated that the active catalyst involves Cu clusters and that these clusters bind to both the azide and alkyne and increase the effective concentration of the reaction partners. Cu inserts into the terminal C-H bond of the alkyne to form a Cu-acetylide, an azide that is bound to a nearby Cu within the cluster then reacts with the Cu-acetylide, as shown in Figure 2.15. It has been estimated that the Cu catalyst increases the rate of the azide/alkyne reaction by 10^7, compared to the uncatalyzed reaction[153].

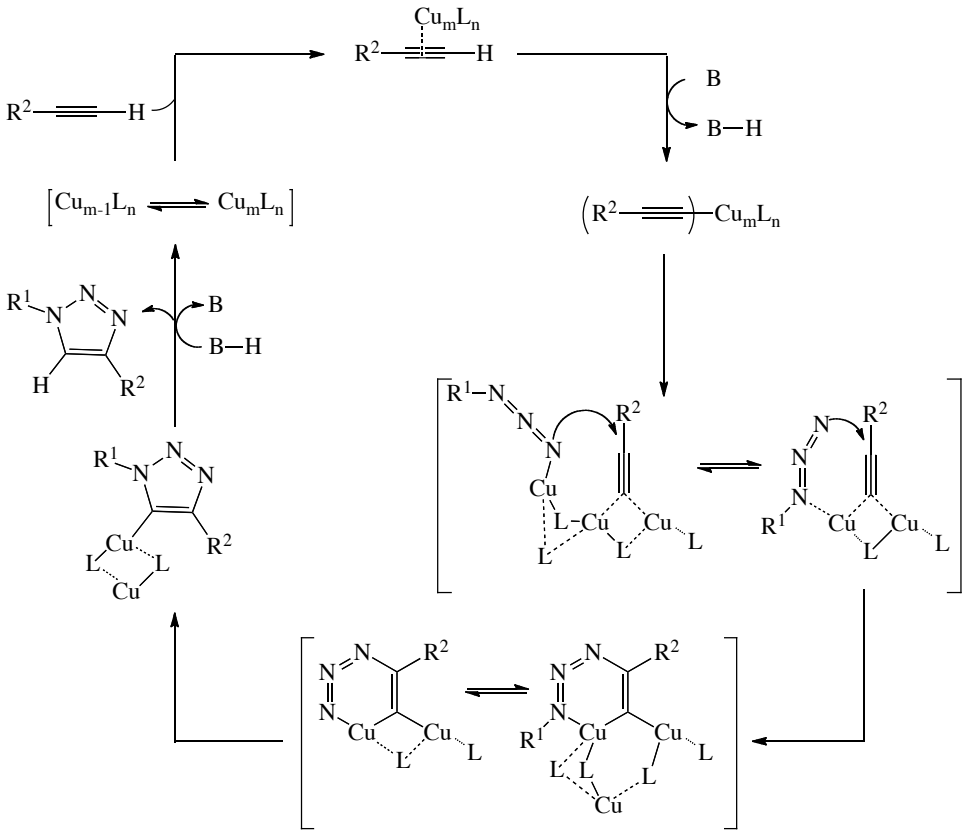

Figure 2.15. Mechanism of copper-catalyzed click reaction.[152]

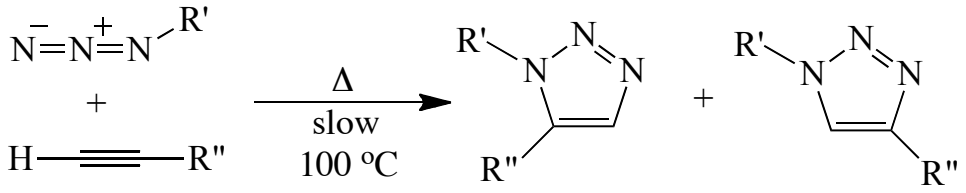

Figure 2.16. Mechanism of thermal 1,3-dipolar cycloaddition between alkyne and azide.

The use of copper in click reactions (albeit at very low catalyst loading ~0.5 mol%) could be problematic for the functionalization of biomolecules but these concerns are not as important for the functionalization of synthetic polymers or materials used for ex-vivo applications. Matyjaszewski and and co-workers[155] made azide functionalized polymers (see Figure 2.17A) via atom transfer radical polymerization, ATRP. For this polymer, there were several azide units per polymer so a subsequent CuAAC functionalization

with alkynes of this polymer would afford a polymer with several triazole units per polymer. Similarly, Hawker *et al.*[156] used nitroxide living radical polymerization to make a polymer that incorporated several alkyne units per polymer (Figure 2.17B). A polymer obtained via a nitroxide living radical polymerization would contain N-O linkages, which are known to decompose under heat or UV irradiation to generate radicals. This instability could be viewed as a favorable attribute for the purpose of making degradable polymers. The alkyne-functionalized polymer could be reacted with azide containing partners to give 1,2,3-triazole functionalized polymers. It must be noted that it is easier to do a click reaction using a polymer that has several azide units per polymer than having several alkyne units per polymer. This is because with several alkyne units in a single polymer, the alkyne moieties might bind to all possible Cu sites in the Cu cluster and reduce the chances of the azide binding to the cluster to increase the effective concentration of the reacting partners.[157]

An interesting use of CuAAC reaction in polymer science is to use the click reaction for the polymerization and not as an end-functionalization strategy. Reek and co-workers[158] described the synthesis of a triazole containing polymer via the polymerization of bis-alkyne/bis-azide monomers (see Figure 2.17D). The triazole containing polymers described all contain multiple triazoles per polymeric unit. The triazole moiety contains two nitrogen atoms with lone pairs of electrons that are not part of the aromatic π-electron cloud and hence are available for binding to metals. Therefore polymers that contain many triazole units per polymer chain could bind to adventitious metals and this might affect their properties. As it is impossible to control the amount or nature of adventitious metals in the environment, the properties of such polymers might

not be predictable under all conditions. The triazole group, on the other hand, could be water-soluble due to its hydrogen-bonding capability. As a result polymers containing several triazole units per polymer might be water-soluble and have unique applicabilities. The controlled use of click chemistry in derivatizing polymers has been described by Hawker and co-workers.[159] In their approach, alkyne groups were placed at the end of the polymer (end-capped) and the ends of the polymer could then be "clicked" with azide-containing monomers, (Figure 2.17C).

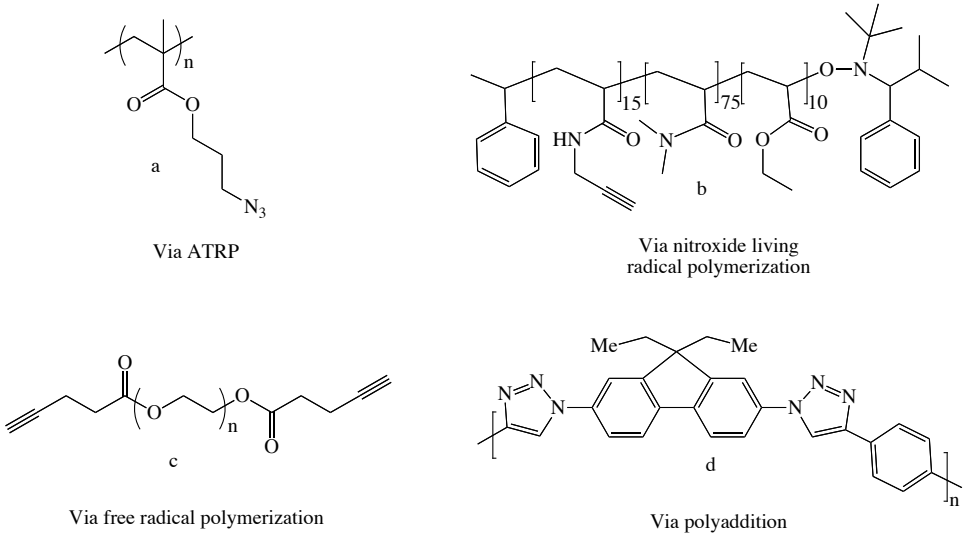

Figure 2.17. "Click"-polymer products. [132,143,155,156,158,159]

Inspired by the utility of click chemistry, we aimed to functionalize our polyolefins with either alkyne or azide units, for subsequent functionalization using click. Living coordination polymerization with or without organozinc or organoaluminum reagents, deliver metal-terminated polymers because it is easier to functionalize the carbon-metal bond at the terminus (which is nucleophilic) with electrophiles. The azide or alkyne units are usually introduced into organic molecules by utilizing nucleophilic azides or alkynes

so it was necessary to first convert the metallated polymers into a polymer with a good leaving group so that the nucleophilic azide or alkyne could be used to functionalize the polymer. Towards this goal, polyethylene was first iodinated as discussed in Section 2 of this chapter.

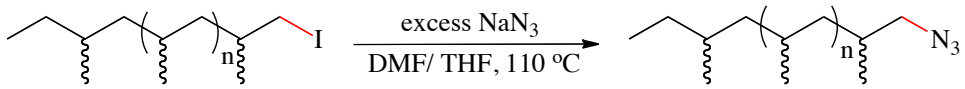

Scheme 2.23. Azide functionalization reaction.

With the terminal iodo-polymer in hand, in meaningful quantities, the iodide group was displaced with the azide anion in DMF/THF co-solvent at 110 ^{o}C (Scheme 2.23). THF was needed in the co-solvent because the iodo-terminated polymer was not soluble in neat DMF. It must be mentioned that azides are usually considered to be explosion hazards and it is not usually recommended to do azidation reactions at high temperatures, but the propensity of a nitrogen containing material to explode relates to the carbon/nitrogen ratio in that the lower this ratio the higher the risk of explosion of the material. The ratio of carbon to nitrogen in the azide-terminated polymer is presumably high, but this reaction was done behind a protective glass shield in compliance with standard safety precautions.

The displacement of the iodo group on the polymer by azide was facilely done. The reaction was monitored by taking an aliquot after an overnight reaction and analyzing this aliquot by NMR. The complete disappearance of NMR resonances (centered around 3.15 and 3.25 ppm) attributed to the α-protons that were germinal to the iodide group in the polymer, and the appearance of new resonance peaks centered at 3.10 and 3.20 ppm (a small upfield shift) were judged to signal the completion of the azide-iodide displacement

reaction. Further evidence of the successful completion of the reaction was obtained via IR, where a new IR peak at 2100 cm^{-1} was consistent with carbon-azide functionality. The azide-terminated polymer was isolated by first evaporating the reaction solution and then re-dissolving the crude product in chloroform. The polymer was then precipitated via the addition of the polymer-chloroform solution into methanol. This strategy gave purer polymer material because the impurities in the polymer are soluble in both chloroform and methanol but the polymer is only soluble in chloroform. Further cleansing of the polymer was achieved by re-dissolving the precipitated polymer in chloroform and passing this through a short pad of silica gel. Evaporation of the chloroform solvent afforded azide-terminated polymer that was good for a subsequent click reaction. ^{1}H and ^{13}C NMR as well as IR of the azide polymer is shown in Figures 2.18-20 and display all the resonance peaks that one would expect for an azide-containing polymer.

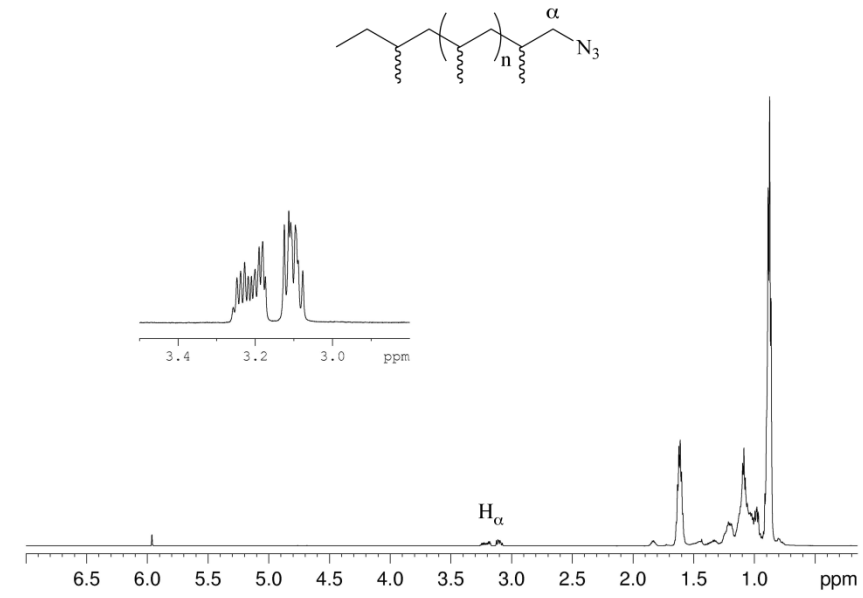

Figure 2.18. ^{1}H NMR (600 MHz, 1,1,2,2-$C_2D_2Cl_4$, 90 °C) of azide terminated *a*PP.

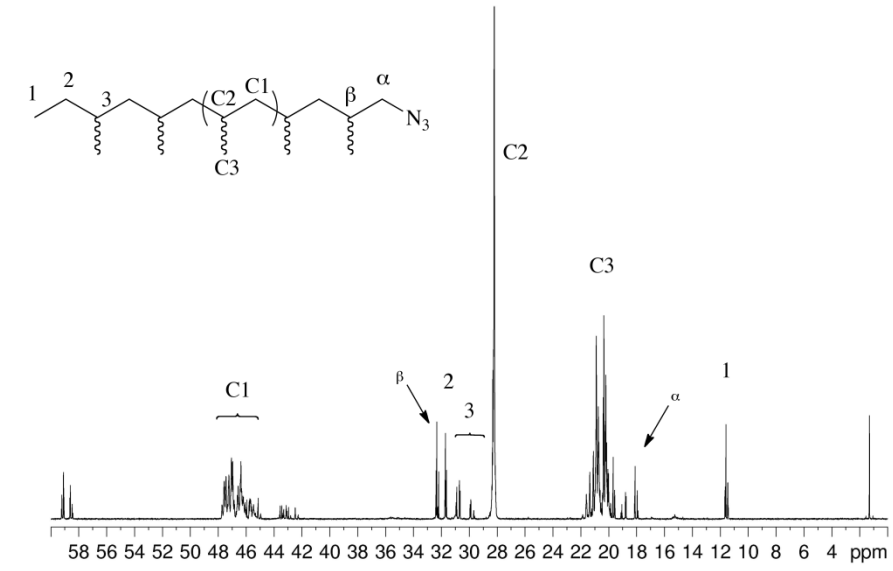

Figure 2.19. ^{13}C NMR (150 MHz, 1,1,2,2-$C_2D_2Cl_4$, 90 °C) of azide terminated *a*PP.

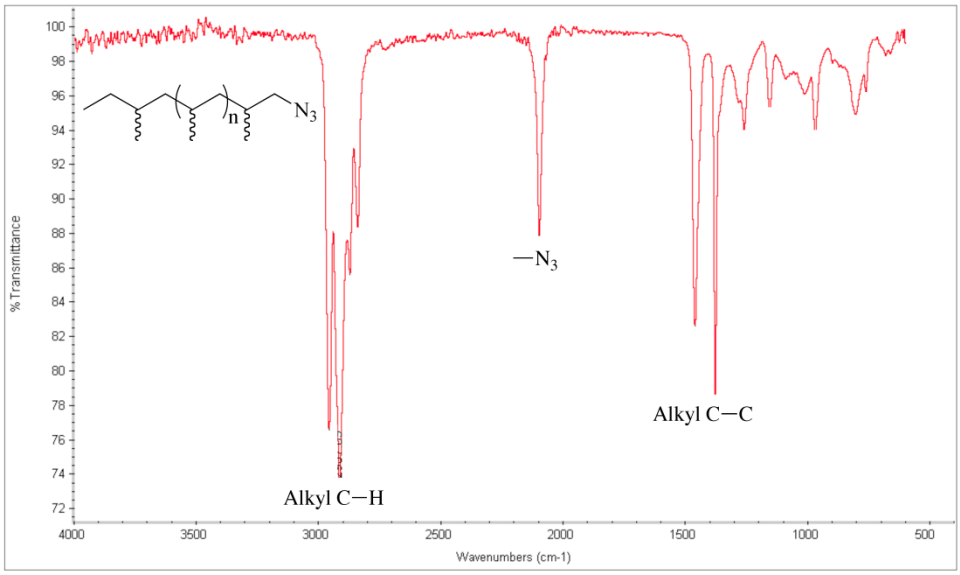

Figure 2.20. Infrared spectrum of azide terminated *a*PP.

2.6.1 Acrylate and Methacrylate Functionalized aPP

With an azide-terminated polymer in hand, the stage was now set to perform the click reaction. This azide-terminated polymer was first dissolved in DMF/THF co-solvent, followed by the addition of propargyl acrylate or methacrylate (see Scheme 2.23 for structures). Cu_2SO_4 and ascorbic acid were then added to the reaction mixture and left to stir overnight. To monitor the progress of this reaction, aliquots of the reaction mixture were taken, solvent evaporated and IR spectra taken of the reaction mixture. The azide functionality has a distinctive IR peak around 2100 cm^{-1} so the disappearance of this IR peak was indicative of the completion of the reaction. After the completion of the click reaction, the solvents were evaporated, the crude material was dissolved in chloroform and this chloroform-polymer solution was added to a flask containing methanol to precipitate the polymer. The rationale for this purification procedure is the same as previously discussed for the cleaning of the azide-terminated polymer. ^{1}H and ^{13}C NMR

as well as IR spectra of the 1,2,3-triazole containing polymer (the triazole unit originates from the addition of the alkyne to the azide) are shown in Figures 2.21-24.

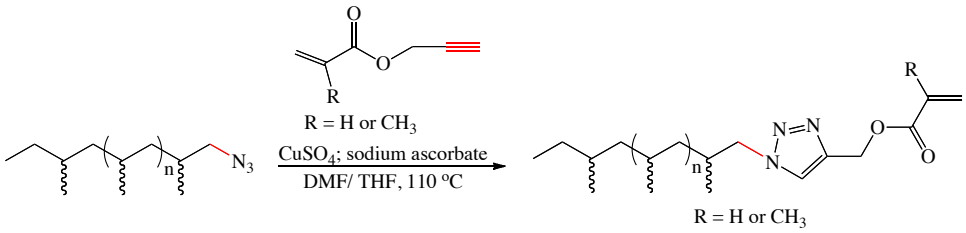

Scheme 2.24. Acrylate/methacrylate functionalization reaction.

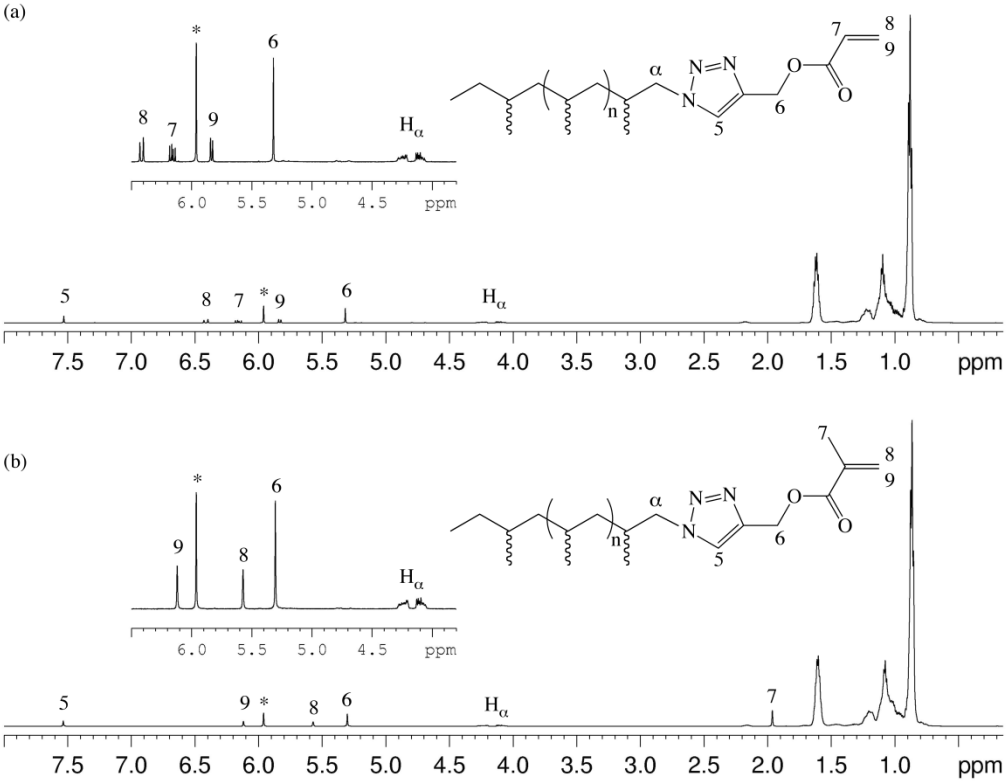

Figure 2.21. ^{1}H NMR (600 MHz, 1,1,2,2-$C_2D_2Cl_4$, 90 °C) of clicked azide polymer-acrylate/methacrylate conjugates.

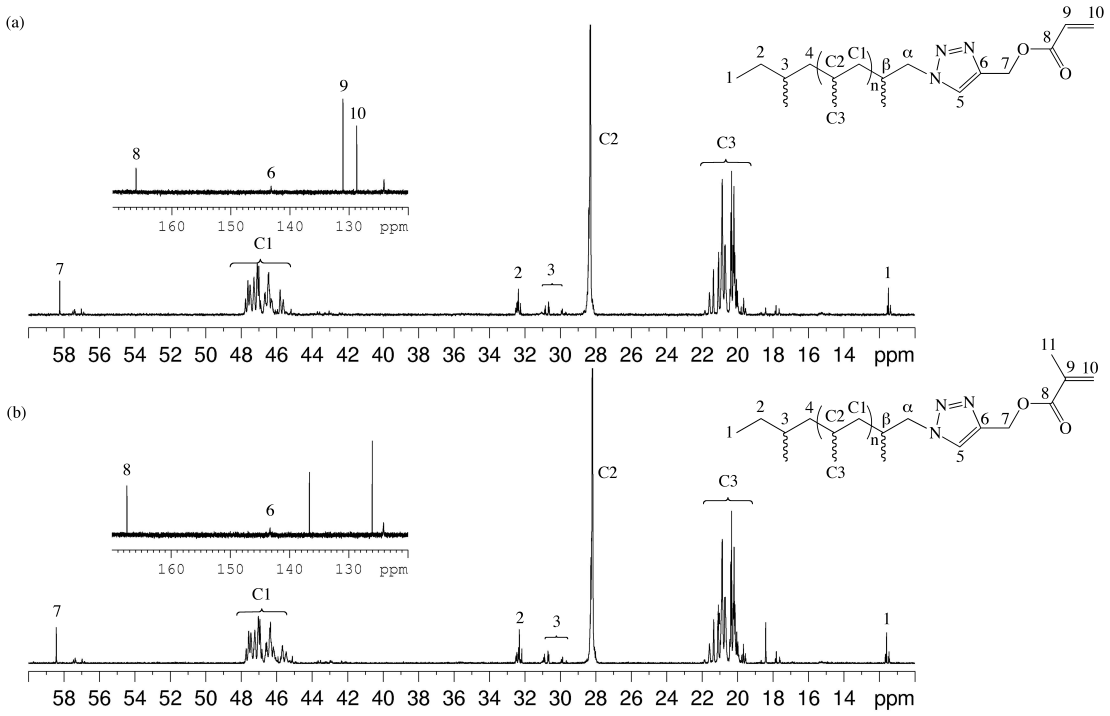

Figure 2.22. ^{13}C NMR (150 MHz, 1,1,2,2-$C_2D_2Cl_4$, 90 °C) of clicked azide polymer-acrylate/methacrylate conjugates.

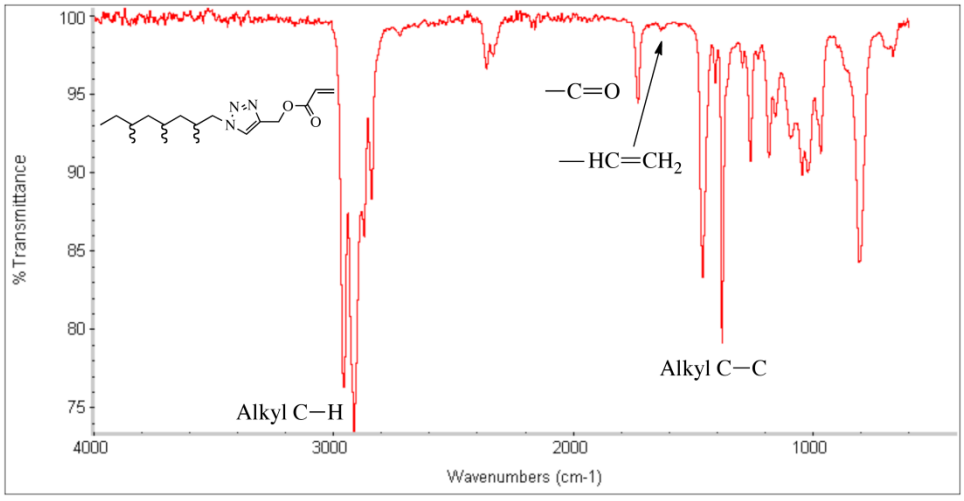

Figure 2.23. IR of clicked azide polymer-acrylate conjugate.

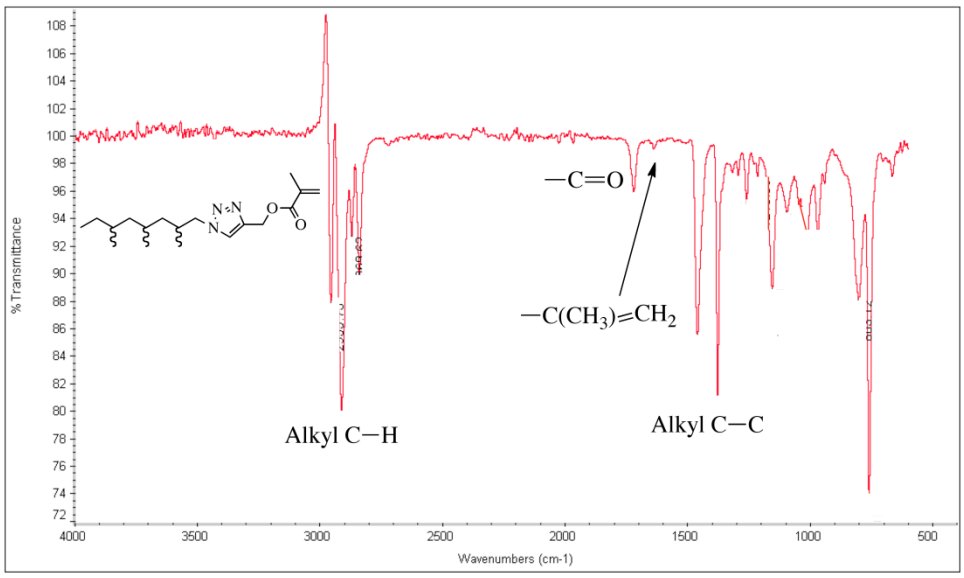

Figure 2.24. IR of clicked azide polymer-methacrylate conjugate.

The mass spectrum (MS) of the starting azide did not show the usual distribution of a polypropene polymer, whereby a distribution with MS differences of 42 corresponding to the propene unit would be expected. It can be assumed that the azide-terminated PP did not ionize easily or that the ionized azide polymer did not "fly" well in the MS instrument. Conversion of the azide to the acrylate1,2,3-triazole would however endow the polymer with several heteroatoms with lone pairs, such as two nitrogens in the triazole moiety, that could be protonated and hence give a good MS. Pleasingly, the acrylate/methacrylate-1,2,3-triazole polymer (obtained from the click reaction between the azide-terminated PP and propargyl acrylate/methacrylate) gave a good MS that showed the characteristic polymer distribution with MS differences of 42 units, corresponding to propene units (see Figures 2.25 and 2.26).

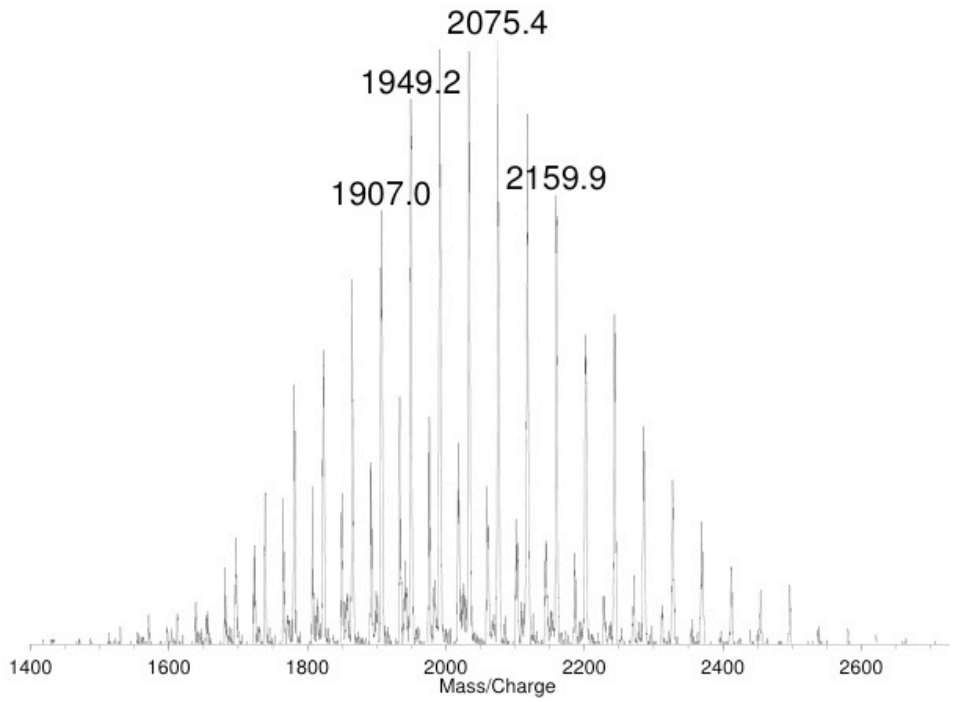

Figure 2.25. MS spectrum of acrylate-1,2,3-triazole PP.

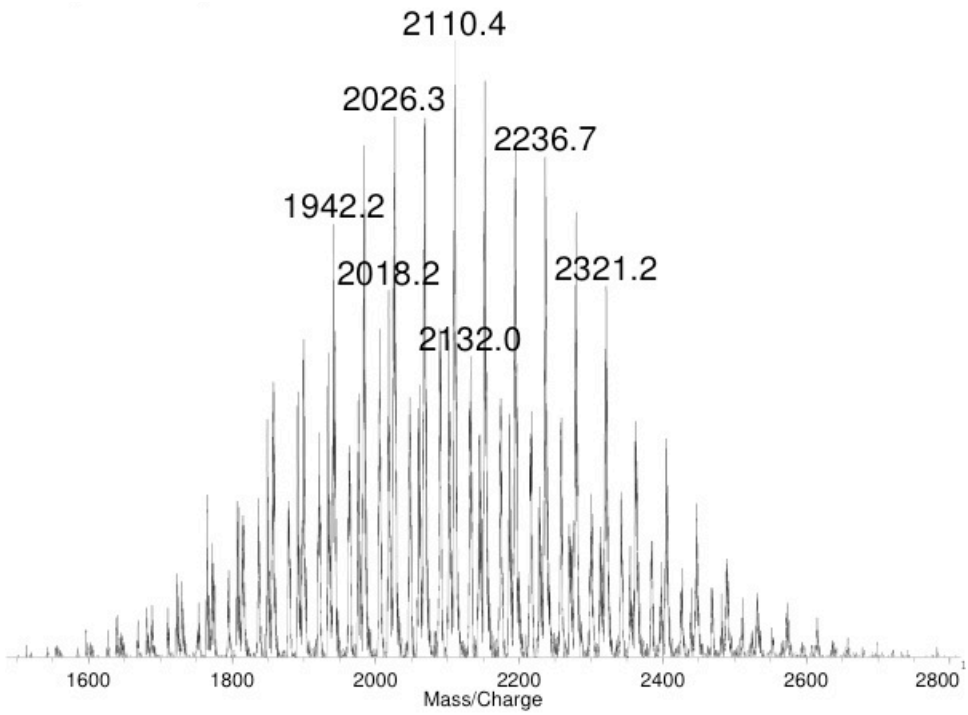

Figure 2.26. MS spectrum of methacrylate-1,2,3-triazole PP.

It is worth noting that the MS of both acrylate/methacrylate-1,2,3-triazole PP (see Figures 2.25 and 2.26) also contained polymeric satellite peaks, which were also separated by 42 units, meaning that these polymers are also functionalized polypropene derivatives. These satellite peaks were off 26 mass units from the main peaks. D'Agosto and co-workers, who also functionalized polyethylene with acrylate and methacrylate also observed these satellite peaks in their MS.[93] Unfortunately, a rationale for these observations has not been hypothesized.

2.6.2 Conversion of azides to amines

The azide group can be converted to amines using a variety of conditions. The amine functionality is as versatile as the azide group and can be transformed into other functionalities via well-established protocols. For example, reaction of an amine-functionalized polymer with carboxyl partners using coupling reagents such as dicyclocarbodiimide (DCC) would lead to amide bond formation. The amine group is also polar and would therefore impart hydrophilic properties to the polymer.

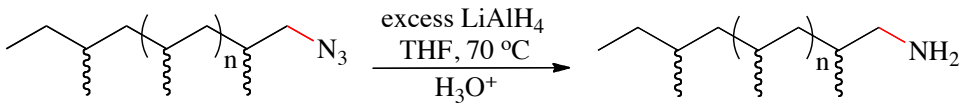

Scheme 2.25. Reduction of azide to a primary amine.

The azide-terminated polymer was reacted with lithium aluminium hydride ($LiAlH_4$) at 70 ^oC in THF, Scheme 2.25. At stirring overnight, the mixture was quenched with acetic acid and the solvent was evaporated off. The crude mixture was then added to a THF/water mixture containing 1M NaOH and stirred overnight. This step was necessary to get rid of any amine-aluminum chelates. The organic layer was separated

and the solution was filtered through Celite, after which the THF solvent was evaporated to afford the amine-terminated polymer. ^{1}H NMR of the amine-terminated polymer showed new peaks centered around 2.6 and 2.7 ppm, assigned to alpha protons to the amine group and a broad peak centered at 3.55 ppm, which was presumed to be the labile NH_2 protons (see Figure 2.27). IR spectra showed disappearance of the azide peak at 2100 cm^{-1}, indicating conversion of the azide functionalized polypropene to the amine-terminated polypropene.

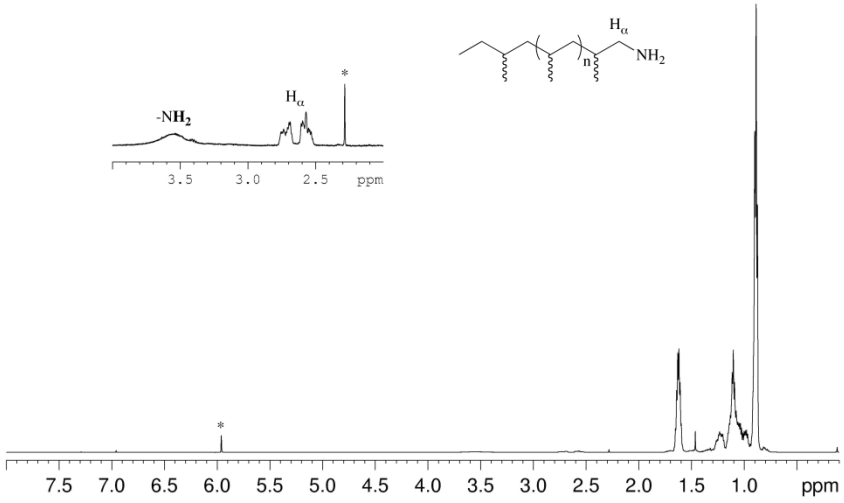

Figure 2.27. ^{1}H NMR (600 MHz, 1,1,2,2-$C_2D_2Cl_4$, 90 °C) of amine-terminated PP.

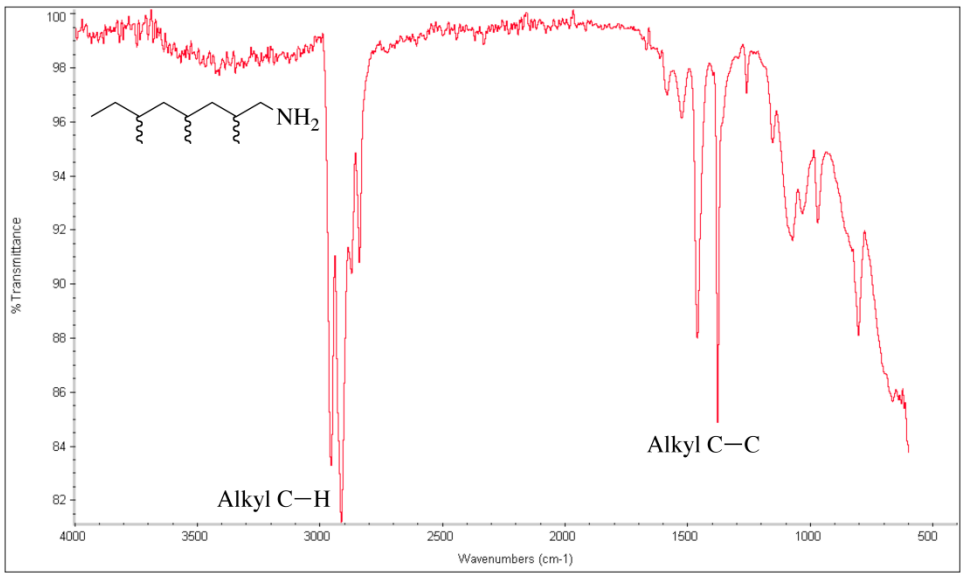

Figure 2.28. IR of amine-terminated PP. The azide peak around 2100 cm^{-1} has disappeared, in line with expectations.

2.9 Alkyne Functionalized Polypropene

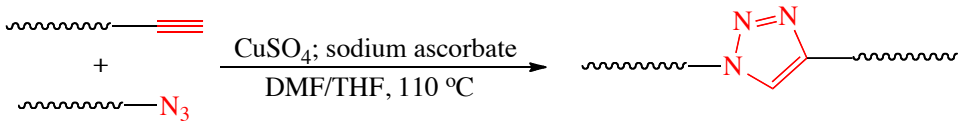

Scheme 2.26. "Clicking" together two polymers to generate block copolymer.

As previously discussed in Section 2.7, the CuAAC reaction is a powerful method to couple two fragments together under mild conditions when one fragment contains an alkyne and the other contains an azide. In Section 2.7, the synthesis of polymeryl azides from polymeryl iodides was described. Access to polymeryl alkyne would allow for the coupling of two different polyolefin chains together whereby one polymer contains an alkyne and the other is terminated with an azide, Scheme 2.26. We therefore became interested in the development of methodologies to convert polymeryl iodides into alkyne-terminated polyolefins, see Scheme 2.27.

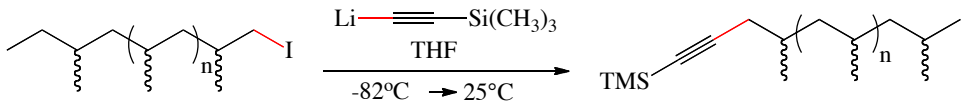

Scheme 2.27. Synthesis of alkyne-terminated polyporopene from iodide functionalized polymer.

Lithiated TMS (trimethylsilane) alkyne in THF (commercially available from Sigma-Aldrich) was added to the polymeryl iodide at -82 ^{o}C and the mixture was allowed to warm to room temperature. The reaction was quenched with methanol and the polymer was precipitated from methanol. ^{1}H NMR showed the appearance of a singlet around 0.18 ppm, attributed to the TMS group on the polymer (see Figure 2.29). There were also some residual resonances from the starting iodide. For example, the resonances of the two alpha protons adjacent to the iodide around 3.2 ppm belonging to the iodide starting material were still present. Integration of the TMS peaks (corresponding to nine protons) at 0.18 and 0.10 ppm (of the alkyne-functionalized aPP) and the alpha protons peak of the starting iodide around 3.2 ppm gave a 2.1:1.0 ratio, implying that the polymer mixture contained 68% starting material and 32% alkyne product. Both the ^{1}H and ^{13}C NMR of the alkyne-terminated polymer (Figures 2.29 and 2.30 respectively) indicate the presence of two alkyne containing polymers (one major peak at 0.18 ppm and a minor peak at 0.10 ppm in the ^{1}H NMR and one major peak at 0.37 ppm and one minor peak at 1.31 ppm in the ^{13}C NMR). The existence of two TMS group peaks could be due to the presence of "two diastereomers", referring to the relative orientation of the two stereocenters closest to the TMS-alkyne group (shown in Scheme 2.28). In principle, there would be more than two diastereomers due to the presence of multiple stereocenters in the polymer but only the last two terminal stereocenters would probably affect the TMS group.

Future optimization of the reaction to achieve complete conversion would probably involve leaving the reaction to stir longer than what was done (1.5 h) or using more equivalence of the lithiated TMS alkyne or adding the lithiated TMS alkyne reagent to the polymeryl iodide as separate aliquots over time (in case the lithiated TMS alkyne is being quenched before the reaction gets completed).

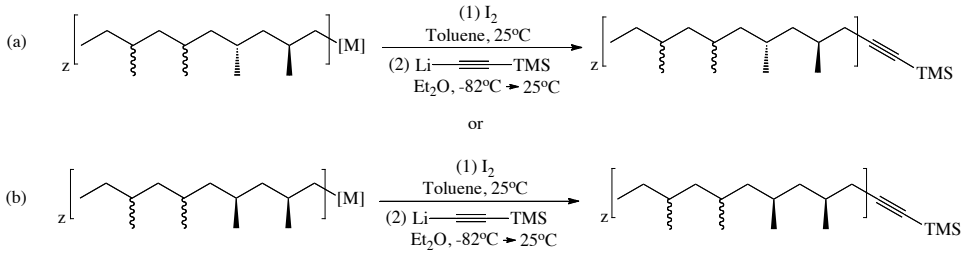

Scheme 2.28. Displacement of iodo group with lithiated TMS alkyne.

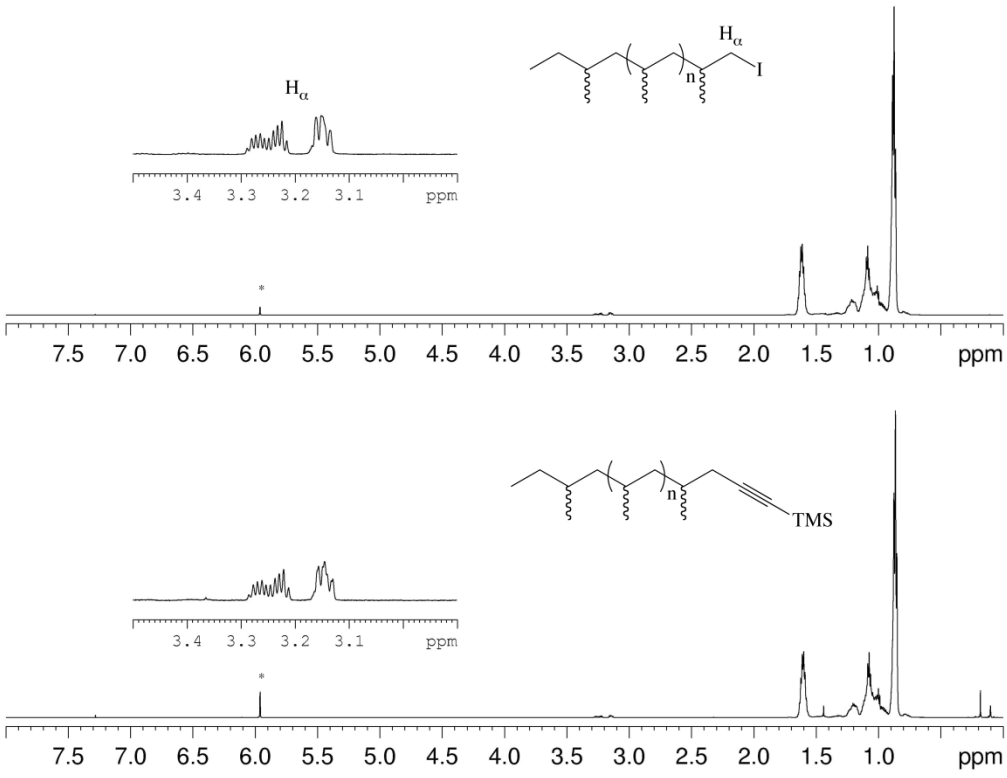

Figure 2.29. ^{1}H NMR (600 MHz, 1,1,2,2-$C_2D_2Cl_4$, 90 °C) of iodide terminated *a*PP (top) and ^{1}H NMR (600 MHz, 1,1,2,2-$C_2D_2Cl_4$, 90 °C) of TMS alkyne functionalized *a*PP (bottom).

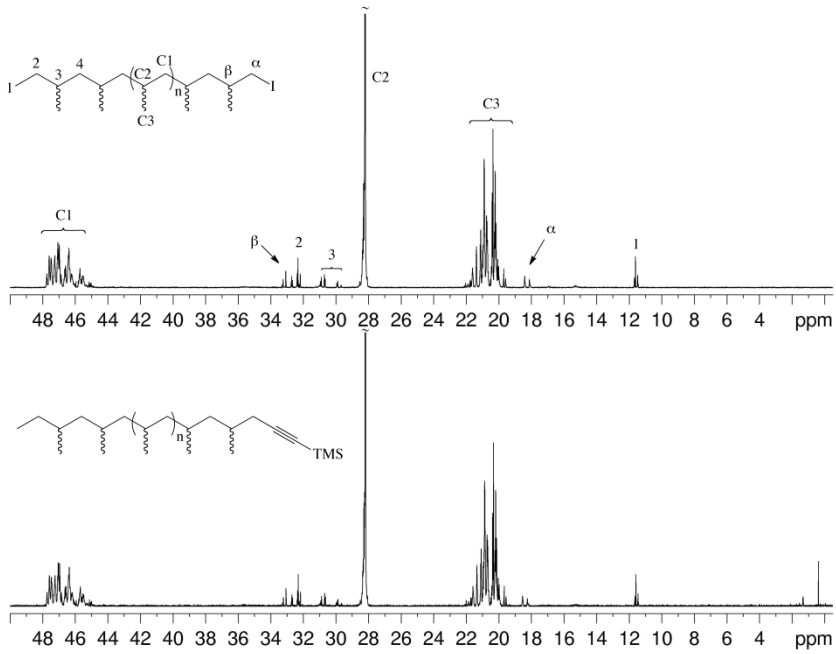

Figure 2.30. ^{13}C NMR (150 MHz, 1,1,2,2-$C_2D_2Cl_4$, 90 °C) of iodide terminated *a*PP (top) and ^{13}C NMR (150 MHz, 1,1,2,2-$C_2D_2Cl_4$, 90 °C) of TMS alkyne functionalized *a*PP (bottom).

2.7 Thiol Functionalized aPP

The addition of the thiol unit (SH) to polymers allow for the modulation of the properties of the polymer via sulfur-specific/selective reactions (shown in Schemes 2.29 and 2.30). The reaction of the thiol group with maleimides is well known and has been utilized by several groups to append moieties that contain the maleimide unit onto macromolecules.[160-163] This reaction proceeds via the 1,4-conjugate addition of the thiolate nucleophile to the α,β-unsaturated unit of maleimides. Hence it is best to conduct the reaction at a slightly basic pH, where the thiol is deprotonated to form the thioate anion. When the pH is raised too high (above pH 8), the thiol selectivity is lost and amines also begin to react with maleimides. Secondly, above pH 8, the maleimide group can also hydrolyze into an unreactive molecule. Macromolecules or polymers that are

conjugated with maleimides can be further functionalized via the hydrolysis of the formed succinimide to succinamide acid via a ring-opening reaction catalyzed by molybdate or chromate.[164] Recently a paper has shown that thioethers obtained from sulfur/maleimide conjugation are not as stable as believed by the community and that in the presence of other thiols, this conjugate can be exchanged[165]. The labile nature of the thioether group in the thiol-maleimide conjugate could be viewed as a plus and used for the preparation of polymers that could be triggered to release a cargo when competing thiols are added. In any case, hydrolysis of the succinimide to succinamide increases the stability of the conjugates.

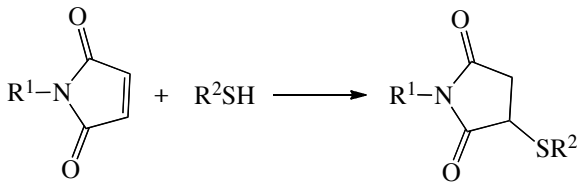

Maleimide Thioether

Scheme 2.29. Thiols add to the α,β-unsaturated unit of a maleimide to form a thioether.

Another strategy that has been used quite extensively to conjugate groups to thiol-containing macromolecules is to react the thiol group with iodo/bromoacetamides to form a thioether. Iodoacetamide is more reactive than bromoacetamide and is the preferred reagent for thiol modification[162,163] (see Scheme 2.30). Iodoacetamides can also react with other functional groups such as amines and readily hydrolyze in basic aqueous solutions so they do not provide as much thiol selectivity as seen with maleimides.

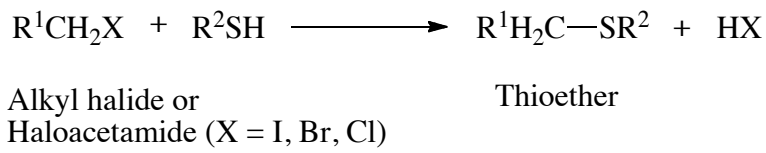

Scheme 2.30. Reaction of thiols with alkyl halides or haloacetamides. For haloacetamides, the order of reactivity is Cl < Br < I.

Gold has a great affinity for thiols and hence most gold surfaces can be decorated with molecules (including polymers) via a facile self-assembling process, if the molecule/polymer contains thiols.[166,167]

2.7.1 Thiol Functionalization via Thioacetate

Due to the potential to functionalize macromolecules that contain thiols with different moieties, the conversion of iodo-terminated polyolefins into thiol-terminated polymers was pursued. The displacement of alkyl iodides with potassium thioacetate was attempted (see Scheme 2.31). Hydrolysis of the thioacetate with hydroxide affords a free thiol (see Scheme 2.32) and has already been demonstrated by others[168-170].

Scheme 2.31. The conversion of iodo-terminated polymer into thioacetate polymer.

Thioactetate functionalized *a*PP was obtained from the iodo-terminated *a*PP. Excess potassium thioacetate was added to a solution of *a*PP-*t*-I in THF and was refluxed at 70 °C overnight. The reaction mixture was slowly cooled to room temperature the following day and then quenched with methanol. Solvents were removed in *vacuo*. The crude polymer was later dissolved in chloroform and titrated into excess methanol. The

crude polymeric product was isolated thereafter and purified via silica gel filtration in chloroform. The final product was dried under vacuum and ^{1}H NMR revealed quantitative conversion of the starting material. The ^{1}H NMR indicated the absence of resonances around 3.2 ppm, which indicates the complete consumption of the iodo-terminated *a*PP starting material. New resonances centered around 2.8 ppm (corresponding to the two alpha protons next to sulfur) and a singlet at 2.35 ppm (corresponding to the methyl group of the thioacetate) were also observed in ^{1}H NMR (see Figure 2.31), supporting the conclusion that the iodide group was successfully displaced by the thioacetate. Further proof of thioacetate functionalization was obtained from IR, which showed the carbonyl stretch at 1680 cm^{-1} (see Figure 3.32).

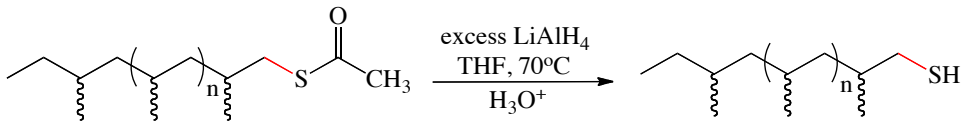

Scheme 2.32. Reduction of thioacetate-terminated *a*PP to thiol-functionalized *a*PP.

After the synthesis of the thioacetate its hydrolysis to the free thiol was investigated. In the presence of trace metals, thiols are known to readily oxidize in air to several species, including disulfides and sulfenic acid.[171] Therefore, it is better to prepare the free polymeryl thiols immediately before conjugation. Nonetheless, the thioacetate was hydrolyzed with $LiAlH_4$ (see Scheme 3.32). ^{1}H NMR of the thiol-terminated polymer did not contain the thioacetate peak of the starting material (singlet peak at 2.35 ppm). Nor did it contain the resonances centered around 2.8 ppm found in the ^{1}H NMR of the starting thioacetate (compare Figures 2.31 and 2.33). Additionally, the IR of the thiol-terminated polymer did not contain the carbonyl stretch at 1680 cm^{-1}, seen in the IR of

the starting thioacetate shown in Figure 2.32. All of these pieces of spectroscopic evidence support the conclusion that the thioacetate was successfully hydrolyzed.

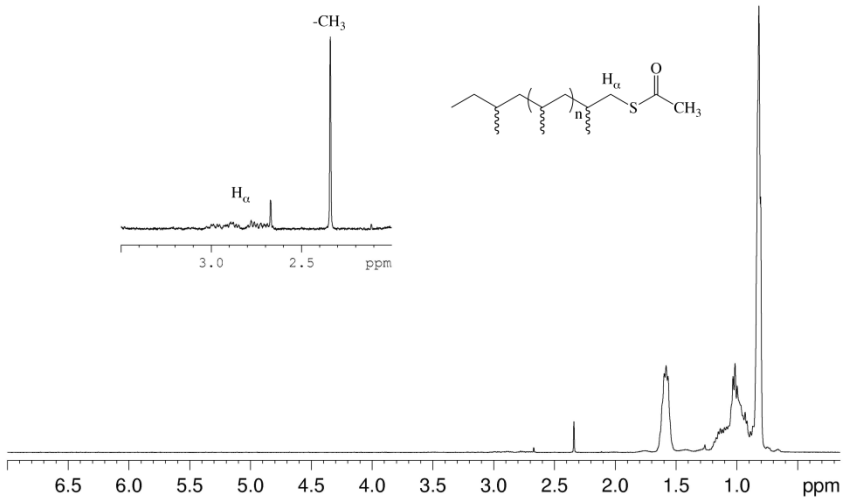

Figure 2.31. ^{1}H NMR (400 MHz, chloroform-d_1, 25°C) of thioacetate functionalized *a*PP showing the characteristic singlet at 2.35 ppm corresponding to the methyl group of the acetate.

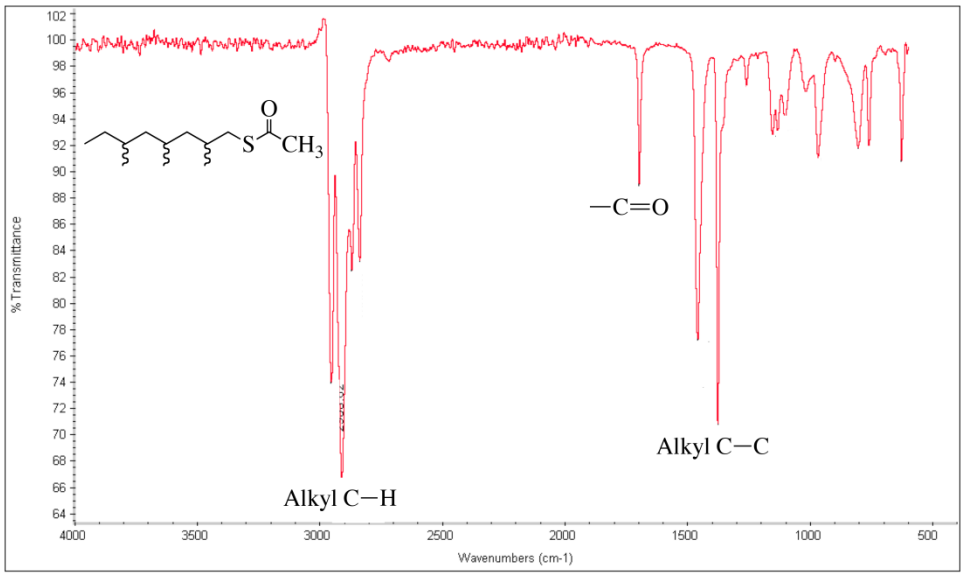

Figure 2.32. IR of thioacetate-terminated *a*PP, showing the characteristic carbonyl stretch of the starting at 1680 cm^{-1}.

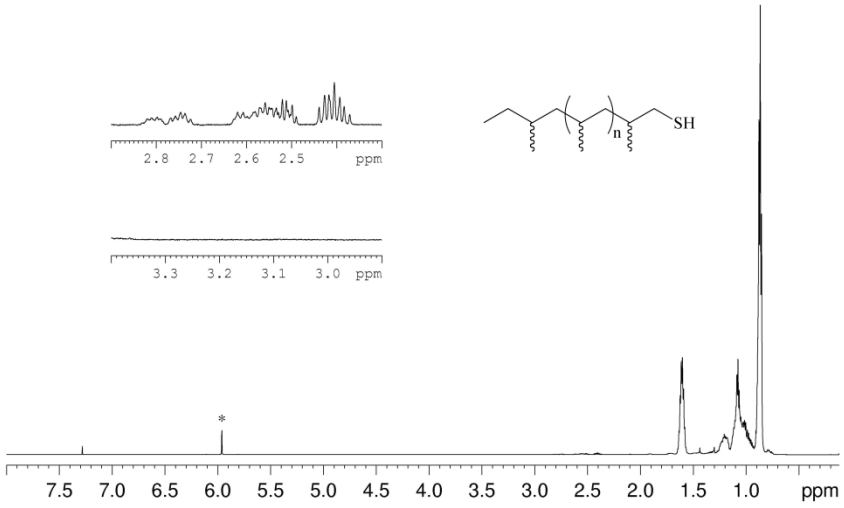

Figure 2.33. ^{1}H NMR (600 MHz, 1,1,2,2-$C_2D_2Cl_4$, 90 °C) of thiol-terminated *a*PP, showing the disappearance of the starting thioacetate resonances and the appearance of new resonances.

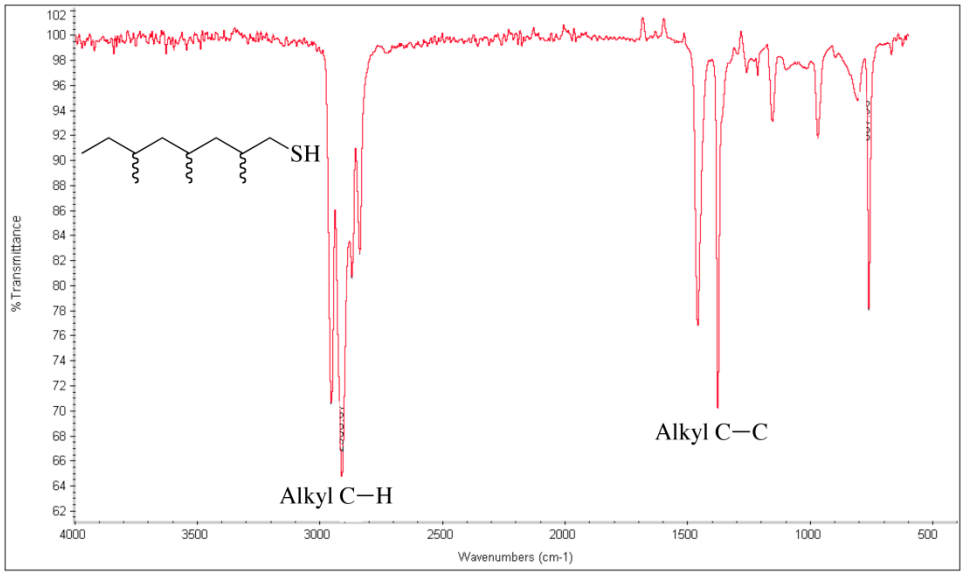

Figure 2.34. IR of thiol-terminated *a*PP, showing the disappearance of the characteristic carbonyl stretch of the starting thioacetate at 1680 cm^{-1}.

2.8 Conclusions

Polyolefins can be readily made in a living fashion using [Cp*HfMe{N(Et)C(Me)N(Et)}][$B(C_6F_5)_4$] (generated from the **Precatalyst III** and one equivalent of the **Cocatalyst I**) as the initiator with dialkyl zinc or trialkyl aluminum as a chain transfer reagent. Polyolefins, however, do not interact well with other materials so there has been a need to functionalize these materials with other moieties in order to improve the performance of polyolefins. A current limitation of the hafnium catalyst used for the synthesis of polyolefins is the incompatibility with several polar functional groups, especially those containing lone pairs of electrons, which coordinate to the catalyst and shut off the catalytic cycle. Post-functionalization of polyolefins with other handles that allow for subsequent conjugation to other moieties or macromolecules holds great potential for the tailoring of the properties of polyolefins. In this chapter, various strategies that were used to post-functionalize polyethene and polypropene were discussed. End-functionalization with the hydroxyl group was readily achieved via the quenching of the polymerization reaction with molecular oxygen. Alkyl halides, especially iodides, are excellent partners for nucleophilic displacement reactions. Iodo-terminated polymers were prepared via the quenching of polymeryl metals with iodine. The iodo-terminated polymer served as an excellent starting material for the synthesis of other end-functionalized polymers, such as azides, alkynes, alkene and thiols. The facile conversion of polymeryl iodide into azide allowed for further functionalization of the polymer using CuAAC click chemistry. The development of end-functionalization protocols of polyolefins has now made value-added polyolefins with several desirable properties highly accessible.

2.9 Future Outlook

Several successes were achieved in tethering different functional groups onto polyolefins, synthesized with Sita's hafnium catalyst system. However, there were synthetic challenges associated with the preparation of polymer precursors that would be end-functionalized with a few other desirable moieties. For example, the nucleophilic displacement of iodide with lithiated alkyne did not smoothly give an alkyne-terminated polymer. Future development of this reaction by others in the Sita group could investigate other strategies to couple alkyne units with iodides, such as copper catalyzed alkynation using a polymeryl iodide and an alkyne Grignard (akin to the copper-catalyzed vinylation reaction using polymeryl iodide and allyl Grignard described in this thesis, see Section 2.6). Secondly, the conversion of hydroxyl-terminated polymers into aldehydes was extensively discussed due to its ability to act as a chemical handle to access other desirable functional groups. In the future, the conversion of these hydroxyl-terminated polymers into aldehydes, via oxidation, and subsequent coupling of the aldehydes with other groups would increase the repertoire of end-functionalized polyolefins.

The conjugation of polyolefins with other polymers or nanostructures may potentially lead to the preparation of smart materials with interesting properties and real world usage. For example, conjugating an azide-containing polyolefin with another polymer bearing an alkyne unit via CuAAC click reaction could potentially lead to "blocky" type polymers with properties that lie between those of the constitutive polymers or even with entirely new properties. Another potential use of the end-functionalization methodology that was developed during my PhD tenure is the conjugation of polyolefins with other nanostructures made of different materials, such as

gold and silver quantum dots etc. Thiol-terminated polyolefins, synthesized from the readily prepared iodo-terminated polyolefin, would be ideal for the conjugation to gold via self-assembly.

Finally, because the ultimate goal of this program is to make polymers with useful properties, future endeavors would look into the processing of these functionalized polyolefins into films etc. and the characterization of the resultant material.

2.10 Experimental

Materials. All manipulations were performed under an inert atmosphere of dinitrogen using either standard Schlenk techniques or a Vacuum Atmospheres glovebox. Dry, oxygen-free solvents were employed throughout. Chlorobenzene was distilled from calcium hydride and toluene was distilled from sodium. Polymer grade ethene and propene were purchased from Matheson Trigas, and passed through activated Q5 and molecular sieves (4 Å). Cp*Hf$(Me)_2$[N(Et)C(Me)N(Et)] (**1**) were prepared according to previously reported procedures. [PhNHMe_2][B$(C_6F_5)_4$] (**2**) and [Ph_3C][B$(C_6F_5)_4$] (**3**) was purchased from Boulder Scientific and used without further purification.

Instrumentation. GPC analyses were performed using a Viscotek GPC system equipped with a column oven and differential refractometer both maintained at 45 °C and four columns also maintained at 45 °C. THF was used as the eluant at a flow rate of 1.0 mL/min. M_n, M_w and M_w/M_n values were obtained using a Viscotek GPC with OmniSEC software (conventional calibration) and ten polystyrene standards (M_n = 580 Da to 3,150 kDa) (from Polymer Laboratories). ^{13}C {^1H} NMR spectra were recorded at 150 MHz, using 1,1,2,2-tetrachloroethane-d_2 as the solvent at 90 ºC. Some ^1H NMR spectra were recorded at 400 mHz, using chloroform-d_1 as the solvent at room temperature. MALDI-

TOF analysis: Solution concentrations were 20 mg/mL for the dithranol matrix and for the analyte with toluene used as solvent. A 5 mg/mL potassium chloride solution in a 9:1 mixture of ethanol and water was used to increase the signal-to-noise ratio. The matrix, analyte and potassium solutions were mixed in a 10:10:1 ratio and spotted from a 1 μL micropipet onto the steel target. After drying, the droplets showed a finely divided crystalline structure. MALDI-TOF was performed on a Shimadzu Axima-CFR in linear mode which provided uncertainties of approximately 1 mass unit . Ions were generated using a 337 nm wavelength nitrogen laser with a pulse duration of the order of 5 ns and a maximum laser energy of 270 μJ. The laser power used was 85. All measurements were performed in the positive mode.

Preparation of *a*PP-*t*-I: In a 250 mL Schlenk flask, to a 20 mL toluene solution of cocatalyst **2** (16.8 mg, 0.021 mmol) at 0 ºC were added the precatalyst **1** (9.1 mg, 0.020 mmol) and $ZnEt_2$ (0.247 g, 2.0 mmol, 100 equiv. to **1**). The flask was then pressurized to 5 psi with propene and the pressure was maintained for 2 h with stirring. Then propene was pumped away via vacuum for 30 min at 0 ºC. The reaction mixture was removed from the glove box and saturated I_2 in toluene solution was added to the $Zn(aPP)_2$ toluene solution at room temperature until the purple color stayed in the reaction solution. The toluene solution was then extracted with 3 × 100 mL 10% NaOH solution, 3 × 100 mL 10% HCl solution and 3 × 100 mL D. I. water. The crude product was stirred under activated carbon and filtered through Celite before being titrated into basic MeOH. The polymer was recovered and dried in *vacuo* to remove toluene before GPC and NMR analysis. Yield: 4.6 g. GPC: M_n = 2.26 kDa, M_w = 2.47 kDa, PDI = 1.09.

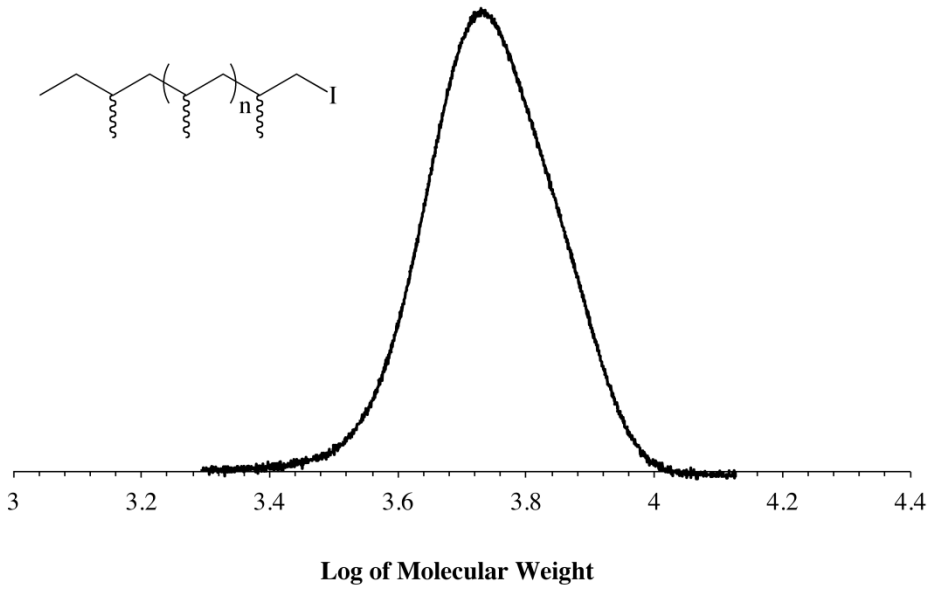

SI 2.1. GPC chromatograph of *a*PP-*t*-I.

Preparation of Al(*a*PP)$_3$ stock solution: In a 250 mL Schlenk flask, to a 20 mL toluene solution of cocatalyst **3** (19.4 mg, 0.021 mmol) at 0 ºC were added the precatalyst **1** (9.1 mg, 0.020 mmol), $ZnEt_2$ in 2 wt% toluene solution (0.124 g, 2.5 mmol, 1 equiv. to **1**) and Al(*i*Bu)$_3$ (0.397 g, 2 mmol, 100 equiv. to **1**). The flask was then pressurized to 5 psi with propene and the pressure was maintained for 20.5 h, 36 h, and 38 h with stirring. Then propene was pumped away via vacuum for 30 min at 0 ºC. Aliquots were taken out for GPC and NMR analysis. The bright yellow Al(*a*PP)$_3$ toluene solution was kept at -25 ºC in freezer. GPC: M_n = 5.49 kDa, M_w = 5.69 kDa, PDI = 1.04.

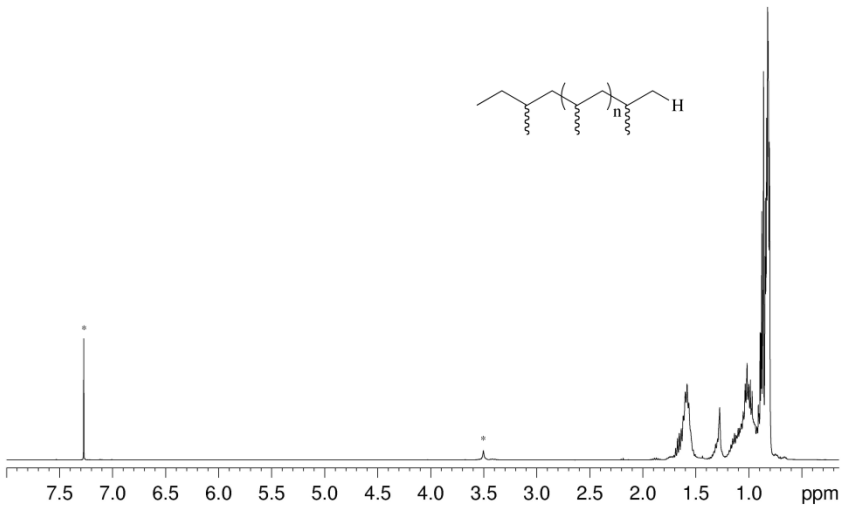

SI 2.2. ^{1}H NMR (400 MHz, chloroform-d_1, 25 °C) of methanol quenched Al(aPP)$_3$/Tol stock solution.

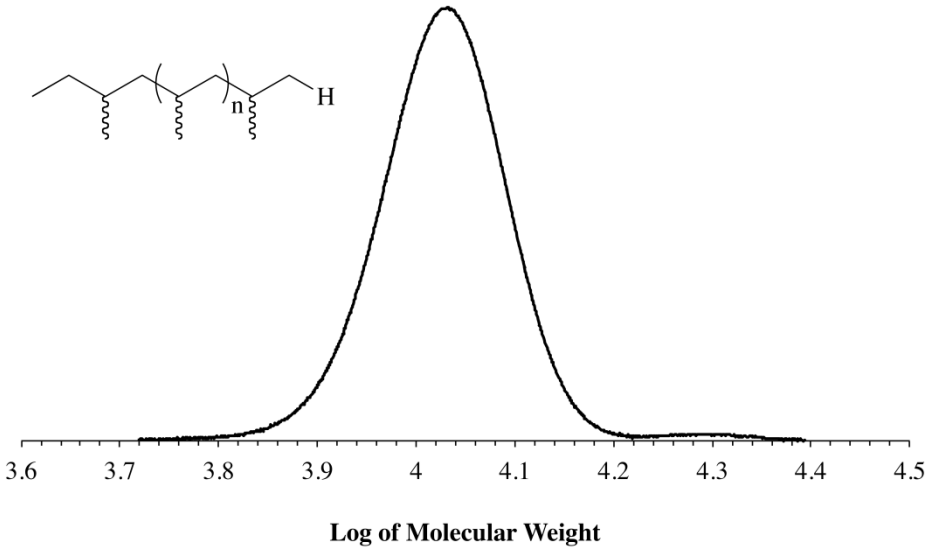

SI 2.3. GPC chromatograph of methanol quenched Al(aPP)$_3$/Tol stock solution.

Preparation of *a*PP-t-OH: The Al(*a*PP)$_3$/ Tol stock solution was transferred to a 100 mL Schlenk flask and placed under dinitrogen at -35 °C for 10 min with stirring. The reaction flask was then pressurized to approximately 3 psi with dioxygen passed over molecular sieves and Dri-Rite for 3 h with the temperature allowed to fluctuate between -35 °C and -25 °C before quenching with 2 mL of acidic methanol. Toluene was removed in *vacuo*, and then the polymer was dissolved in chloroform and purified through 400-mesh silica gel. Solvent was removed under *vacuo* then the final product was collected and dried overnight in *vacuo* before GPC, NMR, DSC and TGA analyses.

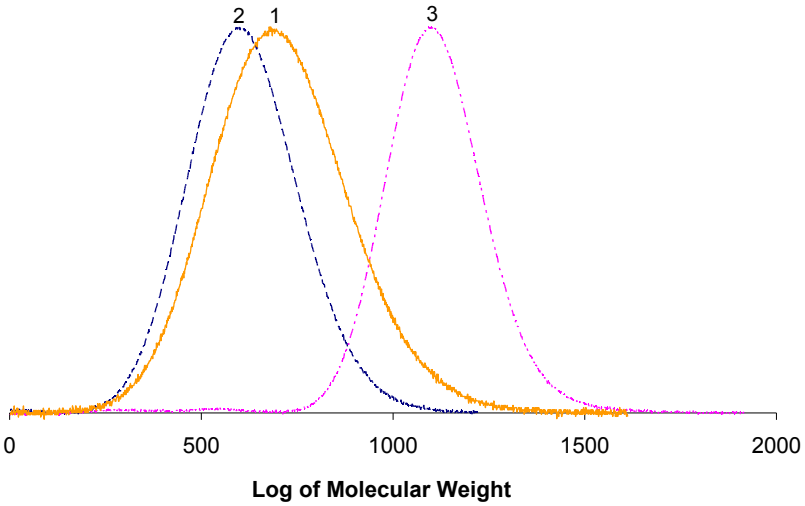

SI 2.4. GPC chromatographs from 1-hydroxy-*a*PP products, where the orange, blue, and pink chromatographs correspond to entries 1-3 in Table 1, respectively.

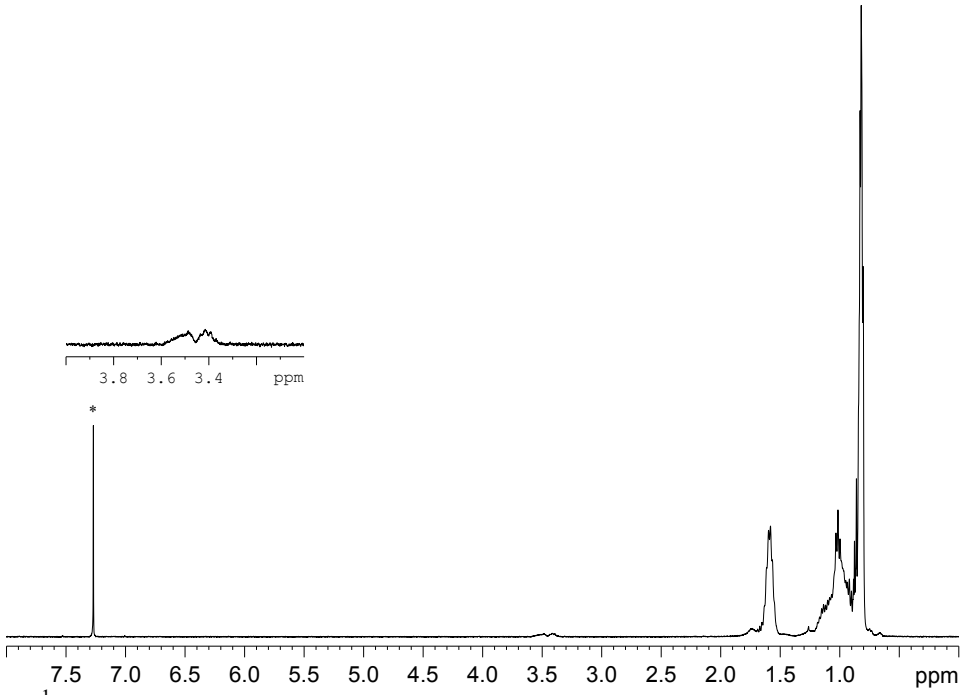

SI 2.5. ^{1}H NMR (400 MHz, chloroform-d_1, 25 ºC) spectrum of 1-hydroxy-*a*PP, corresponding to Entry 1 in Table 1, with the expansion showing the hydroxyl proton and solvent peaks are denoted by asterisks.

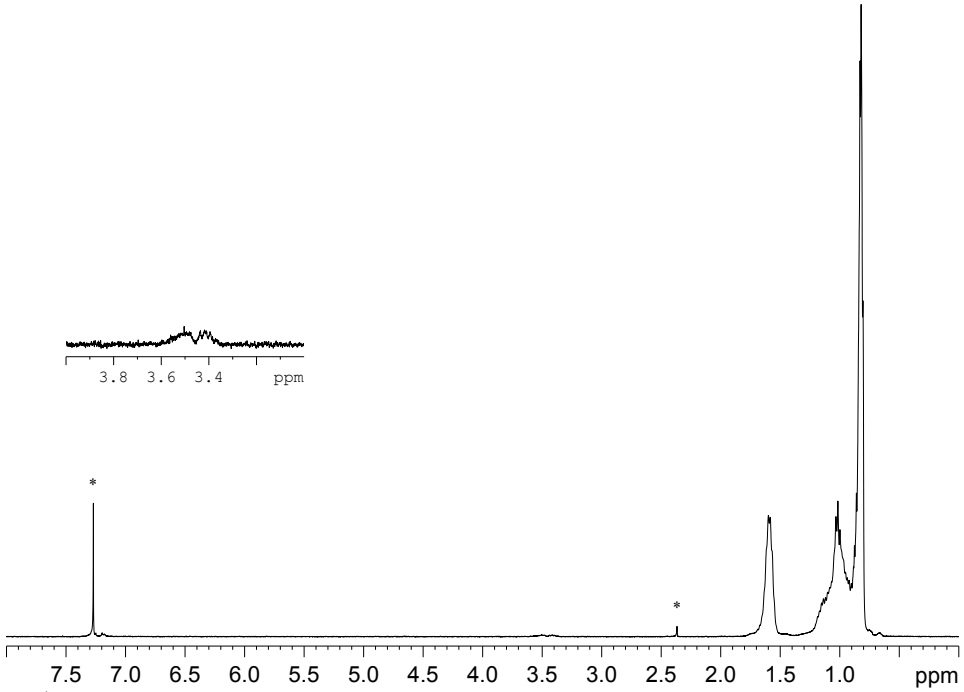

SI 2.6. ^{1}H NMR (400 MHz, chloroform-d_1, 25 ºC) spectrum of 1-hydroxy-*a*PP, corresponding to Entry 2 in Table 1, with the expansion showing the hydroxyl proton and solvent peaks are denoted by asterisks.

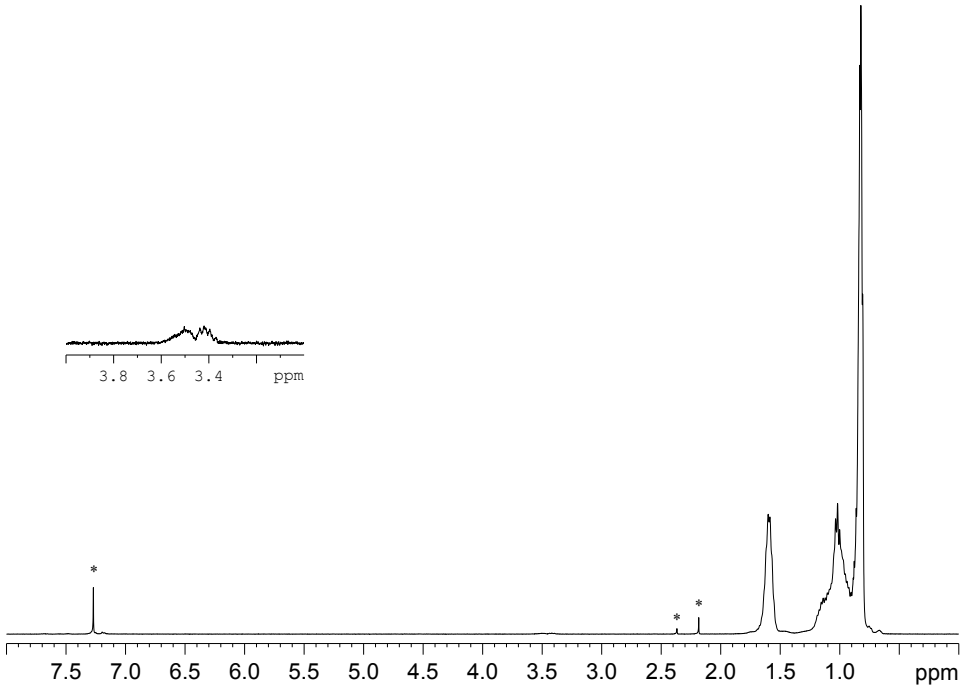

SI 2.7. ^{1}H NMR (400 MHz, chloroform-d_1, 25 ºC) spectrum of 1-hydroxy-*a*PP, corresponding to Entry 3 in Table 1, with the expansion showing the hydroxyl proton and solvent peaks are denoted by asterisks.

Preparation of 1-[I][PPh$_3$]-*a*PP: In a 50 mL Schlenk flask, to 15 mL dry DMF was added 1.0 g triphenylphosphine and 0.5 g 1-iodo-*a*PP dissolved in 1 mL hot toluene. The reaction mixture was allowed to reflux at 110 ºC for 6 days under N_2, after which the solution was precipitated into 100 mL methanol. The crude product was collected via removing all the volatiles under vacuum, followed by washing with chloroform twice and then pumping away chloroform to remove residual DMF. The final product was collected and dried in *vacuo* before NMR and MALDI-TOF-MS analyses.

Preparation of allyl functionalized *a*PP from Grignard: To a 100 mL Schlenk flask was added a polymer solution of 0.5 g *a*PP-*t*-I (0.2 mmol, M_n = 2.50 kDa, PDI=1.07) in THF and 0.48 mL Li_2CuCl_4 (0.002 mmol of 0.10 M in THF) under N_2 atmosphere. 0.6 mL allylmagnesium bromide (0.6 mmol of 1 M in Et_2O) dropwise over approximately 30 min at 0 ^{o}C under nitrogen atmosphere. The orange reaction solution

changed to clear and then to black overtime. The reaction solution was stirred at 0 ^{o}C for 1 h. The solution was then quenched with 20% aqueous acetic acid after which the color changed from black to clear with a grey suspension and then to light purple. The polymer solution was washed with diethyl ether three times to extract the polymeryl species. A saturated aqueous sodium bicarbonate solution was used to wash the Et_2O polymer solution. Excess water was removed by stirring over magnesium sulfate then the polymer solution was dried under *vacuo* to remove volatiles. The final product was dissolved in chloroform and filtered through Celite then analyzed by GPC and NMR analysis. Yield: 0.39 g, GPC: M_n = 5.07 kDa, M_w = 5.58 kDa, PDI = 1.10 (bimodal).

Preparation of *a*PP-*t*-H from *a*PP-*t*-Li: In a 100 mL Schlenk flask, to 2 mL Et_2O solution of 3.16 mL *t*-BuLi (9.0 mmol, 6 equiv. to *a*PP-*t*-I, 2.85 M in pentane) at -82 ºC was added 2.22 g *a*PP-*t*-I (1.43 mmol, M_n = 2.54 kDa by GPC, M_n = 1.55 kDa by ^{1}H NMR, PDI = 1.08) in 8 mL Et_2O dropwise over 30 min. The reaction was stirred at -82 ºC for 1 h, and then warmed up to room temperature in 2 h with stirring. An aliquot (0.5 mL) was then quenched with MeOH and dried under *vacuo* to remove volatiles before for ^{1}H NMR analysis in $CDCl_3$. GPC of *a*PP-*t*-H: M_n = 3.47 kDa, M_w = 3.75 kDa, PDI = 1.08.

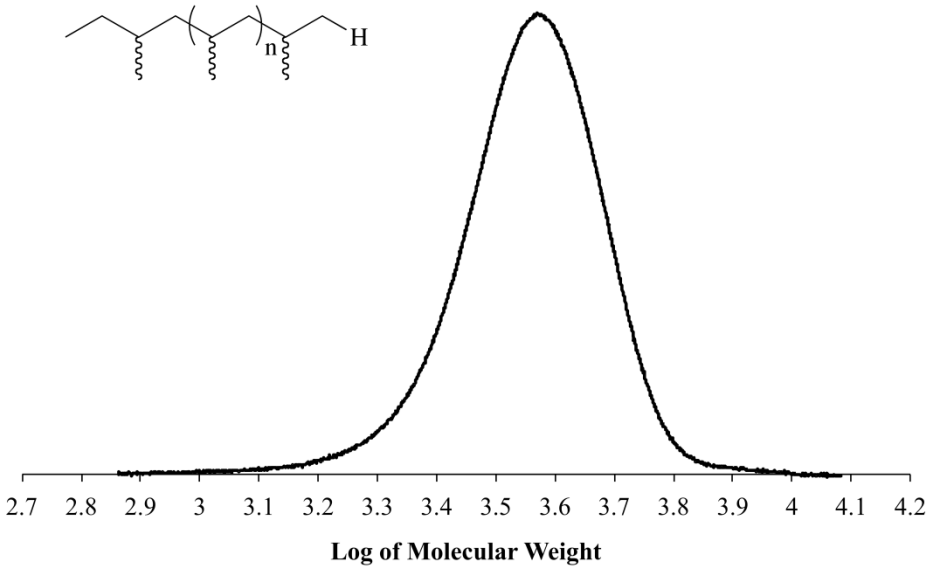

SI 2.8. GPC chromatograph from *a*PP-*t*-H product generated from MeOH quenching of *a*PP-*t*-Li .

Preparation of allyl functionalized *a*PP from *a*PP-*t*-Li: To a 100 mL Schlenk flask with 2 mL Et_2O was added 3.16 mL *t*-BuLi (9.0 mmol, 6 equiv. to *a*PP-*t*-I, 2.85 M in pentane) at -82 ºC over 15 min and allowed to stir for 1 h. A polymer solution of 2.22 g *a*PP-*t*-I (1.43 mmol, M_n = 2.54 kDa by GPC, M_n = 1.55 kDa by ^{1}H NMR, PDI = 1.08) in 8 mL Et_2O was added to the reaction flask at -82 ºC over 30 min. The reaction solution was stirred at -82 ºC for 1 h and then warmed to r.t. over 2 h before being stirred at r.t. overnight under N_2 atmosphere. After stirring overnight, the volatiles were pumped away and the crude product was dissolved in 10 mL $CHCl_3$ and precipitated into 400 mL MeOH and stirred overnight. The following day, the MeOH was decanted and the polymer redissolved in $CHCl_3$ then filtered through silica gel twice. Volatiles were pumped away for a second time to give the final product for NMR and GPC analysis. Yield: 0.98 g. GPC: M_n = 3.67 kDa, M_w = 4.06 kDa, PDI = 1.11.

Preparation of *a*PP-*t*-N_3: In a 250 mL Schlenk flask, 5.00 g *a*PP-*t*-I (2.06 mmol, M_n = 2.43 kDa, PDI = 1.05) was dissolved in 10 mL THF and 40 mL DMF mixed solution. Then 6.70 g NaN_3 (2.06 mmol, 50 equiv. to *a*PP-*t*-I) was added and the reaction solution was heated to 110 ºC overnight. After stirring overnight, the volatiles were pumped away and the crude product was dissolved in 20 mL $CHCl_3$ and precipitated into 800 mL MeOH and stirred overnight. The following day, the MeOH was decanted and the polymer redissolved in $CHCl_3$ then filtered through Celite. Volatiles were pumped away for a second time to give the final product for NMR and GPC analysis. Yield: 4.05 g. GPC: M_n = 2.95 kDa, M_w = 3.11 kDa, PDI = 1.06.

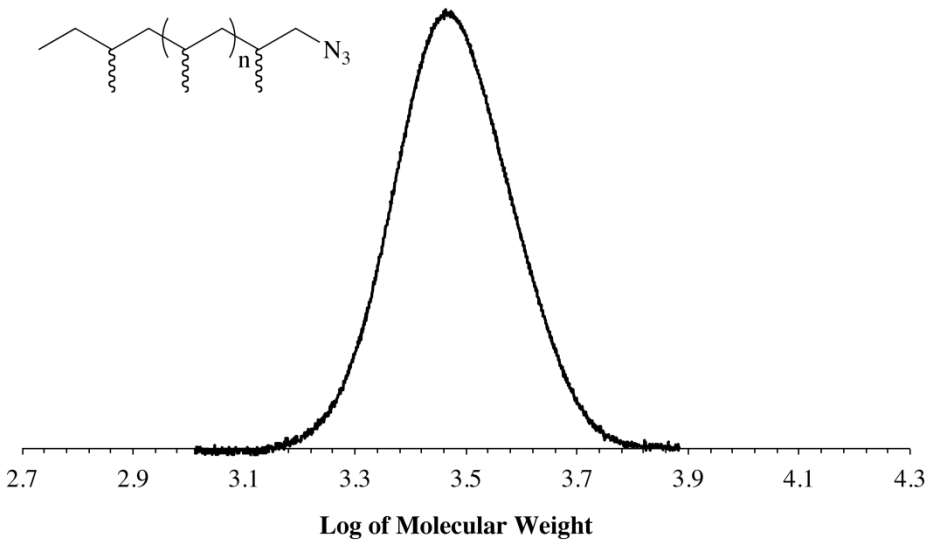

SI 2.9. GPC chromatograph of *a*PP-*t*-N_3.

Preparation of acrylate/methacrylate functionalized *a*PP from aPP-t-N_3: Fresh solutions of propargyl acrylate (275 mg, 2.5 X 10^{-3} mol) or propargyl methacrylate (300 mg, 2.4 X 10^{-3} mol) in 1 mL DMF, $CuSO_4$ (20 mg, 1.25 X 10^{-4} mol) in 1 mL DMF, and sodium ascorbate (50 mg, 2.5 X 10^{-4} mol) in 1 mL DMF were prepared in the glove box

under dinitrogen atmosphere. A solution of *a*PP-*t*-N_3 (0.77 g, 0.318 mmol, M_n = 5.51 kDa by GPC, M_n = 2.43 kDa by ^{1}H NMR, PDI = 1.05) in 5 mL DMF was also prepared in the glove box and added to a 100 mL Schlenk flask. Solutions of propargyl acrylate (0.351 mL, 96.46 mg, 0.954 mmol, 3 equiv.) or propargyl methacrylate (0.395 mL, 118.39 mg, 0.954 mmol, 3 equiv.), sodium ascorbate (0.414 mL, 20.68 mg, 0.1044 mmol, 0.3 equiv.), and $CuSO_4$ (0.381 mL, 7.61 mg, 0.0477 mmol, 0.15 equiv.) were added to the reaction flask. The reaction was heated overnight under nitrogen flow. A color change from yellow to brown was observed. The next day the reaction was cooled to room temperature then quenched with methanol. The volatiles were pumped away and the crude product was dissolved in 20 mL $CHCl_3$ and precipitated into 800 mL MeOH and stirred overnight. The following day, the MeOH was decanted and the polymer redissolved in $CHCl_3$ then filtered through Celite. Volatiles were pumped away for a second time to give the final product for NMR and GPC analysis. Yield of *a*PP-*t*-acrylate: 0.50 g. GPC of *a*PP-*t*-acrylate: The M_n, M_w, and PDI data were unattainable given ongoing instrumentation issues. Yield of *a*PP-*t*-methacrylate: 0.54 g. GPC of *a*PP-*t*-methacrylate: M_n = 6.02 kDa, M_w = 6.35 kDa, PDI = 1.06.

Preparation of *a*PP-*t*-NH_2: In a 100 mL Schlenk flask, 0.76 g a*PP*-t-N_3 (0.31 mmol, M_n = 5.51 kDa by GPC, M_n = 2.43 kDa by ^{1}H NMR, PDI = 1.05) was dissolved in 50 mL THF. Then 0.119 g $LiAlH_4$ (3.13 mmol, 10 equiv. to *a*PP-*t*-N_3) and the reaction solution was refluxed overnight at 70 ºC under N_2 flow. After stirring overnight, the solution was precipitated into 800 mL MeOH and stirred overnight once again. The solution was subsequently filtered to yield a grey solid. The crude polymer was stirred in a 300 mL 50/50 mixture of THF/ basic H_2O. The organic layer was isolated and stirred in the

presence of anhydrous $MgSO_4$ to remove residual water. The THF polymer solution was then filtered through Celite and dried to give the final product for NMR and GPC analysis. Yield: 0.50 g. GPC: M_n = 4.54 kDa, M_w = 4.88 kDa, PDI = 1.07.

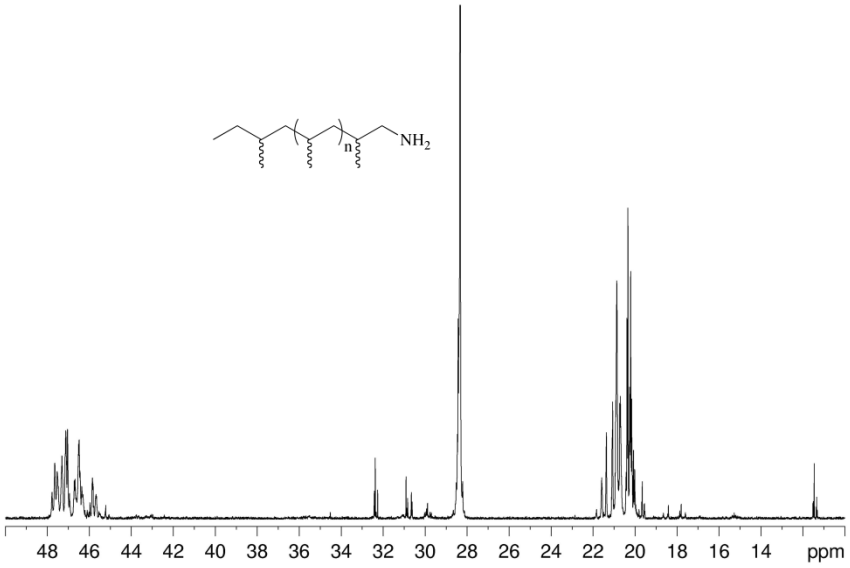

SI 2.10. ^{13}C NMR (150 MHz, 1,1,2,2-$C_2D_2Cl_4$, 90 °C) of amine terminated *a*PP.

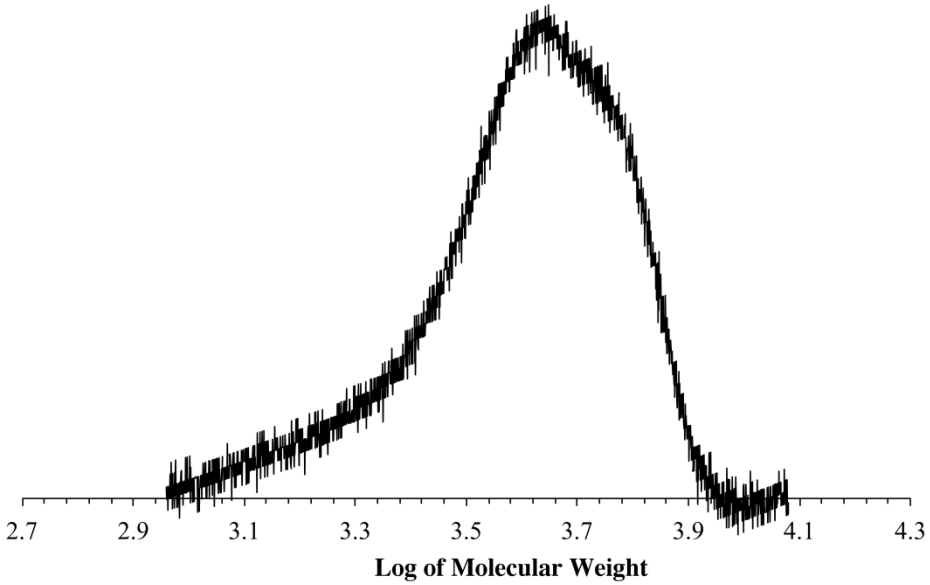

SI 2.11. GPC chromatograph of *a*PP-*t*-NH_2.

Preparation of TMS alkyne functionalized *a*PP from *a*PP-*t*-I: In a 100 mL Schlenk flask, to 3 mL Et_2O solution of *a*PP-*t*-I (1.0 g, M_n = 5.51 kDa by GPC, M_n = 2.43 kDa by ^{1}H NMR, PDI = 1.05) was added 4.93 mL (trimethylsilyl)ethynyl lithium (2.47 mmol, 6 equiv. to *a*PP-*t*-I, 0.5 M in THF) at -82 ºC dropwise over 10 min. The reaction was stirred at -82 ºC for 1 h, and then warmed up to room temperature over 1.5 h with stirring. The reaction mixture was then quenched with MeOH and dried under *vacuo* to remove volatiles before for ^{1}H and ^{13}C NMR analysis. Yield: 0.98 g. GPC: M_n = 5.50 kDa, M_w = 6.19 kDa, PDI = 1.12 (bimodal).

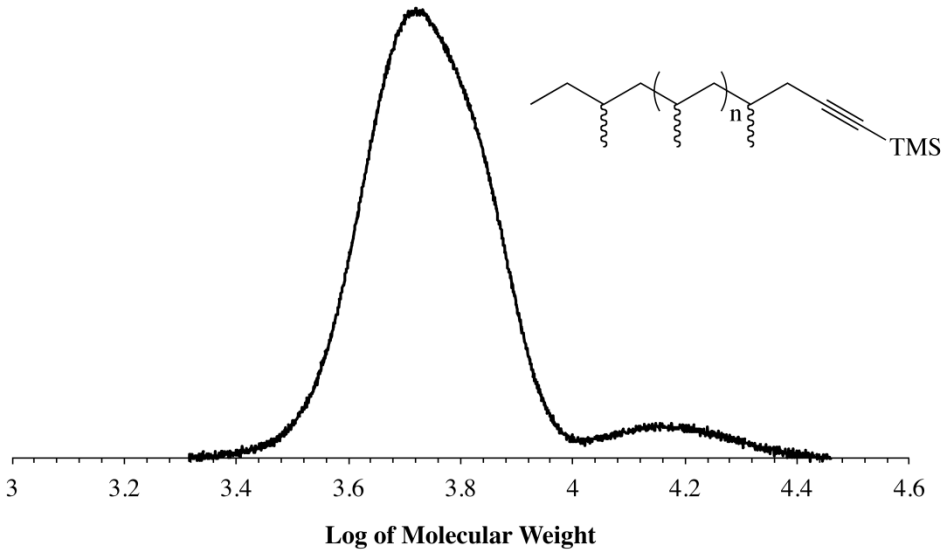

SI 2.12. GPC chromatograph of TMS alkyne functionalized *a*PP.

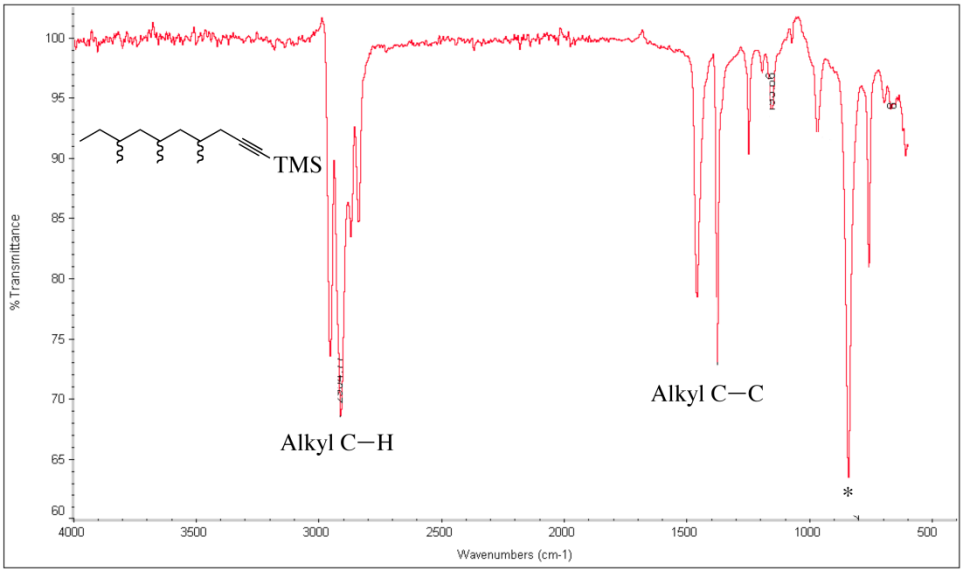

SI 2.13. IR of TMS alkyne functionalized *a*PP.

Preparation of thioacetate functionalized *a*PP from potassium thioacetate: In a 100 mL Schlenk flask, 1.00 g *a*PP-*t*-I (0.41 mmol, M_n = 5.51 kDa by GPC, M_n = 2.43 kDa by ^{1}H NMR, PDI = 1.05) was dissolved in 5 mL THF and 15 mL DMF mixed solution. Then 0.094 g potassium ethanethioate (0.41 mmol, 2 equiv. to *a*PP-*t*-I) was added and the reaction solution was heated to 110 ºC overnight. After stirring overnight, the reaction was quenched with methanol and the volatiles were pumped away and the crude product was dissolved in 10 mL $CHCl_3$ and precipitated into 400 mL MeOH and stirred overnight. The following day, the MeOH was decanted and the polymer redissolved in $CHCl_3$ then filtered through Celite twice. Volatiles were pumped away for a second time to give the final product for NMR and GPC analysis. Yield: 1.01 g. GPC: M_n = 5.30 kDa, M_w = 5.72 kDa, PDI = 1.08.

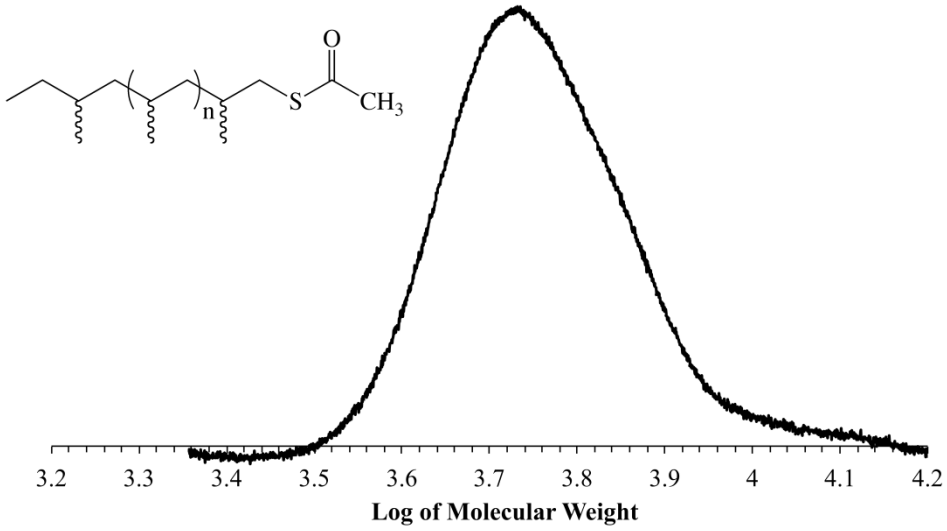

SI 2.14. GPC chromatograph of thioacetate functionalized *a*PP.

Preparation of thiol functionalized *a*PP from thioacetate terminated *a*PP: In a 100 mL Schlenk flask, 0.502 g thioacetate functionalized *aPP* (0.206 mmol, M_n = 5.30 kDa by GPC, M_n = 2.43 kDa by ^{1}H NMR, PDI = 1.08) was dissolved in 50 mL THF. Then 0.078 g $LiAlH_4$ (2.06 mmol, 10 equiv. to *a*PP-*t*-$SOCH_3$) and the reaction solution was refluxed overnight at 70 ºC under N_2 flow. After stirring overnight, the solution was precipitated into 800 mL MeOH and stirred overnight once again. The solution was subsequently filtered through Celite and dried to give the final product for NMR and GPC analysis. Yield: 1.007 g. GPC: M_n = 6.52 kDa, M_w = 7.71 kDa, PDI = 1.18 (polymodal).

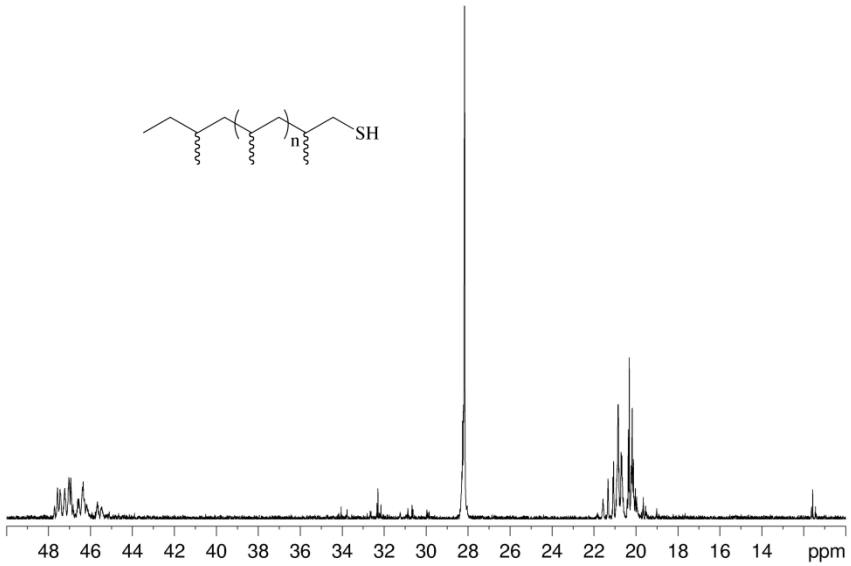

SI 2.15. ^{13}C NMR (150 MHz, 1,1,2,2-$C_2D_2Cl_4$, 90 °C) of *a*PP-*t*-SH.

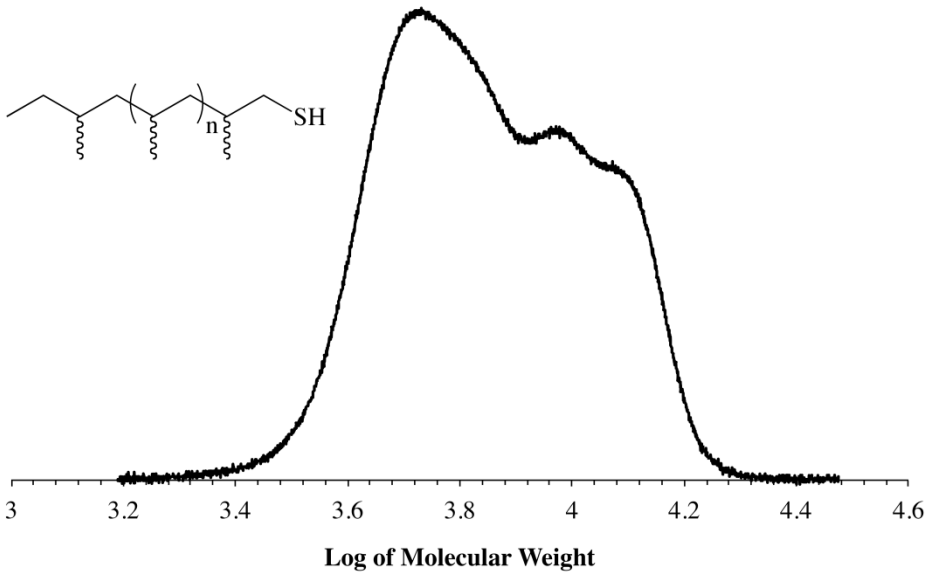

SI 2.16. GPC of thiol functionalized *a*PP.

Chapter 3 : Precision Polymers from Living Coordinative Chain Transfer Polymerization (LCCTP) of Sterically Encumbered Monomers, Norbornene and β-Citronellene

3.1 Background

The previous chapter discussed the polymerization of simple monomers, such as ethene and propene via living coordinative chain transfer using **Precatalyst III** activated by **Cocatalyst I** and their functionalization to produce value-added polyolefin materials. The use of LCCTP for the preparation of copolymers based on ethene and/or propene with sterically encumbered monomers (i.e. non-terminal alkenes or alkenes that contain substitutions *alpha* to the alkene unit) that are more difficult to polymerize than ethene will be examined to determine the scope of the Sita catalyst system. Norbornene and β-Citronellene were chosen for study not only because they are sterically encumbered (per the above definition of being sterically encumbered) but also due to the following desirable properties of these particular monomers: 1) Norbornene is a strained bicyclic monomer so readily partakes in polymerization reactions that release the ring strain (discussed in detail in subsequent section); 2) β-Citronellene contains two alkene units per monomer so polymerization using one of the alkenes would lead to a polymer chain containing multiple alkene handles that could be used for post functionalization. We were also interested in the co-polymerization of these two alkenes with simpler monomers, such as ethene and propene.

3.1.1 Norbornene Polymers

Norbornene, bicyclo[2.2.1]hept-2-ene, is a very valuable monomer that is sterically encumbered because of the tertiary centers (at the 1 and 4 position) that are *alpha* to the alkene unit. Norbornene can be polymerized by three different polymerization techniques as shown in Scheme 3.1, each allowing access to a different type of polymeric material with distinctive structures and properties.[172,173]

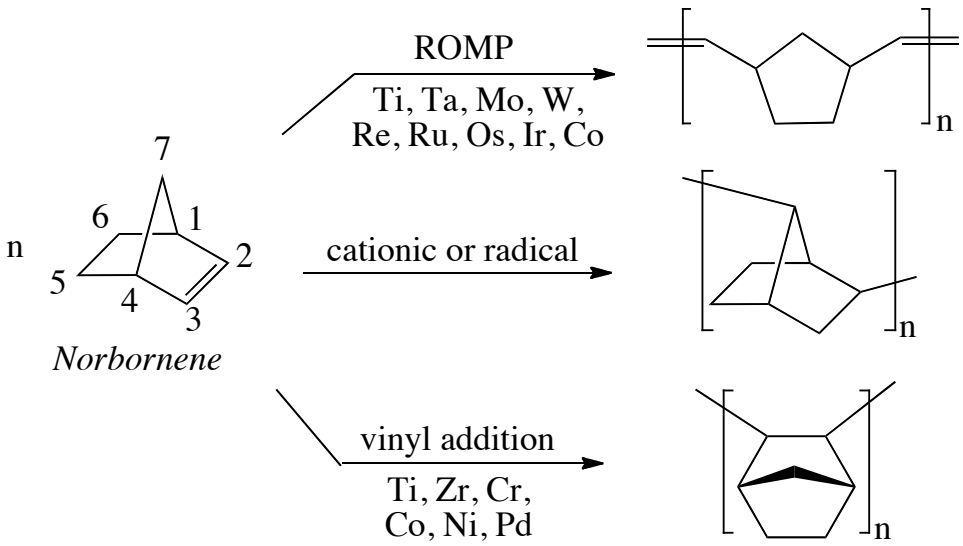

Scheme 3.1. Schematic representation of the three different types of polymerization of norbornene. Reproduced from Janiak and coworkers.[172,173]

Amongst the three polymerization routes shown in Scheme 3.1, ring opening metathesis polymerization is the most well known.[174] The success of this method for polymerizing norbornene is due to the release of ring strain during the polymerization process, generating a polyalkene containing double bonds along the polymer backbone that could be crosslinked to generate elastomeric materials with widespread applicability. Vulcanized polynorbornene materials from ROMP for example, are used in the

production of antivibration, sound damping, and high friction materials such as engine mounts, bumpers, and transmission belts. Moreover, specific grades of polynorbornene, manufactured as Norsorex®[175], have a high affinity for hydrocarbons and can absorb up to ten times its own weight. Consequently these materials, in both powder and rubber form, are routinely used to cleanup oil spills. The industrial production of polynorbornene generally employs heterogeneous catalysts such as tungsten, molybdenum, rhenium or ruthenium. These catalysts are usually used as metal halides (e.g. $RuCl_3$), metal oxides or metal oxochlorides in combination with alkylating agents (e.g. R_4Sn, Et_2AlCl) and promoting agents (e.g. O_2, EtOH, PhOH).[174,176] Conversely, homogenous catalysts based on tungsten[177-182], molybdenum[183-186], ruthenium[187-189], titanium[190], tantalum[191], and osmium[192] have been utilized in academia towards the synthesis of polynorbornene by ROMP. It has been observed that catalyst selection and reaction parameters are essential for the production of polymers with specific properties because these parameters impact structural features such as stereochemistry and tacticity, which influence physical properties such as glass transition temperature and polymer permeability/stability.[193]

The second polymerization pathway shown in Scheme 3.1 (cationic or radical), was first described by Makowiski and coworkers in 1967 for the synthesis polynorbornene.[194-196] This method for norbornene homopolymerization uses typical polymerization initiators such as azoisobutyronitrile (AIBN) for the radical type and $EtAlCl_2$ for the cationic type of polymerization. These modes of polymerization generate polymers having 2,7-connectivity of the norbornene monomer, but can only produce oligomers thus limiting applicability.

The third method for norbornene polymerization, shown in Scheme 3.1, is vinyl addition to norbornene (catalyzed by various transition metals). This method preserves the bicyclic structural unit of the norbornene and the consecutive enchainment is through the double bond only. This reaction is influenced by the ring strain of the cyclic olefin and by the non-planarity of the reacting double bond, which has a symmetric out-of-plane deformation. Polynorbornene produced via this method, like other cycloaliphatic polymers, are known to have high decomposition temperatures, small optical birefringence and high transparency, making them suitable for use in the microelectronic industry.[197,198] However, a limitation of these materials is that their melting points are typically higher (T_m ~ 600 °C) than their decomposition temperatures making processing challenging.[172,199] As a work around solution to this problem, cyclic olefin copolymers (COCs) based on norbornene or norbornene derivatives have been pursued extensively.[200] Although copolymerization with sterically encumbered monomers generally leads to reduction in catalytic activity, the end-use properties and processibility of the final polyolefin materials can be significantly improved with even small incorporated amounts of these comonomers. In this regard, COCs with various comonomer content and microstructures are known to exhibit high transparency and glass transition temperatures (T_g), good processibility, low dielectric constants, biocompatibility, and stability against chemical degradation that render them perfect candidates for use in a broad range of applications in optical, electric and medical fields.[201] In fact, Hoechst (now Ticona) and Mitsui Sekka have jointly trademarked TOPAS®, a highly transparent amorphous thermoplastic COC based on ethene and norbornene synthesized via vinyl addition with a

metallocene catalyst. These materials have wide use applicability in compact discs, toner binder for colored printers, and food and medical packaging.[202]

Considering the industrial importance of ethylene-norbornene (E-NB) based materials, and the need to expand the range of polyolefins that are commercially available, the copolymerization of NB with α-olefins was investigated under LCCTP conditions. Much like other polymeric materials, the properties of these NB based COCs depend on parameters such as the comonomer composition, the distribution of comonomers within the chain, and the chain stereoregularity. These features are influenced by the catalyst precursor used for their synthesis and can therefore be different for each catalyst system and give access to various grades of E-NB polymers. Given that LCCTP allows precise control over molecular weight and composition, while maintaining narrow molecular weight distributions, this polymerization method was investigated for the synthesis of NB co- and terpolymers.[4,69,203-205]

3.1.2 β-Citronellene Polymers

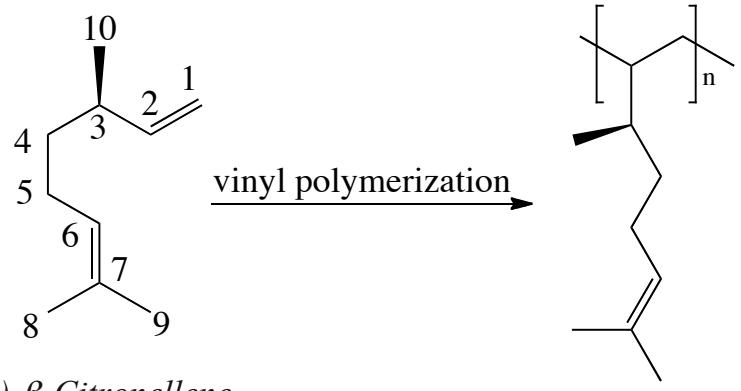

(-)-β-Citronellene

Scheme 3.2. Schematic representation of vinyl polymerization of (-)-β-Citronellene.

Within the realm of sterically encumbered monomers, dienes are also of interest, as they allow incorporation of vinyl groups in the polymer backbone that can be

subsequently functionalized for use in a variety of applications[206], see Scheme 2. The living coordination copolymerization (LCP) of ethene and propene with (-)-β-citronellene (βC), a biomass derived chiral monomer available on a commodity scale from terpene feedstocks[207,208] was also explored for the synthesis of optically active polymers having main chain chirality, which guarantees control over "handedness" and tacticity of the resulting unsaturated polymer.[206]

3.2 Traditional Living Coordination Polymerization (LCP) of Norbornene

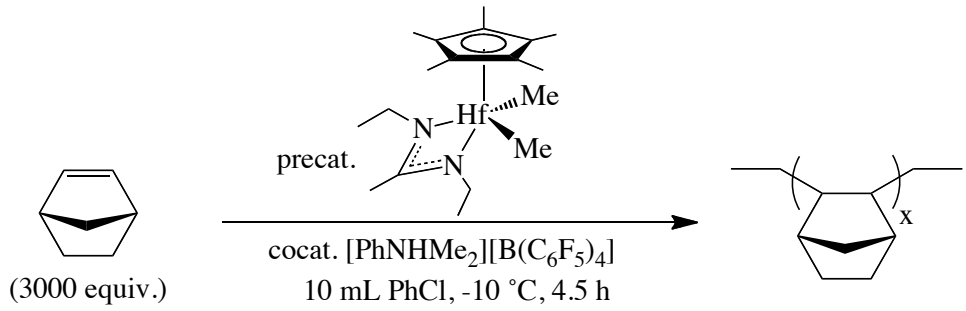

Scheme 3.3. Homopolymerization of norbornene using Precatalyst III.

The homopolymerization of norbornene using **Precatalyst III** activated by **Cocatalyst I** was attempted under non-chain transfer conditions according to Scheme 3 in order to assess the activity of this catalyst system. The catalyst solution (light yellow in color if the catalyst is active) was added to a solution of norbornene in chlorobenzene at -10 ºC. The reaction was allowed to stir at -10 ºC for 4.5 h. The reaction solution remained yellow throughout and no change in viscosity was observed. After 4.5 h the reaction was quenched with methanol and titrated into 800 mL acidic methanol solution in order to precipitate the polymer product. No polymer product was obtained, although the formation of oligomers could not be excluded. It was rationalized that failure to

homopolymerize norbornene using **Precatalyst III** was due to the inability of this catalyst system to accommodate a growing polymer chain containing consecutive sterically encumbered norbornene units. Therefore, the ability to synthesize an ethene-norbornene copolymer (see Section 4.3), whereby the C2 unit from the smaller ethene monomer would provide a "buffer" region to separate the larger norbornene units from one another was investigated.

3.3 LCCTP of ethene and norbornene

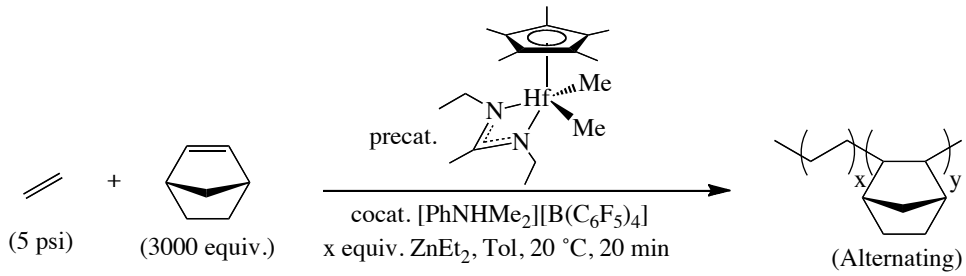

Scheme 3.4. Synthesis of ethene/norbornene copolymers as a function of chain transfer mediator concentration.

The LCCTP copolymerization of ethylene and norbornene was achieved using the transition-metal initiator prepared from a stoichiometric mixture of **Precatalyst III** and **Cocatalyst I** to produce poly(ethene-*co*-norbornene) as shown in Scheme 4. The structural identity of this polymer was confirmed by ^{13}C NMR spectroscopy (Figure 3.2) and DSC (Figure 3.3). As shown in Table 3.1, when an excess of NB (3000 equiv. relative to catalyst) was employed in the comonomer feed, the level of NB incorporation in the copolymer remained constant at ~50% regardless of the number of equivalents of $ZnEt_2$ used as the chain transfer mediator.

Table 3.1. Traditional and Chain Transfer Living Coordination Polymerization of ethene with NB.

Run[a]	$ZnEt_2$ (equiv.)	T_p (min)	T_g (°C)	Yield (g)	Comonomer (mol%)[b]
1	-	30	126.6	3.4	47.7
2	20	20	121.3	2.7	50.0
3	50	20	100.6	2.7	50.2
4	100	20	106.8	6.1	49.5
5	200	20	108.1	7.6	51.3

[a]Conditions: **Precatalyst III** (10 μmol), **Cocatalyst I** (10 μ mol) in 40 Tol at 20°C, NB (60 mmol, 3000 equiv. relative to catalyst) and ethene (~5 psi) except for run 1 were **Precatalyst III** (25 μ mol), **Cocatalyst I** (25 μmol) in 10 PhCl , NB (5 mmol, 500 equiv. relative to catalyst) at 25°C and ethene (~5psi) [b]Calculated from ^{13}C NMR data.

^{1}H NMR (Figure 3.1) indicated the absence of olefinic peaks, indicating that the enchainment is at the alkene segment the of norbornene unit.

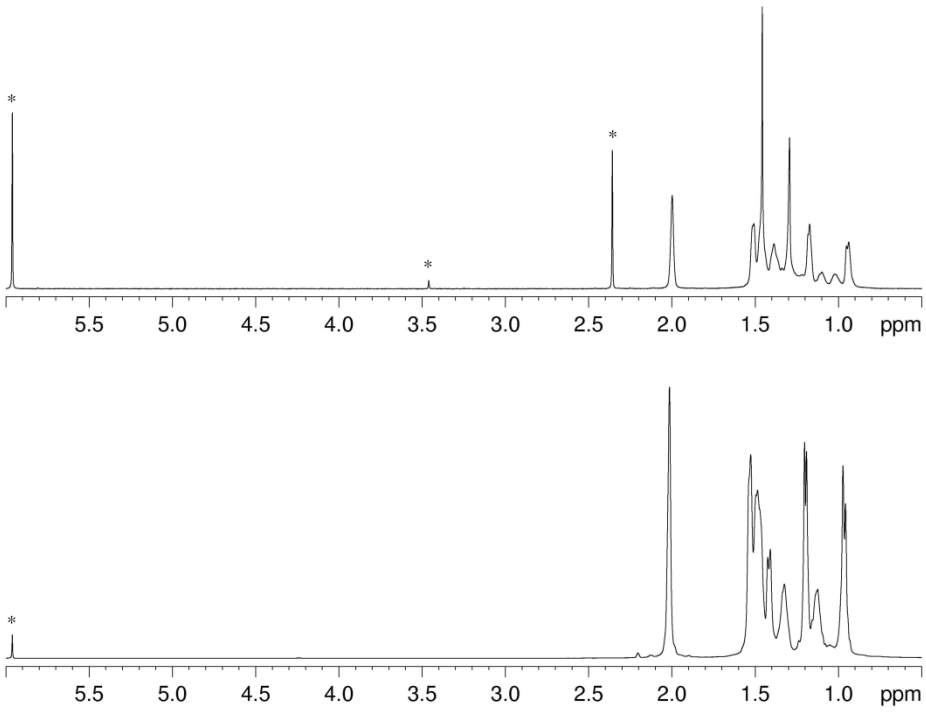

Figure 3.1. ^{1}H NMR (600 MHz, 1,1,2,2-$C_2D_2Cl_4$, 110 ºC) spectrum and resonance assignments for P(E-*co*-NB) copolymers for P(E-*co*-NB) copolymers, from runs 1 and 3 from Table 3.1, synthesized via LCP (top) and LCCTP (bottom) conditions.

^{13}C NMR spectra for these materials confirmed that an alternating copolymer microstructure (E-*alt*-NB) was predominantly obtained each time (see diagnostic ^{13}C NMR peaks at 47.5 and 48 ppm in Figure 3.2). This result is consistent with NB having high comonomer reactivity, relative to E, but due to steric incumberance, NB homopolymerization is strongly disfavored. Indeed, only trace levels of NB-NB dyads can be detected in the ^{13}C NMR spectra of these materials.[209,210]

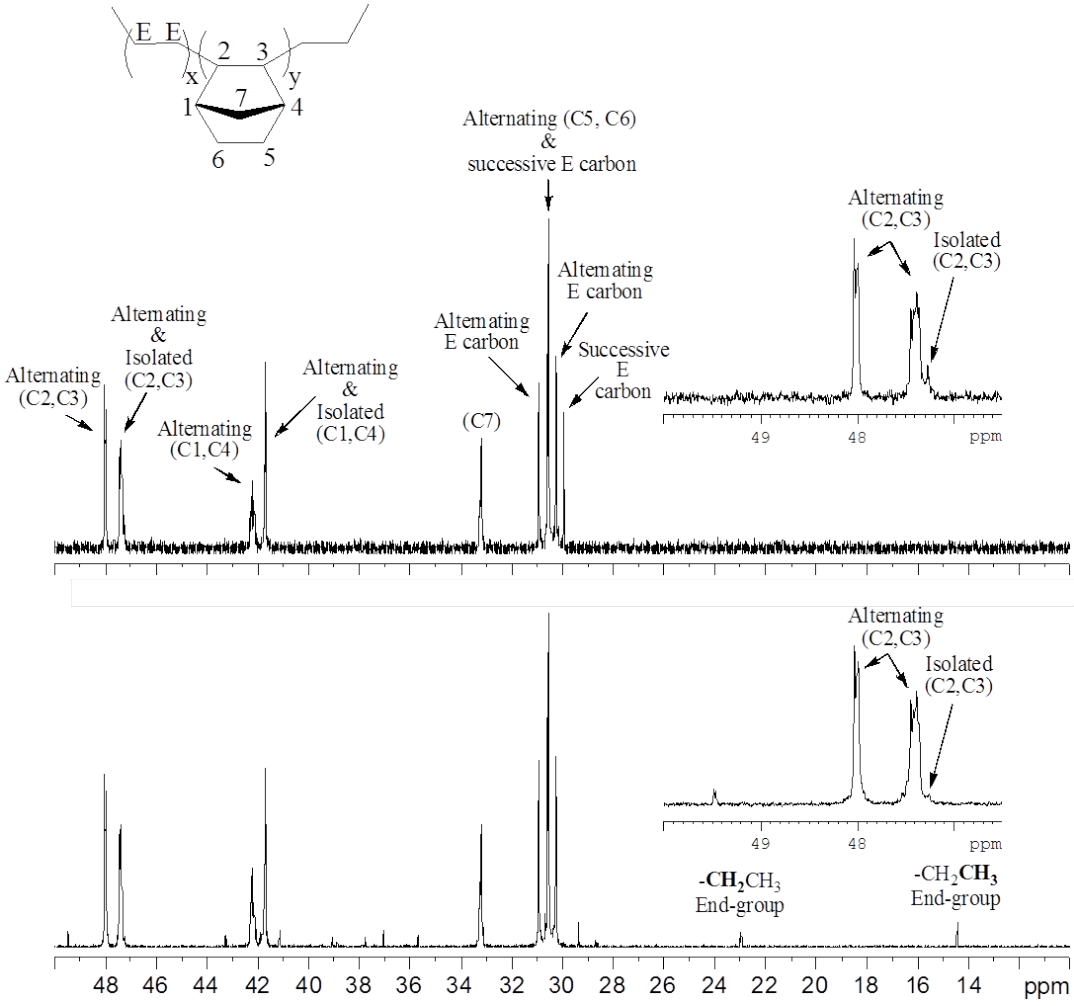

Figure 3.2. ^{13}C NMR (150 MHz, 1,1,2,2-$C_2D_2Cl_4$, 110 ºC) spectrum and resonance assignments for P(E-*co*-NB) copolymers, from runs 1 and 3 from Table 1, synthesized via LCP (top) and LCCTP (bottom) conditions.

The observed increase in yield that was obtained with increasing $ZnEt_2$ equivalents (*cf* runs 2 – 5 in Table 3.1) is consistent with highly efficient chain-transfer occurring between the transition-metal propagating species and the surrogate main-group-metal alkyl. GPC analysis showing a monomodal MW distribution with narrow polydispersity would have augmented the assertion that chain transfer did occur. Unfortunately poly(ethene-*co*-norbornene) was only sparingly soluble in THF, xylene or 1,2,3-trichlorobenzene at room temperature therefore GPC chromatographs of these materials

were unattainable using the in-house GPC Max instrument from Viscotek. Future plans are to analyze these norbornene-based polymers at external facilities that are equipped with high temperature GPCs. Other circumstantial evidences however point to the fact that chain transfer is occurring. For example, increasing the amount of chain transfer reagent led to an increase in the copolymer yield (see Table 3.1). Additionally, the ^{13}C NMR (Figure 3.2A) of the polymer generated under non-chain transfer conditions does not show the end group CH_2CH_3 resonances whereas the ^{13}C NMR (Figure 3.2B) of the copolymer generated under chain transfer conditions contain the end group resonances for CH_2CH_3, implying a decrease in molecular weight with chain transfer use.

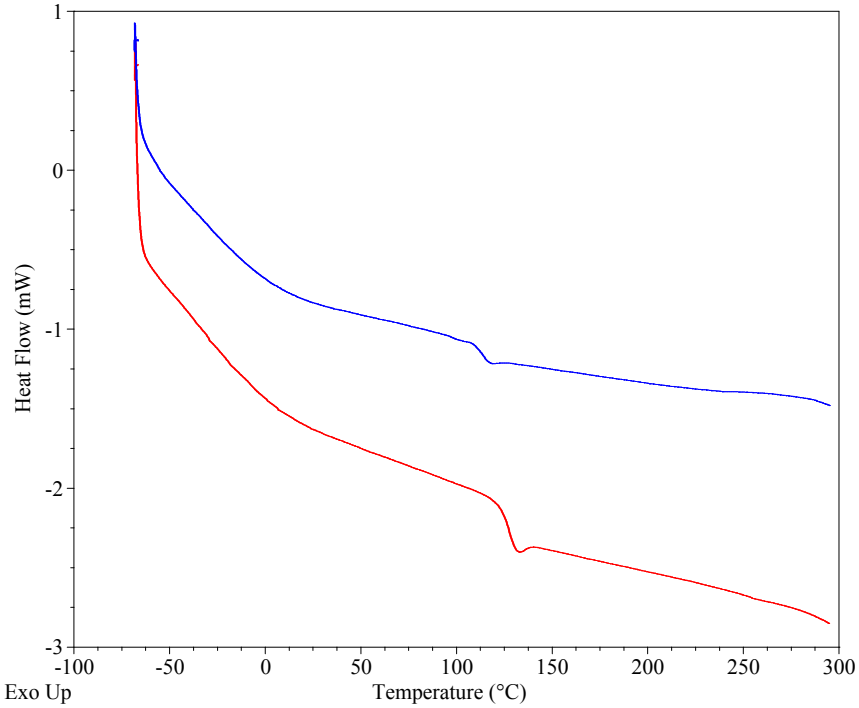

Figure 3.3. DSC curves for P(E-*co*-NB) copolymers synthesized via LCP (red; run 1) and LCCTP (blue run 3) conditions.

A decrease in glass transition temperatures, from 121.3 °C to 108.1 °C, was also observed as the concentration of $ZnEt_2$ in solution was increased and is indicative of the expected decrease in molecular weights of these polymeric materials.

3.4 LCCTP copolymerization of ethene with NB to produce poly(E-co-NB)-blocky-PE

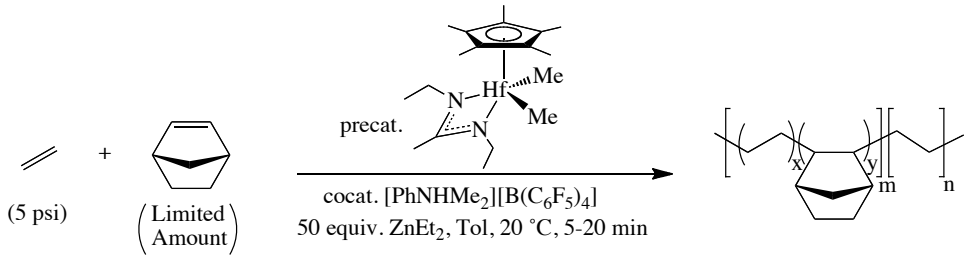

Scheme 3.5. Synthesis of ethene/norbornene block copolymers as a function of norbornene concentration.

In the previous section, alternating ethene/norbornene copolymers were prepared, using excess norbornene monomer. Next, the production of poly(E-*co*-NB)-*b*-PE was investigated using limited amounts of norbornene. The expectation was that by using this strategy, instead of getting alternation between ethyl and norbornyl units in the polymer, a random polymer mainly comprised of polyethyl (PE) units disrupted by isolated norbornyl units would be obtained. By employing the chain transfer mediator $ZnEt_2$, the initiator obtained from **Precatalyst III** and **Cocatalyst I** was able to produce poly(E-*co*-NB)-*b*-PE block copolymers with varying degrees of comonomer incorporation as shown in Table 3.2.

Table 3.2. LCCTP copolymerization of ethene with NB as a function of norbornene feed to produce P(E-*co*-NB)-*b*-PE.

Run[a]	NB (equiv.)	T_g (ºC)	T_m (ºC)	T_c (ºC)	Yield (g)	Comonomer (mol %)[b]	Isolated NB (mol %)[b]
1	50	-	65.3	84.3	0.3	26.5	96.9
2	100	-	71.6	108.0	0.8	30.5	85.3
3	200	-	72.2	97.8	0.9	34.5	65.4
4	500	-	57.4	95.8	0.6	46.9	29.1
5	1000	-	79.2	100.1	1.5	47.0	20.0
6	3000	114.2	-	-	4.2	50.4	5.1

[a]Conditions: **Precatalyst III** (10 μmol), **Cocatalyst I** (10 μmol) and 1.1 M $ZnEt_2$ in toluene (40 mL) at 20 ºC and ethene (~5 psi). Reaction time was 5 min, except in the case of run 10 and 11, which were 7 min and 20 min, respectively. [b] Calculated from ^{13}C NMR data.

When the concentration of NB in the toluene solution was used in limiting amounts, the isolated materials had sharply defined melting and crystallization phase transitions associated with PE-rich segments. However, with larger quantities of NB in the reaction solution, the materials became decidedly amorphous as determined by DSC analysis (see Figure 3.4).

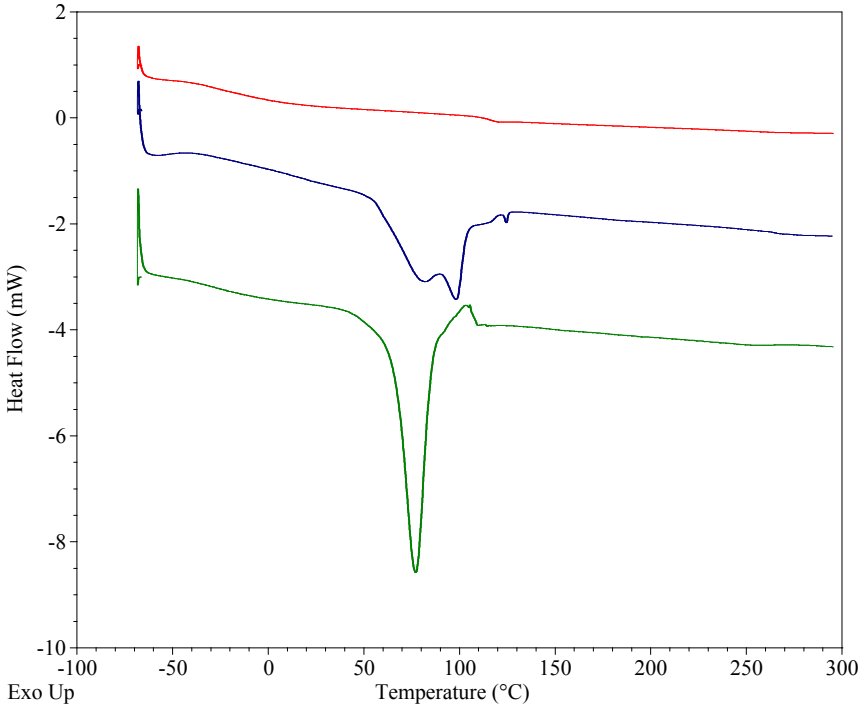

Figure 3.4. DSC curves for P(E-*co*-NB)-b-PE copolymers synthesized via LCCTP with variable amounts of norbornene. Red represents run 1 of Table 2 (3000 equiv. NB), blue represents run 4 of Table 2 (500 equiv. NB) and green represents run 6 of Table 2 (50 equiv. NB).

These observations are in agreement with the ^{13}C NMR spectra shown in Figure 3.5 that confirm lower levels of NB incorporation for the more crystalline materials (the region between 47 and 48 ppm in the ^{13}C NMR spectrum is a good window to determine the level of comonomer alternation). The data in Table 3.2 also clearly reveals that the level of NB comonomer incorporation in the final material is dependent upon the concentration of NB in solution. The comonomer incorporation increases from 26.5% to 50.4% as the equivalents of NB increases from 50 to 3000. Also important is that as the comonomer feed becomes increasingly limited in NB, a shift from an E-*alt*-NB copolymer microstructure to one that consists almost exclusively of isolated NB units is evident by both Table 3.2 and Figure 3.5 (^{13}C NMR data).

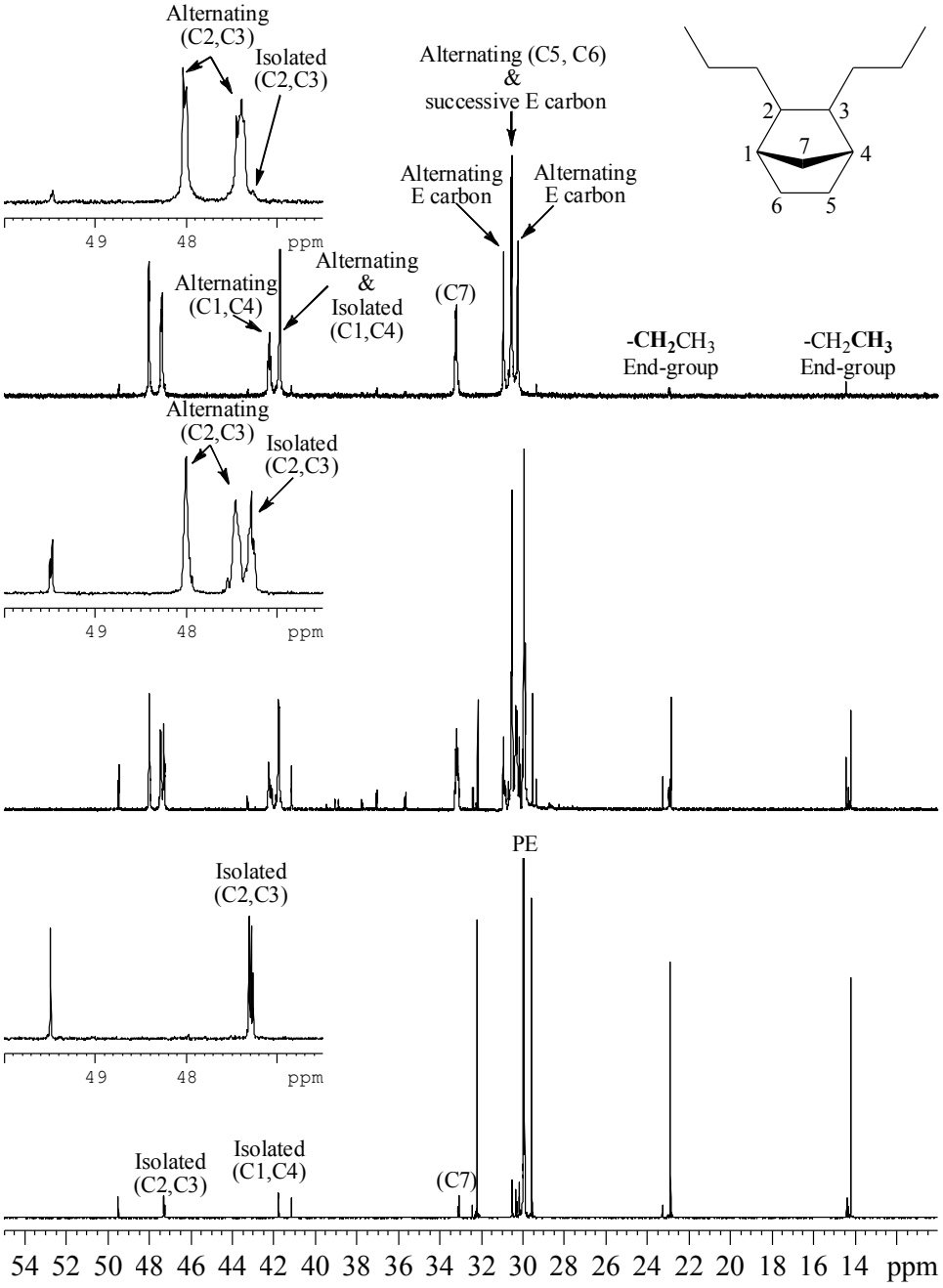

Figure 3.5. ^{13}C NMR (150 MHz, 1,1,2,2-$C_2D_2Cl_4$, 110 ºC) spectrum and resonance assignments for P(E-*co*-NB)-*b*-PE copolymers, from runs 1, 4, and 6 from Table 3.1, synthesized via 50 (bottom) 500 (middle) and 3000 (top) equivalents NB respectively.

With this information in hand, it was possible to design and synthesize poly(E-*co*-NB)-*b*-PE block copolymers consisting of variable incorporated amounts of NB that are associated with either isolated or alternating copolymer microstructures from a single class of initiators – simply by employing different concentrations of NB in solution.

3.5 LCCTP of higher α-olefins and norbornene

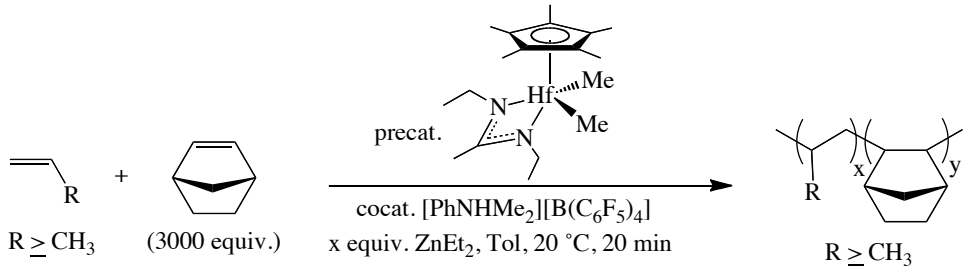

Scheme 3.6. Attempted copolymerization of norbornene with higher alkenes.

Having established that ethene could be co-polymerized with norbornene to give different polymers, depending on the relative amount of norbornene in the comonomer feed, it was of interest to know if higher alkenes (such as propene, 1-hexene, etc.) could also copolymerize with norbornene. Unfortunately, although it was determined that the catalyst was active (evidenced by the solution being yellow, which is an indication of an active catalyst) no polymer (homo or copolymer) was obtained when propene, 1-hexene, 1-octene or vinylcyclohexane were used as the other monomer. In the absence of norbornene, it is known that higher alkenes such as propene, 1-hexene, vinylcyclohexane, 1-octene etc. can be polymerized under reaction conditions utilized in Chapter 2. Therefore the absence of at least a homopolymer suggests two possibilities: a) the polymerization was initiated by norbornene (which is expected to react faster than a propene) but steric factors prevented further monomer incorporation or b) the

polymerization was initiated by propene, 1-hexene, 1-octene or vinylcyclohexane followed by incorporation of norbornene but once again, steric factors prevented further chain propagation. Plausibly a catalyst that has a more open active site, which would accommodate more sterically hindered monomers, such as norbornene, might facilitate the preparation of copolymers containing sterically encumbered units.

3.6 LCCTP terpolymerization of ethene with NB and higher α-olefins

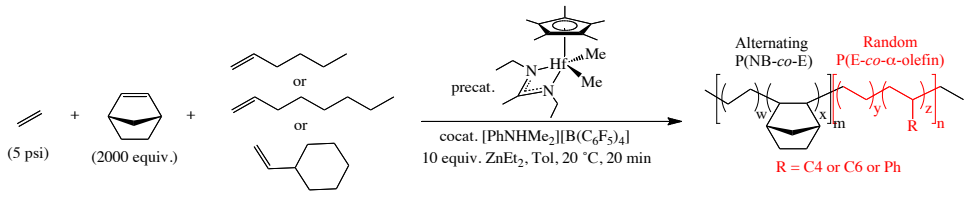

Scheme 3.7. Terpolymerization of ethene, norbornene, and higher olefins.

Norbornene or norbornene/ethene derived polymers have several desired properties suitable for end-use applications. To further diversify the properties of norbornene-derived polymers, we sought strategies that would allow for the incorporation of additional groups into the polymer. The inability of the active hafnium catalyst, generated from **Precatalyst III** and **Cocatalyst I,** to yield P(H-*co*-NB) both in the presence and absence of chain transfer reagent $ZnEt_2$ enabled the synthesis of P(E-*co*-NB)-*b*-P(E-*co*-H) block copolymers via a "one-pot" terpolymerization as shown in Table 3.3, and confirmed by ^{13}C NMR analysis. NB can insert into the metal-methyl bond however it appears that due to sterics NB is unable to insert next to another NB unit thereby allowing ethene insertion, ultimately leading to the observed alternating structure. Yet still, unlike ethene, larger monomers such as 1-hexene and propene are unable to undergo subsequent insertion into the metal-norbornene bond via **Precatalyst III**. As a

result, P(E-*co*-NB)-*b*-P(E-*co*-α-olefin) block copolymers can be synthesized quite easily, since NB only allows generation of P(E-*co*-NB) even in the presence of higher α-olefins. However, when the NB is consumed, ethene will copolymerize with α-olefins present in the reaction solution.

Table 3.3. Terpolymerization of ethene with NB and higher α-olefins via LCCTP.

Run[a]	**co-monomer (equiv.)**	**$ZnEt_2$ (equiv.)**	**Yield (g)**	**T_g (°C)**	**T_m (°C)**	**T_c (°C)**	**NB (mol%)**	**co-monomer (mol%)**
1	C6 (2000)	10	2.5	117.4	94.6	68.5	47.5	9.3
2	C8 (2000)	10	3.0	-	80.6	45.4	46.9	13.6
3	VCH (2000)	10	2.3	-	103.1	101.8	42.0	15.1

Table 3.3 shows data corresponding to ethene/norbornene terpolymers synthesized using 1-hexene, 1-octene, and vinylcylcohexane as the higher α-olefins. In the case of the 1-hexene analog, ^{13}C NMR (Figure 3.6) and DSC (Figure 3.7) evidence the presence of 1-hexene in the polymer product. ^{13}C resonances corresponding to random displacement of ethene/1-hexene throughout the polymer chain are labeled in Figure 3.6 and were utilized to calculate a comonomer incorporation of 9.3%.

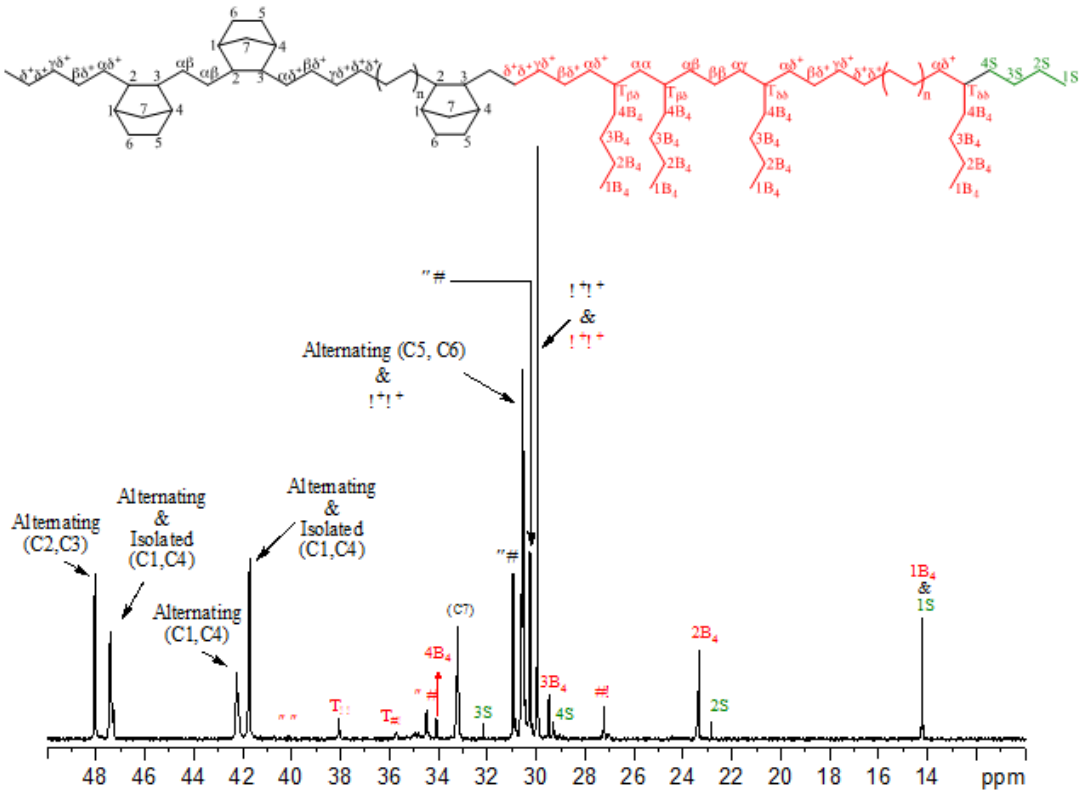

Figure 3.6. ^{13}C NMR of E/NB-*b*-E/H.

DSC curves for this material were even more telling, as the amorphous and crystalline character that would be expected for individual poly(E-*co*-NB) and poly(E-*co*-H) copolymers, respectively, were also revealed in the DSC of the poly(E-co-NB)-*b*-poly(E-*co*-H) terpolymer material, which is typical in a block copolymer type system.

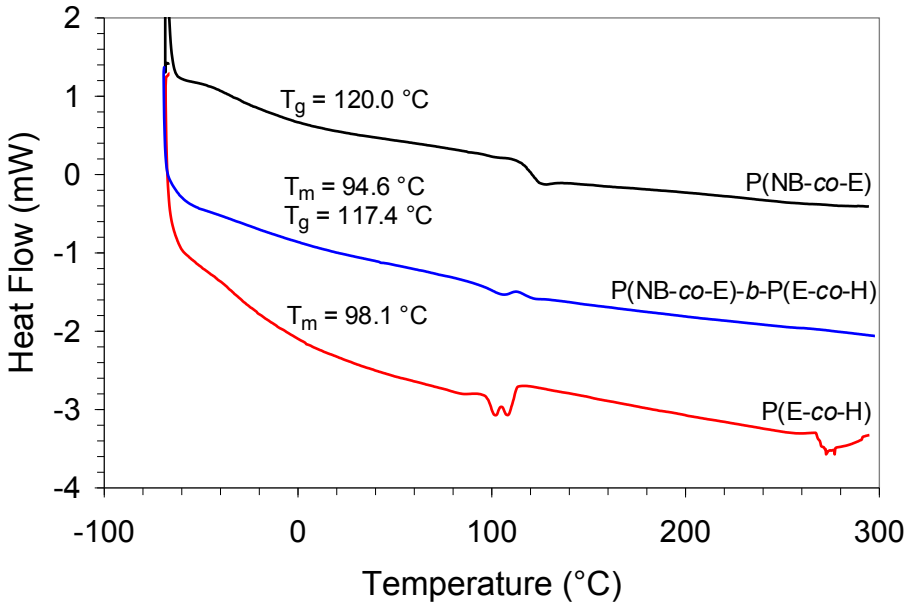

Figure 3.7. DSC of P(NB-co-E)-b-P(E-co-H) showing both a glass transition temperature and melting point that supports successful terpolymerization.

DSC of the terpolymer, shown in Figure 3.7, revealed a glass transition temperature at 117.4 °C and a melting endotherm at 94.6°C. Unlike in the case of the 1-hexene terpolymer, the DSC of the 1-octene and vinylcyclohexane analogs generated under otherwise identical reaction conditions, only showed melting endotherms at 80.6 °C and 103.1 °C respectively. Comonomer contents calculated from the ^{13}C NMRs of poly(E-co-NB)-b-poly(E-co-O) and poly(E-co-NB)-b-poly(E-co-VCH) were 13.6% and 15.1% respectively (Figures 3.8 and 3.9) which supports successful incorporation of the higher α-olefin. Unfortunately even with comonomer incorporation ranging from approximately 9% to 14%, these terpolymers were not soluble in THF, xylene, or trichlorobenzene at room temperature making GPC analysis unattainable in house.

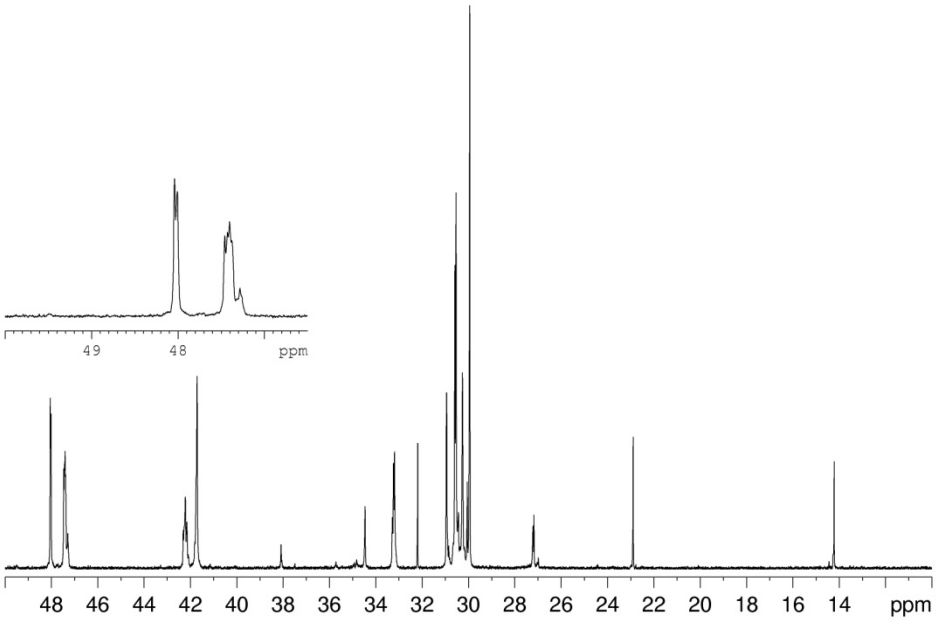

Figure 3.8. ^{13}C NMR of P(E-co-NB)-b-P(E-co-O) from terpolymerization of ethene, norbornene and 1-octene.

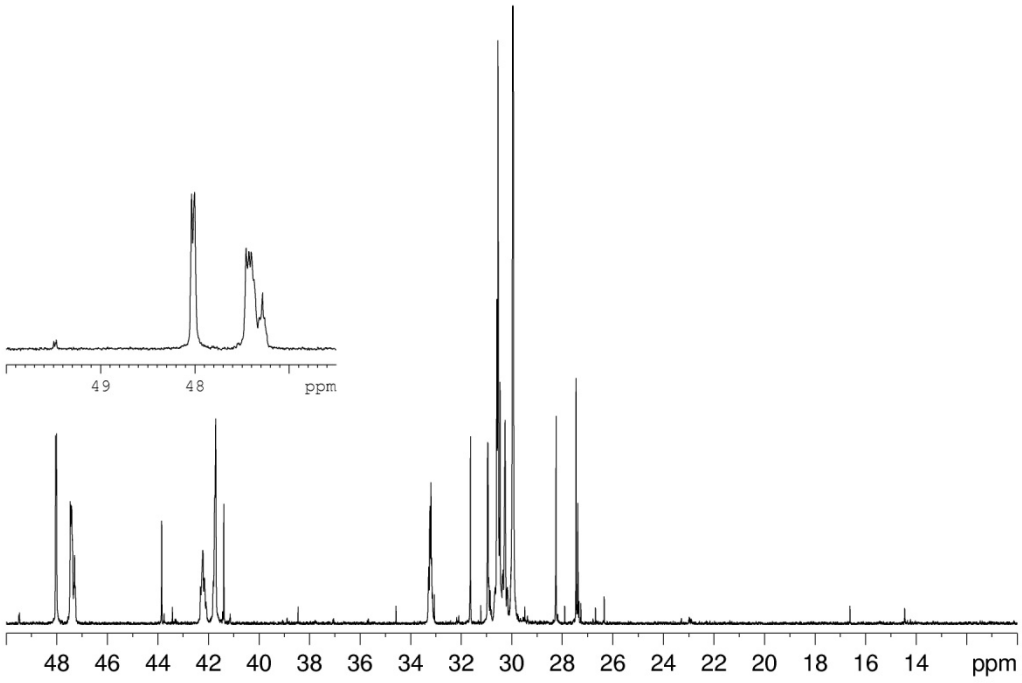

Figure 3.9. ^{13}C NMR of P(E-co-NB)-b-P(E-co-VCH) from terpolymerization of ethene, norbornene and vinylcyclohexane.

3.7. Modulation of Comonomer Incorporation in NB Terpolymers

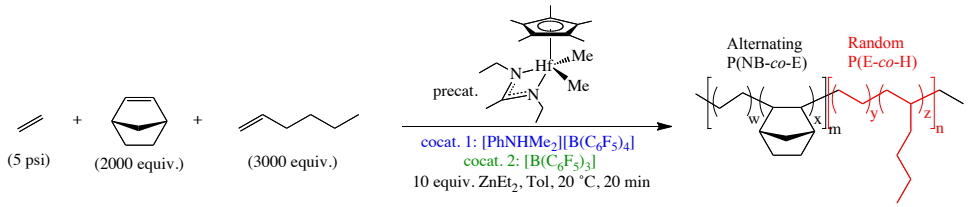

Scheme 3.8. Terpolymerization of ethene, norbornene, and 1-hexene via reversible chain-transfer between ion pairs.

It was recently demonstrated that LCCTP coupled with fast and reversible chain transfer between "tight" and "loose" ion pairs could be used to modulate comonomer relative reactivities in ethene/α-olefin and ethene/cycloalkene copolymers. This

approach was exploited to generate different grades of P(E-*co*-NB)-*b*-P(E-*co*-H) materials by copolymerization with a single transition metal precatalyst (**Precatalyst II** or **Precatalyst III**). Three P(E-*co*-NB)-*b*-P(E-*co*-H) materials were synthesized by LCCTP copolymerization of ethene, 1-hexene and norbornene with three different ratios of "loose", [Cp*HfMe{N(Et)C(Me)N(Et)}][$B(C_6F_5)_4$], and "tight", [Cp*HfMe{N(Et)C(Me)N(Et)}][$MeB(C_6F_5)_3$], ion pairs generated in situ from activation of **Precatalyst III** with: (run 1 of Table 3.4) only the borate **Cocatalyst I**, (run 2 of Table 3.4) a 1:1 mixture of the two cocatalysts, **Cocatalyst I** and **Cocatalyst II**, and (run 3 of Table 3.4) only the borane **Cocatalyst II**. In each case, CCTP copolymerization of E and NB was performed using 50 equiv. of $ZnEt_2$ and 500 equiv. NB in the presence of 3000 equiv. H (relative to **Precatalyst III**) in toluene at 20°C and at ethene pressure of 5 psi. The three samples have not yet been analyzed by GPC due to their insolubility in THF, xylene or 1,2,3-trichlorobenzene at room temperature. However, a decrease in yield (activity) and melting points were observed as the concentration of the tight-ion-pair propagating species increased, serving as additional evidence of successful modulation of 1-hexene content. ^{13}C NMR spectroscopic and microstructural analysis revealed that 1-hexene incorporation increased from 2.0% to 6.5% as the population of loose ion pairs increased. No evidence of chain termination by β-hydrogen-atom transfer was observed in ^{1}H NMR spectra, suggesting a living system.

Table 3.4. Terpolymerization of ethene, norbornene, and 1-hexene via reversible chain-transfer between ion pairs.

Run	Cocatalyst I : II	T_m (ºC)	T_c (ºC)	Yield (g)	NB (mol %)	H (mol %)
1	1 : 0	91.0	105.9	2.1	33.4	6.5
2	1 : 1	89.1	95.5	1.8	39.2	3.9
3	0 : 1	72.4	105.6	1.5	38.8	2.0

Finally, DSC analysis (Figure 3.10) revealed only a melting point transition although ^{13}C NMR also showed norbornene incorporations of 33.4%, 39.3%, and 38.8% for runs 1-3 in Table 3.4 respectively, which confirms the presence of both H and NB in the polymer product. Like the 1-hexene terpolymers discussed in the previous section, poly(NB-*co*-E)-*b*-(poly(E-*co*-H) samples were insoluble in GPC solvents at room temperature so molecular weights and polydispersity indices were not determined.

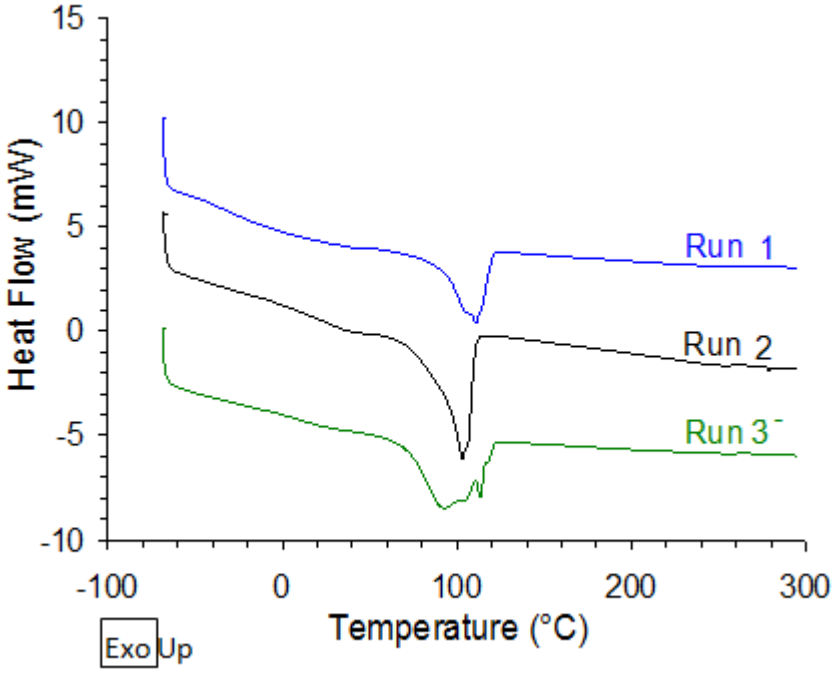

Figure 3.10. DSC curves of poly(E-*co*-NB)-*b*-poly(E-*co*-H) materials prepared using reversible chain transfer between ion pairs methodology.

3.8 Homopolymerization of β-Citronellene via Living Coordination Polymerization

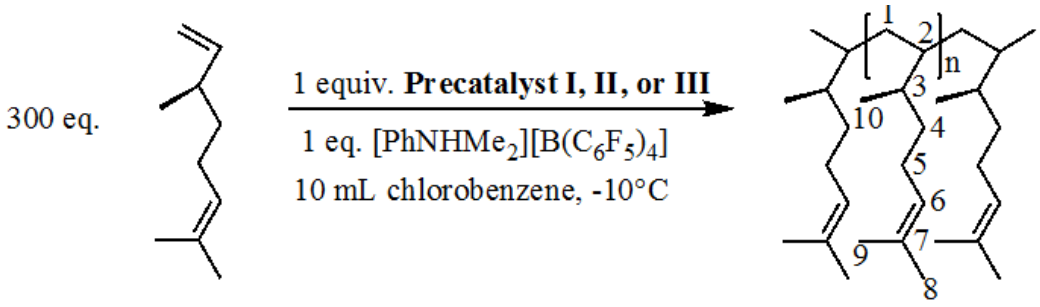

Scheme 3.9. Scheme for β-Citronellene Homopolymerization.

As previously mentioned, functionalized polymers are of interest for the fabrication of smart materials. One method for the functionalization of polymers is to use monomers having latent groups that can act as a handle for further functionalization. β-Citronellene is considered to be sterically encumbered because there is a tertiary center next to the terminal alkene and the internal alkene is trisubstituted. The monomer contains one internal alkene unit and an additional terminal one. β-Citronellene additionally contains a chiral center, therefore polymers that incorporate this monomer would be optically active and could have interesting optical properties. β-Citronellene is a commodity from terpene feedstocks and is commercially available.

Table 3.5. Living homopolymerization of (-)-β-citronellene.

Entry	Precatalyst	Yield (mg)	T_m (℃)	T_c (℃)	M_n (kDa)	M_w (kDa)	PDI
1	**I**	433	160.4	155.8	54.0	66.0	1.2
2	**II**	872	175.0	168.0	80.0	105.0	1.3
3	**III**	613	169.4	165.2	47.0	57.0	1.2

Conditions: Polymerizations were conducted in 10 mL chlorobenzene using equimolar (25μmol) amounts of **Precatalyst I, Precatalyst II, or Precatalyst III** and **Cocatalyst I** using 300 equiv. of (-)-β-citronellene at -10 °C for 16 h.

In order to gain a qualitative sense of activity, homopolymerizations of β-citronellene were carried out using three of Sita's catalysts as described in Table 3.5. After 16 h of polymerization using the C_1-symmetric **Precatalyst I** and **Cocatalyst I**, it was determined that the sterically hindered monomer was indeed able to insert into the metal-carbon bond to produce poly(β-citronellene) homopolymer. As expected given the symmetry of the catalyst, the resulting homopolymer was crystalline with a melting endotherm at 160 °C. However due to the low yield, C_s-symmetric **Precatalysts II** and **III** were subsequently investigated, given their more sterically accessible metal centers. **Precatalysts II** and **III** also produced crystalline materials, producing slightly better yields. It is worth noting that poly(βC) yielded from **Precatalyst II** had molecular weights that were much higher than the other two precatalysts. This is likely due to the use of a cyclopentadiene rather than a pentamethylcyclopentadiene unit in the catalyst motif, which creates a more open environment for monomer insertion. ^{1}H NMR of the poly(β-citronellene) homopolymers revealed resonances assignments around 5.1 ppm, 1.7 ppm, and 1.6 ppm corresponding to the internal alkene (6) and the methyl groups at the 9 and 8 position respectively, as shown in Figure 3.11. Moreover, ^{13}C NMR resonances around 131 ppm and 125 ppm evidence the internal alkene, as illustrated in Figure 3.12.

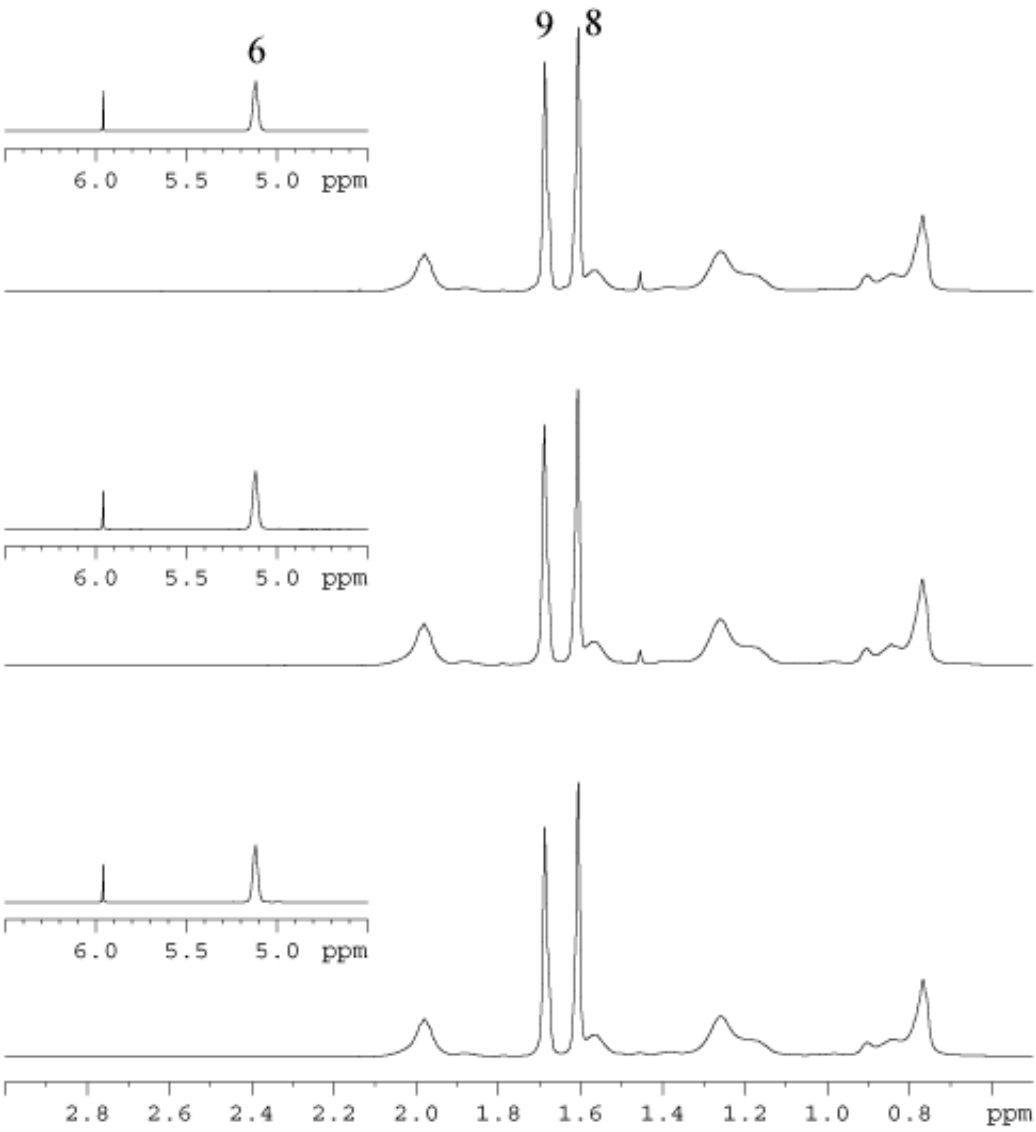

Figure 3.11. ^{1}H NMR (150 MHz, 1,1,2,2-$C_2D_2Cl_4$, 90ºC) spectrum and resonance assignments of poly(β-citronellene) from entry 1 (top), entry 2 (middle) and entry 3 (bottom) in Table 3.1..

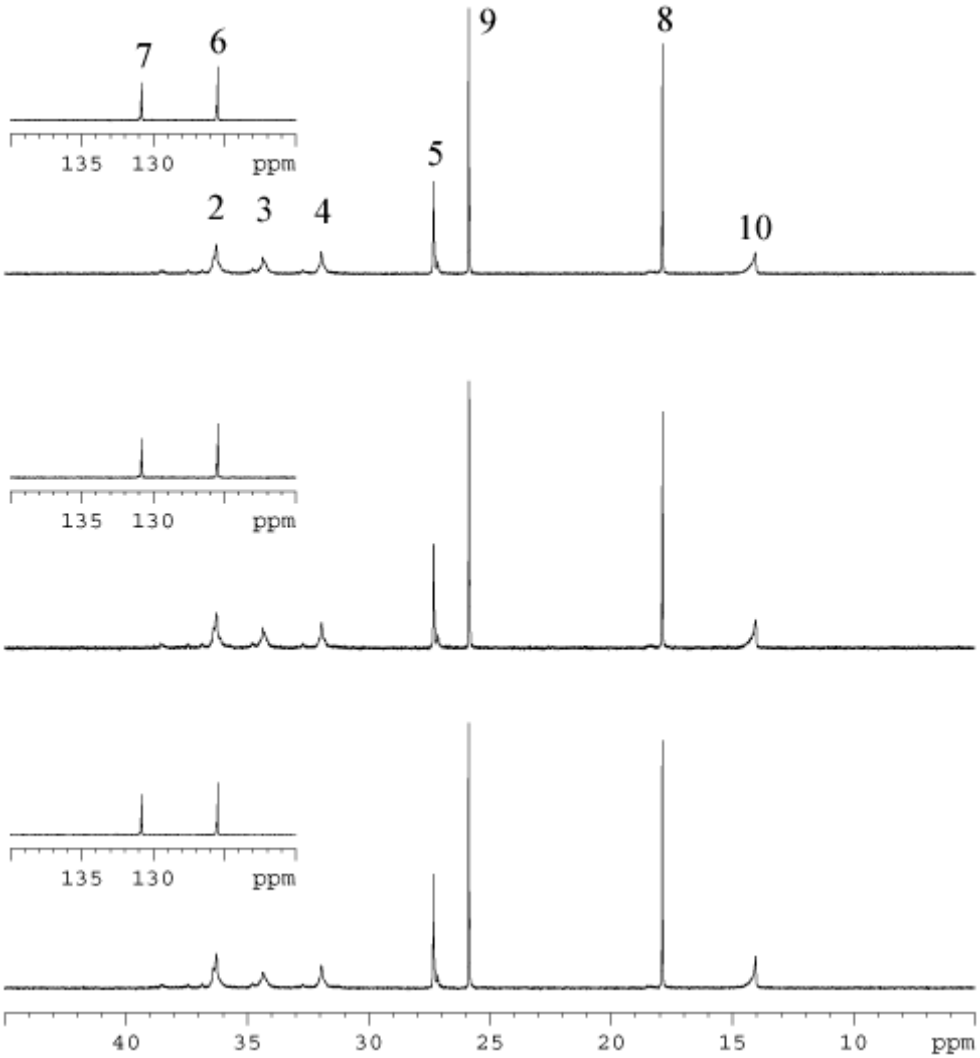

Figure 3.12. ^{13}C NMR (150 MHz, 1,1,2,2-$C_2D_2Cl_4$, 90ºC) spectrum and resonance assignments of poly(β-citronellene) from entry 1 (top), entry 2 (middle) and entry 3 (bottom) in Table 1.

3.9 Living Coordination Polymerization of α-olefin with β-Citronellene

The emergence of ethene-propene-diene terpolymers (EPDM) as a dominant elastomer in applications that demand excellent chemical and thermal stability has lead to substantial intereste in the modification of polyolefins. The functionalization of the hydrocarbon main chain of polyolefins can improve properties of EPDM in the realm of

science. The application of non-conjugated dienes for copolymerization with ethene via transition-metal-based catalysts is one avenue being investigated.[211]

Earlier reports by Dolatkhani,[211,212] and coworkers demonstrated the homopolymerization of β-citronellene with unspecified optical purity using heterogeneous titanium-based catalysts and vanadium-based catalytic systems, for which the ^{13}C NMR spectrum was provided. Santos[213] and coworkers later reported the successful copolymerization of ethene with β-citronellene of unspecified optical purity via a silicon-based catalyst with constrained geometry, where small quantities of β-citronellene ranging from 0.041 M to 0.186 M were used in the copolymerization. These studies resulted in percent incorporations of only 0.3 and 1.2 percent weight average molecular weight distributions from 27-57 kDa, and polydispersities from 2.3 to 4.9.[208,214].

Table 3.6. Living coordination polymerization of ethene with (-)-β-citronellene.

Entry	Precatalyst	T_p (min)	Yield (g)	T_m (℃)	T_c (℃)	Comonomer (mol%)
[α]1	III	30	0.88	108.2	100.9	2.7
[α]2	II	13	0.59	100.5	91.1	11.0
[β]3	III	30	1.51	99.0	104.1	3.3
[β]4	II	30	1.24	116.0	110.2	4.0

[α]Conditions: Polymerizations were conducted in 10 mL chlorobenzene using equimolar (25μmol) amounts of **Precatalyst II** or **Precatalyst III** and **Cocatalyst I** using 500 equiv. of (-)-β-citronellene and 5 psi ethene at 25 °C (entries 1 and 2). Polymerizations corresponding to entries 3 and 4 were conducted under LCCTP conditions using 20 equiv. of diethylzinc in 40 mL toluene. Comonomer incorporation was calculated from ^{13}C NMR data.

Given the successful polymerization of βC via Sita's catalysts, copolymerizations of βC with ethene and propene were attempted to produce more robust polyolefin based materials that are equipped with latent groups that can be utilized as a handle. Living

coordination polymerization of E with βC at an ethene pressure of 5 psi at 25 °C was carried out using **Precatalyst III** or **II** with **Cocatalyst I** both in the presence and absence of chain transfer reagent, $ZnEt_2$, to obtain poly(E-*co*-βC) materials. Copolymer compositional analysis by ^{13}C NMR indicated 2.7% and 11.0% respectively, via traditional coordination polymerization and 3.3% and 4.0% βC incorporation in the case of the CCTP product, as shown in entries 1 and 2 of Table 3.6. This is a remarkably high value in comparison to the 1.2% incorporation reported by Santos et al.[213] using a titanium-based constrained geometry catalyst (CGC). Higher comonomer content was observed in the case of **Precatalyst II**, which is likely due to the lesser amount of steric bulk associated with having a Cp (Cp = η^5-C_5H_5) versus Cp* (Cp* = η^5-C_5Me_5) half-sandwich catalyst system in addition to cyclohexyl groups positioned in the plane rather than ethyl groups positioned outside of the plane. DSC characterization further confirmed comonomer incorporation by unveiling a crystalline state with melting endotherms ranging from 99.0°C to 116.0°C and crystallization exotherms ranging from 91.1°C to 110.2°C. Also worth mentioning, is the presence of ^{13}C resonances at 126 ppm and 131 ppm confirming the preservation of the internal double bond as shown in Figure 3.13.

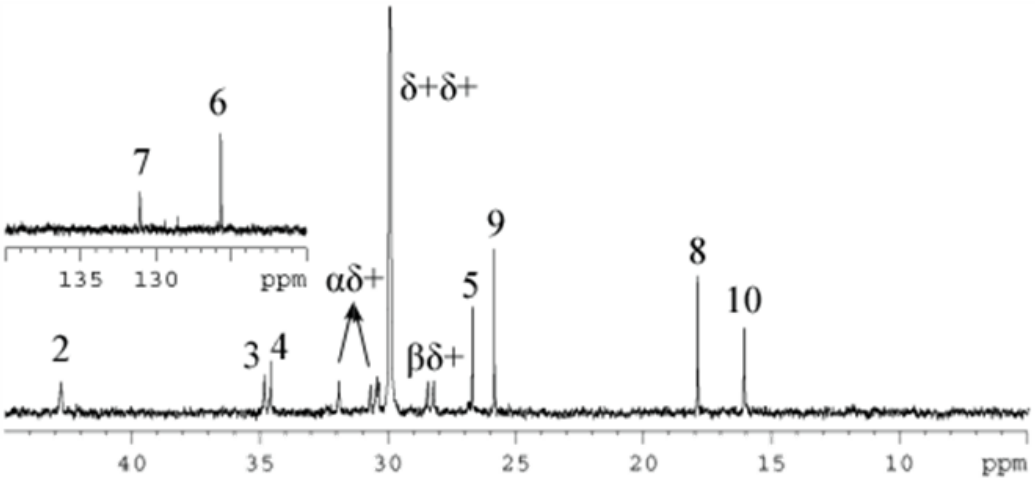

Figure 3.13. ^{13}C NMR (600 MHz, 1,1,2,2-$C_2D_2Cl_4$, 90ºC) spectrum and resonance assignments of poly(E-*co*-βC) from run 1 in Table 3.6.

Unfortunately, GPC of poly(E-*co*-βC) materials were not acquired because of their lack of solubility in THF, xylene, ot 1,2,3-trichlorobenzene. Finally, when compressed at 120°C for 20 min using a Carver melt press and then cooled at room temperature for 15 min, the non-chain transfer material yielded a hard opaque plastic while the chain transfer materials yielded a high melting wax.

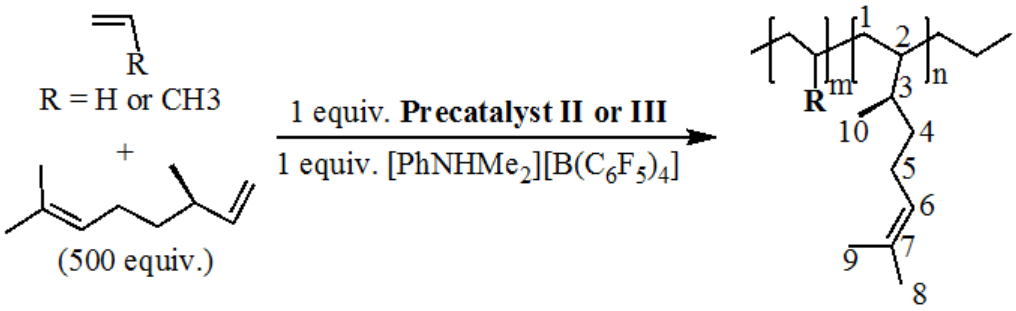

Scheme 3.10. Scheme for copolymerization of BC with a-olefin.

3.10 Conclusions

Synthesis of poly(E-*co*-NB) cyclic olefin copolymers via both traditional coordination copolymerization and LCCTP copolymerization was achieved towards the

production of virtually completely alternating materials with seemingly variable molecular weights. Block copolymers having one block of poly(E-*co*-NB) random copolymer, having either alternating, isolated or some combination of the two microstructures, and another block of PE were also generated and used for the elucidation of resonance assignments. LCCTP together with rapid and reversible chain transfer between tight and loose ion pairs enabled the synthesis of or poly(E-*co*-NB)-b-poly(E-*co*-H) polymers with different quantities of 1-hexene incorporated in the polyethylene backbone. Also, traditional coordinative copolymerization and/or LCCTP gave way to poly(E-co-βC) copolymers with units of unsaturations along the polymer backbone that can be further functionalized or cross-linked as in the case of EPDM materials. Overall, successful extension of the range of new polyolefin materials were achieved via the copolymerization of sterically hindered monomers with readily available ethene and propene was achieved.

3.11 Experimentals

Materials. All manipulations were performed under an inert atmosphere of dinitrogen using either standard Schlenk techniques or a Vacuum Atmospheres glovebox. Dry, oxygen-free solvents were employed throughout. Chlorobenzene was distilled from calcium hydride and toluene was distilled from sodium. Polymer grade ethene and (1:9) ethene to propene mixed gas was purchased from Matheson Trigas, and passed through activated Q5 and molecular sieves (4 Å). **Precatalyst II** and **Precatalyst III** were prepared according to previously reported procedures. **Cocatalyst I** and **Cocatalyst II** were purchased from Boulder Scientific and used without further purification.

Instrumentation. ^{13}C $\{^{1}H\}$ NMR spectra were recorded at 150 MHz, using 1,1,2,2-tetrachloroethane-d_2 as the solvent at 110 ºC. Thermal analyses were performed on a TA Instruments DSC Q1000 calibrated with indium and sapphire using hermetically sealed aluminum sample pans holding 10mg of material. Samples were heated and cooled at a rate of 10 ˚C/min and dinitrogen was used as the sample purge gas at a flow rate of 50 mL/min. In DSC analyses, heat flows (mW) less than zero were deemed endothermic while those greater than zero were considered exothermic. Glass transition (T_g), melting onset (T_m) and crystallization onset (T_c) temperatures were obtained using a heat/cool/heat method on a DSC Q1000 with TA Series Explorer.

Procedure for living coordination copolymerization of ethene with NB (run 1 in Table 3.1). In a 250 mL Schlenk flask, ethene (5 psi) was equilibrated to a 9 mL chlorobenzene solution containing cocatalyst **2** (21.0 mg, 0.026 mmol) and comonomer NB (1.177 g, 12.5 mmol) at 25 °C for 30 min. A 1 mL chlorobenzene solution of precatalyst **1** (11.4 mg, 0.025 mmol) was then added to the flask to initiate the polymerization. After stirring for 30 min at 20 °C, ethene charging was stopped. The polymer solution was immediately quenched with 1 mL methanol and subsequently precipitated into 800 mL of acidic methanol (10% concentrated HCl) to isolate the polymer. The final product was collected after decanting the methanol solution and dried overnight in *vacuo* before DSC and NMR analyses.

Procedure for LCCTP copolymerization of ethene E with NB (runs 2-5 in Table 3.1). In a 250 mL Schlenk flask, ethene (5 psi) was equilibrated to a toluene solution

containing 1.1 M $ZnEt_2$ (50 equiv. to 3000 equiv. relative to **1**) and 3000 equiv. of comonomer NB (5.649 g, 60 mmol) at 20 °C for 20 min. A 1 mL chlorobenzene solution of cocatalyst **2** (8.4 mg 0.0105 mmol) and precatalyst **1** (4.6 mg, 0.010 mmol) was added to the flask to initiate the polymerization. After stirring for 20 min at 20 °C, ethene charging was stopped. The polymer solution was immediately quenched with 1 mL methanol and subsequently precipitated into 800 mL of acidic methanol (10% concentrated HCl) to isolate the polymer. The final product was collected after decanting the methanol solution and dried overnight in *vacuo* before DSC and NMR analyses.

Procedure for preparation of P(E-*co*-NB)-*b*-E block copolymers (run 1-6 in Table 3.2). In a 250 mL Schlenk flask, to a 40 mL toluene solution of 1.1 M $ZnEt_2$ in 15 wt% toluene solution (412 mg, 0.5 mmol, 50 equiv. relative to **1**) at 20 ºC was added from 50 equiv. to 3000 equiv. of NB (165 mg, 0.2 mmol to 2.825 g, 30 mmol). The flask was then pressurized to slightly above 1 atm (5 psi) with ethene and the pressure was maintained for 30 min with stirring. Then a 1 mL solution of cocatalyst **2** (8.0 mg, 0.010 mmol) and the precatalyst **1** (4.6 mg, 0.010 mmol) were added to the reaction flask and the flask was immediately repressurized to 5 psi with ethene and maintained for 5 min with stirring, after which time, ethene charging was stopped. The polymer solution was immediately quenched with 1 mL methanol and subsequently precipitated into 800 mL of acidic methanol (10% concentrated HCl) to isolate the polymer. The final products were collected and dried overnight in *vacuo* before DSC and NMR analyses.

Procedure for terpolymerization of ethene and 1-hexene with NB (run 1 in Table 3.3). In a 250 mL Schlenk flask, of ethene (5 psi) was equilibrated to a toluene solution containing 1.1 M $ZnEt_2$ (247 mg, 2 mmol, 200 eq), H (5.049 g, 60 mmol) and NB (5.649 g, 60 mmol) at 20 °C for 30 min. A 1 mL chlorobenzene solution of cocatalyst **3** or/and **4** and precatalyst **1** was added to the flask to initiate the polymerization. After stirring for 20 min at 20 °C, ethene charging was stopped. The polymer solution was immediately quenched with 1 mL methanol and subsequently precipitated into 800 mL of acidic methanol (10% concentrated HCl) to isolate the polymer. The final product was collected after decanting the methanol solution and dried overnight in *vacuo* before DSC and NMR analyses.

Preparation of P(E-*co*-NB)-*b*-P(E-*co*-H) block copolymers (runs 1 to 3 in Table 3.4). In a 250 mL Schlenk flask, to a 40 mL toluene solution of $ZnEt_2$ in 15 wt% toluene solution (412 mg, 0.5 mmol, 50 equiv.) at 20 ºC was added some amount of NB and H (2.525 g, 30 mmol, 3000 equiv.). The flask was then pressurized to slightly above 1 atm (5 psi) with ethene and the pressure was maintained for 30 mins with stirring. Then a 1 mL solution of cocatalyst **3** (8.0 mg, 0.010 mmol) and the precatalyst **1** (4.6 mg, 0.010 mmol to **1**) was added to the reaction flask and the flask was immediately repressurized to 5 psi with ethene and the pressure maintained for 30 mins with stirring after which ethene charging was stopped. The polymer solution was immediately quenched with 1 mL methanol and subsequently precipitated into 800 mL of acidic methanol (10% concentrated HCl) to isolate the polymer. The final products were collected and dried overnight in *vacuo* before GPC, DSC and NMR analyses.

General procedure for living polymerization of (-)-β-Citronellene (runs 1 to 3 in Table 3.5): In a 100 mL Round-bottom flask, to 10 mL chlorobenzene at -10 °C were added the 25 μmol cocatalyst **4** and the 25 μmol precatalyst **1,2 or 3**. Then 300 equivalents (1.037 g) of 25μmol (-)-β-citronellene were then added to the reaction flask for 16 h with stirring before quenching with 0.5 mL of methanol. The chlorobenzene solution was precipitated into 800 mL of methanol to isolate the polymer. The final product was collected after decanting the methanol solution and dried overnight in *vacuo* before GPC, DSC and NMR analyses.

General procedure for living copolymerization of ethene and (-)-β-Citronellene (run 1 and 2 in Table 3.6): In a 250 mL Schlenk flask, to 9 mL chlorobenzene at 25 °C was added 500 equivalents (1.728 g) of 25 μmol (-)-β-citronellene. The flask was then pressurized to slightly above 1atm (~5 psi) with ethene and the pressure was maintained for 10min with stirring. Subsequently, the flask was depressurized and 25 μmol of the cocatalyst **4** and the precatalyst **2** were dissolved in 1 mL chlorobenzene and transferred to the Schlenk flask which was immediately repressurized to slightly above 1atm (~5 psi) with ethene where it remained isobaric for 30min with stirring before quenching with 0.5 mL of methanol. The chlorobenzene solution was precipitated into 800 mL of methanol to isolate the polymer. The final product was collected after decanting the methanol solution and dried overnight in *vacuo* before GPC and NMR analyses.

General procedure for living coordinative chain-transfer copolymerization of ethene and (-)-β-Citronellene (run 3 and 4 in Table 3.6): In a 250 mL Schlenk flask, to a 40 mL toluene solution of $ZnEt_2$ at 25 °C was added 500 equivalents (1.728 g) of 25 μmol (-)-β-citronellene. The flask was then pressurized to slightly above 1atm (~5 psi) with ethene and the pressure was maintained for 10 min with stirring. Subsequently, the flask was depressurized and 25 μmol of the cocatalyst **4** and the precatalyst **2** were dissolved in 1 mL toluene and transferred to the Schlenk flask which was immediately repressurized to slightly above 1 atm (~5 psi) with ethene where it remained isobaric for 30min with stirring before quenching with 0.5 mL of methanol. The chlorobenzene solution was precipitated into 800 mL of methanol to isolate the polymer. The final product was collected after decanting the methanol solution and dried overnight in *vacuo* before GPC and NMR analyses.

General procedure for living polymerization of (-)-β-Citronellene: In a 100 mL Round-bottom flask, to 10 mL chlorobenzene at -10 °C were added the 25 μmol cocatalyst **4** and the 25 μmol precatalyst **1,2 or 3**. Then 300 equivalents (1.037 g) of 25 μmol (-)-β-citronellene were then added to the reaction flask for 16 h with stirring before quenching with 0.5 mL of methanol. The chlorobenzene solution was precipitated into 800 mL of methanol to isolate the polymer. The final product was collected after decanting the methanol solution and dried overnight in *vacuo* before GPC, DSC and NMR analyses.

General procedure for living random copolymerization of ethene and (-)-β-Citronellene: In a 250 mL Schlenk flask, to 9 mL chlorobenzene at 25 °C was added 500 equivalents (1.728 g) of 25 μmol (-)-β-citronellene. The flask was then pressurized to slightly above 1atm (~5 psi) with ethene and the pressure was maintained for 10min with stirring. Subsequently, the flask was depressurized and 25 μmol of the cocatalyst **4** and the precatalyst **2** were dissolved in 1 mL chlorobenzene and transferred to the Schlenk flask which was immediately repressurized to slightly above 1atm (~5 psi) with ethene where it remained isobaric for 30 min with stirring before quenching with 0.5 mL of methanol. The chlorobenzene solution was precipitated into 800 mL of methanol to isolate the polymer. The final product was collected after decanting the methanol solution and dried overnight in *vacuo* before GPC and NMR analyses.

General procedure for living random coordinative chain transfer copolymerization of ethene and (-)-β-Citronellene: In a 250 mL Schlenk flask, to a 40 mL toluene solution of $ZnEt_2$ at 25 °C was added 500 equivalents (1.728 g) of 25 μmol (-)-β-citronellene. The flask was then pressurized to slightly above 1 atm (~5 psi) with ethene and the pressure was maintained for 10min with stirring. Subsequently, the flask was depressurized and 25 μmol of the cocatalyst **4** and the precatalyst **2** were dissolved in 1 mL toluene and transferred to the Schlenk flask which was immediately repressurized to slightly above 1 atm (~5 psi) with ethene where it remained isobaric for 30 min with stirring before quenching with 0.5 mL of methanol. The chlorobenzene solution was precipitated into 800 mL of methanol to isolate the polymer. The final product was

collected after decanting the methanol solution and dried overnight in *vacuo* before GPC and NMR analyses.

General procedure for living random copolymerization of propene and (-)-β-Citronellene: In a 250 mL Schlenk flask, to 9 mL chlorobenzene at -10 °C was added 500 equivalents (1.728 g) of 25 μmol (-)-β-citronellene. The flask was then pressurized to slightly above 1 atm (~5 psi) with propene and the pressure was maintained for 10min with stirring. Subsequently, the flask was depressurized and 25 μmol of the cocatalyst **4** and the precatalyst **2** were dissolved in 1 mL chlorobenzene and transferred to the Schlenk flask which was immediately repressurized to slightly above 1 atm (~5 psi) with propene where it remained isobaric for 2 hours with stirring before quenching with 0.5 mL of methanol. The chlorobenzene solution was precipitated into 800 mL of methanol to isolate the polymer. The final product was collected after decanting the methanol solution and dried overnight in *vacuo* before GPC and NMR analyses.

Chapter 4 : Rod-Coil Block Copolymers from Pure Polyolefins

4.1 Background

A great deal of attention has been focused on block copolymers, because of their ability to self assemble into a variety of nanostructures through microphase separation of chemically distinct macromolecular blocks.[215] The propensity of block copolymers to phase separate is dependent on the characteristics of the separate polymers chain domains that comprise the block copolymers. In block copolymers having only amorphous polymer chains, phase separation is thermodynamically controlled because of repulsion between dissimilar blocks. In completely crystalline, rod-rod, block copolymers phase separation is crystallization induced. In other words, phase separation is dictated by the rate of crystallization and block length of each polymer chain, as shown by Register et al. and Hamley et al.[216,217] In block copolymers having both amorphous and crystalline blocks, rod-coil, microphase separation and crystallization of the rod components compete, resulting in self assembly at a smaller scale than typically obtained in coil-coil systems.[218]

While equilibrium phase diagrams based on self-consistent mean field theory (SCFT)[219] exist for classical coil-coil diblock copolymers and predicts phase separation of spherical, cylindrical, gyroid, and lamellae morphologies, theoretical studies predict a diversity of structures in rod-coil diblock copolymers.[220] These phases include zigzag, wavy lamellar, arrowhead, puck, smectic, and nematic phases with spherical, vesicular, rectangular or cylindrical nanodomains and have been observed in polymer and protein rod-coil systems.[220] Over the years, there have been a number of theoretical studies based on analytical free energy calculations and scaling relationships[221-224], random phase

approximation (RGA)[225,226], and SCFT[227-230] for example. These studies have predicted transitions between nematic, smetic, bilayer, and "puck", and isotropic phases (shown in Figure 1) which can be characterized by four parameters.[231] The four parameters[223,224,229,232,233] are: the product of the degree of polymerization and the Flory-Huggins interaction parameter, χN, and the volume fraction of the two blocks, φ (χN and φ as in coil-coil systems), the product of the degree of polymerization and the Maier-Saupe parameter, μN, and the coil to rod length ratio, v. The Flory-Huggins interaction measures the local repulsion between rod coil segments. The Maier-Saupe parameter is an alignment parameter that accounts for the liquid crystalline interactions between rod-like polymers.[234] The coil to rod length ratio represents the mismatch in scaling dimensions between the rod and coil, which leads to a difference in their characteristic length or the interfacial area occupied as a function of molecular weight. Segalman and coworkers recently reported a universal phase diagram based on theoretical and experimental studies of PPV-*b*-PI, poly(alkoxyphenylenevinylene) rods and polyisoprene coils that predict lamellar, nematic, and isotropic phases when χN or μN is plotted versus coil fraction, as seen in Figure 2.[231,235] This phase diagram is incomplete and does not provide a rationale for the thermodynamics of the system. While, this phase diagram accounts for equilibrium morphologies, there are a host of microstructures that have been observed within the lamellar and nematic regions that are not accounted for. Thus, in depth studies of rod-coil block copolymers that self-assemble into morphologies not represented in the equilibrium phase diagram are essential if a thorough understanding of how to control self-assembly is to be attained.

Figure 4.1. Illustration of molecular packing in possible rod-coil block copolymer microphases. From left to right the phases are bilayer, smectic A-like monolayer, smectic C-like monolayer, nematic, and isotropic. While regions of the lamellar, nematic, and isotropic phases can be clearly demarcated on the phase diagram, discerning between the lamellar structures is more difficult. On the basis of domain spacing, the two monolayer phases are the most probable lamellar morphologies, with transitions in rod tilt and chain stretching occurring as the polymers are heated through the order-disorder transition. Reproduced from Segalman and coworkers.[231]

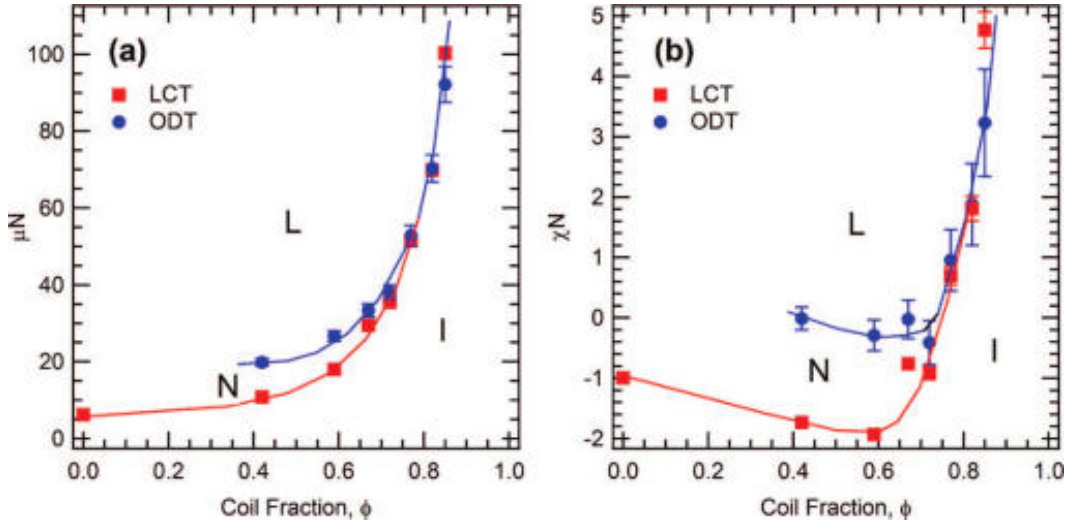

Figure 4.2. Universal phase diagram for weakly segregated rod-coil block copolymers. The universal phase diagram, where the temperature axis has been replaced by either χN or μN, is applicable to any system with a rod-coil molecular shape and can be used in a predictive capacity for functional rod coil systems. The phase diagram shows that increasing χN or μN results in the formation of nanostructured phases and liquid crystalline ordering, respectively. Phases are identified as lamellar (L), nematic (N), and isotropic (I). Reproduced from Segalman and coworkers.[235]

As stated, polyolefins are often first considered for use in any application, making them the largest volume polymers in the plastics industry. This is primarily due

to their benign nature, excellent cost performance value, and ease of recyclability, proccessability and fabrication. In addition to being able to phase separate into nanometer scale microstructures, rod-coil copolymers from such materials also possess thermoplastic elastomeric properties. This typically occurs in materials having at least two blocks that are hard at room temperature separated by blocks with a glass transition temperature (T_g) below room temperature, if the low T_g block volume is large.[236] The hard domains serve as thermally reversible crosslinks promoting recoverable elasticity in the soft phase and rendering the use of vulcanates unnecessary to evoke thermoplastic elastomeric properties. Block polyolefins have the ability to produce different grades of thermoplastic elastomers due to their ability to self assemble into a multitude of morphologies. Thus a range of new plastics having a variety of properties can be obtained from block polyolefins. New plastics made from block polyolefins have the potential to outcompete plastics that are currently on the market because these plastics contain harmful plasticizers (added to provide elasticity) and have been the subject of recent safety concerns.

In 2009, Hustad and co-workers at the Dow Chemical company reported polyethylene polymers that can form photonic crystals.[237] Photonic crystals are periodic dielectric materials that manipulate and control the movement of light. In essence, materials able to rotate light in the visible light region of the electromagnetic spectrum were produced on an industrial scale from pure polyolefins bearing no functionality. Despite the potential applications of polyethylene photonic crystals in the fabrication of devices, very little studies have been done on polyethylene photonic crystals, in contrast to the vast amounts of literature that exist for photonic crystals made from functionalized

polymers.[238] The reason why these pure polyolefin systems have not been studied in detail probably stems from the lack of synthetic routes to generate these materials. Until recently, anionic, cationic, ring opening, and radical-based living polymerization were the primary means utilized to synthesize polyolefins.[8]

Hillmyer and coworkers investigated a series of symmetric EPE (E = poly(ethylene-*co*-1-butene) and P = poly(ethylene-*alt*-propylene)) triblock copolymers with various molecular weights in order to establish a relationship between melt segregation strength, equilibrium morphologies, solid-state microstructures and mechanical properties.[239] The polyolefins used were synthesized via sequential anionic polymerization of symmetric poly(1,4-butadiene)-*b*-poly(1,4-isoprene)-*b*-poly(1,4-butadiene), BIB, then subsequently hydrogenated.

The aforementioned systems have allowed better understanding of the phase behavior in rod coil systems and the mechanical properties of the resultant bulk materials. This greater level of understanding has certainly been facilitated by living Ziegler-Natta polymerization, which allows the polymerization of α-olefins.[8] Additionally, the large scale production of these block polyolefin materials can also be achieved as shown by Hustad *et al*.[237,240] Despite the progress made in this field, there still exists a monumental gap in knowledge between how the optical properties of the self-assembled polymers, observed by Hustad *et al*., relate to the morphology or mechanical properties of the polymers.

4.2 Synthesis of Rod-Coil Block Copolymers based on α-Olefins and 1,5-Hexadiene

The Sita group is interested in how the microstructures of block polyolefins affect the physical and mechanical properties of the polymers. It is expected that insights

gained from such investigations would be used for the tailored synthesis of polyolefins having specific properties. In 2000, Sita and coworkers reported the first class of homogeneous catalysts that facilitate both living and stereospecific Ziegler-Natta polymerization of an α-olefin.[65]

My aim was to use the methodology reported by a previous PhD student in the Sita group, Jayaratne, to make block copolymers and study the phase behaviors of these polymers.[241]

4.2.1 Synthesis of Rod-Coil Block Copolymers based on α-Olefins and 1,5-Hexadiene

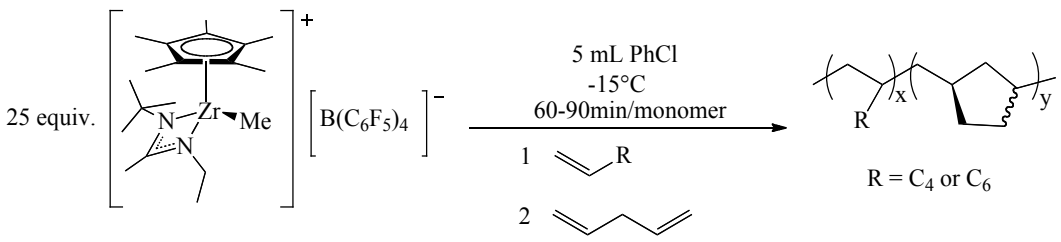

Scheme 4.1. Synthesis of PMCP-based diblock polyolefins.

Table 4.1. Synthesis of *iso*-α-olefin/PMCP diblock copolymers.

Entry	α-olefin	HD	R	T_p (°C)	M_w	M_n	PDI	T_m (°C)	T_c (°C)
1	89 (90)	89 (90)	C_4	-10	49,300	35,700	1.38	75	83
2	89 (90)	89 (90)	C_4	-15	38,700	30,700	1.26	86	80
3	89 (60)	89 (60)	C_4	-15	27,600	21,100	1.30	81	86
4	89 (90)	89 (90)	C_6	-15	19,800	17,800	1.11	74	86

Polymerizations were conducted in 5 mL chlorobenzene using equimolar (25 μmol) amounts of **Precatalyst I** and **Cocatalyst I**; Values correspond to the number of monomer equivalents and those in parentheses to polymerization times in minutes.

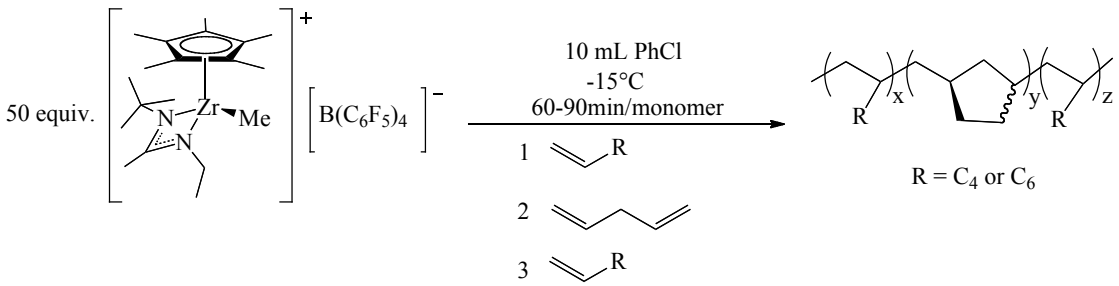

Scheme 4.2. Synthesis of PMCP-based triblock polyolefins.

Table 4.2. Synthesis of *iso*-α-olefin/PMCP triblock copolymers.

Entry	α-olefin	HD	α-olefin	R	T_p (°C)	M_w	M_n	PDI	T_m (°C)	T_c (°C)
5	77 (90)	77 (90)	77 (90)	C_4	-10	65,500	42,600	1.54	70	86
6	77 (60)	77 (60)	77 (60)	C_4	-15	42,200	32,200	1.30	73	86
7	77 (90)	77 (90)	77 (90)	C_6	-15	45,600	31,000	1.47	70	86

Polymerizations were conducted in 10 mL chlorobenzene using equimolar (50 μmol) amounts of **Precatalyst I** and **Cocatalyst I**; Values correspond to the number of monomer equivalents and those in parentheses to polymerization times in minutes.

The block copolymers were synthesized following reported literature.[241] Briefly, this was done by adding the α-olefin of choice (either 1-hexene or 1-octene) to a chlorobenzene solution containing equimolar amounts of **Precatalyst I** and **Cocatalyst I** for some prescribed time as specified in Tables 1 and 2. Subsequent addition of some amount of 1,5-hexadiene to the reaction solution yield the crystalline segment of the block copolymer. In cases where diblock copolymers were targeted, the polymerization was subsequently terminated with the addition of methanol. However in cases where triblock copolymers were targeted, an extra aliquot of α-olefin was added to the reaction flask and the solution was stirred for some allotted time, after which the reaction was terminated using methanol. The hexadiene-based block copolymers were isolated after precipitation of the chlorobenzene reaction solution into excess acidic methanol solution.

Tables 1 and 2 give molecular weights, polydispersity indices as well as thermal properties of the polymers that were synthesized. It is worth noting that the polydispersities of the block copolymers ranged from 1.11 to 1.54, which is slightly broader than the PDIs reported by Jayaratne.[241] Nonetheless, phase behaviors of these polymers were still probed. Focus was placed on the analysis of the 1-octene based diblock and triblock copolymer because molecular weight distributions were a bit narrower. Given that isotactic poly(1-hexene) and poly(1-octene) both have glass transition temperatures below the melting point of the crystalline block that allows mobility of the coil polymer chains, the phase behavior should be virtually identical.

4.3 Ps-tm AFM and TEM Imaging of isotactic PO/PMCP Block Copolymers

The ability to prepare *iso*-PO/PMCP block copolymers through sequential monomer addition was confirmed, though improvements are required. The microphase separated morphologies at the surface of this rod-coil block copolymer were investigated by phase sensitive tapping mode atomic force microscopy, ps-tm AFM. In ps-tm AFM the phase difference between the driving signal of the piezo oscillating the cantilever and the phase lag of the cantilever oscillation, which results from variations in material properties such as adhesion and viscoelasticity, can be exploited in order to map out the surface morphology of rod-coil block copolymers as shown in Figure 3.[242,243] Images revealed microphase separation into a cylindrical morphology with soft domains of poly(1-octene) (PO) surrounded by hard PMCP cylinders parallel to the surface, marking the production of the first class of microphase separated polyolefin materials of well-defined structure by living Ziegler-Natta polymerization.

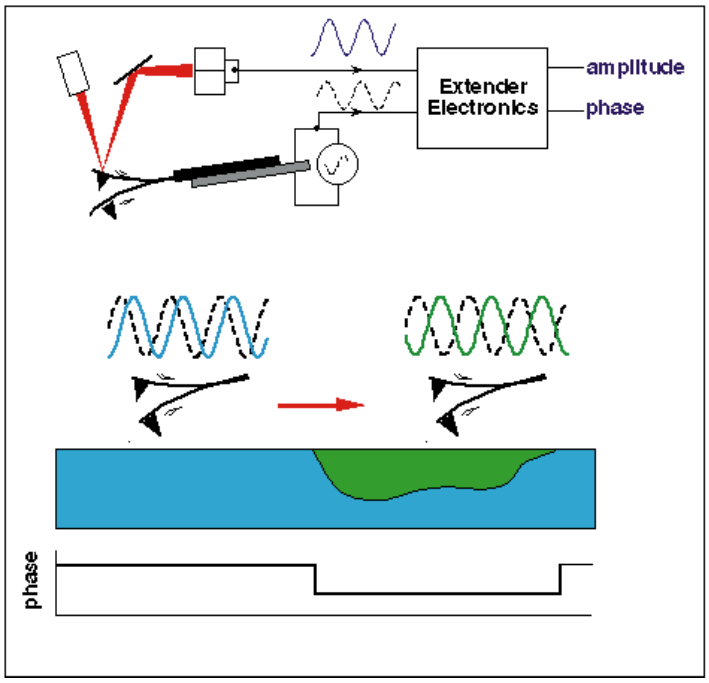

Figure 4.3. Phase imaging uses the Extender Electronics Module to measure the phase lag of the cantilever oscillation (solid wave) relative to the piezo drive (dashed wave). The amplitude signal is used simultaneously by the NanoScope III controller for Tapping Mode feedback. Spatial variations in sample properties cause shifts in the cantilever phase (bottom) which are mapped to produce the phase images shown here. Reproduced from Digital Instruments' K.L. Babcock and C.B. Prater.[243]

Height and phase maps for samples 4 and 7, (*iso*-PO/PMCP di- and triblock) obtained after spin casting from toluene solution onto crystalline silicon substrates, established that thin films of 4 (~ 30 nm thick) self assembled into a trinity of microstructures while thin films of 7 having the same thickness display complex yet uniformed morphology upon phase separation. Figures 4a-4c display AFM images of the nanostructures observed for the *iso*-PO triblock copolymer.

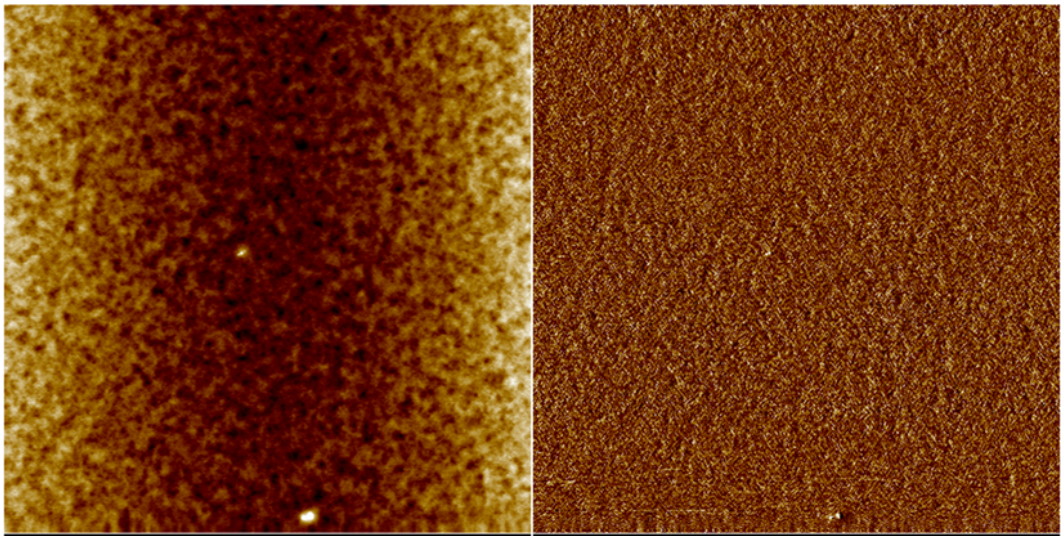

Figure 4.4 a. 10μm X 10μm ps-tm AFM height (left) and phase maps (right) of 34 nm thick unannealed film spun from 1 wt% *iso*-PO/PMCP triblock (entry 7) at 6000 rpm for 1 min.

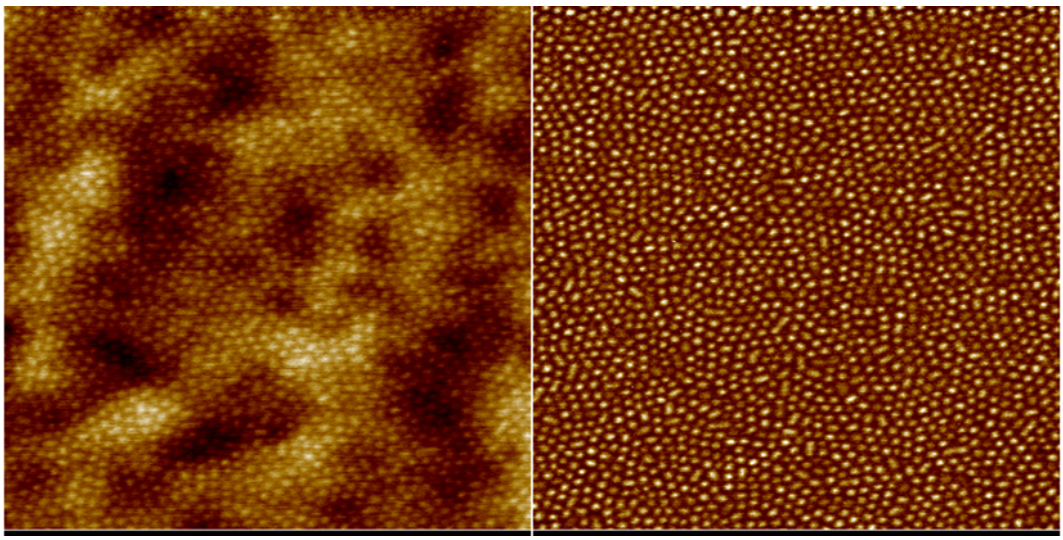

Figure 4.4 b. 1μm X 1μm ps-tm AFM height (left) and phase maps (right) of 34 nm thick unannealed film spun from 1 wt% *iso*-PO/PMCP triblock (entry 7) at 6000 rpm for 1 min.

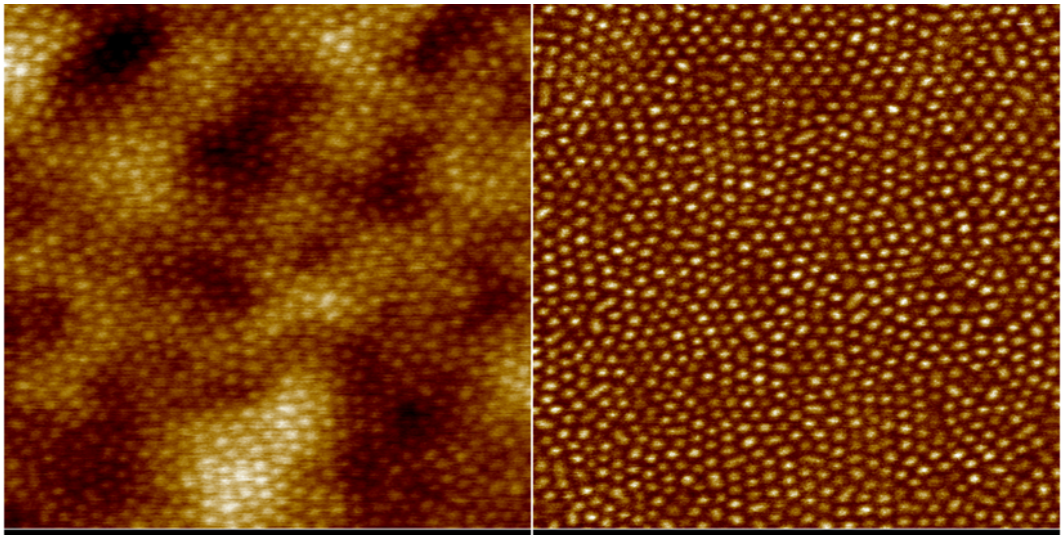

Figure 4.4 c. 700 nm X 700 nm ps-tm AFM height (left) and phase maps (right) of 34 nm thick unannealed film spun from 1 wt% *iso*-PO/PMCP triblock (entry 7) at 6000 rpm for 1 min.

The height map illustrates height gradients on the surface of the 29 nm thin film, where low regions are shown in brown and the high regions are white. Although the 10 X 10 μm phase image seems relatively flat, the 1 X 1 μm and 700 X 700 nm phase maps reveal hard crystalline hexagonally packed spherical nanostructures (white) with diameters of ~15-20 nm arranged in a continuous matrix of soft amorphous (dark brown) segments. Also observed were "defects" where the spheres are elongated. This could indicate that the morphology is cylindrical, rather than spherical, with the majority of cylinders aligned perpendicular to the surface and a small percentage aligned parallel to the surface. When the height and phase map are compared side by side there appears to be no changes in nanostructure between the low and high height regions of the thin film, a possible indication that the film thickness is commensurate with the domain spacing or fully quantized.[244]

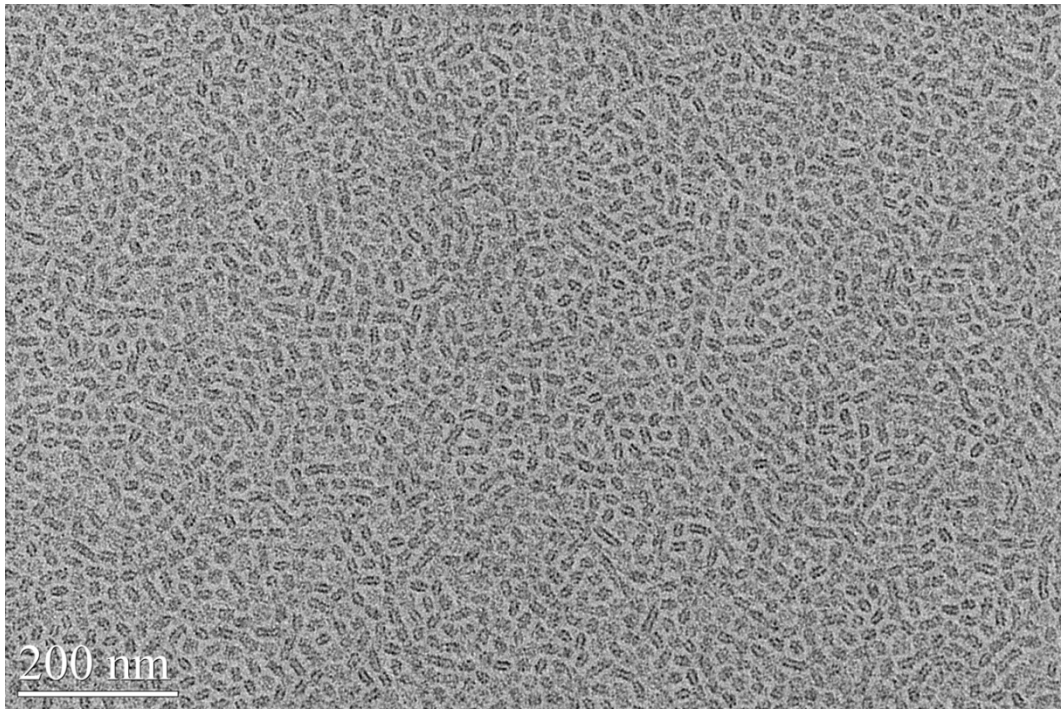

Figure 4.4 d. 200 nm TEM image of 32 nm thick unannealed film spun from 1 wt% *iso*-PO/PMCP triblock (entry 7) at 6000 rpm for 1min and stained for 60min with RuO_4.

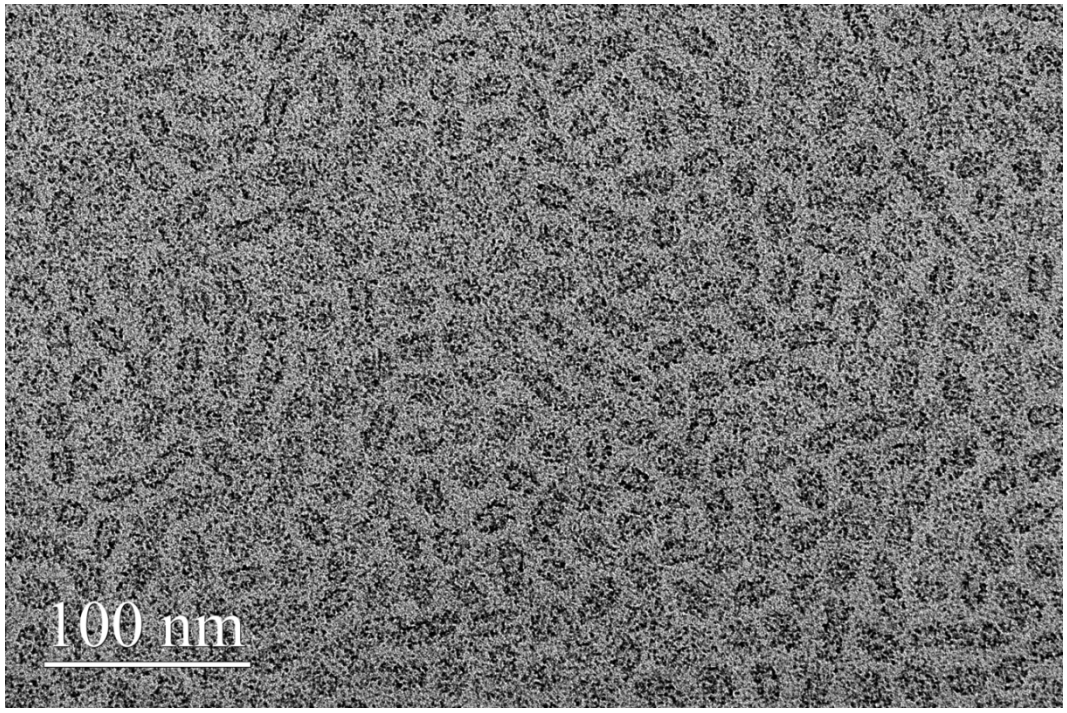

Figure 4.4 e. 100 nm TEM image of 32 nm thick unannealed film spun from 1 wt% *iso*-PO/PMCP triblock (entry 7) at 6000 rpm for 1min and stained for 60min with RuO_4.

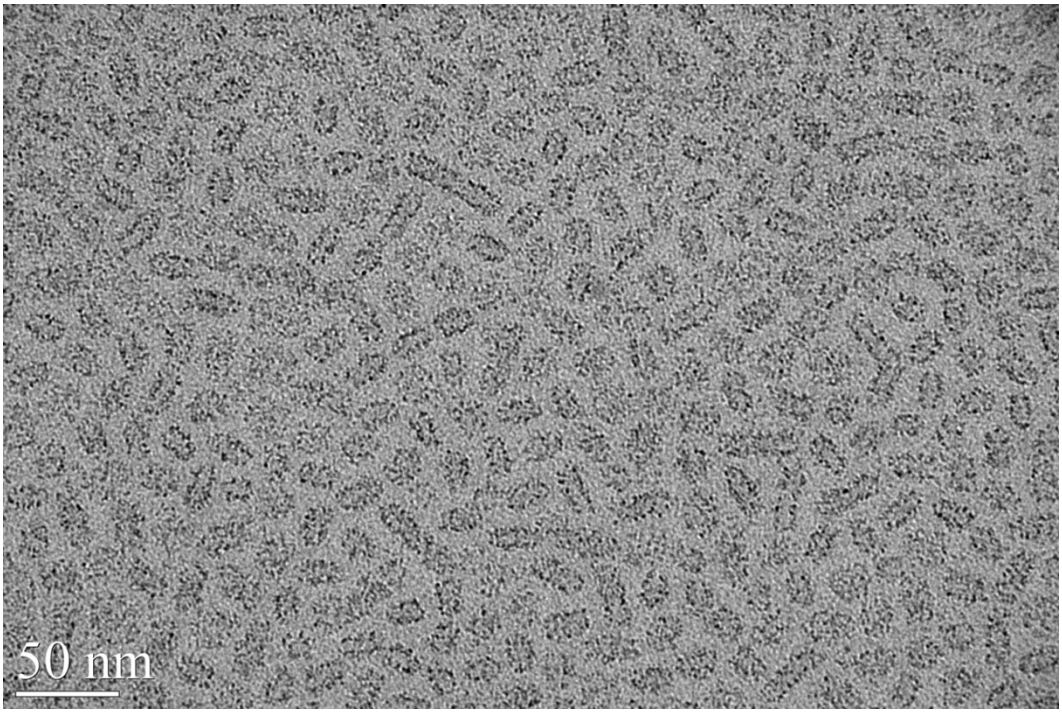

Figure 4.4 f. 50 nm TEM image of 32 nm thick unannealed film spun from 1 wt% *iso*-PO/PMCP triblock (entry 7) at 6000 rpm for 1 min and stained for 60 min with RuO_4.

Convinced that the triblock copolymer phase separated into either cylinders aligned perpendicular to the surface because of hexagonal packing, TEM imaging was conducted on a 32 nm thick film by Wonseok Hwang of the Sita group, shown in Figures 4d-4f. Samples were prepared by spin coating 1 wt% *iso*-PO/PMCP on a carbon coated mica surface then transferring the film to a 600 mesh copper gilder grid and staining with ruthenium tetroxide for 60 minutes. TEM did not reveal lamellae, cylindrical, or spherical morphology, instead it showed short oval shaped rod-like structures scattered along the surface. Furthermore, TEM images depicted the short rod like morphology to be the amorphous regions. Darker domains in the TEM images are due to more intense staining of that region. Since RuO_4 has a greater diffusivity in the less dense amorphous regions they are thus represented by the darker grey color. This result is contrary to what was seen in the AFM phase maps, which indicated crystalline cylinders in an amorphous

matrix. In order to better understand the morphology that resulted from the self assembly of the *iso*-PO/PMCP triblock copolymer, the phase behavior diblock system was probed, as it is not influence by the additional coil-coil interactions and can be utilized to obtain fundamental information about the phase behavior in rod-coil polyolefin systems.

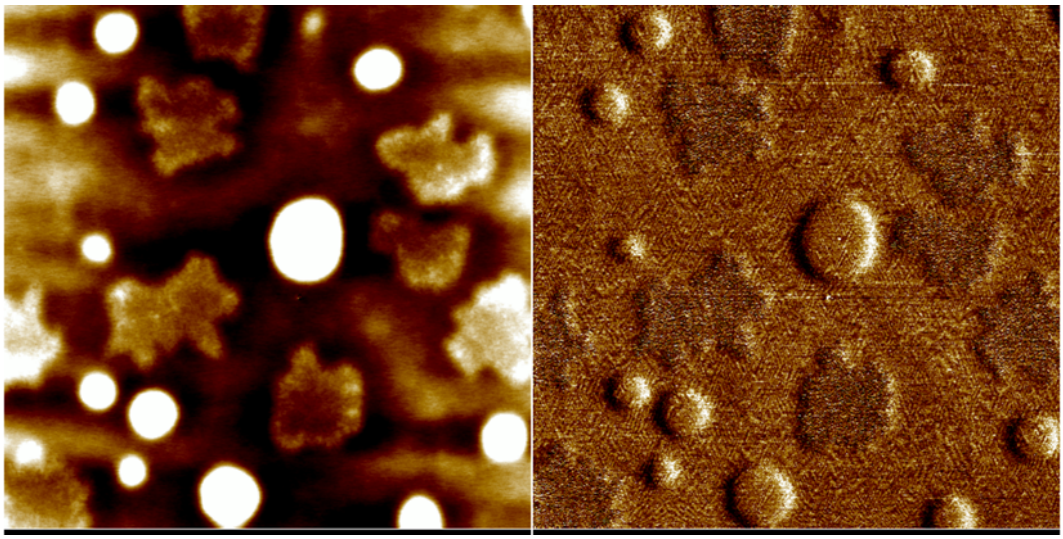

Figure 4.5 a. 10 µm X 10 µm ps-tm AFM height (left) and phase maps (right) of 29 nm thick unannealed film spun from 1 wt% *iso*-PO/PMCP diblock (entry 4) at 6000 rpm for 1 min.

The 10 µm X 10 µm height and phase map of the diblock copolymer was not flat as in the case of the triblock copolymer. In fact, randomly scattered high spherically shaped regions 500 nm - 2 µm in size and lower irregularly shaped regions about 2 µm in size were observed on the 34 nm thick film surface, as shown in Figure 5a. A difference in morphology in these regions seems evident from the 10 µm scan, thus each region was probed. A 3 µm X 3 µm height and phase map seen in Figure 5b-5d, undoubtedly illustrates regions with high cylindrical domains ~20 nm in size packed parallel to the surface and lower bicontinuous regions ~20 nm in size surrounded by spherical domains.

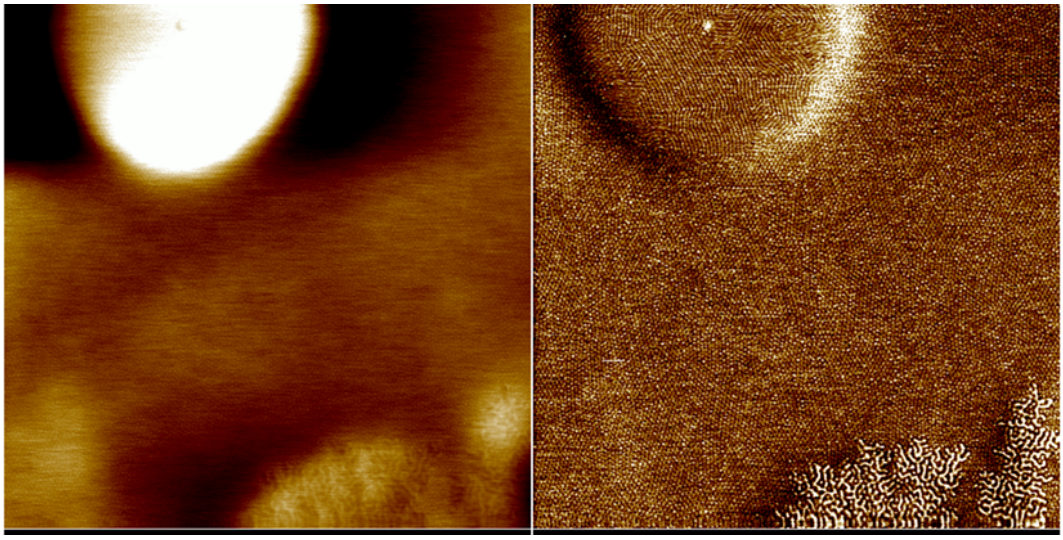

Figure 4.5 b. 3 μm X 3 μm ps-tm AFM height (left) and phase maps (right) of 29 nm thick unannealed film spun from 1 wt% *iso*-PO/PMCP diblock (entry 4) at 6000 rpm for 1 min.

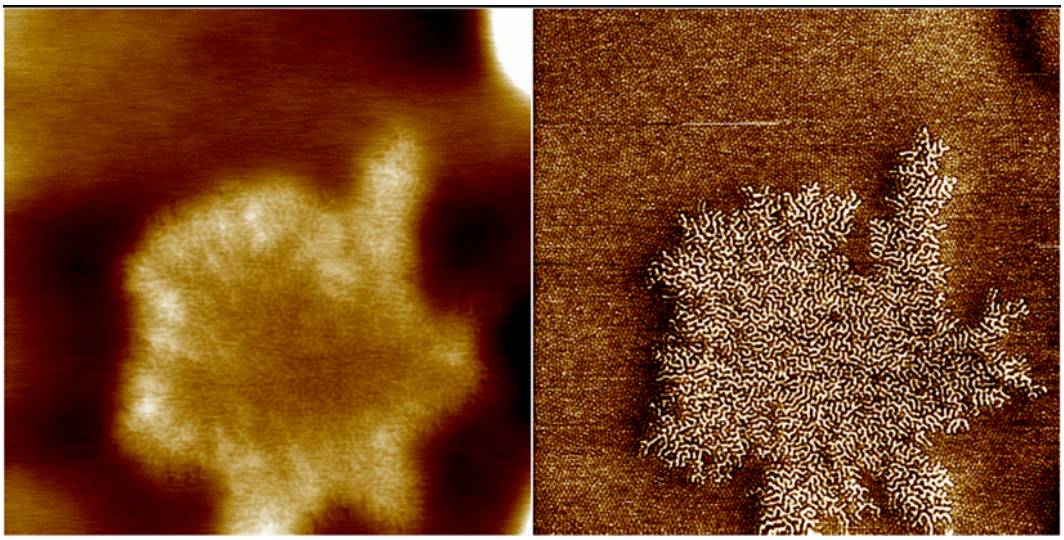

Figure 4.5 c. 3 μm X 3 μm ps-tm AFM height (left) and phase maps (right) of 29 nm thick unannealed film spun from 1 wt% iso-PO/PMCP diblock (entry 4) at 6000 rpm for 1 min.

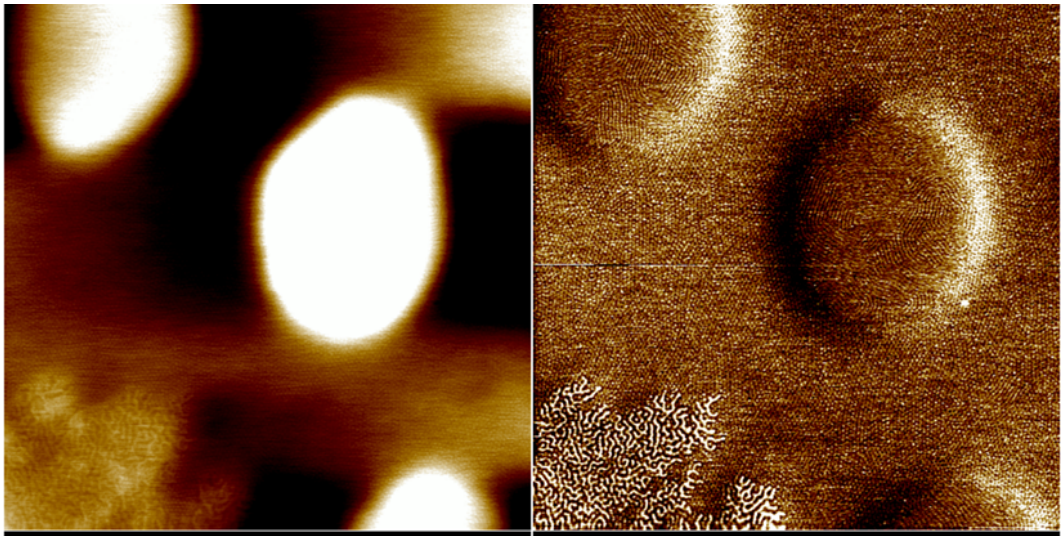

Figure 4.5 d. 3 μm X 3 μm ps-tm AFM height (left) and phase maps (right) of 29 nm thick unannealed film spun from 1 wt% *iso*-PO/PMCP diblock (entry 4) at 6000 rpm for 1 min.

This distribution of phase behavior can be rationalized by the height differences in the film, where the spheres observed could be a monolayer of cylinders aligned perpendicular to the surface; the high regions could represent a bilayer of cylinders, and the bicontinuous region could be islands that result because of an unquantized increase in height. Evidence of this reorientation was obtained from vertical distance measurements taken on using the Nanscope III program. The vertical distance between the flat spherical surface and the region with parallel cylinders was about 16 nm. The vertical distance between the flat spherical region and the bicontinuous islands was about 8 nm. The diameter of the spheres in the flat region was approximately 15-20 nm. Also possible is that both the parallel cylinders and the bicontinuous microstructure resulted from unquantized domain spacings; this is dependent on whether or not the domain size is 15 or 20 nm. Determining the microstructure in thinner and thicker films can allow further elucidation of height effects on the morphology of these materials.

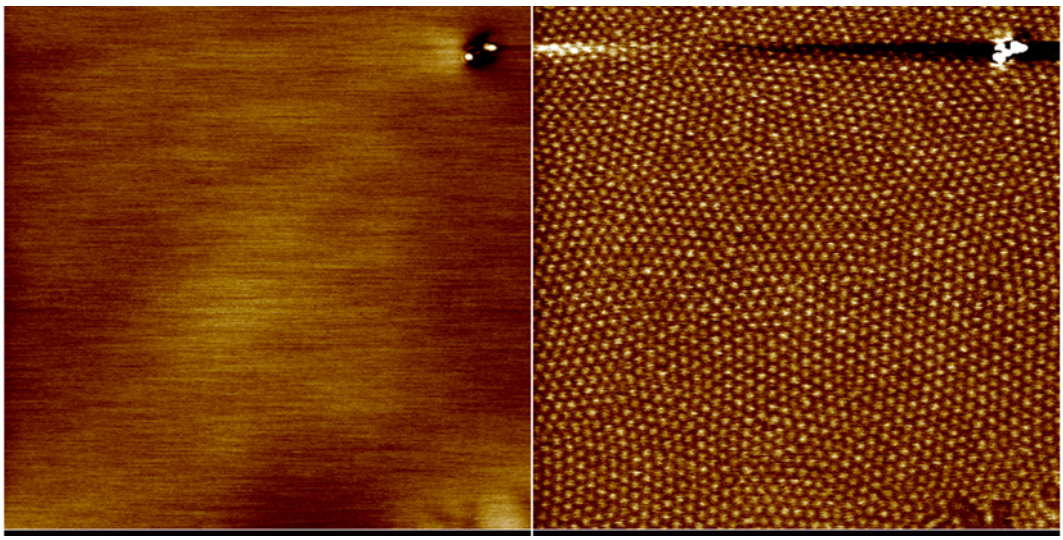

Figure 4.5 e. 1 μm X 1 μm ps-tm AFM height (left) and phase maps (right) of 29 nm thick unannealed film spun from 1 wt% *iso*-PO/PMCP diblock (entry 4) at 6000 rpm for 1 min.

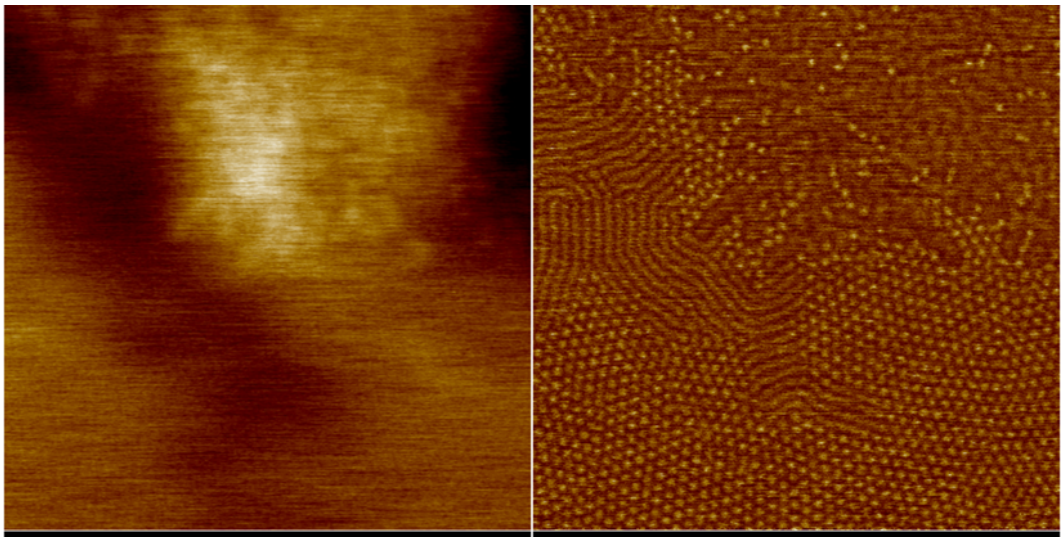

Figure 4.5 f. 1 μm X 1 μm ps-tm AFM height (left) and phase maps (right) of 29 nm thick unannealed film spun from 1 wt% *iso*-PO/PMCP diblock (entry 4) at 6000 rpm for 1 min.

The bottom left corner of the 1 X 1 μm phase image of the *iso*-PO diblock shows a defect, therefore this material was further investigated. Additional probing uncovered the coexistence of three phases represented by spheres (~20 nm), "brain-coral" (~20 nm) and lamellae or parallel cylindrical regions (~30-40 nm) as shown in Figure 5e-5f, which

may or may not be due to lack of quantization. In this case the height map shows the brain-coral to be the highest, and the lamellae like region to be the lowest with the spheres in the mid height region. The vertical distance between the spheres and the "brain-coral" is about 3 nm. The distance between the lamellae like regions and the flat spherical region is about 4 nm. Thermal annealing of these materials prior to imaging to eliminate solvent effects may allow distinction between these observed morphologies and the thermodynamically stable morphologies.

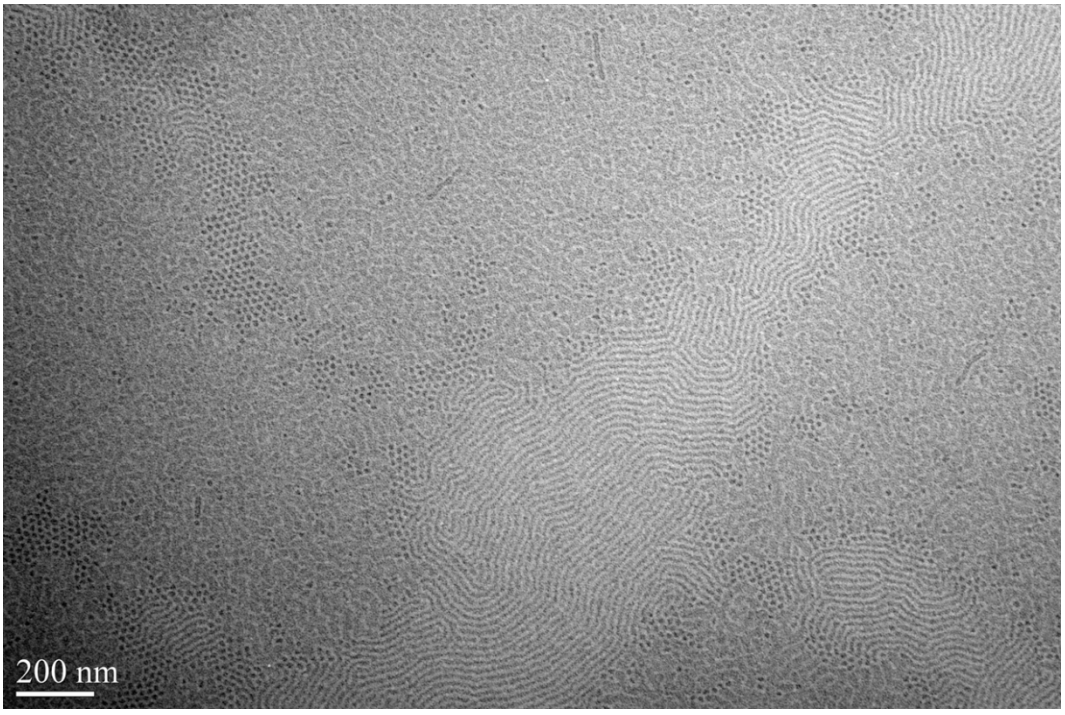

Figure 4.6 a. 200 nm TEM image of 32 nm thick unannealed film spun from 1 wt% *iso*-PO/PMCP diblock (entry 4) at 6000 rpm for 1 min and stained for 60 min with RuO_4.

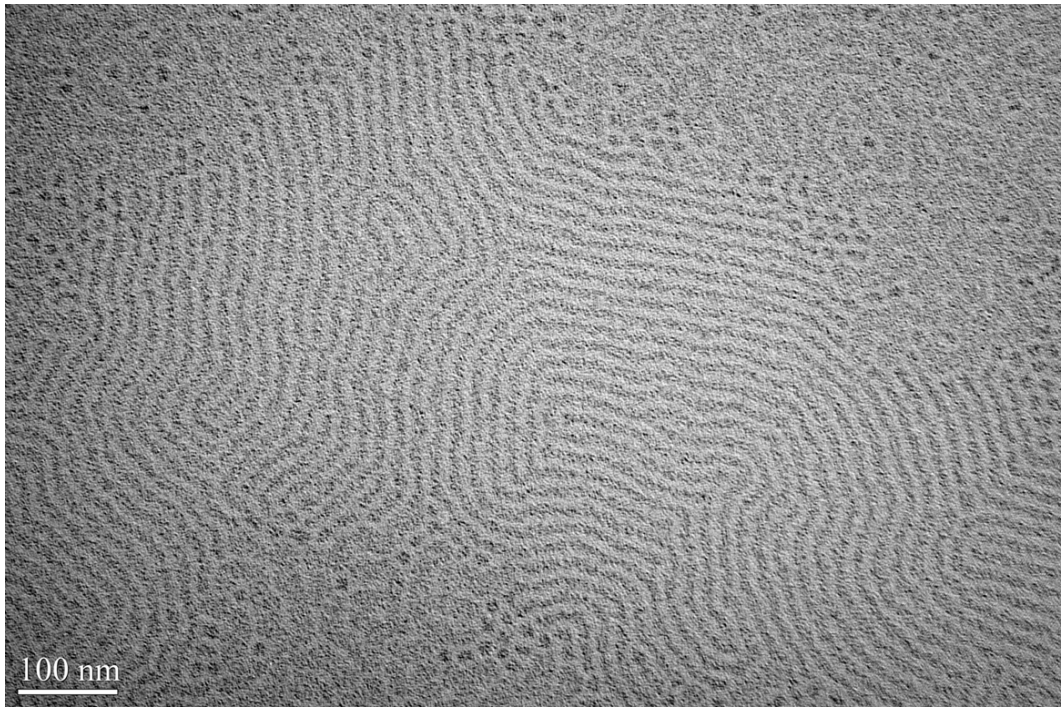

Figure 4.6 b. 100 nm TEM image of 32 nm thick unannealed film spun from 1 wt% *iso*-PO/PMCP diblock (entry 4) at 6000 rpm for 1 min and stained for 60 min with RuO_4.

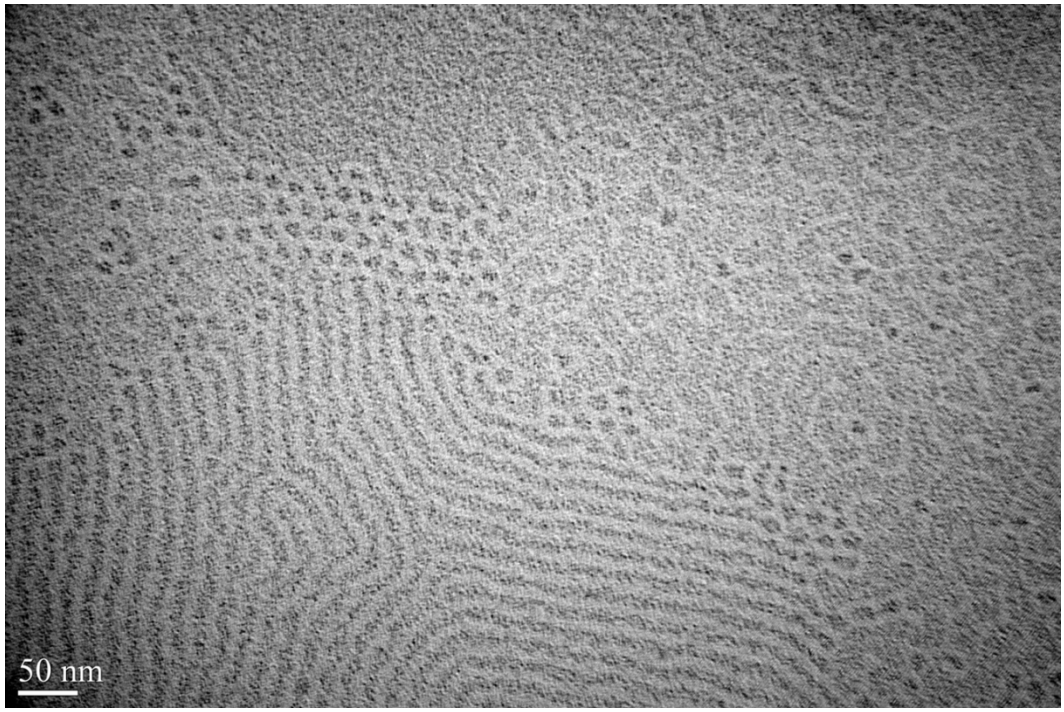

Figure 4.6 c. 50 nm TEM image of 32 nm thick unannealed film spun from 1 wt% *iso*-PO/PMCP diblock (entry 4) at 6000 rpm for 1 min and stained for 60 min with RuO_4.

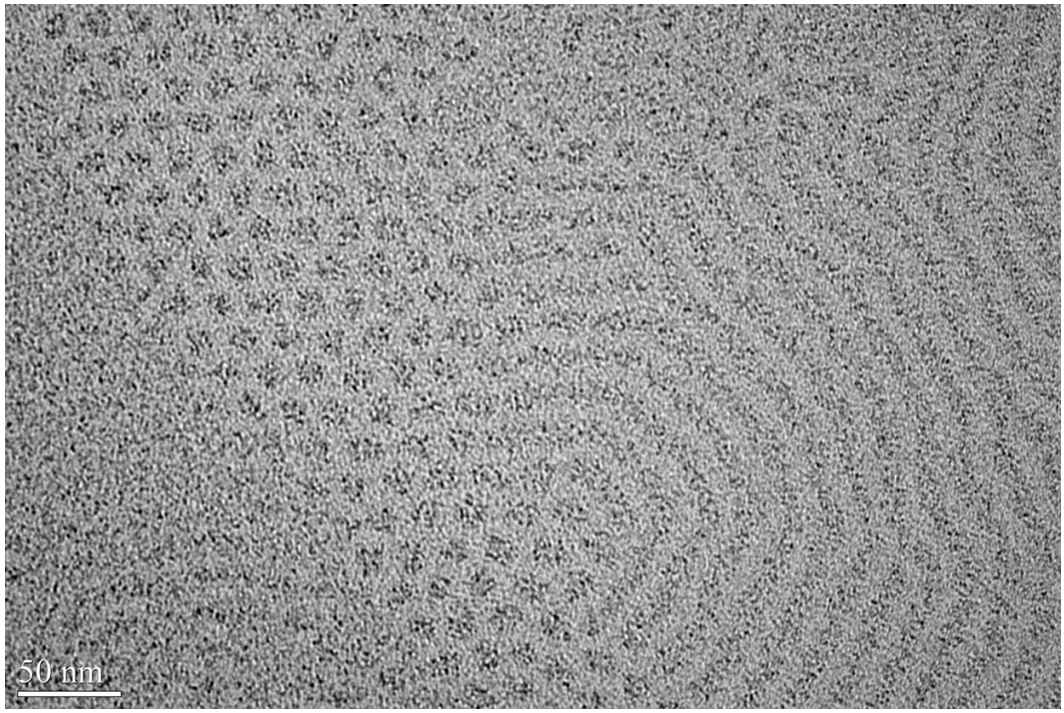

Figure 4.6 d. 50 nm TEM image of 32 nm thick unannealed film spun from 1 wt% *iso*-PO/PMCP diblock (entry 4) at 6000 rpm for 1 min and stained for 60 min with RuO_4.

As in the case of the triblock, TEM was utilized in attempts to distinguish between a spherical and cylindrical morphology. TEM images, Figures 6a-6d, obtained from the *iso*-PO/PMCP diblock show a trinity of nanostructures as seen in ps-tm AFM phase maps. The low, lightest grey, regions seem to have lamellae morphology, while the higher regions, darker grey, showed bicontinuous or "brain coral" type morphology. Hexagonally packed spheres or cylinders aligned perpendicular to the surface was observed around the perimeter of bicontinuous domains. Like in the case of the triblock copolymer, TEM showed inversion of hard and soft regions when compared to AFM images. Block copolymer/homopolymer blends can be used to distinguish between amorphous and crystalline regions. In theory, the addition of coil homopolymers should result in the expansion of the amorphous region. Hence, if the dark lamellae regions are amorphous the domain size should increase. If the domain size of the matrix increased

rather than that of the lamellae regions, it would indicate an amorphous matrix. In this case, the preferential staining of the crystalline regions could be attributed to units of unsaturations from the pendant vinyl groups produced from the polymerization of 1,5-hexadiene.

Attempts were made to synthesize isotactic PH/PMCP diblock copolymer under reaction conditions analogous to those reported by Jayaratne et al.[241], since they had already shown to be successful in the production of narrow polydispersity (PDI<1.1) block copolymers. While NMR spectroscopy showed these conditions to be effective in the synthesis of *iso*-PH/PMCP diblock copolymer, GPC chromatograph showed it to be ineffective for the production of narrow molecular weight distribution materials. GPC revealed a trimodal chromatograph, having a low intensity high molecular weight peak of 91.7 kDa and a low intensity low molecular weight peak of 14.2 kDa in addition to a high intensity peak representative of the bulk of the material. The overall PDI of the material was 1.38 in contrast to the previous PDI of 1.05. The high molecular weight peak could be due to crosslinking of the polymer chain, as ^{1}H NMR shows peaks in the olefinic region indicating the presence of vinyl groups resulting from the 1,2-insertion of 1,5-hexadiene. The low molecular weight peak can be attributed to impurities being introduced to the reaction solution with sequential addition of the second and third monomer, which could render a portion of the catalyst in solution inactive. Precipitation of polymer from the reaction solution prior to termination is another possible reason for the presence of the low molecular weight peak.

4.4 Conclusions

Very exciting observations regarding the phase separation of pure polyolefin rod-coil systems based on 1-octene and 1,5-hexadiene were reported, however given the inhomogeneity observed by gel permeation chromatography, it is imperative that other hydrocarbon based systems be probed. A polyolefin rod-coil block copolymer system having a narrow monomodal molecular weight distribution would be better suited as a model system to investigate the unique phase behavior of hydrocarbon based block copolymers, because the self-assembled nanostructures observed could then be attributed to the incompatibility of the covalently link polymer chain and completely independent of the bimodal character of the polymer being analyzed. Elucidation of phase behavior of these simple saturated polyolefins serve to provide a thorough understanding of structural parameters that impact the self-assembly of rod-coil block copolymers. Correlation of this phase behavior with physical and mechanical properties will allow the rational design of polymeric materials having specifically targeted properties. The inexpensive and large scale production of these benign materials having limitless properties can find use in a variety of applications within numerous commercial industries.

4.5 Experimental

All manipulations were performed under an inert atmosphere of dinitrogen using either standard Schlenk techniques or a Vacuum Atmospheres glovebox. Dry, oxygen-free solvents were employed throughout. Chlorobenzene was distilled from calcium hydride. The 1-hexene, 1,5-hexadiene, 1-octene, and 4-methylpentene monomers were vacuum transferred from NaK prior to use in polymerizations. **Precatalyst I** was prepared according to previously reported procedures. **Cocatalyst I** was purchased from Strem

Chemicals and used without further purification. GPC analyses were performed using a Viscotek GPC system equipped with a column oven and differential refractometer both maintained at 45 °C and four columns also maintained at 45 °C. THF was used as the eluant at a flow rate of 1.0 mL/min. M_n, M_w and M_w/M_n values were obtained using a Viscotek GPC with OmniSEC software (conventional calibration) and ten polystyrene standards (M_n = 580 Da to 3,150 kDa) (from Polymer Laboratories). Thermal analyses were performed on a TA Instruments DSC Q1000 calibrated with indium and sapphire using hermetically sealed aluminum sample pans holding approximately 10 mg of material. Samples were heated and cooled at a rate of 10 ˚C/min and dinitrogen was used as the sample purge gas at a flow rate of 50 mL/min. T_m, T_c values were obtained using a heat/cool/heat method on a DSC Q1000 with TA Series Explorer and TA Universal Analysis software. In DSC analyses, heat flows (mW) less than zero were deemed endothermic while those greater than zero were considered exothermic. $\{^1H\}$ NMR spectra were recorded at 100 MHz, using chloroform-d_1 as the solvent at 25 °C.

General procedure for living polymerization of iso-poly(1-hexene)/ poly(methylene-1,3-cyclopentane) block copolymer: In a 50 mL round-bottom flask or 20 mL vial, to 5 mL chlorobenzene at -10 °C or -15 °C were added the 25 μmol **Cocatalyst I** and the 25 μmol **Precatalyst I**. Then 89 or 178 equivalents (188 mg or 377 mg) of 25 μmol 1-hexene were added to the reaction flask for 30 min to 90 min with stirring before the immediate addition of 50, 89, 178 equivalents (103 mg, 183 mg, or 365 mg) 25 μmol 1,5-hexadiene with stirring for 30 min to 90 min before quenching with 0.5 mL of methanol. The chlorobenzene solution was precipitated into 400 mL of methanol and 2 mL hydrochloric acid solution to isolate the polymer. The final product was collected after

decanting the methanol solution and dried overnight in *vacuo* before GPC, DSC and NMR analyses.

General procedure for living polymerization of iso-poly(1-hexene)/ poly(methylene-1,3-cyclopentane)/iso-poly(1-hexene) block copolymer: In a 50 mL round-bottom flask or 20 mL vial, to 10 mL chlorobenzene at -10 °C or -15 °C were added the 25 μmol or 50 μmol **Cocatalyst I** and the 25 μmol or 50 μmol **Precatalyst I**. Then 77 equivalents (162 mg or 324 mg) of 25 μmol or 50 μmol 1-hexene were added to the reaction flask for 30 min to 90 min with stirring before the immediate addition of 50 or 77 equivalents (158 mg or 316 mg) 1,5-hexadiene with stirring for 60 min to 90 min. Subsequently, 77 equivalents (162 mg or 324 mg) of 25 μmol or 50 μmol 1-hexene were added to the reaction flask for 60 min to 90 min with stirring before quenching with 0.5 mL of methanol. The chlorobenzene solution was precipitated into 400 mL of methanol and 2 mL hydrochloric acid solution to isolate the polymer. The final product was collected after decanting the methanol solution and dried overnight in *vacuo* before GPC, DSC and NMR analyses.

General procedure for living polymerization of iso-poly(1-octene)/ poly(methylene-1,3-cyclopentane) block copolymer: In a 20 mL vial, to 5 mL chlorobenzene at -15 °C were added the 25 μmol **Cocatalyst I** and the 25 μmol **Precatalyst I**. Then 89 equivalents (250 mg) of 25 μmol 1-octene were added to the reaction flask for 90 min with stirring before the immediate addition of 89 equivalents (183 mg) 25 μmol 1,5-hexadiene with stirring for 90 min before quenching with 0.5 mL of methanol. The chlorobenzene solution was precipitated into 400 mL of methanol and 2 mL hydrochloric

acid solution to isolate the polymer. The final product was collected after decanting the methanol solution and dried overnight in *vacuo* before GPC, DSC and NMR analyses.

General procedure for living polymerization of iso-poly(1-octene)/ poly(methylene-1,3-cyclopentane)/ iso-poly(1-octene) block copolymer: In a 20 mL vial, to 10 mL chlorobenzene at -15 °C were added the 50 μmol **Cocatalyst I** and the 50 μmol **Precatalyst I**. Then 77 equivalents (432 mg) of 50 μmol 1-octene were added to the reaction flask for 90 min with stirring before the immediate addition of 77 equivalents (316 mg) 1,5-hexadiene with stirring for 90 min. Subsequently, 77 equivalents (432 mg) of 50 μmol 1-octene were added to the reaction flask for 90 min with stirring before quenching with 0.5 mL of methanol. The chlorobenzene solution was precipitated into 400 mL of methanol and 2 mL hydrochloric acid solution to isolate the polymer. The final product was collected after decanting the methanol solution and dried overnight in *vacuo* before GPC, DSC and NMR analyses.

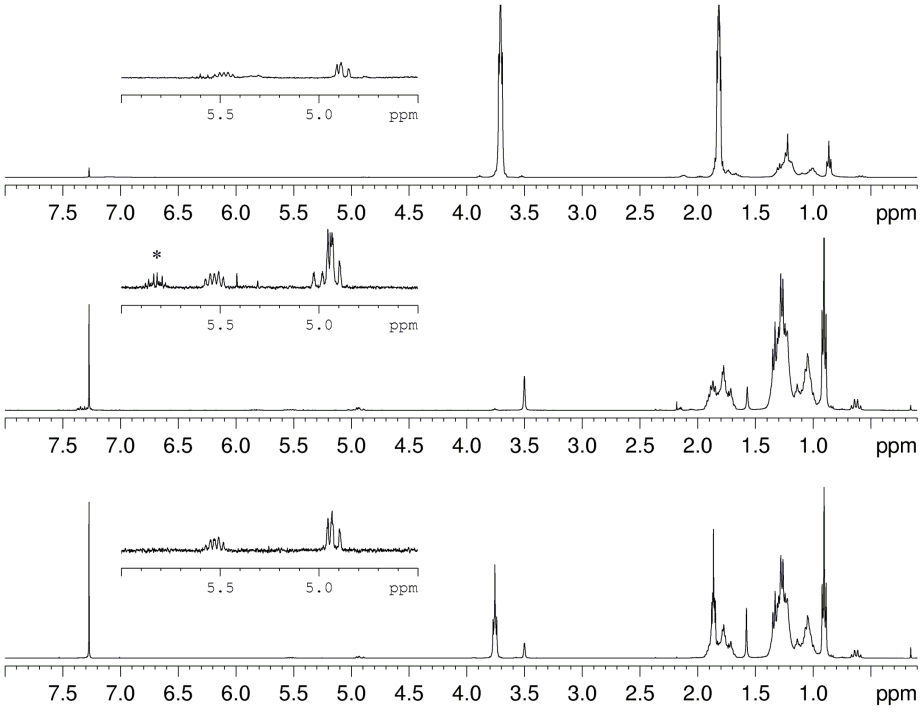

SI 4.1. ^{1}H NMR (400 MHz, chloroform-d_1, 25 ºC) spectrum of *iso*-poly(1-hexene)/ PMCP diblock copolymer with the expansion showing vinyl groups resulting from 1,2-insertion of 1,5-hexadiene. The asterisk corresponds to impurities. Entries 1-3 are shown in order from top to bottom.

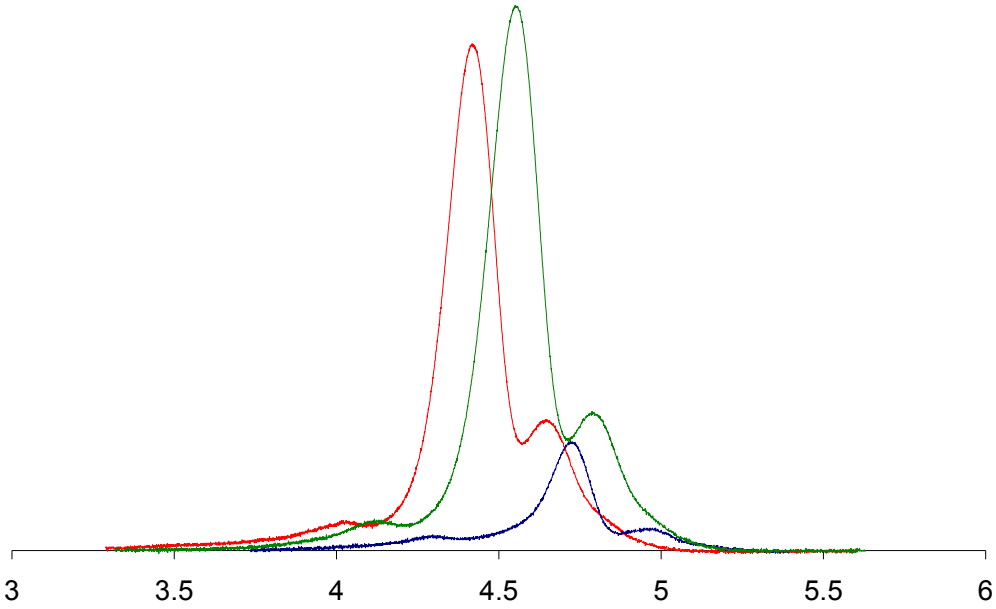

SI 4.2. GPC chromatographs from *iso*-poly(1-hexene)/ PMCP diblock copolymers, where the red, blue, and green chromatographs correspond to entries 1-3, respectively.

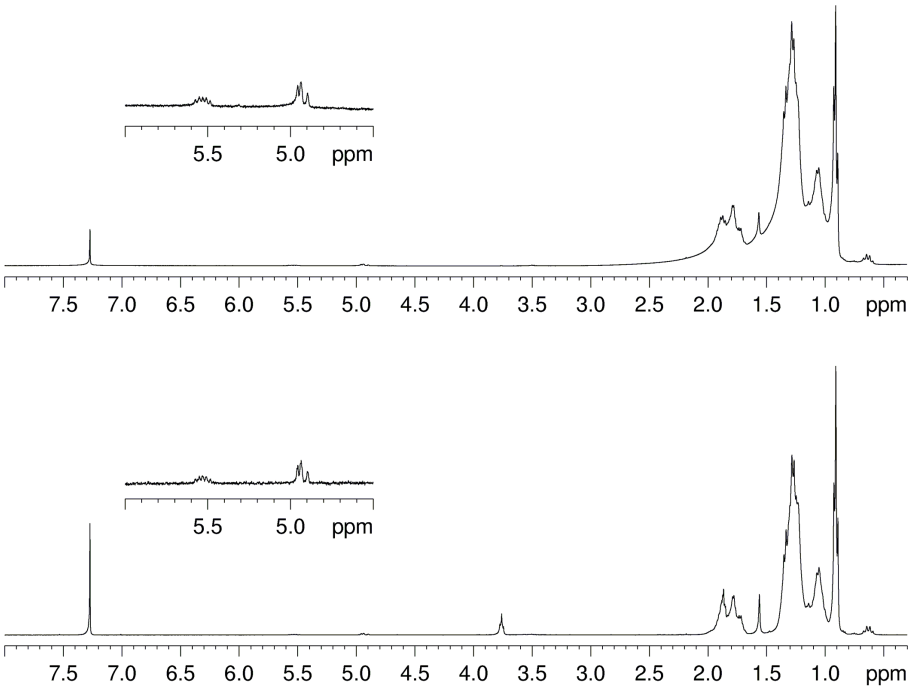

SI 4.3. ^{1}H NMR (400 MHz, chloroform-d_1, 25 ºC) spectrum of *iso*-poly(1-hexene)/ PMCP triblock copolymer with the expansion showing vinyl groups resulting from 1,2-insertion of 1,5-hexadiene. Entries 5 and 6 are shown from top to bottom respectively.

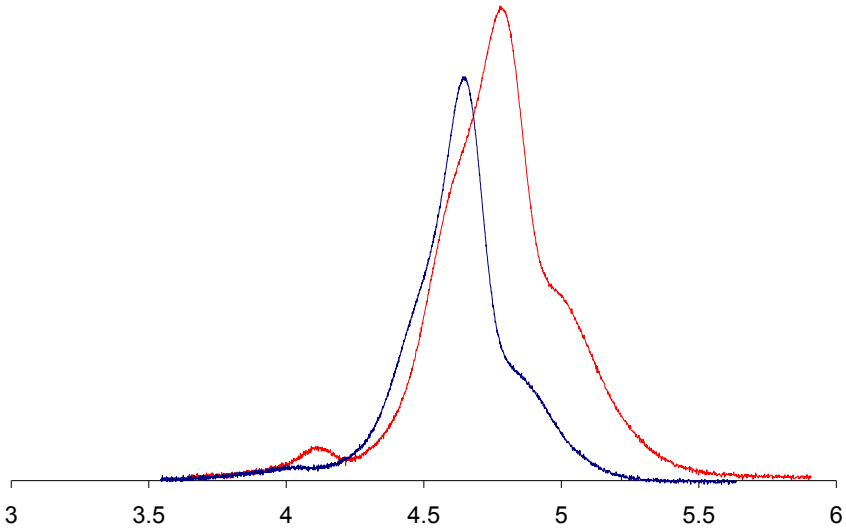

SI 4.4. GPC chromatographs from *iso*-poly(1-hexene)/ PMCP triblock copolymers, where the red and blue chromatographs correspond to entries 5 and 6, respectively.

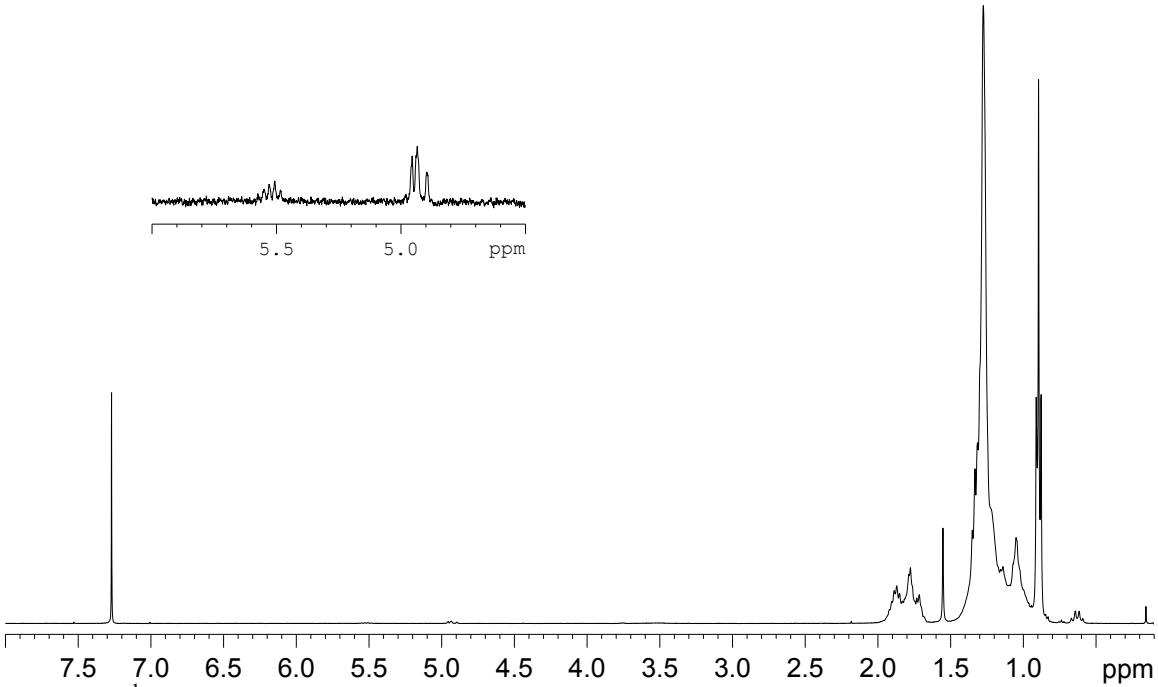

SI 4.5. ^{1}H NMR (400 MHz, chloroform-d_1, 25 ºC) spectrum of *iso*-poly(1-octene)/ PMCP diblock copolymer with the expansion showing vinyl groups resulting from 1,2-insertion of 1,5-hexadiene (entry 4).

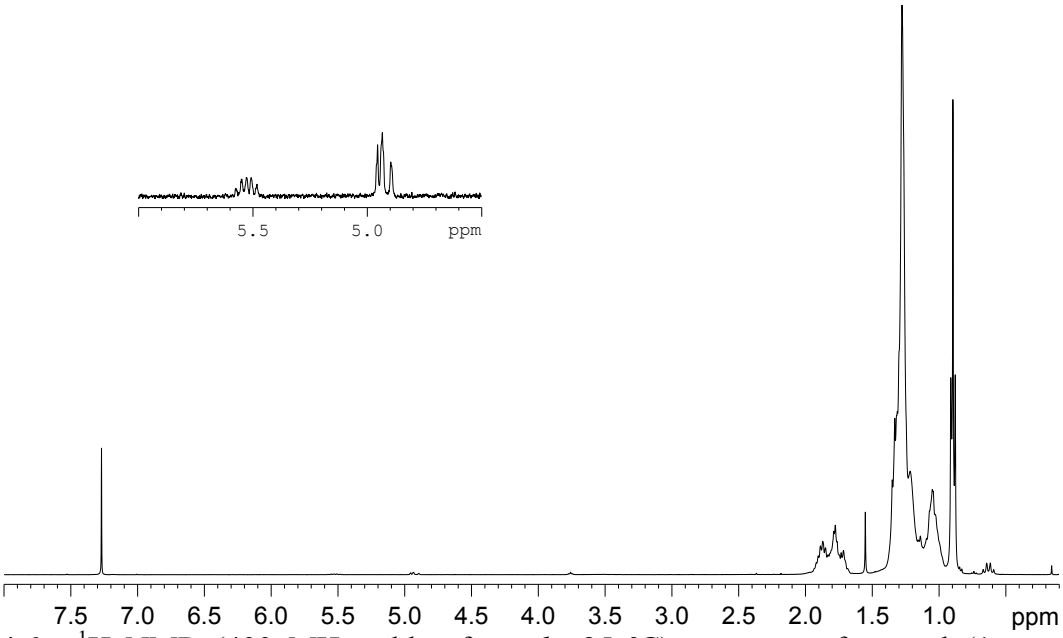

SI 4.6. ^{1}H NMR (400 MHz, chloroform-d_1, 25 ºC) spectrum of *iso*-poly(1-octene)/ PMCP triblock copolymer with the expansion showing vinyl groups resulting from 1,2-insertion of 1,5-hexadiene (entry 7).

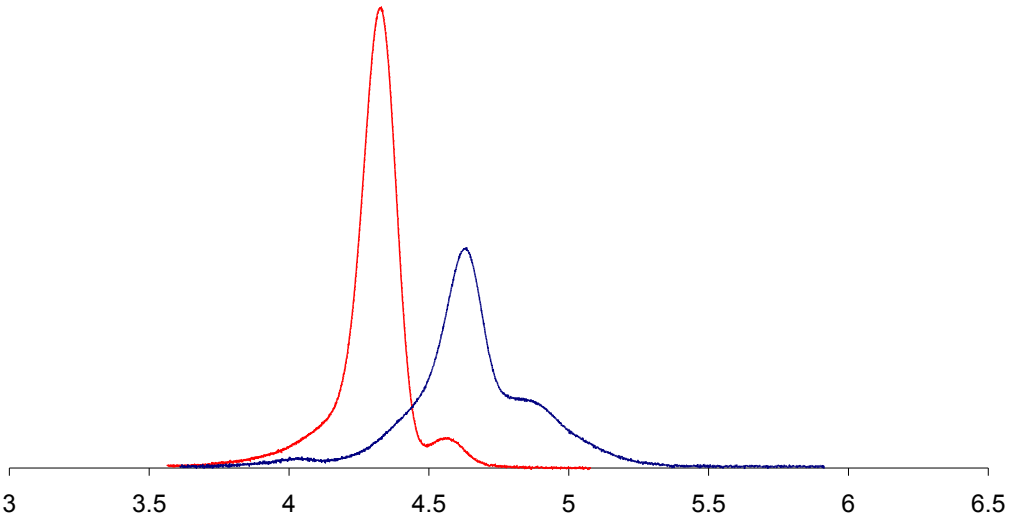

SI 4.7. GPC chromatographs from *iso*-poly(1-octene)/ PMCP block copolymers where the red and blue chromatographs correspond to entries 4 and 7, respectively.

.

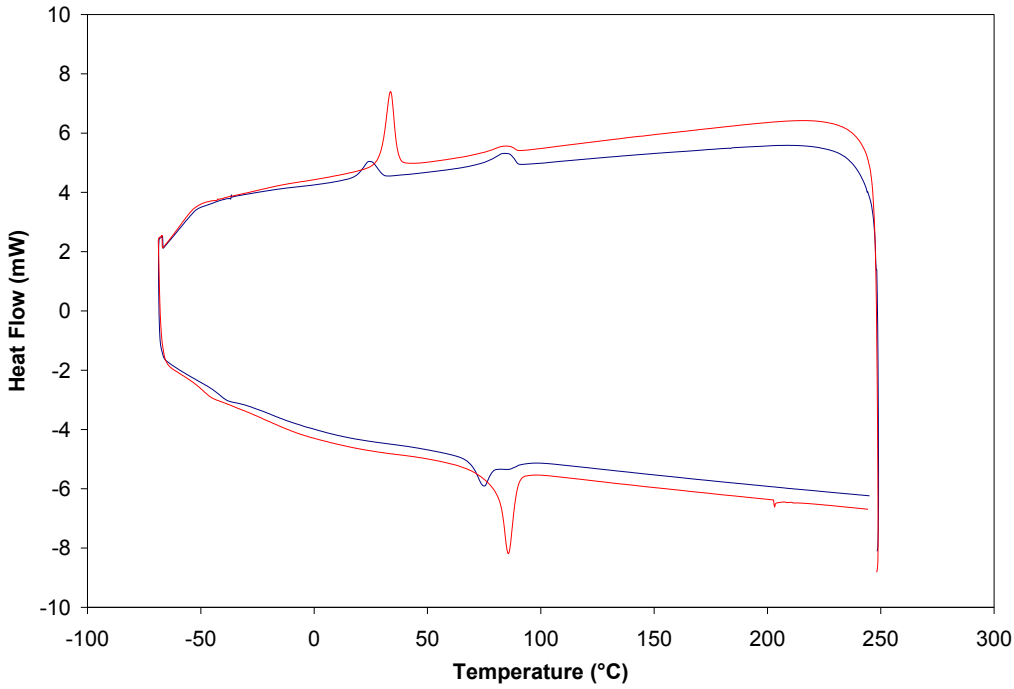

SI 4.8. DSC heating and cooling curves from *iso*-poly(1-hexene)/ PMCP di- and tri-block copolymers where the red and blue curves correspond to entries 3 and 6, respectively.

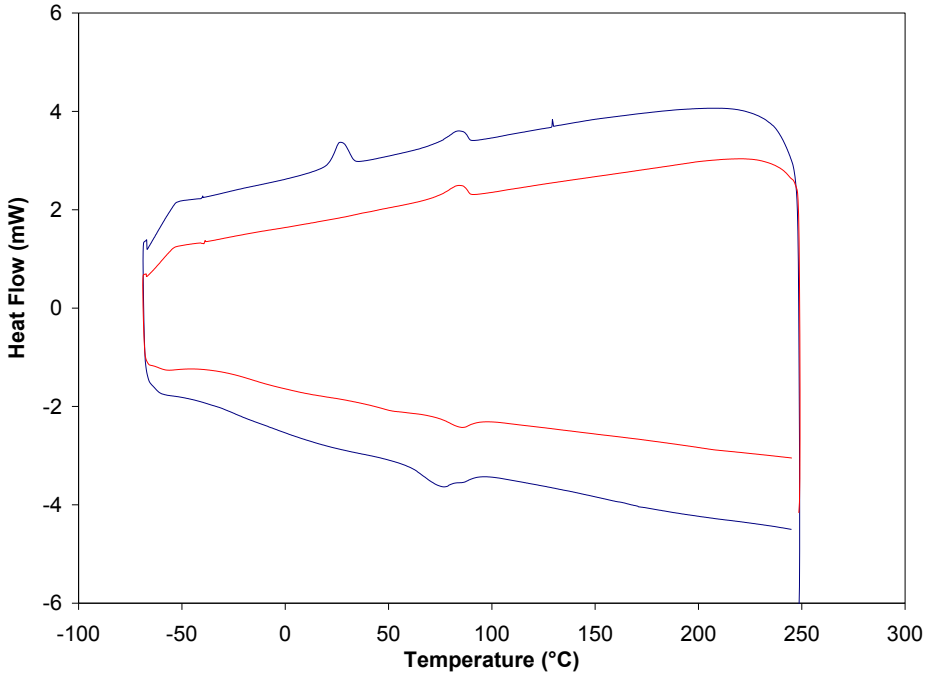

SI 4.9. DSC heating and cooling curves from *iso*-poly(1-octene)/ PMCP di- and tri-block copolymers where the red and blue curves correspond to entries 4 and 7, respectively.

Chapter 5 : Matrix Assisted Laser Desorption/Ionization Time-of-Flight Mass Spectrometry (MALDI-TOF MS) of Precision Polyolefins from Living Coordinative Chain Transfer Polymerization (LCCTP)

5.1 Background

As discussed in previous chapters, the detailed structural and molecular characterization of polymeric materials is essential, given that these parameters significantly influence the chemical and physical properties, which dictate their end-use properties. Over the years, societal dependence on polyolefin materials in particular has skyrocketed. Therefore research efforts have understandably been geared towards the synthesis of new catalyst systems that can produce novel polyolefins in a controlled fashion, allowing the tailoring of molecular weight, composition, and stereochemistry.[8] The concern however, is that the shortage of techniques for the characterization of these new materials limits our ability to understand how the structure (both electronic and sterics) of a catalyst affects the structure and hence the property of a polymer.

General techniques that are utilized for the structural characterization of polymers include NMR spectroscopy, gel permeation chromatography (GPC), infrared spectroscopy (IR), mass spectrometry (MS), light scattering (LS), and differential scanning calorimetry (DSC). Amongst these characterization methods, NMR and mass spectrometry are the most powerful techniques. NMR reveals quantitative information about the chemical and architecture composition of polymers while MS gives quantitative information about molecular weight and molecular weight distributions. NMR is a versatile tool that works on both polar and non-polar molecules while mass spectrometry is limited to polymers having polar, unsaturated, or aromatic functional groups that can

be ionized. As a result, hydrocarbon polymers such as polyethene and polypropene are virtually unanalyzable via this technique. As a workaround solution to this problem, scientists have added metal cations to polymers in order to facilitate the cationization of low molecular weight (M_n < 2 kDa) hydrocarbons (polyethene[245,246], saturated crude oil fractions[247], long chain alkanes[248] and hydrogenated polybutadiene[249]) by matrix assisted laser desorption/ionization time-of-flight mass spectrometry, MALDI-TOF MS. However, this method is restricted to low molecular weight hydrocarbons and results in cationization that is not well understood, making qualitative analysis difficult.[250] Baur, Wallace and coworkers of NIST reported another method that can be utilized for the analysis of hydrocarbon polymers that involves the covalent attachment of charged species (PPh_3^+) unto the polyethylene chain end.[250,251] These functionalized polyethene materials generated strong MALDI signals that could be processed via traditional MALDI analysis techniques given the presence of lone pairs on which cationization can take place. Given the ability to produce end-group functionalized polyolefins (discussed in Chapter 2) it was of interest to utilize the aforementioned technique to determine the feasibility of MALDI-TOF MS as a routine characterization method for the evaluation of new polyolefins and catalyst systems. MALDI is a soft ionization technique that can produce intact ions of a polymeric analyte upon irradiation with a pulsed laser beam in the presence of a matrix compound that minimizes interactions among polymeric analytes and between the analyte and the target surface. Ions produced can then separated based on their mass-to-charge (*m/z*) ratios using a time-of-flight analyzer to give direct access to molecular weight information for synthetic polymers.

5.2 MALDI-TOF MS for Homopolymer Characterization

In order to evaluate the utility of MALDI-TOF MS as a technique, initial focus was geared towards the analysis of low molecular weight polypropene and polyethene materials. This would allow the establishment of optimum sample preparation methods and instrument parameters on a relatively simple system.

5.2.1 Sample Preparation

In light of the fact that the unfunctionalized polyolefin material cannot be ionized via mass spectrometry, it was imperative that time was invested in the creation of a chemical modification method that would allow the polymer to be ionized with good signal. *a*PP was functionalized by first adding an iodide to the terminus (as described in Chapter 2) and then displacing the iodide with triphenylphosphine to give a phosphonium polymer. Initially, the iodide terminated polypropene precursor was dissolved in 1 mL hot xylene and transferred to a Schlenk flask containing excess triphenylphosphine in 15 mL xylene then refluxed at 110 °C. The reaction was monitored by ^{1}H NMR over two weeks, after which it was determined that the reaction was complete based on the disappearance of resonances at 3.2 ppm representing protons alpha to the iodide group of *a*PP-*t*-I. In order to minimize reaction time, a new reaction protocol was attempted. The iodinated polymer was dissolved in 1 mL hot toluene then transferred to a Schlenk flask containing excess triphenylphosphine in 15 mL dimethylformamide (DMF), then refluxed at 110 °C for 4 days, after which an aliquot was taken and the reaction was deemed to be complete (quantitative conversion) based on ^{1}H NMR analysis in dueterated chloroform. The polymeryl solution was later precipitated into 300 mL methanol. The crude product was collected by removing volatiles under vacuo. The

crude material was then washed with chloroform twice and then placed under vacuum to remove chloroform and residual DMF. This method became the standard procedure used to generate all charged phosphonium-functionalized polymeric materials discussed herein. Additional evidence for the successful functionalization of the polymer with phosphonium unit came from MALDI-TOF spectra, which showed strong MS signals (discussed later in this chapter). It is worth noting that making conclusions about the exact composition of the polymer based on a MALDI-TOF analysis of the phosphonium functionalized polymers has certain limitations. For example, it is assumed that all of the *a*PP-t-I polymer chains reacted with triphenylphosphine at equal rates to give phosphonium polymers. If this assumption is incorrect then the molecular weight values and distribution would be skewed, because unfunctionalized chains would not be represented in the molecular weight data acquired via MALDI-TOF MS. However the ^{1}H NMR analysis of the crude reaction mixtures of both the iodination and phosphine displacement reactions were quantitative, therefore the MS molecular weight distribution should be representative of the bulk material.

With a good chemical modification procedure towards the generation of a charged polymer in hand, efforts were then focused on determining sample preparation parameters that would be best suited for the MALDI-TOF MS analysis of these polyolefin materials. Considering that the polyolefin would only possess a polar functionality at the chain end, finding a matrix compound that would improve the desorption efficiency of the polymer analytes into the gas phase.[252] Matrices suitable for MALDI-TOF analysis have high molar extinction coefficients that the wavelength of the laser used, are stable under vacuum, and compatible with solvents used in sample

preparation. Little is known about what qualities make a particular compound a good matrix; as such matrices must be identified by trial and error. All things considered, finding a matrix that performed satisfactorily as a MALDI matrix for these end functionalized polyolefin samples was crucial. No MALDI-TOF signal was observed using trans retinoic acid but a strong signal was observed with use of dithranol. Thus, dithranol became the standard matrix of choice. Toluene or chloroform was utilized as a solvent and required no heating to put the polymeric analyte into solution. Typically, both the matrix and analyte solution concentrations were 20 mg/mL. A solution containing potassium chloride (5 mg/mL) in a 9:1 mixture of ethanol and water was used to increase the signal-to-noise ratio. The matrix, analyte and potassium solutions were mixed in a 10:10:1 ratio and spotted using a 1 μL micropipet onto the steel target. After drying, the droplets showed a finely divided crystalline structure.

MALDI-TOF was performed on a Shimadzu Axima-CFR in linear mode, which provided uncertainties of approximately 1 mass unit. Ions were generated using a 337 nm wavelength nitrogen laser with a pulse duration on the order of 5 ns and a maximum laser energy of 270 μJ. The laser power used for all reported spectra was 85, but several laser energies were investigated to determine optimum laser power. See Section 5.2.2 for details. All measurements were performed in the positive mode. The instrument was calibrated with bradykinin fragment 1-7 (peak at 757.4 Da), $P_{14}R$ synthetic peptide (peak at 1,533.9 Da), and bovine insulin (peak at 5,730.6 Da), which provide uncertainties of less than a few mass units.

5.2 Accuracy and precision of MALDI-TOF MS

To determine if MALDI-TOF would be a good tool to routinely characterize polyolefins, it was important to determine the uncertainties associated with the MALDI-TOF MS measurements of the phosphonium-terminated polymers. The determination of the accuracy and precision of the method is discussed herein.

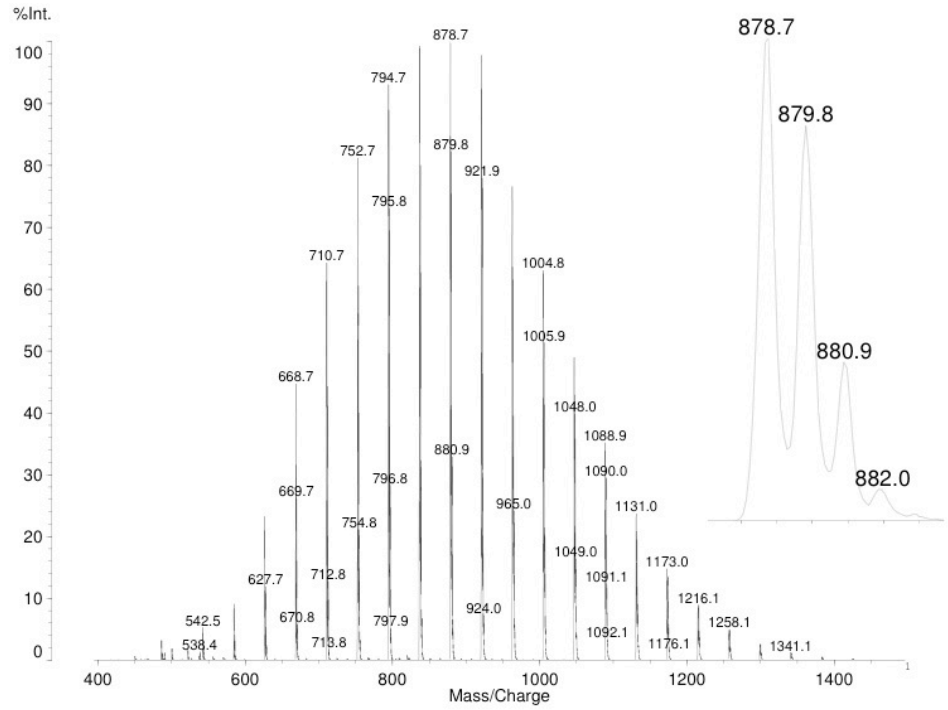

Figure 5.1 MALDI-TOF MS spectrum evidencing successful modification of *a*PP-*t*-I to the phosphonium functionalized *a*PP, 1-[PPh_3]-*a*PP^+. Inset represents isotropic distributions of peak at the center of the molecular weight distribution.

MALDI-TOF MS spectra for atactic polypropene and polyethene modified with a phosphonium end group through functionalization with triphenylphosphine are shown in Figures 5.1 and 5.3, respectively. No smoothing or baseline corrections were made for the data presented in these figures as such isotopic distributions can be observed easily in the figure insets. These isotopic distributions show the precision of MALDI-TOF, as

differences are on average only 1 g/mol. MALDI-TOF signal corresponding only to the chemically modified charged polymer chains are represented in the spectra. Repeat patterns of 42 g/mol was shown for the polypropene materials, which corresponds to the molecular weight of one propene monomer unit and therefore provides further evidence that the polymer being analyzed is indeed a polypropene-derived polymer.

MALDI-TOF MS detection of the phosphonium polymer is based on the ionized polymeryl species striking the time of flight detector to produce a current that reflects the number of ions present, the number average (M_n) and weight average (M_w) molecular weights. The polydispersity index (PDI) of a polymer can be tabulated directly from the MALDI-TOF MS data. To do this, the number of oligomers having some specific molecular weight should be determined first. This can be achieved according to Equation 5.1, where the signal intensity (peak area), S_i, of a specific oligomer mass m_i is directly proportional to the number of polymer molecules at that oligomer mass, n_i and k is a constant independent of m_i.

$$S_i = kn_i \tag{5.1}$$

Next, the total mass of the polymer can be calculated by taking the sum of the product of the total measured mass and the total signal intensity over all oligomers, *i,* as shown in Equation 5.2.

$$\sum_i S_i m_i = k \sum_i n_i m_i \tag{5.2}$$

Dividing the sum over all oligomers of Equation 5.1 by the total mass of Equation 5.2,

gives the M_n of the polymer independent of *k* since *k* in the numerator and denominator cancel out Equation 5.3.

$$\sum_i S_i m_i \Big/ \sum_i S_i = k \sum n_i m_i \Big/ k \sum_i n_i \qquad (5.3)$$

The M_w of the polymer can also be determined independent of *k* by dividing the mass of a specific oligomer by the total mass of the polymer sample to determine the weight fraction, then taking the sum of the product of the weight fraction of the oligomer and the mass of that oligomer according to Equation 5.4. The ratio of the weight average molecular weight to the number average molecular weight can then be used to describe the overall molecular weight distribution, which is also referred to as the polydispersity index (Equation 5.5).

$$\sum_i S_i m_i^2 \Big/ \sum_i S_i m_i = k \sum n_i m_i^2 \Big/ k \sum_i n_i m_i \qquad (5.4)$$

$$M_w \Big/ M_n = PDI \qquad (5.5)$$

Calculated M_n, M_w, PDI values for *a*PP were 904 g/mol, 927 g/mol, and 1.02 respectively. The calculation of these values is based on integrated peak area values determined using the PeakFit program then applying the equations discussed above (Equations 5.3, 5.5 and 5.6). The M_n value of 904 g/mol corresponds to an incorporation of about 20 ethene monomer units in the polymer chain in addition to the ethyl group (29 g/mol) at one end (from $ZnEt_2$) and the phosphonium group (262 g/mol) at the other end. The number average molecular weight value calculated based on the MALDI-TOF data was similar to values attained from GPC (M_n = 916 g/mol) and ^{1}H NMR (M_n = 651

g/mol) analysis of the iodide terminated polypropene chain. The M_n value obtained from GPC was greater than the value from ^1H NMR, which was in turn larger than that of the MALDI-TOF MS number average molecular weight. These discrepancies could be due to the absence of some polymer chains from the MALDI-TOF data due to lack of phosphonium functionalization, though this is likely not the case given nearly 100% conversion to the charged polymeric species. A more plausible explanation for the differences between MS and GPC calculation of polymer weight is due to the fact that molecular weight calculations by the GPC used in this work was based on a set of polystyrene standards and utilized refractive index for weight calculation (an indirect method) whereas molecular weight determination by MS determination is a more direct method. As mentioned in the Chapter 1, molecular weight values obtained from GPC that uses light scattering to determine polymer weight are more accurate however it is not effective for the determination of low molecular weight polymers. There is also a certain degree of uncertainty associated with the MALDI-TOF data because the calculated molecular weight is based on the integration of the MALDI-TOF signal, which has uncertainty due to both instrument and experimental set-up factors. The accuracy of the MALDI-TOF values was also validated by electron spray ionization mass spectrometry (ESI MS) taken on the JOEL AccuTOF-CS instrument. As can be gleaned from Figure 5.2 below, the molecular weight distribution is very similar to that obtained from MALDI-TOF MS. In fact, the molecular weight distribution is centered around 870 g/mol as compared to 879 g/mol in the MALDI-TOF spectra in Figure 5.1 above. The repeat units are also 42 g/mol as in the case of MALDI-TOF MS.

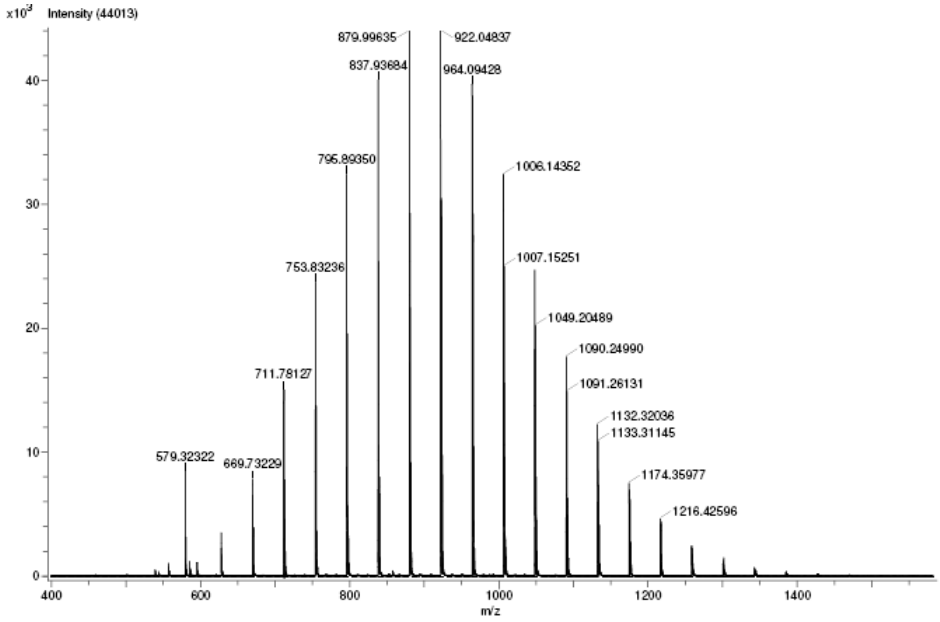

Figure 5.2. ESI-MS data for 1-[PPh_3][I]-*a*PP.

Similar to the case of the aPP material, repeat patterns for PE were also very pronounced, except the repeat values were 28 g/mol, in line with the mass of an ethene monomer unit. Calculated M_n, M_w, and PDI values for the PE material are 622 g/mol, 627 g/mol and 1.01, respectively based on peak area calculations according to the Equations 5.3, 5.4 and 5.6. This M_n value corresponds to about 21 incorporations of ethene monomer units during polymerization. GPC (M_n = 884) and ^{1}H NMR (M_n = 427) analysis number average molecular weight values were greater than values determined via MALDI-TOF in the case of PE also.

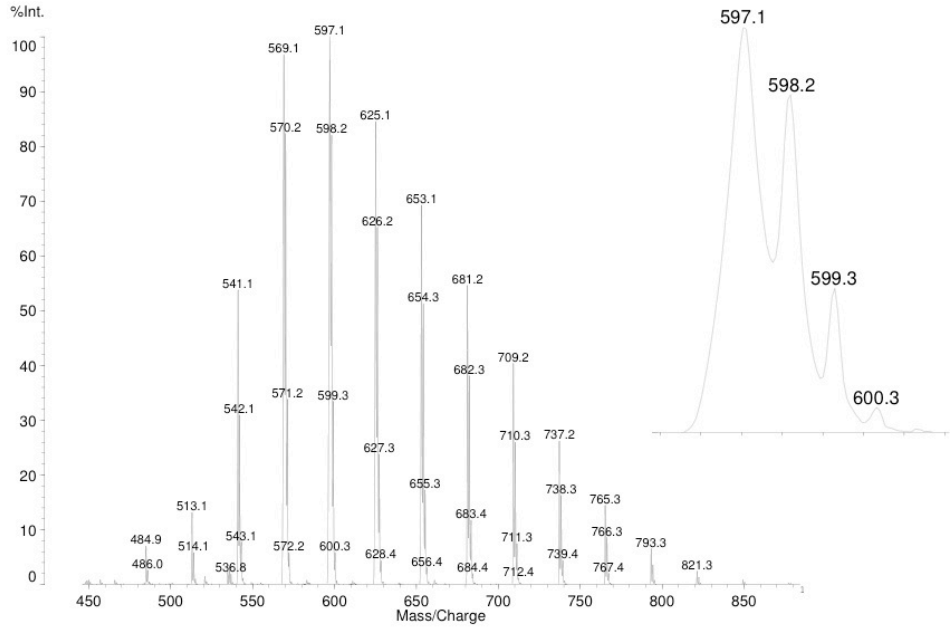

Figure 5.3 MALDI-TOF MS spectrum evidencing successful modification of PE-*t*-I to the phosphonium functionalized PE. Inset represents isotropic distributions of peak at the center of the molecular weight distribution.

As mentioned previously, the instrument parameters directly impact the molecular weight values and overall molecular weight distribution that is attained from MALDI-TOF MS. One parameter in particular, laser power, was shown to affect the molecular weight distribution in the MALDI-TOF spectrum and is discussed more in depth below. The laser power is the optical power output of the laser beam utilized to ionize the polymeric material. The power of the irradiating laser is an important factor in MALDI analysis because the laser power may have a greater effect on the intensities of lower molecular weight polymers. If the laser energy is not high enough a MALDI-TOF signal will be weak for the higher molecular weight polymer chains. On the other hand if the laser power is set too high, the polymer chains begin to fragment. Given that the molecular weight values are calculated based on the intensity/area for each peak seen in the spectra, the absence of some higher molecular weight polymer chains (caused by low

laser power) or presence of extra lower molecular weight polymer chains (caused by fragmentation and high laser power) can severely impact the molecular weight data calculated. As such, it is imperative that an "optimum" laser power be determined for each polymer sample being analyzed.

Figure 5.4, illustrates mass spectra for 1-[PPh_3]-*t*-aPP taken at five different laser energies, two below threshold power, one at the threshold laser power and two below threshold. If the spectra 4A and 4B attained at LP = 60 and LP = 70 respectively are compared, it can be observed that the.4B not only gives a stronger signal for the molecular weights in the distribution but also new peaks around 1200 g/mol are now present. This can be interpreted to mean that the laser power is too low at LP = 60 because it cannot irradiate the longer polymer chains, making LP = 70 a better setting. When spectra 4B and 4C are compared, at LP = 85 not only can one see peaks associated with higher molecular weight polymer chains around 1400 g/mol can be observed, but the intensity of all other peaks in the distribution are more intense thus, LP = 85 is the better laser energy to use for this sample. When spectra 4C and 4D are evaluated, for each sample the peaks attained at 85 LP are superior. When the laser power was increased, the average molecular weight peak shifts from 879 g/mol to 795 g/mol and a decrease in intensity of high molecular weight species and an increase in lower molecular weight species was also observed. This suggests some degree of fragmentation of the polymeryl species; as the laser power is increased, the higher molecular weight polymers begin to fragment into lower molecular weight polymers and therefore the amount of lower molecular weight polymers in the sample increases.[253-257] Moreover, when the laser energy is further increased to LP = 125 (4E), not only did the average molecular value

shift even lower to 752 g/mol but the overall distribution began to flatten, which is another indicator that the LP is too high and probably all the polymer species (both higher and lower molecular weights) have fragmented into even smaller fragments that lie outside the analysis window. At LP = 125, the intensities of the peaks relative to one another are similar to when LP = 105, but the overall signal strengths are lower than when LP = 105. After considering all of these observations, the 'optimum' laser power was determined to be LP = 85. This value became the standard laser energy used, as it consistently represented the laser power at threshold. However it is important to note that only at this laser energy did we observe an accurate depiction of the molecular weight distribution, reinforcing the importance of instrument parameters.

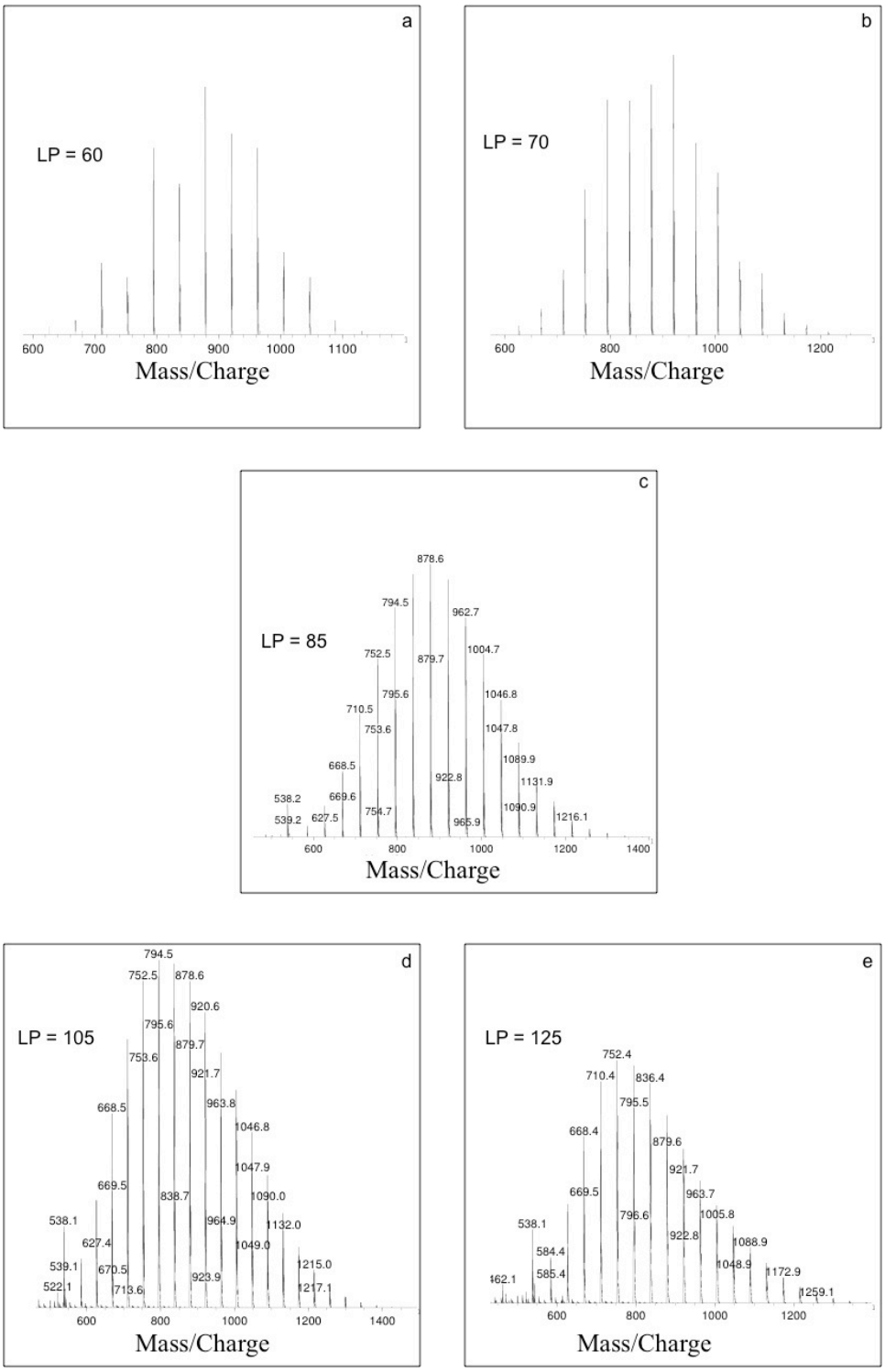

Figure 5.4 MALDI-TOF MS spectra of phosphonium functionalized *a*PP at various laser powers.

5.3 MALDI-TOF MS for Copolymer Characterization

With the successful MS characterization of polypropene and polyethylene homopolymers done, we decided to pursue the characterization of two copolymers, poly(ethene-*b*-propene) and poly(propene-*co*-1-octene). MALDI-TOF MS however does not allow one to distinguish between random and block copolymers. Furthermore, in cases where the molecular weights of the two different monomers overlap it becomes challenging to uncover compositional information about the polymeric material. In the case of the poly(ethene-*b*-propene) material for example, a polymer having six ethene monomer incorporations and zero propene monomer incorporations (MW with end groups = 459.67 g/mol) would have the same mass as a polymer chain having 3 ethene monomer incorporations and 2 propene monomer incorporations (MW with end groups 459.67), therefore compositional information is not deducible. The same is true in the case of the poly(propene-*co*-1-octene) copolymer, as there is overlap at every interval of three incorporations of 1-octene monomer (ie. The mass of propene = 28, octene = 0 overlaps with propene = 20, octene = 3 and propene = 12, octene = 6). However, in the case of the poly(E-*b*-P) material, total molecular weight distribution information was acquired based on the mass spectrum shown in Figure 5.5. Isotopic distributions matched expected distribution (based upon values calculated using the IDCalc isotope distribution calculator). These values were separated by only 1 g/mol mass difference, meaning that the precision of MALDI-TOF MS for characterization of these types of polymers is 1 g/mol. Distinct repeat patterns of 14 g/mol which represents the difference between the mass of a propene monomer (42 g/mol) and an ethene monomer (28 g/mol), which is expected given that this polymer is a block copolymer. Number average and weight average molecular weight values were calculated by treating the monomers being

incorporated into the polymer chain as one monomer (i.e. E = 28 g/mol and P = 42 g/mol so total monomer mass = 70 g/mol). Mass spectra revealed peaks corresponding to 3 to 17 monomer incorporations for which peak area data was acquired using PeakFit. M_n, M_W, and PDI values tabulated after deconvolution of the monomodal mass spectrum were 983 g/mol, 1001 g/mol and 1.02 respectively, indicating that the reaction was indeed living and therefore resulted in homogeneity of the polymeric product.

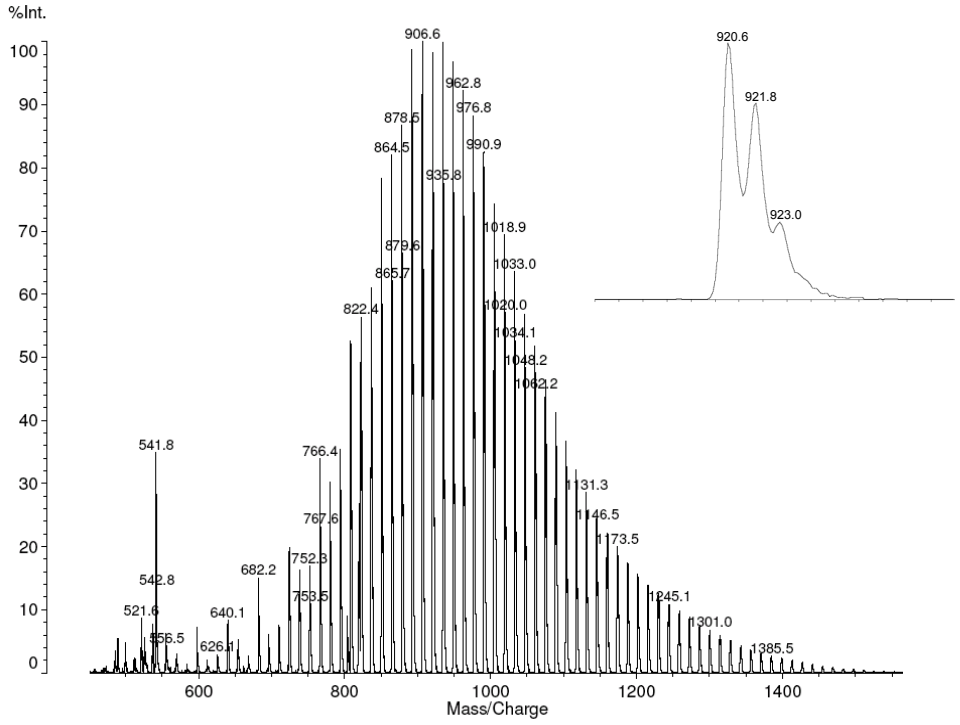

Figure 5.5. MALDI-TOF-MS of 1-[PPh_3]-PE-*b*- *a*PP^+.

Analysis of the poly(propene-*co*-1-octene) showed a monomodal symmetric molecular weight distribution, illustrated in Figure 5.6. In this case, determining the overall molecular weight distribution was not feasible given the extensive overlap between oligomers having differing compositions of 1-octene and propene monomers but the same mass. Therefore although this copolymer of propene and 1-octene revealed qualitative information regarding the precision of MALDI-TOF MS and the living nature

of the chain transfer polymerization, quantitative information about the molecular weight distribution was not uncovered. However as shown in Figure 5.6, the molecular weight distribution was centered around 2053 g/mol.

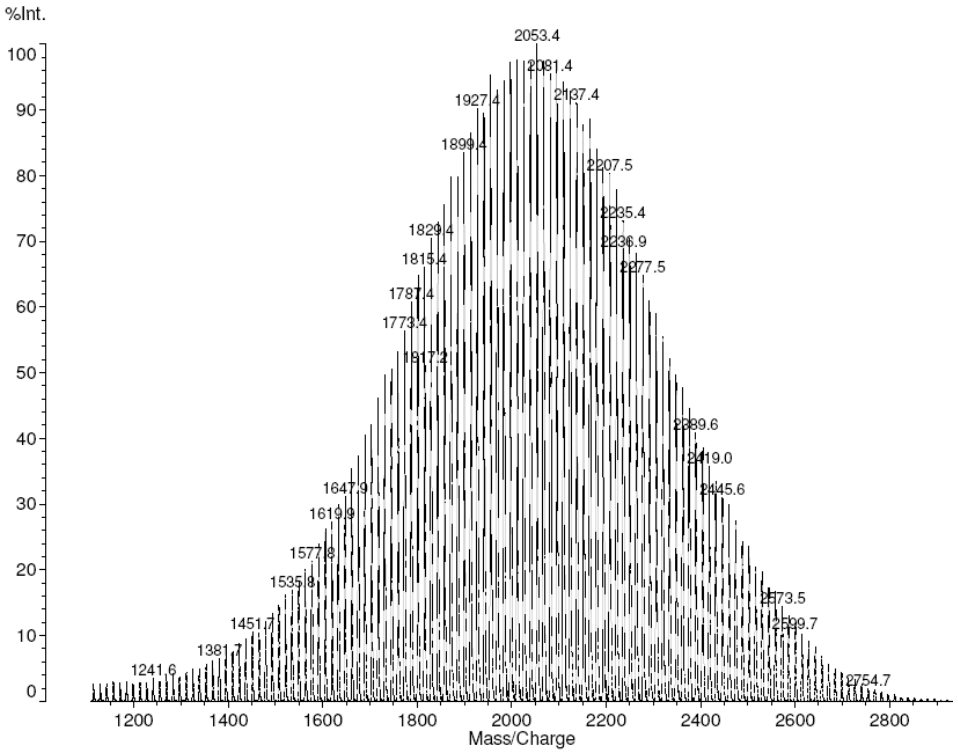

Figure 5.6. MALDI-TOF MS of poly(P-*co*-O) material.

5.4 The Utility of MALDI-TOF MS as a Powerful Characterization Tool in the Analysis of Ethene-Cyclopentene Copolymers

After establishing reliable sample preparation and instrument parameters for the analysis of polyolefin materials by MALDI-TOF MS the utility of the method was evaluated using three phosphonium functionalized poly(ethene-*co*-cyclopentene) samples. Low molecular weight copolymers based on ethene and cyclopentene were targeted because there is virtually no overlap between masses until ethene (E) insertions exceed 16 incorporations and cylcopentene (CP) insertions exceed 6 incorporations (i.e.

when E = 17 and CP = 0 to 6 oligomer masses are equal to when E = 0 and CP = 7 to 13). The in depth analyses of these poly(ethene-*co*-cyclopentene) materials were critical in order to validate an extension of living coordinative chain-transfer polymerization (LCCTP) to include the rapid and reversible chain transfer between two populations of "tight" and "loose" propagating ion pairs. If successful, this method would allow the level of comonomer incorporated into the polymer chain to be regulated through variations in the cocatalysts used to activate the hafnium or zirconium based precatalyst. Generating many grades of polyethene-based polymeric materials from a single precatalyst would be an amazing accomplishment, mainly because a new precatalyst is generally required to modulate the comonomer content while preserving all other parameters. See Chapter 1.7 for the proposed mechanism. This is probably the primary reason why the design and synthesis of homogeneous single-site catalysts has remained at the forefront of the polymerization field. MALDI-TOF analyses of these ethene and cyclopentene based copolymers were all expected to show narrow monomodal molecular weight distributions. However, the cyclopentene content should increase as the ratio of borate comonomer ("loose" ion pair) used to activate the precatalyst is increased as was shown by ^{13}C NMR taken by Jia Wei.[258]

The three phosphonium-functionalized copolymers used for this study were prepared via LCCTP copolymerization of ethene (E) and cyclopentene (CP). **Precatalyst II** was used to generate three different populations of ion pairs, by activation with one equivalent of 1) only the borate **Cocatalyst I** 2) a 1:1 mixture of borate and borane **Cocatalysts I and II respectively** 3) only the borane **Cocatalyst II.** All LCCTP reactions were carried out in the presence of 50 equivalents of $ZnEt_2$ and 3000

equivalents of cyclopentene (relative to the Zr precatalyst) in toluene at 25 °C and at ethene pressures of 5 psi, then quenched with a slight excess of I_2 as a solution in toluene to generate the iodo-terminated poly(E-*co*-CP) polymers. The iodide functionalized poly(E-*co*-CP) copolymers were later converted to their phosphonium counterparts, α-[I][Ph_3P]-poly(E-*co*-CP), by heating as a solution in dimethylformamide (DMF) with an excess of triphenylphospine at 110 °C for 3 days. All phosphonium-functionalized samples were then prepared via the dried-droplet method for MALDI-TOF analysis, according to Section 5.2.1.

The MALDI-TOF MS spectra for all three poly(E-*co*-CP) samples revealed narrow overall molecular weight distributions, but each spectra also showed several narrow distributions within the overall distribution representing varying degrees of CP incorporation within the copolymer, see Figure 5.7. When 100% **Cocatalyst I** (borate) was used to activate the precatalyst there are eight distinct molecular weight distributions, representing 3-10 cyclopentene incorporations, each having M_n values ranging from 720 g/mol to 1669 g/mol, PDI values ranging from 1.01 to 1.04, and cyclcopentene incorporation ranging from 29.8% to 36.9%. These eight distributions combined have an overall number average molecular weight of 1146 g/mol, polydispersity index of 1.06 and comonomer incorporation of 34.0% as shown in Figure 5.7A. It is also worth noting that deconvolution of MALDI-TOF peaks revealed the presence of polymer chains having zero incorporations of ethene while having up to seven consecutive enchainments of cyclcopentene. Given the bulkiness of the cyclopentene monomer and higher rate of insertion of ethene this was not at all expected. Recall that ^{13}C NMR did not indicate any diads or triads present in the copolymer architecture and the fact that MALDI-TOF MS

analysis revealed the presence of diads and triads showcases the power of MALDI-TOF MS. The level of cyclopentene incorporation for this sample and samples of the like, were calculated based on van Herk *et al*.[259] Isotopic distributions observed were in agreement with those predicted using IDCalc isotopic distribution calculator, which allows one to view the expected isotope distribution for biological and polymeric molecules measured by mass spectrometry. Differences in peak values were 28 g/mol for each individual molecular weight distribution. When 100% $[PhNHMe_2][B(C_6F_5)_3]$ (borane) was used to activate zirconium precatalyst, six distinct molecular weight distributions, representing 0-5 cyclopentene units per polymer chain, were identified after deconvolution of peak using the PeakFit program. Peaks that made up each individual distribution were separated by 28 g/mol, see Figure 5.7C. No polymer chains made up of only cyclopentene were observed in this polymeric product, indicating lower reactivity of cyclopentene in this system.

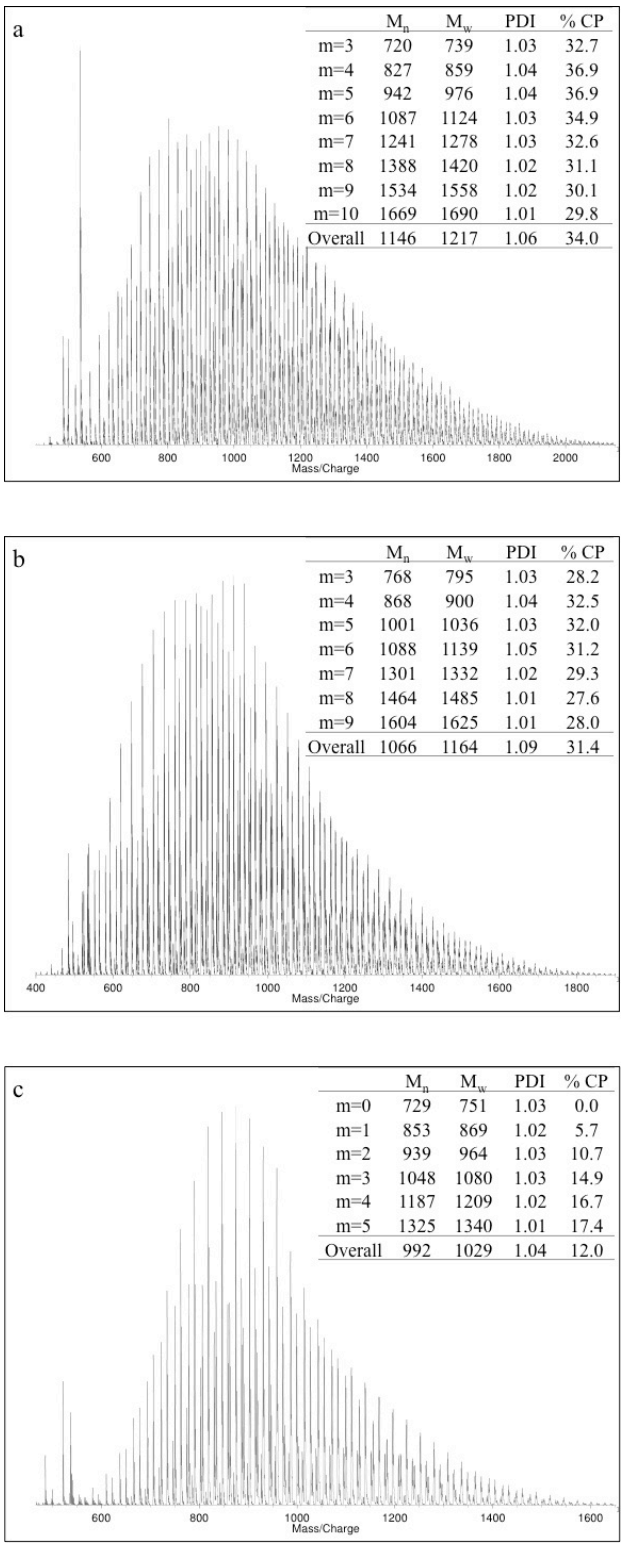

a

	M_n	M_w	PDI	% CP
m=3	720	739	1.03	32.7
m=4	827	859	1.04	36.9
m=5	942	976	1.04	36.9
m=6	1087	1124	1.03	34.9
m=7	1241	1278	1.03	32.6
m=8	1388	1420	1.02	31.1
m=9	1534	1558	1.02	30.1
m=10	1669	1690	1.01	29.8
Overall	1146	1217	1.06	34.0

b

	M_n	M_w	PDI	% CP
m=3	768	795	1.03	28.2
m=4	868	900	1.04	32.5
m=5	1001	1036	1.03	32.0
m=6	1088	1139	1.05	31.2
m=7	1301	1332	1.02	29.3
m=8	1464	1485	1.01	27.6
m=9	1604	1625	1.01	28.0
Overall	1066	1164	1.09	31.4

c

	M_n	M_w	PDI	% CP
m=0	729	751	1.03	0.0
m=1	853	869	1.02	5.7
m=2	939	964	1.03	10.7
m=3	1048	1080	1.03	14.9
m=4	1187	1209	1.02	16.7
m=5	1325	1340	1.01	17.4
Overall	992	1029	1.04	12.0

Figure 5.7 MALDI-TOF MS spectra of phosphonium functionalized poly(E-*co*-CP) samples. Where (a) represents run 1, (b) represents run 2, (c) represents run 3 in Table 5.1.

M_n, PDI, and percent CP incorporation for each individual molecular weight distribution ranged from 729 g/mol to 1325 g/mol, 1.01 to 1.03, and 0.0 to 17.4, respectively. Altogether these distributions gave an overall number average molecular weight, PDI, and cyclopentene incorporation of 992 g/mol, 1.04, and 12.0%, respectively. The final ethene-cyclopentene copolymer was synthesized using a 1:1 ratio of borate to borane. MALDI-TOF analysis of this material also showed narrow total molecular weight distributions. However, the number average molecular weight and cyclopentene incorporation values were lower than those achieved from 100% borate and higher than those acquired using 100% borane as cocatalysts. Overall M_n, PDI, and percent comonomer incorporation were 1066 g/mol, 1.09, and 31.4%, respectively. This distribution was made up of seven individual molecular weight distributions, representing 3-9 cyclopentene units incorporated per polymer chain. Numbered average molecular weights, polydispersity indices, and cyclopentene incorporation ranged from 768 g/mol to 1604 g/mol, 1.01 to 1.05, and 27.6% to 32.5% respectively. Unlike in the case of the borate copolymer, no poly(cyclopentene) polymers were observed in this material. However, polymer chains having primarily cyclopentene units (2-6 CP units) and only one ethene unit were observed once again indicating that the CP activity increases with use of the borate cocatalyst.

As discussed in Section 5.2, phosphonium functionalized cyclopentene copolymers, unlike their unfunctionalized counterpart, can be ionized by MALDI-TOF and analyzed by conventional methods to determine molecular weight and molecular weight distributions. Nevertheless, the molecular weight indices and copolymer composition values calculated from the MALDI-TOF data cannot be regarded as

quantitative without extensive standardization.[260] Nonetheless the qualitative data extracted from MALDI-TOF MS proved to be extremely useful, when combined with GPC, ^{1}H NMR, and ^{13}C NMR data and will therefore be discussed in a qualitative sense to evaluate the proposed synthetic methodology. Firstly, the lack of evidence of chain termination by β-hydrogen-atom transfer by ^{1}H NMR spectra was supported by the narrow molecular weight distributions observed for all three copolymers by MALDI-TOF and GPC analysis, thus verifying the living character of LCCTP by reversible chain transfer between ion pairs. GPC data can provide the overall polydispersity of the polymer sample but MALDI-TOF gave a more in depth picture of the nature of the molecular weight distribution than what could be extracted from the GPC data alone. Furthermore, exclusive enchainment in 1,2-fashion was revealed by microstructural and end-group analyses by ^{13}C NMR spectroscopy. ^{13}C NMR also disclosed that the level of cyclopentene incorporation decreased (from 16 to 9 percent) as the population of tight ion pairs increased see Table 5.1. This observation was also seen by MALID-TOF analysis, which also showed that the percent of CP incorporated decreased from 34 to 12 percent as the ratio of borane to borate was increased. Finally, both GPC and MALDI-TOF analysis showed monomodal molecular weight distributions, where the yield (activity) and M_n values were inversely proportional to the concentration of the tight-ion pair propagating species of **Precatalyst II** activated by **Cocatalyst I,** which supports the efficacy of this LCCTP extension. However there are inconsistencies between M_n values obtained from GPC, ^{13}C NMR spectroscopic end-group analysis and MALDI-TOF MS analysis. M_n values for all cyclopentene copolymers obtained from GPC analysis was higher than those from NMR, which were larger than those calculated from MALDI-TOF

spectra. This is likely due to the intrinsic deficiencies in polymer standards and GPC columns for low- molecular-weight analyses and the lack of optimization of all instrument parameters for MALDI-TOF analysis. Although not exactly the same, the MALDI-TOF data obtained for the three α-[I][Ph_3P]-poly(E-*co*-CP) samples showed molecular-weight distributions that were very much in line with the M_n values derived by NMR spectroscopy.

Table 5.1. Data for I-poly(E-*co*-CP) obtained from LCCTP with reversible exchange between ion pairs. Percent incorporations from NMR analysis were calculated by Jia Wei.

Run	Cocatalyst **I** : **II**	mol% CP^{α}	mol% CP^{β}	mol% $\%CP^{\gamma}$
1	1 : 0	15.6	15.6	34.0
2	1 : 1	11.4	11.6	31.4
3	0 : 1	8.7	8.7	12.0

[α]Determined from ^{13}C NMR analysis[261,262]
[β]Determined from ^{1}H NMR analysis[263]
[γ]Determined from MALDI-TOF MS analysis[259]

5.5 Conclusion

In summary, MALDI-TOF MS was established as a powerful tool to analyze polymers synthesized via LCCTP. Of note, MALDI-TOF analysis of the polymer samples allowed for a more detailed analysis of the polymer composition and polydispersity than what GPC could reveal. We conclude from the MALDI-TOF analysis of these polymers that LCCTP coupled with fast and reversible chain transfer between tight and loose ion pairs is a good strategy to synthesize an array of novel polyethene-based copolymers from a single precatalyst, as evidenced by the qualitative increase in the molar percentage of cyclopentene incorporation as the population of the loose ion pair increased relative to the population of the tight ion pair.

5.6 Experimental

MALDI-TOF analysis: Solution concentrations were 20 mg/mL for the dithranol matrix and for the analyte with toluene used as solvent. A 5 mg/mL potassium chloride solution in a 9:1 mixture of ethanol and water was used to increase the signal-to-noise ratio. The matrix, analyte and potassium solutions were mixed in a 10:10:1 ratio and spotted from a 1 μL micropipet onto the steel target. After drying, the droplets showed a finely divided crystalline structure. MALDI-TOF was performed on a Shimadzu Axima-CFR in linear mode, which provided uncertainties of approximately 1 mass unit. Ions were generated using a 337 nm wavelength nitrogen laser with a pulse duration of the order of 5 ns and a maximum laser energy of 270 μJ. The laser power used was 85. All measurements were performed in the positive mode.

Preparation of *a*PP-*t*-PPh$_3$: In a 50 mL Schlenk flask, to 15 mL dry DMF was added 1.0 g triphenylphosphine and 0.5 g *a*PP-t-I dissolved in 1 mL hot toluene. The reaction mixture was allowed to reflux at 110 ºC for 4 days under, after which the solution was precipitated into 300 mL methanol. The crude product was collected via removing all the volatiles under vacuum, followed by washing with chloroform twice and then pumping away chloroform to remove residual DMF. The final product was collected and dried in vacuo before GPC, NMR and MALDI-TOF-MS analyses. Yield: 0.20 g. GPC: M_n = 1.12 kDa, M_w = 1.29 kDa, PDI = 1.15.

Preparation of PE-t-PPh$_3$: In a 50 mL Schlenk flask, to 15 mL dry DMF was added .4 g triphenylphosphine and 0.2 g PE-t-I dissolved in 1 mL hot toluene. The reaction mixture was allowed to reflux at 110 ºC for 3 days under, after which the

solution was precipitated into 100 mL methanol. The crude product was collected via removing all the volatiles under vacuum, followed by washing with chloroform twice and then pumping away chloroform to remove residual DMF. The final product was collected and dried in vacuo before GPC, NMR and MALDI-TOF-MS analyses. GPC: M_n = 884 kDa, M_w = 968 kDa, PDI = 1.09.

Synthesis of α-iodo-poly(P-*co*-O): The following description represents a typical procedure for P and O copolymerization in toluene followed by end-group functionalization using iodine. In a 250 mL Schlenk flask, to 40 mL toluene at 25 ºC was added O (4.08 g, 60.0 mmol) and $ZnEt_2$ (823 mg, 1.0 mmol) as 15 wt% (1.1 M) solution in toluene. Then the flask was pressurized 5 psi with propene and equilibrated for 30 min. A clear yellow mixture solution of cocatalyst **2** (8.0 mg, 0.010 mmol), cocatalyst **5** (5.1 mg, 0.010 mmol), and precatalyst **6** (8.2 mg, 0.020 mmoL) in 1.0 mL chlorobenzene was added to the reaction flask to initiate polymerization. Polymerization temperature was maintained at 0 ± 3 ºC. After 30 min, a slightly excess of iodine (558 mg, 2.2 mmol) was added until a purple color persisted in the reaction solution. The reaction solution was then precipitated into 600 mL basic methanol (10% NaOH) to isolate the polymer. The final product was collected after decanting the methanol solution, washed with acidic methanol and methanol and dried in vacuum before GPC and NMR analyses. Yield: 2.1 g. GPC analysis: M_W = 2.78 kDa; M_n = 2.46 kDa; PDI = 1.14.

Synthesis of α-[I][PPh_3]-poly(P-*co*-O): The following description represents a typical procedure for synthesis of α-[I][PPh_3]-poly(P-*co*-O) from α-iodo-poly(P-*co*-O). In

a 50 mL Schlenk flask, to 15 mL dry DMF was added 0.6 g of triphenylphosphine and 0.3 g α-iodo-poly(P-*co*-O) dissolved in 1 mL hot toluene. The reaction mixture was allowed to reflux at 110 ºC for 3 days under N_2. The crude product was collected via removing all the volatiles under vacuum, followed by washing with chloroform twice and then pumping away chloroform to remove residue DMF. The final product was collected and dried overnight in vacuum before NMR and MALDI-TOF-MS analyses.

Synthesis of α-[I][PPh_3]-poly(E-*co*-CP): The following description represents a typical procedure for synthesis of α-[I][PPh_3]-poly(E-*co*-CP) from α-iodo-poly(E-*co*-CP). In a 50 mL Schlenk flask, to 15 mL dry DMF was added 0.6 g of triphenylphosphine and 0.3 g α-iodo-poly(E-*co*-CP) dissolved in 1 mL hot toluene. The reaction mixture was allowed to reflux at 110 ºC for 3 days under N_2. The crude product was collected via removing all the volatiles under vacuum, followed by washing with chloroform twice and then pumping away chloroform to remove residue DMF. The final product was collected and dried overnight in vacuum before NMR and MALDI-TOF-MS analyses.

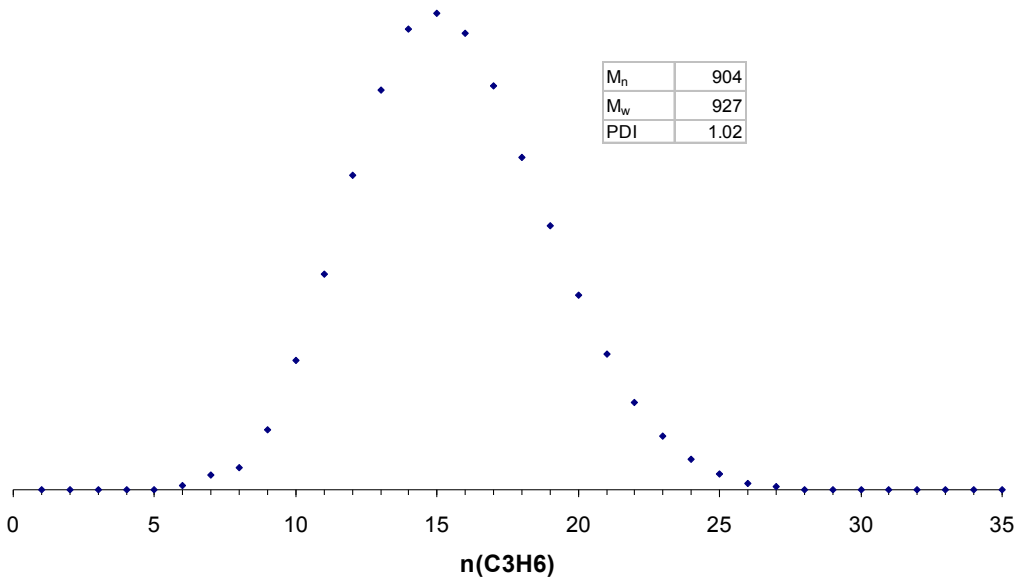

SI 5.1. Deconvoluted MALDI-TOF-MS of 1-[PPh_3]-*a*PP^+.

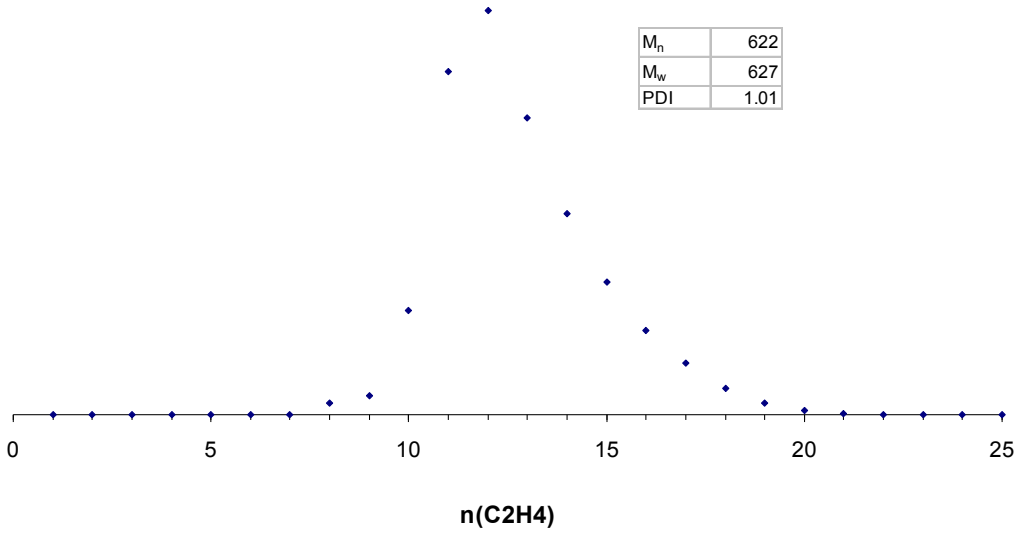

SI 5.2. Deconvoluted MALDI-TOF-MS of 1-[PPh_3]-PE^+.

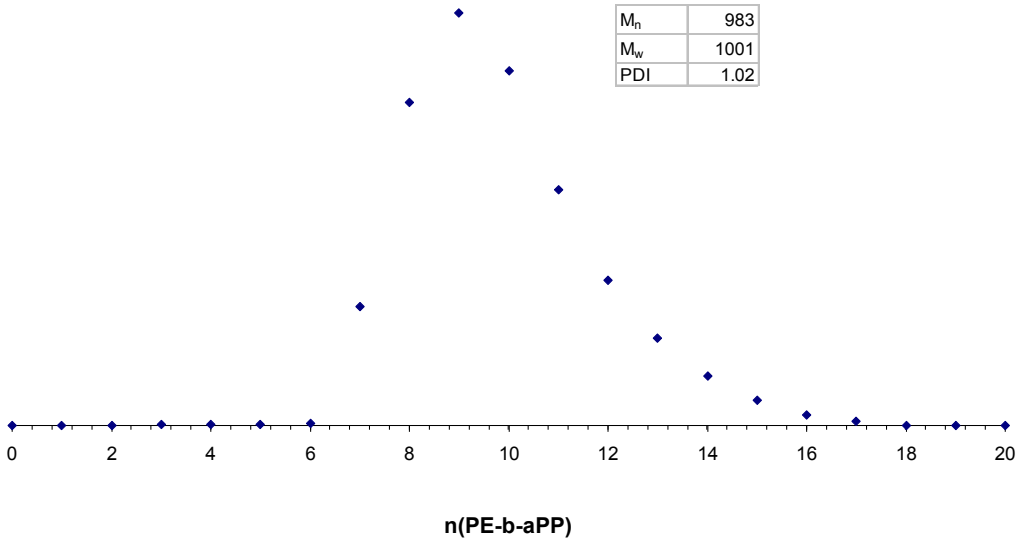

SI 5.3. Deconvoluted MALDI-TOF-MS of 1-[PPh_3]-PE-*b*-*a*PP^+.

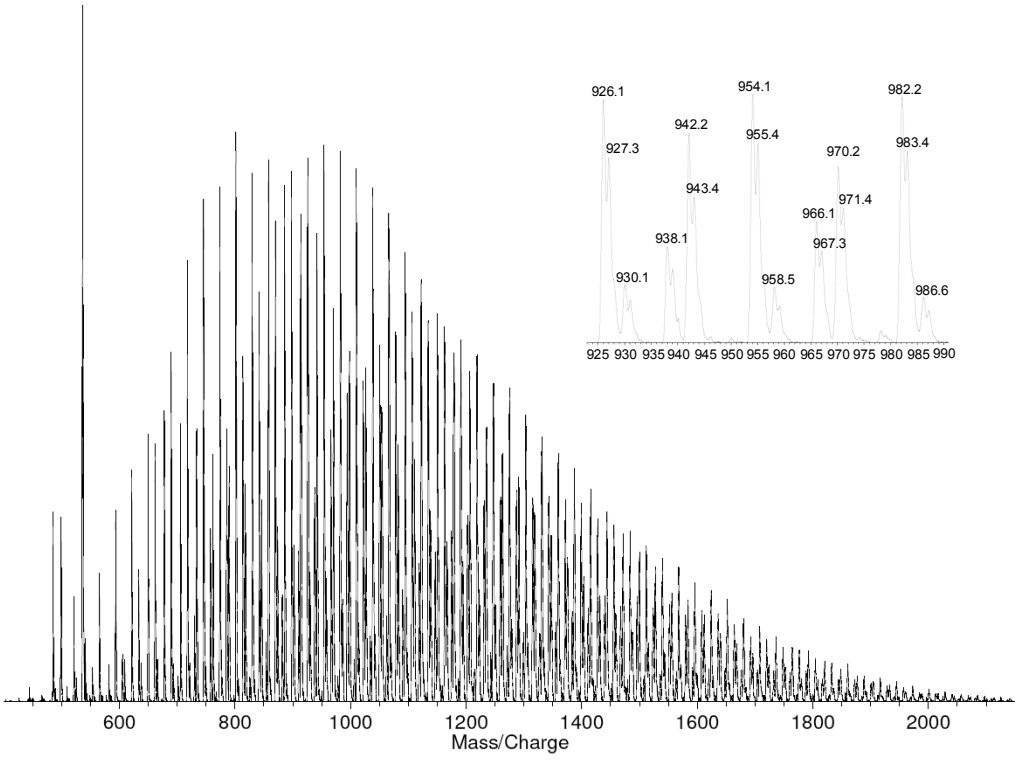

SI 5.4. MALDI-TOF-MS data for 1-[PPh_3][I^-]-PE-*co*-PCP via borate cocatalyst.

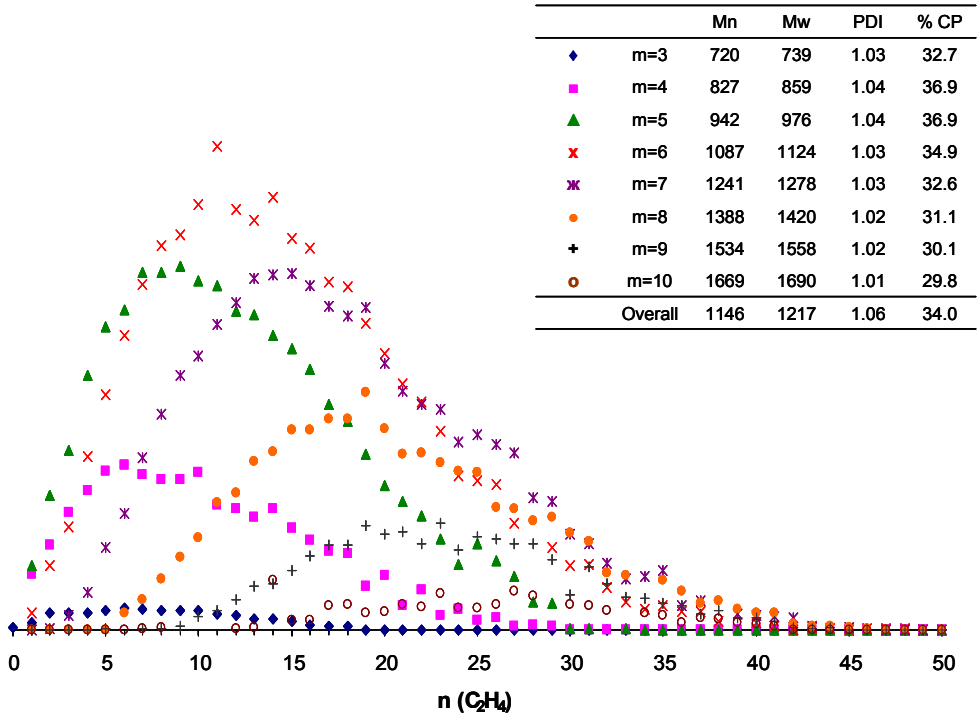

		Mn	Mw	PDI	% CP
♦	m=3	720	739	1.03	32.7
■	m=4	827	859	1.04	36.9
▲	m=5	942	976	1.04	36.9
×	m=6	1087	1124	1.03	34.9
✱	m=7	1241	1278	1.03	32.6
●	m=8	1388	1420	1.02	31.1
+	m=9	1534	1558	1.02	30.1
○	m=10	1669	1690	1.01	29.8
	Overall	1146	1217	1.06	34.0

SI 5.5. Deconvoluted MALDI-TOF-MS data for 1-[PPh_3][I^-]-PE-*co*-PCP via borate cocatalyst.

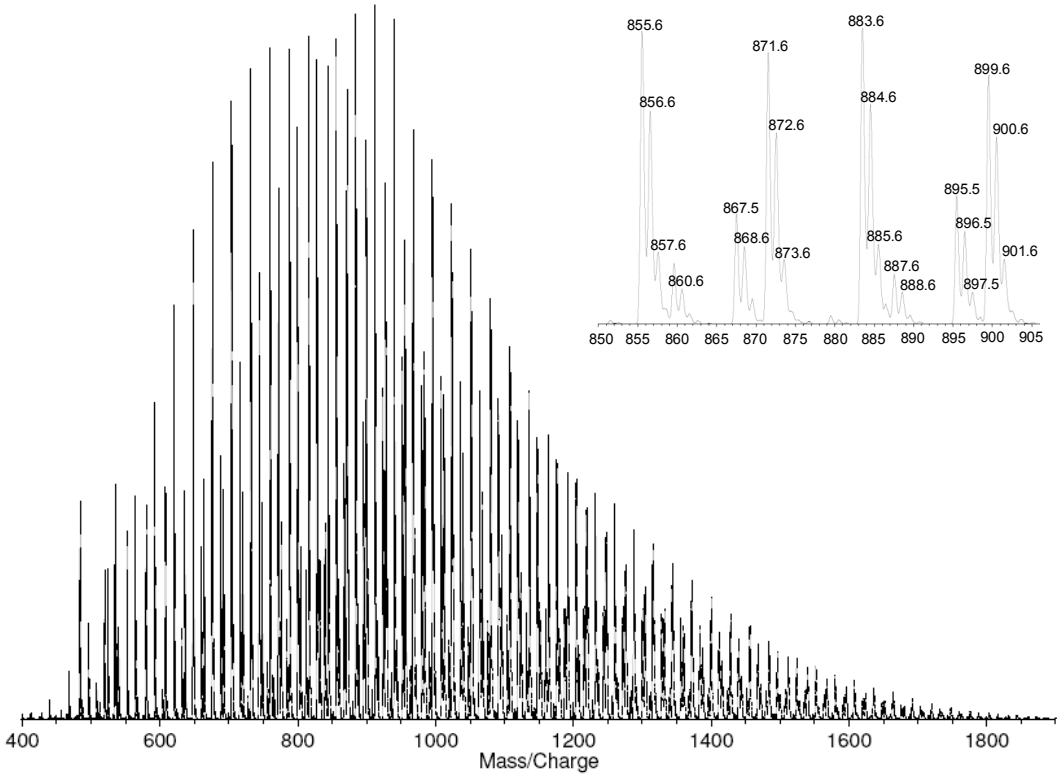

SI 5.6. Deconvoluted MALDI-TOF-MS data for 1-[PPh_3][I^-]-PE-*co*-PCP via borate cocatalyst.

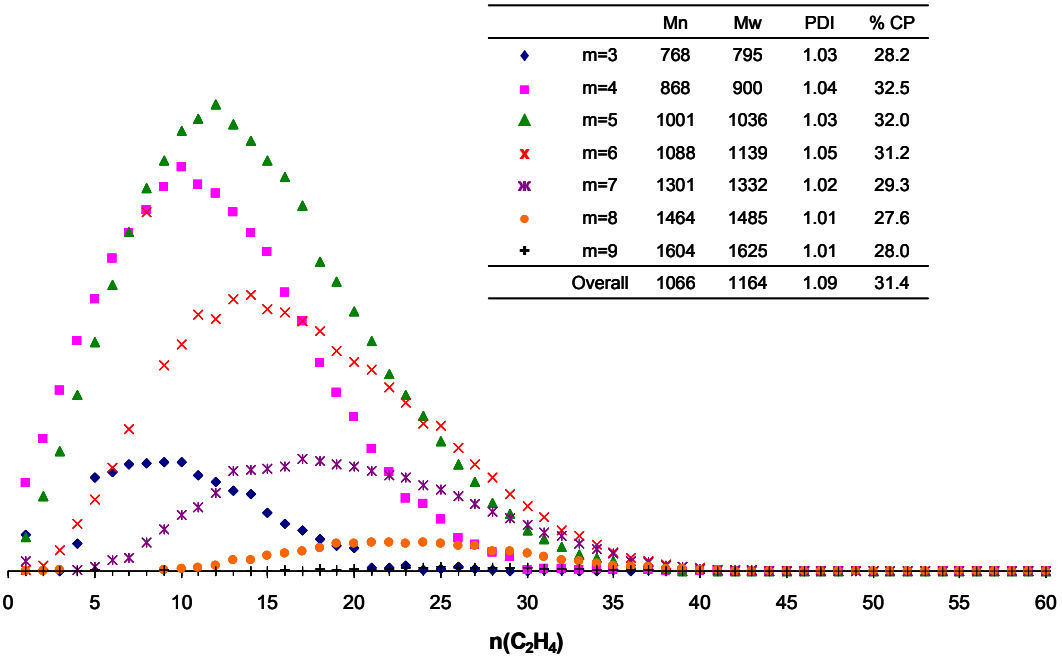

		Mn	Mw	PDI	% CP
♦	m=3	768	795	1.03	28.2
■	m=4	868	900	1.04	32.5
▲	m=5	1001	1036	1.03	32.0
x	m=6	1088	1139	1.05	31.2
ж	m=7	1301	1332	1.02	29.3
●	m=8	1464	1485	1.01	27.6
+	m=9	1604	1625	1.01	28.0
	Overall	1066	1164	1.09	31.4

SI 5.7. Deconvoluted MALDI-TOF-MS data for 1-[PPh_3][I^-]-PE-*co*-PCP via a 1:1 ratio of borate and borane cocatalysts.

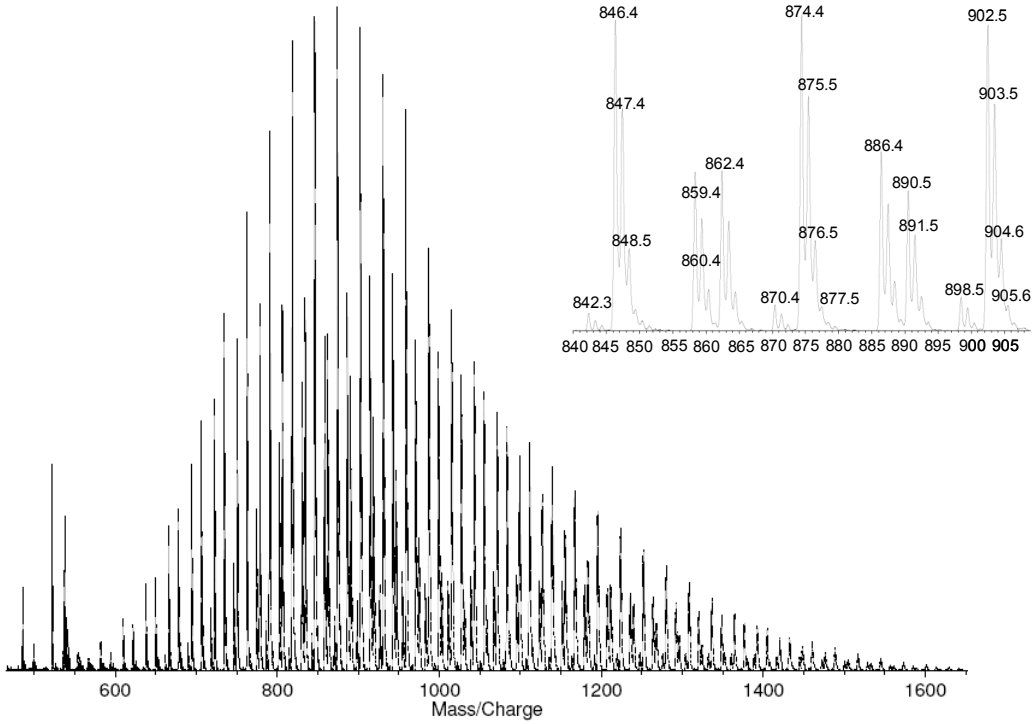

SI 5.8. MALDI-TOF-MS data for 1-[PPh_3][I^-]-PE-*co*-PCP via borane cocatalyst.

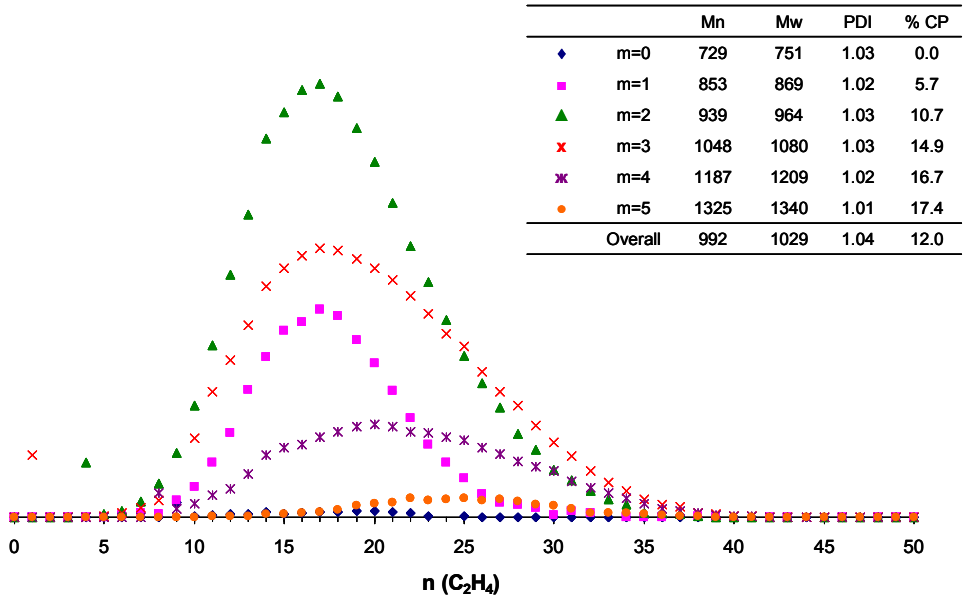

		Mn	Mw	PDI	% CP
◆	m=0	729	751	1.03	0.0
■	m=1	853	869	1.02	5.7
▲	m=2	939	964	1.03	10.7
×	m=3	1048	1080	1.03	14.9
✱	m=4	1187	1209	1.02	16.7
●	m=5	1325	1340	1.01	17.4
	Overall	992	1029	1.04	12.0

SI 5.9. Deconvoluted MALDI-TOF-MS data for 1-[PPh_3][I^-]-PE-*co*-PCP via borane cocatalyst.

References

(1) Peacock, A. *Handbook of Polyethylene. Structures, Properties, and Applications*; Marcel Dekker, Inc.: New York, 2000.

(2) Knuuttila, H.; Lehtinen, A.; Nummila-Pakarinen, A. *Long-Term Properties of Polyolefins* **2004**, *169*, 13-27.

(3) Pasquini, N.; Addeo, A. *Polypropylene Handbook*; Hanser: Ohio, 2005.

(4) Sita, L. R. *Angew. Chem. Int. Ed.* **2009**, *48*, 2464-2472.

(5) Coates, G. W. *Dalton Trans.* **2002**.

(6) Bamford, C. H. *The kinetics of vinyl polymerization by radical mechanisms*; Academic Press: Utah, 1958.

(7) Walling, C. *Free radicals in solution*; Wiley: New York, 1957.

(8) Domski, G. J.; Rose, J. M.; Coates, G. W.; Bolig, A. D.; Brookhart, M. *Prog. Polym. Sci.* **2007**, *32*, 30-92.

(9) Quirk, R. P.; Lee, B. *Polym. Int.* **1992**, *27*, 359-367.

(10) Muller, A. H. E.; Matyjaszewski, K. *Controlled and living polymerizations: methods and materials*; Wiley: New York, 2009.

(11) Szwarc, M.; Levy, M.; Milkovich, R. *J. Am. Chem. Soc.* **1956**, *78*, 2656-2657.

(12) Hirao, A.; Loykulnant, S.; Ishizone, T. *Prog. Polym. Sci.* **2002**, *27*, 1399-1471.

(13) Hirao, A.; Kato, H.; Yamaguchi, K.; Nakahama, S. *Macromolecules* **1986**, *19*, 1294-1299.

(14) Nakahama, S.; Hirao, A. *Prog. Polym. Sci.* **1990**, *15*, 299-335.

(15) Hirao, A.; Nakahama, S. *Prog. Polym. Sci.* **1992**, *17*, 283-317.

(16) Hsieh, H. L.; Quirk, R. P. *Anionic polymerization: principles and practical applications*; Marcel Dekker, Inc.: New York, 1996.

(17) Morton, M. *Anionic polymerization: principles and practice*; Academic Press: Utah, 1983.

(18) Holden, G.; Milkovich. R.; Belgian Patent 627652, 1963.

(19) Walter, H. M.; Schwaben, H. D.; Bueschl, R.; Bronstert, K.; Echte, A.; Deutsch Patent 3730886, 1989.

(20) Knoll, K.; Niessner, N. *Macromol. Symp.* **1998**, *132*, 231-243.

(21) Quirk, R. P.; Chen, W.-C. *J. Polym. Sci., Part A: Polym. Chem.* **1984**, *22*, 2993-3000.

(22) Uhrig, D.; Mays, J. W. *J. Polym. Sci., Part A: Polym. Chem.* **2005**, *43*, 6179-6222.

(23) Higashimura, T.; Kishiro, O. *Polym. J.* **1977**, *9*, 87-93.

(24) Higashimura, T.; Mitsuhashi, M.; Sawamoto, M. *Macromolecules* **1979**, *12*, 178-182.

(25) Miyamoto, M.; Sawamoto, M.; Higashimura, T. *Macromolecules* **1984**, *17*, 2228-2230.

(26) Miyamoto, M.; Sawamoto, M.; Higashimura, T. *Macromolecules* **1984**, *17*, 265-268.

(27) Faust, R.; Kennedy, J. P. *Polym. Bull.* **1986**, *15*, 317-323.

(28) Faust, R.; Kennedy, J. P. *J. Polym. Sci., Part A: Polym. Chem.* **1987**, *25*, 1847-1869.

(29) Kennedy, J. P.; Ivan, B. *Designed polymers by carbocationic macromolecular engineering: theory and practice*; Hanser: Ohio, 1992.

(30) Matyjaszewski, K. *Cationic polymerizations: mechanisms, synthesis, and applications*; Marcel Dekker, Inc.: New York, 1996.

(31) Salamone, J. C. *Polymeric materials encyclopedia: H-L*; CRC Press, 1996.

(32) Aoshima, S.; Kanaoka, S. *Chem. Rev.* **2009**, *109*, 5245-5287.

(33) Puskas, J. E.; Michel, A.; Barghi, S. *Ionic polymerizations and related processes*; Kluwer: New York, 1999.

(34) Buback, M.; van Herk, A. M. *Radical Polymerization: Kinetics and Mechanism*; John Wiley & Sons, Inc.: New York, 2007.

(35) Matyjaszewski, K.; Kubisa, P.; Penczek, S. *J. Polym. Sci., Polym. Chem. Ed*. **1974**, *12*, 1333-1336.

(36) Matyjaszewski, K.; Sigwalt, P. *Polym. Int.* **1994**, *35*, 1-26.

(37) Matyjaszewski, K. *Prog. Polym. Sci.* **2005**, *30*, 858-875.

(38) Georges, M. K.; Veregin, R. P. N.; Kazmaier, P. M.; Hamer, G. K. *Macromolecules* **1993**, *26*, 2987-2988.

(39) Hawker, C. J.; Bosman, A. W.; Harth, E. *Chem. Rev.* **2001**, *101*, 3661-3688.

(40) Wayland, B. B.; Poszmik, G.; Mukerjee, S. L.; Fryd, M. *J. Am. Chem. Soc* **1994**, *116*, 7943-7944.

(41) Poli, R. *Angew. Chem. Int. Ed.* **2006**, *45*, 5058-5070.

(42) Wang, J.-S.; Matyjaszewski, K. *J. Am. Chem. Soc.* **1995**, *117*, 5614-5615.

(43) Matyjaszewski, K.; Xia, J. *Chem. Rev.* **2001**, *101*, 2921-2990.

(44) Matyjaszewski, K. *Macromolecules* **1999**, *32*, 9051-9053.

(45) Moad, C. L.; Moad, G.; Rizzardo, E.; Thang, S. H. *Macromolecules* **1996**, *29*, 7717-7726.

(46) Lowe, A. B.; McCormick, C. L. *Prog. Polym. Sci.* **2007**, *32*, 283-351.

(47) Moad, G.; Rizzardo, E.; Thang, S. H. *Polymer* **2008**, *49*, 1079-1131.

(48) Chauvin, Y. *Angew. Chem. Int. Ed.* **2006**, *45*, 3740-3747.

(49) Grubbs, R. H. *Angew. Chem. Int. Ed.* **2006**, *45*, 3760-3765.

(50) Schrock, R. R. *Angew. Chem. Int. Ed.* **2006**, *45*, 3748-3759.

(51) Buchmeiser, M. R. *Chem. Rev.* **2000**, *100*, 1565-1604.

(52) Frenzel, U.; Nuyken, O. *J. Polym. Sci., Part A: Polym. Chem.* **2002**, *40*, 2895-2916.

(53) Grubbs, R. H. *Handbook of metathesis: Applications in polymer synthesis*; Wiley: New York, 2003.

(54) Jean-Louis Hérisson, P.; Chauvin, Y. *Angew. Makromol. Chem.* **1971**, *141*, 161-176.

(55) Benson, S. W.; Cruickshank, F. R.; Golden, D. M.; Haugen, G. R.; O'Neal, H. E.; Rodgers, A. S.; Shaw, R.; Walsh, R. *Chem. Rev.* **1969**, *69*, 279-324.

(56) Webster, O. W. *Science* **1991**, *251*, 887-893.

(57) Jacobson, H.; Stockmayer, W. H. *J. Chem. Phys.* **1950**, *18*, 1600-1606.

(58) Benedicto, A. D.; Claverie, J. P.; Grubbs, R. H. *Macromolecules* **1995**, *28*, 500-511.

(59) Chen, Z.-R.; Claverie, J. P.; Grubbs, R. H.; Kornfield, J. A. *Macromolecules* **1995**, *28*, 2147-2154.

(60) Rule, J. D.; Moore, J. S. *Macromolecules* **2002**, *35*, 7878-7882.

(61) Watson, K. J.; Anderson, D. R.; Nguyen, S. T. *Macromolecules* **2001**, *34*, 3507-3509.

(62) Ziegler, K. *Advances in Organometallic Chemistry*; Academic Press, **1968**, 6, 1-17.

(63) Natta, G.; Pino, P.; Corradini, P.; Danusso, F.; Mantica, E.; Mazzanti, G.; Moraglio, G. *J. Am. Chem. Soc.* **1955**, *77*, 1708-1710.

(64) Ziegler, K.; Holzkamp, E.; Breil, H.; Martin, H. *Angew. Chem. Int. Ed. Engl.* **1955**.

(65) Jayaratne, K. C.; Sita, L. R. *J. Am. Chem. Soc.* **2000**, *122*, 958-959.

(66) Zhang, Y.; Keaton, R. J.; Sita, L. R. *J. Am. Chem. Soc.* **2003**, *125*, 9062-9069.

(67) Harney, M. B.; Zhang, Y.; Sita, L. R. *Angew. Chem. Int. Ed.* **2006**, *45*, 6140-6144.

(68) Harney, M. B.; Zhang, Y.; Sita, L. R. *Angew. Chem. Int. Ed.* **2006**, *45*, 2400-2404.

(69) Zhang, W.; Sita, L. R. *J. Am. Chem. Soc.* **2007**, *130*, 442-443.

(70) Busico, V.; Carbonniere, P.; Cipullo, R.; Pellecchia, R.; Severn, J. R.; Talarico, G. *Macromol. Rapid Commun.* **2007**, *28*, 1128-1134.

(71) Zhang, W.; Wei, J.; Sita, L. R. *Macromolecules* **2008**, *41*, 7829-7833.

(72) Wei, J.; Zhang, W.; Sita, L. R. *Angew. Chem. Int. Ed.* **2010**, *49*, 1768-1772.

(73) Wei, J.; Zhang, W.; Wickham, R.; Sita, L. R. *Angew. Chem. Int. Ed.* **2010**.

(74) Boffa, L. S.; Novak, B. M. *Chem. Rev.* **2000**, *100*, 1479-1494.

(75) Chung, T. C. *Functionalization of polyolefins*; Academic Press, 2002.

(76) T.C, C. *Progress in Polymer Science* **2002**, *27*, 39-85.

(77) The Dow Chemical Company website

(78) Nakayama, Y.; Kawai, K.; Fujita, T. *J. Jpn. Pet. Inst.* **2010**, *53*, 111-129.

(79) Nomura, K. *J. Synth. Org. Chem Jpn.* **2010**, *68*, 1150-1158.

(80) Nakamura, A.; Ito, S.; Nozaki, K. *Chem. Rev.* **2009**, *109*, 5215-5244.

(81) Nomura, K.; Kitiyanan, B. *Curr. Org. Synth.* **2008**, *5*, 217-226.

(82) Mathers, R. T.; Coates, G. W. *Chem. Commun.* **2004**, 422-423.

(83) Boaen, N. K.; Hillmyer, M. A. *Chem. Soc. Rev.* **2005**, *34*, 267-275.

(84) Hong, M.; Liu, J.-Y.; Li, B.-X.; Li, Y.-S. *Macromolecules* **2011**, *44*, 5659-5665.

(85) Huang, H.; Niu, H.; Dong, J.-Y. *J. Polym. Sci., Part A: Polym. Chem.* **2011**, *49*, 2222-2232.

(86) Amin, S. B.; Marks, T. J. *Angew. Chem. Int. Ed.* **2008**, *47*, 2006-2025.

(87) Bonnet, F.; Barbier-Baudry, D.; Dormond, A.; Visseaux, M. *Polym. Int.* **2002**, *51*, 986-993.

(88) Hong, M.; Pan, L.; Ye, W.-P.; Song, D.-P.; Li, Y.-S. *J. Polym. Sci., Part A: Polym. Chem.* **2010**, *48*, 1764-1772.

(89) Nomura, K.; Liu, J.; Fujiki, M.; Takemoto, A. *J. Am. Chem. Soc.* **2007**, *129*, 14170-14171.

(90) Wei, J.; Wickham, R.; Sita, L. R. *Polymer Preprints* **2010**, *51*, 370-371.

(91) Lopez, R. G.; Boisson, C.; D'Agosto, F.; Spitz, R.; Boisson, F.; Bertin, D.; Tordo, P. *Macromolecules* **2004**, *37*, 3540-3542.

(92) Godoy Lopez, R.; D'Agosto, F.; Boisson, C. *Prog. Polym. Sci.* **2007**, *32*, 419-454.

(93) Briquel, R.; Mazzolini, J.; Le Bris, T.; Boyron, O.; Boisson, F.; Delolme, F.; D'Agosto, F.; Boisson, C.; Spitz, R. *Angew. Chem. Int. Ed.* **2008**, *47*, 9311-9313.

(94) Briquel, R.; Mazzolini, J.; Le Bris, T.; Boyron, O.; Boisson, F.; Delolme, F.; D'Agosto, F.; Boisson, C.; Spitz, R. *Angew. Chem. Int. Ed.* **2008**, *120*, 9451-9453.

(95) Huang, J.-M.; Zhang, J.-F.; Dong, Y.; Gong, W. *J. Org. Chem. 76*, 3511-3514.

(96) Luderer, M. R.; Bailey, W. F.; Luderer, M. R.; Fair, J. D.; Dancer, R. J.; Sommer, M. B. *Tetrahedron: Asymmetry* **2009**, *20*, 981-998.

(97) Denmark, S. E.; Fu, J. *Chem. Rev.* **2003**, *103*, 2763-2794.

(98) Cho, C. S.; Motofusa, S.-I.; Ohe, K.; Uemura, S.; Shim, S. C. *J. Org. Chem.* **1995**, *60*, 883-888.

(99) Schlosser, M. In *Topics in Stereochemistry*; John Wiley & Sons, Inc.: New York, 2007, p 1-30.

(100) Wittig, G.; Geissler, G. *Justus Liebigs Annalen der Chemie* **1953**, *580*, 44-57.

(101) Edmonds, M.; Abell, A. In *Modern Carbonyl Olefination*; Wiley: New York, 2004, p 1-17.

(102) Maercker, A. In *Organic Reactions*; John Wiley & Sons, Inc.: New York, 2004.

(103) Marini, F. *Seminars in Organic Synthesis, "A. Corbella" Summer School, 33rd, Gargnano, Italy, June 23-27, 2008* **2008**, 199-222.

(104) Vedejs, E.; Peterson, M. J. In *Topics in Stereochemistry*; John Wiley & Sons, Inc.: New York, 2007, p 1-157.

(105) Schlosser, M.; Christmann, K. F. *Angew. Chem. Int. Ed.* **1966**, *5*, 126-126.

(106) Horner, L.; Hoffmann, H.; Wippel, H. G. *Chem. Ber.* **1958**, *91*, 61-63.

(107) Horner, L.; Hoffmann, H.; Wippel, H. G.; Klahre, G. *Chem. Ber.* **1959**, *92*, 2499-2505.

(108) Wadsworth, W. S. *Organic Reactions*; John Wiley & Sons, Inc.: New York, 2004.

(109) Wadsworth, W. S.; Emmons, W. D. *J. Am. Chem. Soc.* **1961**, *83*, 1733-1738.

(110) Julia, M.; Paris, J.-M. *Tetrahedron Lett.* **1973**, *14*, 4833-4836.

(111) Kocienski, P. J.; Lythgoe, B.; Ruston, S. *J. Chem. Soc., Perkin Trans. 1* **1978**, 829-834.

(112) Peterson, D. J. *J. Org. Chem.* **1968**, *33*, 780-784.

(113) Ager, D. J. *Organic Reactions*; John New & Sons, Inc.: New York, 2004.

(114) Staden, L. F. v.; Gravestock, D.; Ager, D. J. *Chem. Soc. Rev.* **2002**, *31*, 195-200.

(115) Tebbe, F. N.; Parshall, G. W.; Reddy, G. S. *J. Am. Chem. Soc.* **1978**, *100*, 3611-3613.

(116) Gilbert, J. C.; Weerasooriya, U. *J. Org. Chem.* **1982**, *47*, 1837-1845.

(117) Tholey, A.; Wittmann, C.; Kang, M.-J.; Bungert, D.; Hollemeyer, K.; Heinzle, E. *J. Mass Spectrom.* **2002**, *37*, 963-973.

(118) Dirksen, A.; Dawson, P. E. *Bioconjugate Chem.* **2008**, *19*, 2543-2548.

(119) Schellekens, M. A. J., Eindhoven : Technische Universiteit Eindhoven, 2002.

(120) Edwards, K.L., *Mater. Des.* **2004**, *25*, 529-533.

(121) Ma, J.; Cheng, C.; Sun, G.; Wooley, K. L. *J. Polym. Sci., Part A: Polym. Chem.* **2008**, *46*, 3488-3498.

(122) Ma, J.; Cheng, C.; Sun, G.; Wooley, K. L. *Macromolecules* **2008**, *41*, 9080-9089.

(123) Ornelas, C.; Mary, D.; Cloutet, E.; Aranzaes, J. R.; Astruc, D. *J. Am. Chem. Soc.* **2008**, *130*, 1495-1506.

(124) David, R. L. A.; Kornfield, J. A. *Macromolecules* **2008**, *41*, 1151-1161.

(125) Mathers, R. T.; Coates, G. W. *Chem. Commun.* **2004**.

(126) Cherian, A. E.; Sun, F. C.; Sheiko, S. S.; Coates, G. W. *J. Am. Chem. Soc.* **2007**, *129*, 11350-11351.

(127) Debuigne, A.; Poli, R.; De Winter, J.; Laurent, P.; Gerbaux, P.; Wathelet, J.-P.; Jerome, C.; Detrembleur, C. *Macromolecules* **2010**, *43*, 2801-2813.

(128) Johnson, D. K.; Donohoe, J.; Kang, J. *Synth. Commun.* **1994**, *24*, 1557-1564.

(129) Cali, P.; Begtrup, M. *Synthesis* **2002**, *2002*, 0063,0066.

(130) Jensen, A. E.; Dohle, W.; Sapountzis, I.; Lindsay, D. M.; Vu, V. A.; Knochel, P. *Synthesis* **2002**, *2002*, 0565,0569.

(131) Sapountzis, I.; Knochel, P. *Angew. Chem. Int. Ed.* **2002**, *41*, 1610-1611.

(132) Binder, W. H.; Sachsenhofer, R. *Macromol. Rapid Commun.* **2007**, *28*, 15-54.

(133) Kolb, H. C.; Finn, M. G.; Sharpless, K. B. *Angew. Chem. Int. Ed.* **2001**, *40*, 2004-2021.

(134) Meldal, M. *Macromol. Rapid Commun.* **2008**, *29*, 1016-1051.

(135) Lutz, J.-F. *Angew. Chem. Int. Ed.* **2008**, *47*, 2182-2184.

(136) Baskin, J. M.; Bertozzi, C. R. *Click Chemistry for Biotechnology and Materials Science*; John Wiley & Sons, Inc.: New York, 2009, p 29-51.

(137) Nwe, K. B., Martin W. *Cancer Biotherapy & Radiopharmaceuticals* **2009**, *24*, 289-302.

(138) van Dijk, M.; Rijkers, D. T. S.; Liskamp, R. M. J.; van Nostrum, C. F.; Hennink, W. E. *Bioconjugate Chem.* **2009**, *20*, 2001-2016.

(139) Colombo, M.; Bianchi, A. *Molecules* **2010**, *15*, 178-197.

(140) Crowley, J. D.; Lee, A.-L.; Kilpin, K. J. *Aust. J. Chem.* **2011**, *64*, 1118-1132.

(141) Lühr, S.; Holz, J.; Börner, A. *ChemCatChem* **2011**, *3*, 1708-1730.

(142) Le Droumaguet, B.; Velonia, K. *Macromol. Rapid Commun.* **2008**, *29*, 1073-1089.

(143) Binder, W. H.; Sachsenhofer, R. *Macromol. Rapid Commun.* **2008**, *29*, 952-981.

(144) Baskin, J. M.; Bertozzi, C. R. *QSAR Comb. Sci*. *26*, 1211-1219.

(145) Michael, A. *Journal für Praktische Chemie* **1893**, *48*, 94-95.

(146) Huisgen, R. *Proceedings of the Chemical Society of London* **1961**, 357-&.

(147) Huisgen, R. *Angew. Chem. Int. Ed.* **1968**, *80*, 329-337.

(148) Huisgen, R. *Pure & Appl. Chem* **1989**, *61*, 613-628.

(149) Huisgen, R.; Sauer, J.; Sturm, H. J.; Markgraf, J. H. *Chem. Ber.* **1960**, *93*, 2106-2124.

(150) Huisgen, R.; Szeimies, G.; Möbius, L. *Chem. Ber.* **1967**, *100*, 2494-2507.

(151) Meldal, M.; Tornoe, C. W. *Chem. Rev.* **2008**, *108*, 2952-3015.

(152) Tornoe, C. W.; Christensen, C.; Meldal, M. *J. Org. Chem.* **2002**, *67*, 3057-3064.

(153) Rostovtsev, V. V.; Green, L. G.; Fokin, V. V.; Sharpless, K. B. *Angew. Chem. Int. Ed.* **2002**, *41*, 2596-2599.

(154) Lwowski, W. *1,3-Dipolar Cycloaddit. Chem.* **1984**, *1*, 559-651.

(155) Tsarevsky, N. V.; Bernaerts, K. V.; Dufour, B.; Du Prez, F. E.; Matyjaszewski, K. *Macromolecules* **2004**, *37*, 9308-9313.

(156) Malkoch, M.; Thibault, R. J.; Drockenmuller, E.; Messerschmidt, M.; Voit, B.; Russell, T. P.; Hawker, C. J. *J. Am. Chem. Soc.* **2005**, *127*, 14942-14949.

(157) Rodionov, V. O.; Fokin, V. V.; Finn, M. G. *Angew. Chem. Int. Ed.* **2005**, *117*, 2250-2255.

(158) van Steenis, D. J. V. C.; David, O. R. P.; van Strijdonck, G. P. F.; van Maarseveen, J. H.; Reek, J. N. H. *Chem. Commun.* **2005**, 4333-4335.

(159) Malkoch, M.; Vestberg, R.; Gupta, N.; Mespouille, L.; Dubois, P.; Mason, A. F.; Hedrick, J. L.; Liao, Q.; Frank, C. W.; Kingsbury, K.; Hawker, C. J. *Chem. Commun.* **2006**, 2774-2776.

(160) Becer, C. R.; Hoogenboom, R.; Schubert, U. S. *Angew. Chem. Int. Ed.* **2009**, *48*, 4900-4908.

(161) Hall, D. J.; Van Den Berghe, H. M.; Dove, A. P. *Polym. Int.* **2011**, *60*, 1149-1157.

(162) Kade, M. J.; Burke, D. J.; Hawker, C. J. *J. Polym. Sci., Part A: Polym. Chem.* **2010**, *48*, 743-750.

(163) Lowe, A. B. *Polymer Chemistry* **2010**, *1*, 17-36.

(164) Kalia, J.; Raines, R. T. *Bioorg. Med. Chem. Lett.* **2007**, *17*, 6286-6289.

(165) Baldwin, A. D.; Kiick, K. L. *Bioconjugate Chem.* **2011**, *22*, 1946-1953.

(166) Bain, C. D.; Troughton, E. B.; Tao, Y. T.; Evall, J.; Whitesides, G. M.; Nuzzo, R. G. *J. Am. Chem. Soc.* **1989**, *111*, 321-335.

(167) Love, J. C.; Estroff, L. A.; Kriebel, J. K.; Nuzzo, R. G.; Whitesides, G. M. *Chem. Rev.* **2005**, *105*, 1103-1170.

(168) Liras, M.; Garcia, O.; Quijada-Garrido, I.; PariÃÅs, R. *Macromolecules* **2011**, *44*, 1335-1339.

(169) Zhai, L.; Pilston, R. L.; Zaiger, K. L.; Stokes, K. K.; McCullough, R. D. *Macromolecules* **2002**, *36*, 61-64.

(170) Nakashima, H.; Furukawa, K.; Ajito, K.; Kashimura, Y.; Torimitsu, K. *Langmuir* **2004**, *21*, 511-515.

(171) Davis, F. A.; Billmers, R. L. *J. Am. Chem. Soc.* **1981**, *103*, 7016-7018.

(172) Janiak, C.; Lassahn, P. G. *J. Mol. Catal. A: Chem.* **2001**, *166*, 193-209.

(173) Blank, F.; Janiak, C. *Coordination Chem. Rev.* **2009**, *253*, 827-861.

(174) K.J. Ivin, J. C. M. *Olefin Metathesis and Metathesis Polymerization* San Diego, 1997.

(175) Bhowmick, A. K.; Stephens, H. L. *Handbook of elastomers*; Marcel Dekker, Inc.: New York, 2001.

(176) Schuster, M.; Blechert, S. *Angew. Chem. Int. Ed.* **1997**, *36*, 2036-2056.

(177) Kress, J.; Wesolek, M.; Osborn, J. A. *J. Chem. Soc., Chem. Commun.* **1982**, 514-516.

(178) Kress, J.; Osborn, J. A. *J. Am. Chem. Soc.* **1983**, *105*, 6346-6347.

(179) Aguero, A.; Kress, J.; Osborn, J. A. *J. Chem. Soc., Chem. Commun.* **1985**, 793-794.

(180) Kress, J.; Osborn, J. A.; Greene, R. M. E.; Ivin, K. J.; Rooney, J. J. *J. Chem. Soc., Chem. Commun.* **1985**, 874-876.

(181) Kress, J.; Osborn, J. A.; Greene, R. M. E.; Ivin, K. J.; Rooney, J. J. *J. Am. Chem. Soc.* **1987**, *109*, 899-901.

(182) Schrock, R. R.; Feldman, J.; Cannizzo, L. F.; Grubbs, R. H. *Macromolecules* **1987**, *20*, 1169-1172.

(183) Murdzek, J. S.; Schrock, R. R. *Macromolecules* **1987**, *20*, 2640-2642.

(184) Murdzek, J. S.; Schrock, R. R. *Organometallics* **1987**, *6*, 1373-1374.

(185) Bazan, G. C.; Schrock, R. R.; Cho, H. N.; Gibson, V. C. *Macromolecules* **1991**, *24*, 4495-4502.

(186) Heroguez, V.; Fontanille, M. *J. Polym. Sci., Part A: Polym. Chem.* **1994**, *32*, 1755-1760.

(187) Schwab, P.; France, M. B.; Ziller, J. W.; Grubbs, R. H. *Angew. Chem. Int. Ed.* **1995**, *34*, 2039-2041.

(188) Hafner, A.; Van Der Schaaf, P. A.; Miihlebach, A. *Chimia Int. J. Chem.* **1996**, *50*, 131-134.

(189) Schwab, P.; Grubbs, R. H.; Ziller, J. W. *J. Am. Chem. Soc.* **1996**, *118*, 100-110.

(190) Gilliom, L. R.; Grubbs, R. H. *J. Am. Chem. Soc.* **1986**, *108*, 733-742.

(191) Wallace, K. C.; Liu, A. H.; Dewan, J. C.; Schrock, R. R. *J. Am. Chem. Soc.* **1988**, *110*, 4964-4977.

(192) Brumaghim, J. L.; Girolami, G. S. *Organometallics* **1999**, *18*, 1923-1929.

(193) Steinhäusler, T.; Koros, W. J. *J. Polym. Sci., Part B: Polym. Phys.* **1997**, *35*, 91-99.

(194) Kennedy, J. P.; Makowski, H. S. *J. Macromol. Sci. Part A Pure Appl. Chem.* **1967**, *1*, 345-370.

(195) Gaylord, N. G.; Mandal, B. M.; Martan, M. *J. Polym. Sci.: Polym. Lett. Ed.* **1976**, *14*, 555-559.

(196) Gaylord, N. G.; Deshpande, A. B.; Mandal, B. M.; Martan, M. *J. Macromol. Sci. Part A Pure Appl. Chem.* **1977**, *11*, 1053-1070.

(197) Ahmed, S.; Bidstrup, S. A.; Kohl, P. A.; Ludovice, P. J. *J. Phys. Chem. B* **1998**, *102*, 9783-9790.

(198) Grove, N. R.; Kohl, P. A.; Bidstrup Allen, S. A.; Jayaraman, S.; Shick, R. *J. Polym. Sci., Part B: Polym. Phys.* **1999**, *37*, 3003-3010.

(199) Kaminsky, W.; Bark, A.; Dake, I. *Studies in Surface Science and Catalysis*; Elsevier, **1990**, 56, 425-438.

(200) Tritto, I.; Boggioni, L.; Ferro, D. R. *Coord. Chem. Rev.* **2006**, *250*, 212-241.

(201) Kaminsky, W.; Bark, A.; Arndt, M. *Makromol. Chem. Macromol. Symp.* **1991**, *47*, 83-93.

(202) Brekner, M. J.; Osan, F.; Rohrmann, J.; Antberg, M. Deutsch Patent 5324801, 1994.

(203) Wei, J.; Zhang, W.; Sita, L. R. *Angew. Chem. Int. Ed.* **2010**, *122*, 1812-1816.

(204) Wei, J.; Zhang, W.; Wickham, R.; Sita, L. R. *Angew. Chem. Int. Ed.* **2010**, *49*, 9140-9144.

(205) Zhang, W.; Wei, J.; Sita, L. R. *Macromolecules* **2008**, *41*, 7829-7833.

(206) Sita, L. R. *Macromolecules* **1995**, *28*, 656-657.

(207) Wilbur, J. M.; Marvel, C. S. *J. Polym. Sci., Part A: Gen. Pap.* **1964**, *2*, 4415-4423.

(208) Dolatkhani, M.; Cramail, H.; Deffieux, A. *Macromol. Chem. Phys.* **1995**, *196*, 3091-3105.

(209) Fujita, M.; Coates, G. W. *Macromolecules* **2002**, *35*, 9640-9647.

(210) Lin, Y.-C.; Yu, K.-H.; Huang, S.-L.; Liu, Y.-H.; Wang, Y.; Liu, S.-T.; Chen, J.-T. *Dalton Trans.* **2009**, 9058-9067.

(211) Dolatkhani, M.; Cramail, H.; Deffieux, A. *Macromol. Chem. Phys.* **1995**, *196*, 3091-105.

(212) Dolatkhani, M.; Cramail, H.; Deffieux, A. *Macromol. Chem. Phys.* **1996**, *197*, 2481-2491.

(213) Santos, J. M.; Ribeiro, M. R.; Portela, M. F.; Cramail, H.; Deffieux, A.; Antinolo, A.; Otero, A.; Prashar, S. *Macromol. Chem. Phys.* **2002**, *203*, 139-145.

(214) Santos, J. M.; Ribeiro, M. R. r.; Portela, M. F.; Cramail, H.; Deffieux, A.; Antiæolo, A.; Oterz, A.; Prashar, S. *Macromol. Chem. Phys.* **2002**, *203*, 139-145.

(215) Hamley, I. W. *Introduction to Soft Matter*; John Wiley & Sons, Inc.: New York, 2000.

(216) Hamley, I. W.; Castelletto, V.; Castillo, R. V.; Muller, A. J.; Martin, C. M.; Pollet, E.; Dubois, P. *Macromolecules* **2004**, *38*, 463-472.

(217) Myers, S. B.; Register, R. A. *Macromolecules* **2008**, *41*, 6773-6779.

(218) Klok, H. A.; Lecommandoux, S. *Adv. Mater.* **2001**, *13*, 1217-1229.

(219) Gompper, G.; Schick, M. *Soft Matter: Polymer melts and mixtures*; Wiley: New York, 2006.

(220) Ji-Zhong, C.; Zhao-Yan, S.; Cheng-Xiang, Z.; Li-Jia, A.; Zhen, T. *J. Chem. Phys.* **2008**, *128*, 074904.

(221) Halperin, A. *Europhys. Lett.* **1989**, *10*, 549-553.

(222) Halperin, A. *Macromolecules* **1990**, *23*, 2724-2731.

(223) Semenov, A. N. *Mol. Cryst. Liq. Cryst. Sci.* **1991**, *209*, 191 - 199.

(224) Williams, D. R. M.; Fredrickson, G. H. *Macromolecules* **1992**, *25*, 3561-3568.

(225) de Gennes, P. G. *Scaling concepts in polymer physics*; Cornell University Press, 1979.

(226) Nedoma, A. J.; Robertson, M. L.; Wanakule, N. S.; Balsara, N. P. *Industrial & Engineering Chemistry Research* **2007**, *47*, 3551-3553.

(227) Muller, M.; Schick, M. *Macromolecules* **1996**, *29*, 8900-8903.

(228) Netz, R. R.; Schick, M. *Phys. Rev. Lett.* **1996**, *77*, 302.

(229) Matsen, M. W.; Barrett, C. *J. Chem. Phys.* **1998**, *109*, 4108-4118.

(230) Li, W.; Gersappe, D. *Macromolecules* **2001**, *34*, 6783-6789.

(231) Olsen, B. D.; Segalman, R. A. *Macromolecules* **2005**, *38*, 10127-10137.

(232) Reenders, M.; ten Brinke, G. *Macromolecules* **2002**, *35*, 3266-3280.

(233) Victor, P.; Venkat, G. *J. Chem. Phys.* **2004**, *120*, 5824-5838.

(234) Singh, S. *Phys. Rep.* **2000**, *324*, 107-269.

(235) Olsen, B. D.; Shah, M.; Ganesan, V.; Segalman, R. A. *Macromolecules* **2008**, *41*, 6809-6817.

(236) Hotta, A.; Cochran, E.; Ruokolainen, J.; Khanna, V.; Fredrickson, G. H.; Kramer, E. J.; Shin‖, Y.-W.; Shimizu‖, F.; Cherian, A. E.; Hustad, P. D.;

Rose, J. M.; Coates, G. W. *Proceedings of the National Academy of Sciences of the United States of America* **2008**.

(237) Hustad, P. D.; Marchand, G. R.; Garcia-Meitin, E. I.; Roberts, P. L.; Weinhold, J. D. *Macromolecules* **2009**, *42*, 3788-3794.

(238) Lange, B.; Fleischhaker, F.; Zentel, R. *Nanophotonic Materials*; Wiley: New York, 2008, p 39-61.

(239) Koo, C. M.; Wu, L.; Lim, L. S.; Mahanthappa, M. K.; Hillmyer, M. A.; Bates, F. S. *Macromolecules* **2005**, *38*, 6090-6098.

(240) Hustad, P. D.; Kuhlman, R. L.; Arriola, D. J.; Carnahan, E. M.; Wenzel, T. T. *Macromolecules* **2007**, *40*, 7061-7064.

(241) Jayaratne, K. C.; Keaton, R. J.; Henningsen, D. A.; Sita, L. R. *J. Am. Chem. Soc.* **2000**, *122*, 10490-10491.

(242) Schmitz, I.; Schreiner, M.; Friedbacher, G.; Grasserbauer, M. *Appl. Surf. Sci.* **1997**, *115*, 190-198.

(243) Babcock, K. L.; Prater, C. B.; *Phase Imaging: Beyond Topography;* Digital Instruments, Inc.: Santa Barbara, 2009.

(244) Segalman, R. A. *Mater. Sci. Eng., R*; **2005**, *48*, 191-226.

(245) Kuhn, G.; Weidner, S.; Just, U.; Hohner, G. *J. Chromatogr. A* **1996**, *732*, 111-117.

(246) Hinderling, C.; Chen, P. *Int. J. Mass spectrom.* **2000**, *195-196*, 377-383.

(247) Dutta, T. K.; Harayama, S. *Anal. Chem.* **2001**, *73*, 864-869.

(248) Chen, R.; Li, L. *J. Am. Soc. Mass. Spectrom.* **2001**, *12*, 367-375.

(249) Kahr, M. S.; Wilkins, C. L. *J. Am. Soc. Mass. Spectrom.* **1993**, *4*, 453-460.

(250) Bauer, B. J.; Wallace, W. E.; Fanconi, B. M.; Guttman, C. M. *Polymer* **2001**, *42*, 09949-09953.

(251) Lin-Gibson, S.; Brunner, L.; Vanderhart, D. L.; Bauer, B. J.; Fanconi, B. M.; Guttman, C. M.; Wallace, W. E. *Macromolecules* **2002**, *35*, 7149-7156.

(252) Hillenkamp, F.; Karas, M.; Beavis, R. C.; Chait, B. T. *Anal. Chem.* **1991**, *63*,1193A-1203A.

(253) Belu, A. M.; DeSimone, J. M.; Linton, R. W.; Lange, G. W.; Friedman, R. M. *J. Am. Soc. Mass. Spectrom.* **1996**, *7*, 11-24.

(254) Chaudhary, A. K.; Critchley, G.; Diaf, A.; Beckman, E. J.; Russell, A. J. *Macromolecules* **1996**, *29*, 2213-2221.

(255) Feast, W.; Hamilton, L.; Rannard, S. *Polym. Bull.* **1997**, *39*, 347-352.

(256) Lehrle, R. S.; Sarson, D. S. *Polym. Degrad. Stab.* **1996**, *51*, 197-204.

(257) Wetzel, S. J.; Guttman, C. M.; Flynn, K. M.; Filliben, J. J. *J. Am. Soc. Mass. Spectrom.* **2006**, *17*, 246-252.

(258) Wei, J., University of Maryland, 2012.

(259) Willemse, R. X. E.; Staal, B. B. P.; Donkers, E. H. D.; van Herk, A. M. *Macromolecules* **2004**, *37*, 5717-5723.

(260) Wallace, W. E.; Blair, W. R. *Int. J. Mass spectrom.* **2007**, *263*, 82-87.

(261) Kaminsky, W.; Spiehl, R. *Angew. Makromol. Chem.* **1989**, *190*, 515-526.

(262) Jerschow, A.; Ernst, E.; Hermann, W.; Mueller, N. *Macromolecules* **1995**, *28*, 7095-7099.

(263) Naga, N.; Imanishi, Y. *Macromol. Chem. Phys.* **2002**, *203*, 159-165.